The Bell System Technical Journal

Vol. XXV *April, 1946* *No. 2*

The Magnetron as a Generator of Centimeter Waves

By J. B. FISK, H. D. HAGSTRUM, and P. L. HARTMAN

Introduction

LATE in the summer of 1940, a fire control radar operating at 700 megacycles per second was in an advanced state of development at the Bell Telephone Laboratories. The pulse power of this radar was generated by a pair of triodes operating near their upper limit of frequency. Even when driven to the point where tube life was short, the generator produced peak power in each pulse of only two kilowatts, a quantity usable but marginal. Although the triodes employed had not been designed for high voltage pulsed operation, they were the best available. This is an example of how development of radar in the centimeter wave region was circumscribed by the lack of a generator of adequate power and reasonable life expectancy. Moreover, the prospects of improvement of the triode as a power generator at these wavelengths and extension of its use to shorter wavelengths were not bright. Solution of the problem by means of power amplification was remote. A new source of centimeter wave power was urgently needed.

For the British, who were at war, the problem was even more urgent. They had undertaken a vigorous search for a new type of generator of sufficiently high power and frequency to make airborne radar practicable in the defense against enemy night bombers. They found a solution in the multiresonator magnetron oscillator, admirably suited to pulsed generation of centimeter waves of high power.

In the fall of 1940, an early model of this magnetron operating at ten centimeters was brought to the United States for examination. The first American test of its output power capabilities was made on October 6, 1940 in the Bell Telephone Laboratories' radio laboratory at Whippany, N. J. This test confirmed British information and demonstrated that a generator now existed which could supply several times the power that our triodes delivered and at a frequency four times as great. The most important restraint on the development of radar in the centimeter wavelength region had now been removed.

A number of pressing questions remained to be answered, however. Could the new magnetron be reproduced quickly and in quantity? Was its

operating life satisfactory? Could its efficiency and output power be substantially increased? Could one construct similar magnetrons at forty centimeters, at three centimeters, even at one centimeter? Could the magnetron oscillator be tuned conveniently? One by one, during the war years, all of these questions have been answered in the affirmative. In many instances, but not without detours and delays, results have been better than expected or hoped for.

The British magnetron was first reproduced in America at the Bell Telephone Laboratories for use in its radar developments and those at the Radiation Laboratory of the National Defense Research Committee which was then being formed at the Massachusetts Institute of Technology. Since that time, extensive research and development work has been carried on in our Laboratories, in other industrial laboratories, and in the laboratories of the National Defense Research Committee. Several manufacturers have produced the resultant designs. Magnetron research and development was also carried on in Great Britain by governmental and industrial laboratories. There has been continuous interchange of information among all these laboratories through visits and written reports. Magnetron and radar developments have been greatly accelerated by this interchange.

Multicavity magnetron oscillators are now available for use as pulsed and continuous wave generators at wavelengths from approximately 0.5 to 50 centimeters. The upper limit of peak power is now about 100 kilowatts at 1 centimeter, 3 megawatts at 10 centimeters. Operating voltages may be less than 1 kilovolt or more than 40 kilovolts. The magnetic fields essential to operation range from 600 to 15,000 gauss. Tunable magnetrons now exist for many parts of the centimeter wave region. The tuning range for pulsed operation at high voltage is about $\pm 5\%$. It is as much as $\pm 20\%$ for low voltage magnetrons. Magnetrons may now be tuned electronically, making frequency modulation possible. Present magnetron cathodes are rugged and have long life. Even for high frequency magnetrons where current density requirements are most severe, research has made available rugged cathodes with adequate life. Magnetrons are built to withstand shock and vibration without change in characteristics. Designs have been compressed and in some cases the magnet has been incorporated in the magnetron structure in the interest of light weight for airborne radar equipments.

PART I of this paper is a general discussion of present knowledge concerning the magnetron oscillator. As such it is largely a discussion of what has come to be common knowledge among those who have carried out wartime developments. It brings together in one place results of work done by all the magnetron research groups including that at our Laboratories. PART I supplies the background necessary to understanding the

discussion in PART II of the magnetrons developed at the Bell Laboratories during the war. More complete presentations of the experimental and theoretical work done on the magnetron during the war are soon to be published by other research groups.

The material written up during the war has appeared as secret or confidential reports issued by the British Committee on Valve Development (CVD Magnetron Reports), by the Radiation Laboratories at the Massachusetts Institute of Technology and at Columbia University, and by the participating industrial laboratories. No attempt has been made in PART I to indicate the specific sources of the work done since 1940. To fit the wartime development of magnetrons into the sequence of previous developments, specific references are made to publications appearing in the literature prior to 1940.

The nature and scope of PART II of the paper are discussed more fully in its introductory Section, 11. GENERAL REMARKS.

PART I

THE MAGNETRON OSCILLATOR

1. GENERAL DESCRIPTION

1.1 *Description:* The multicavity magnetron oscillator has three principal component parts: an electron interaction space, a multiple resonator system, and an output circuit. Each of these is illustrated schematically in Fig. 1. The electron interaction space is the region of cylindrical symmetry between the cathode and the multisegment anode. In this region electrons emitted from the cylindrical cathode move under the action of the DC radial electric field, the DC axial magnetic field, and the RF field set up by the resonator system between the anode segments. These electronic motions result in a net transfer of energy from the DC electric field to the RF field. The RF interaction field is the fringing electric field appearing between the anode segments, built up and maintained by the multicavity resonator in the anode block. RF energy fed into the resonator system by the electrons is delivered through the output circuit to the useful load. The output circuit shown in Fig. 1 consists of a loop, inductively coupled to one of the hole and slot cavities, feeding a coaxial line.

To operate such a magnetron oscillator, one must place it in a magnetic field of suitable strength and apply a voltage of proper magnitude to its cathode, driving the cathode negative with respect to the anode. This voltage may be constant or pulsed. In the latter case, the voltage is applied suddenly by a so-called pulser or modulator for short intervals, usually of about one microsecond duration at a repetition rate of about 1000 pulses per second. With suitable values of the operating parameters, the magnetron

oscillates as a self excited oscillator whenever the DC voltage is applied. The energy available at the output circuit may be connected, as in a radar set, to an antenna or, as in a laboratory experimental setup, may be absorbed in a column of water.

1.2 *Analogy to Other Oscillators:* In its fundamental aspects, the magnetron oscillator is not unlike other and perhaps more familiar oscillators. In particular, instructive analogies may be drawn between the magnetron oscillator, the velocity variation oscillator, and the simple triode oscillator. In Fig. 2 is depicted schematically the parallelisms between these types of oscillators and a simplified equivalent lumped constant circuit.

In the triode of Fig. 2(a), as in the gap of the second cavity of the velocity variation tube of Fig. 2(b) and in the interaction space of the magnetron

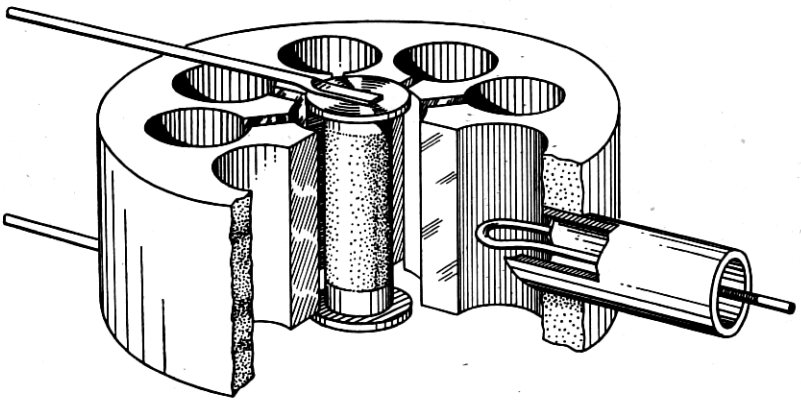

Fig. 1.—A schematic diagram designed to show the principal component parts of a centimeter wave magnetron oscillator. The resonator system and output circuit each represents one of several types used in magnetron construction.

oscillator of Fig. 2(c), electrons are driven against RF fields set up by the resonator or "tank circuit," to which they give up energy absorbed from the primary DC source. In each type of oscillator there is operative a mechanism of "bunching" which allows electrons to interact with the RF field primarily when the interaction will result in energy transfer *to* the RF field. In the triode oscillator this is accomplished by the grid, whose RF potential is supplied by the "tank circuit" in proper phase with respect to the RF potential on the anode. In the velocity variation oscillator, bunching is accomplished by variation of the electron velocities in the gap of the first cavity, followed by drift through the intervening space to the second gap. The first cavity is driven in proper phase by a feed back line from the second cavity. In the magnetron oscillator, as is to be described in detail later, electron interaction with the RF fields is such as to group the electrons into

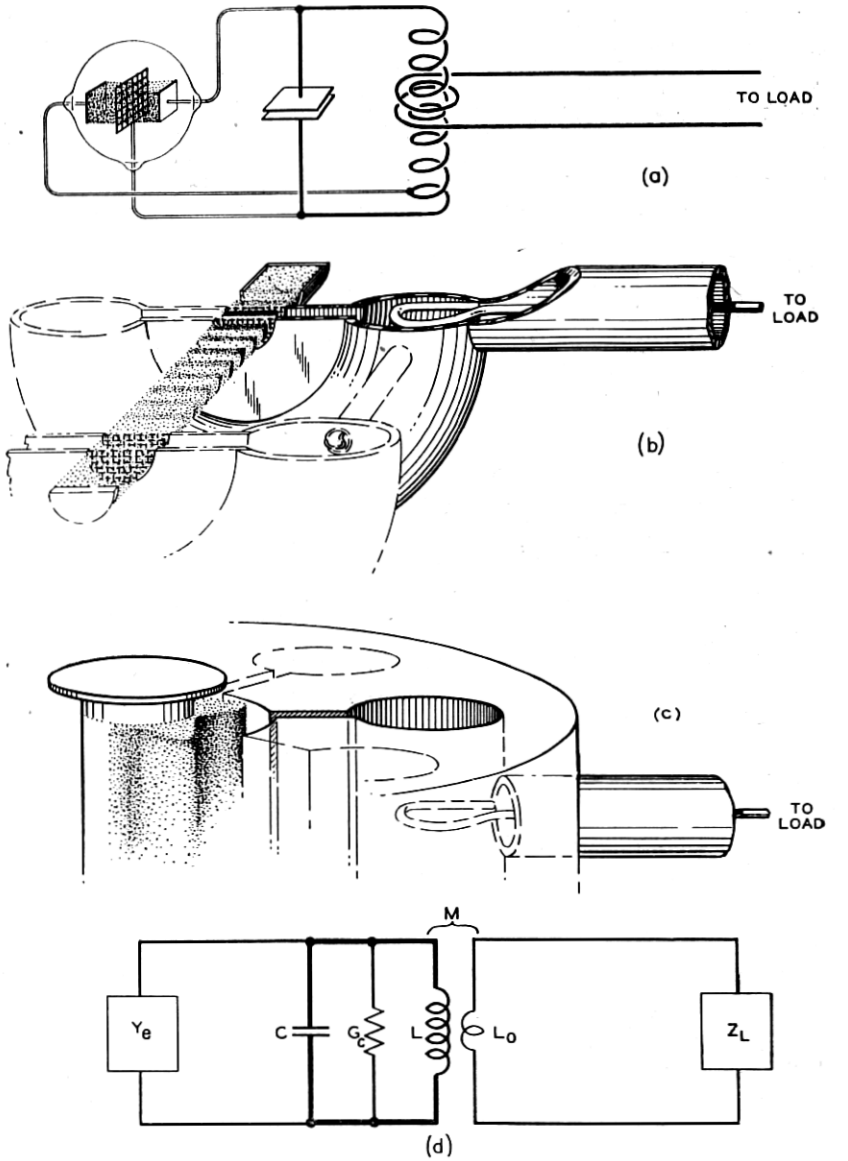

Fig. 2.—A schematic diagram depicting the parallelism among the conventional triode oscillator, the velocity variation oscillator, the centimeter wave magnetron and an equivalent lumped constant circuit. In the figure an attempt is made to align corresponding parts vertically above one another.

bunches or "spokes" which sweep past the gaps in the anode, in phase for favorable interaction with the RF fields across the gaps. The bunching field

is thus the same field as that to which energy is transferred. In this sense the magnetron oscillator is perhaps more properly analogous to the reflex type of velocity variation oscillator, in which a single cavity is used both as "buncher" and "catcher"; the electrons, after traversing the gap once, are turned back in the proper phase in the drift space so as to pass through the gap again in the opposite direction.

Each type of oscillator has a resonator in which energy is stored and which synchronizes the flow of energy from the electrons into it by the means of self excitation. In each type, energy is extracted from the resonator by an output circuit at a rate which, under steady state conditions, equals that of influx from the electron interaction, minus the losses in the resonator itself.

1.3 *Use of Equivalent Circuits:* In many instances the understanding of electromagnetic oscillators is made easier and analytic treatment made possible by use of an equivalent circuit with lumped constants. Of several possible types, one of the simpler and more frequently used for the magnetron oscillator is shown in Fig. 2. This may appear in the case of the multicavity magnetron to be an oversimplification as it does not account for the fact that the resonant frequency of the magnetron resonator system is many valued. A magnetron resonator, being made up of a number of coupled resonating cavities, is capable of supporting several modes of oscillation. These modes of oscillation have different resonant frequencies and correspond to different configurations of the electromagnetic fields. By means to be discussed, however, magnetron resonators can be made to oscillate "cleanly" in one of these modes and may thus be represented for many purposes by a simple L-C circuit having a single resonance.

The output circuit of the oscillator is also amenable to treatment by equivalent lumped constant circuits which account for its behavior with accuracy. More general, four terminal network theory has also been applied in the study and design of impedance transformations in this part of the oscillator.

Finally, the electrons, which in a sense are connected to the circuit formed by the resonator and the load, may also be treated by circuit concepts. The electrons moving in the space between the cathode and anode, by virtue of their presence and motion, induce charge fluctuations on the anode segments. The time derivative of these fluctuations is equivalent to an RF current flowing into the anode from the interaction space. This current and the RF voltage on the anode, bearing a definite phase relationship, make possible the definition of an admittance called the average electronic admittance, $Y_e = G_e + jB_e$. Since the electrons are being driven against RF fields in the interaction space, this admittance looking into the electron stream has a negative conductance term. Unlike usual circuit admittances, the electronic admittance is nonlinear, being a function of the voltage

amplitude of oscillation, V_{RF}, as well as of other parameters governing the electronic behavior of the oscillator, such as voltage and magnetic field. It is not known *a priori* but may be deduced from measurements on the operating oscillator and its circuit.

A necessary condition for oscillation, applicable to the magnetron as to any oscillator, is that, on breaking the circuit at any point, the sum of the admittances looking in the two directions is zero. Thus, if the circuit is broken at the junction of electrons and resonator, as is convenient, the electronic admittance, Y_e, looking from the circuit into the electron stream, must be the negative of the circuit admittance, Y_s, looking from the electron stream into the circuit.

With these remarks, of general applicability to all types of electromagnetic oscillators, the discussion will be continued for the centimeter wave magnetron oscillator in particular. As far as is possible, the electronic interaction space, resonator system, and output circuit of the device will be taken up in that order. The function and operation of each part will be described; then the principles of its design, and its relation to previous magnetron development will be indicated.

1.4 *Electron Motions in Electric and Magnetic Fields—The DC Magnetron:* Before beginning the discussion of the electronics of the magnetron oscillator, it would be well to review briefly electron motions in various types and combinations of electric and magnetic fields, and the operation of the DC magnetron.[1]

An electron, of charge e and mass m, moving in an electric field of strength E, is acted upon by a force, independent of the electron's velocity, of strength eE, directed oppositely to the conventional direction of the field. If the field is constant and uniform, the motion of the electron is identical to that of a body moving in a uniform gravitational field.

An electron moving in a magnetic field of strength B, however, is acted upon by a force which depends on the magnitude of the electron's velocity, v, on the strength of the field, and on how the direction of motion is oriented with respect to the direction of the field. The force is directed normal to the plane of the velocity and magnetic field vectors and is of magnitude proportional to the velocity, the magnetic field, and the sine of the angle, θ, between them. Thus the force is the cross or vector product of $\vec{v}$ and $\vec{B}$,

$$\vec{F} = e[\vec{v} \times \vec{B}], \qquad F = Bev \sin \theta.$$

An electron moving parallel to a magnetic field ($\sin \theta = 0$) feels no force. One moving perpendicular to a uniform magnetic field ($\sin \theta = 1$) is con-

[1] The cylindrical DC magnetron was reported by A. W. Hull, Phys. Rev. 18, 31 (1921).

strained to move in a circle by the magnetic force at right angles to its path. Since this force is balanced by the centrifugal force, the radius, ρ, of the circular path depends on the electron's momentum and the strength of the field; that is,

$$Bev = \frac{mv^2}{\rho},$$

yielding

$$\rho = \frac{mv}{eB}. \tag{1}$$

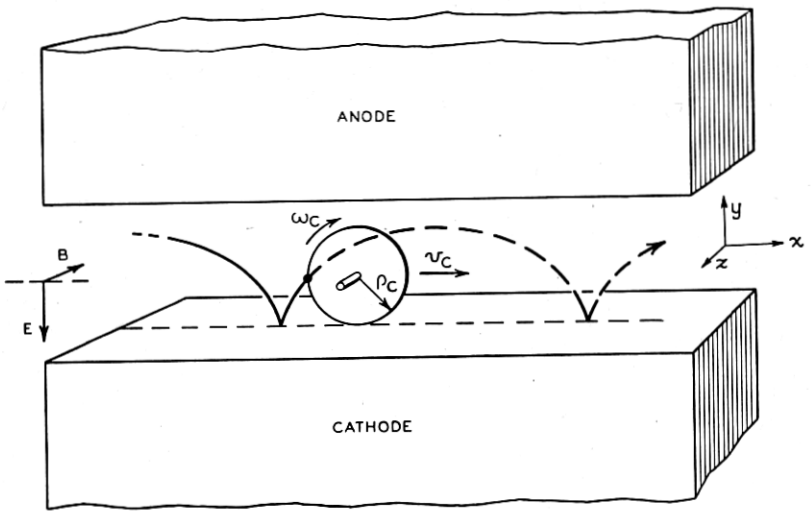

Fig. 3.—The cycloidal path of an electron which started from rest at the cathode in crossed electric and magnetic fields for the case of parallel plane electrodes. The mechanism of generation of the orbit by a point on the periphery of a rolling circle is depicted.

The time, T_c, required to traverse the circle is independent of the radius and hence of the velocity of the electron; $T_c = 2\pi\rho/v = 2\pi m/eB$. Thus, the angular frequency of traversing the circular path, the so-called cyclotron frequency, depends on the magnetic field alone and is given by,

$$\omega_c = 2\pi f_c = 2\pi\frac{1}{T_c} = \frac{e}{m}B. \tag{2}$$

In the magnetron, electron motion in crossed electric and magnetic fields is involved. Consider first such motion between two parallel plane electrodes, neglecting space charge. If, as in Fig. 3, the electric field is directed in the negative y direction and the magnetic field in the negative z direction, the equations of motion of the electron are:

$$\left.\begin{aligned} \frac{d^2x}{dt^2} &= \frac{eB}{m}\frac{dy}{dt}, \\ \frac{d^2y}{dt^2} &= \frac{e}{m}\left(E - B\frac{dx}{dt}\right), \\ \frac{d^2z}{dt^2} &= 0. \end{aligned}\right\} \tag{3}$$

The particular case of most interest here is that for which the electron starts from rest at the origin. The equations of motion then yield a cycloidal orbit given by the parametric equations:

$$\left.\begin{aligned} x &= v_c t - \rho_c \sin \omega_c t = \rho_c(\omega_c t - \sin \omega_c t), \\ y &= \rho_c(1 - \cos \omega_c t), \end{aligned}\right\} \tag{4}$$

in which:

$$v_c = \frac{E}{B}, \tag{5}$$

$$\rho_c = \frac{m}{e}\frac{E}{B^2}, \tag{6}$$

$$\omega_c = \frac{e}{m}B. \tag{7}$$

This motion may be regarded as a combination of rectilinear motion of velocity v_c in the direction of the x axis, perpendicular to both E and B, and of motion in the xy plane about a circular path of radius ρ_c, at an angular frequency ω_c, the cyclotron frequency. Fig. 3 shows the resulting cycloidal path and its generation by a point on the periphery of the rolling circle. In the case of cylindrical geometry, it is often convenient to think in terms of the plane case.

In the case of cylindrical geometry with radial electric and axial magnetic fields, the electron orbit, neglecting space charge, approximates an epicycloid generated by rolling a circle around on the cylindrical cathode. The orbit is not exactly an epicycloid because the radial motion is not simple harmonic, which state of affairs arises from the variation of the DC electric field with radius. The approximation of the epicycloid to the actual path is a convenient one, however, because the radius of the rolling circle, its angular frequency of rotation, and the velocity of its center, for the epicycloid, all approximate those for the cycloid of the plane case. These approximations improve with increasing ratio of cathode to anode radii. Several electron orbits in a DC cylindrical magnetron are shown in Fig. 4 for several magnetic fields.

It is clear from this simplified picture of the orbits in a DC cylindrical magnetron without space charge, that, at a given electric field, an electron orbit for a sufficiently strong magnetic field may miss the anode completely and return to the cathode. The critical magnetic field at which this is just possible is called the cut-off value, B_c. For a given voltage between cathode and anode, as the magnetic field is increased, the current normally passed by the device falls rather abruptly at B_c. A current versus magnetic field curve, together with electron orbits corresponding to four regions of the

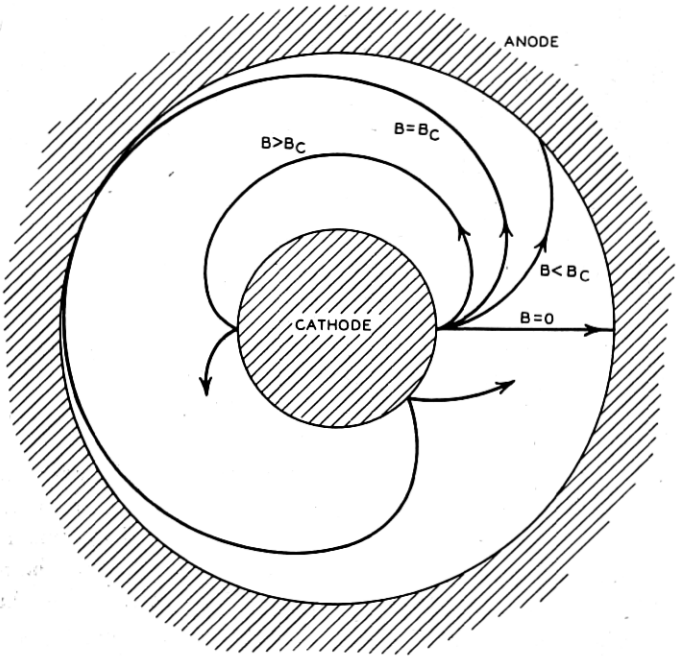

Fig. 4.—Electron paths in a cylindrical DC magnetron at several magnetic fields above and below the cut-off value, B_c. The electrons are assumed to be emitted from the cathode with zero initial velocity.

curve, are shown in Fig. 5. For the case of parallel plane electrodes, the cut-off relation between the critical anode potential, V_c, and magnetic field, B_c, and the electrode separation, d, for the parallel plane case, is obtained by equating the electrode separation to the diameter of the rolling circle. Thus,

$$d = 2\,\frac{m}{e}\left(\frac{V_c}{d}\right)\frac{1}{B_c^2},$$

from which

$$V_c = \frac{eB_c^2 d^2}{2m}.$$

For the cylindrical case, the relation may be shown to be

$$V_c = \frac{eB_c^2 r_a^2}{8m}\left[1 - \left(\frac{r_c}{r_a}\right)^2\right]^2, \tag{8}$$

in terms of cathode and anode radii, r_c and r_a.

2. Types of Magnetron Oscillators

2.1 *Definitions:* The DC magnetron may be converted into an oscillator, suitable for the generation of centimeter waves, by introducing RF fields into the anode-cathode region. This may be done by applying between anode

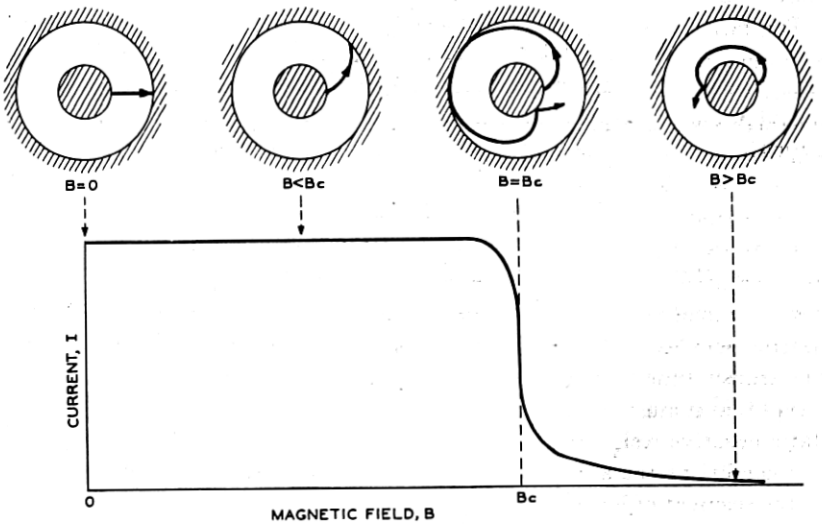

Fig. 5.—Variation of current passed by a cylindrical DC magnetron at constant voltage, plotted as a function of magnetic field. The orbits of electrons occurring at four different magnetic fields are shown above the corresponding regions of the current characteristic.

and cathode RF voltage from a resonant circuit, in which case the electrons interact with the superposed radial RF field. Or, it may be done by splitting the magnetron anode into two or more segments between which the RF voltage is applied. Then the electrons interact with the fringing RF fields existing between the segments. The problem of understanding the electronics of the multicavity magnetron oscillator is that of understanding how an electron, subject to the constraints placed upon its motion by the DC axial magnetic and DC radial electric fields, can move so as to interact favorably with the RF field; how an electron interacting unfavorably is rejected; and why, on the average, the electrons transfer more energy to the RF field than they take from it.

On the basis of the nature of the electronic mechanism by means of which energy is transferred to the RF field, it is now convenient to distinguish three types of magnetron oscillators.[2] The *negative resistance magnetron oscillator* depends on the existence of a static negative resistance characteristic between the two halves of a split anode.[3] The *cyclotron frequency magnetron oscillator* operates by virtue of resonance between the period of RF oscillation and the period of the cycloidal motion of the electrons (rolling circle or cyclotron frequency).[4] The *traveling wave magnetron oscillator* depends upon resonance, that is, approximate equality, between the mean translational velocity of the electrons and the velocity of a traveling wave component of the RF interaction field.[5]

The magnetron oscillator with which this paper is primarily concerned is of the traveling wave type. The other magnetron types are discussed briefly for the sake of completeness and because an understanding of them enhances one's grasp of the entire subject and places the traveling wave magnetron oscillator in its proper historical perspective.

2.2 *The Negative Resistance Magnetron Oscillator—Type I:* In the negative resistance magnetron oscillator,[6] the anode is split parallel to the axis into two halves, between which the RF circuit is attached. The electrons emitted by the cathode must move under the combined action of the DC radial electric and DC axial magnetic fields together with the RF electric field existing between the two semicylinders forming the anode. The transit time from cathode to anode is not involved in the mechanism except that it must be small relative to the period of the RF oscillation. The static negative resistance characteristic arises from the fact that under certain conditions the allowable orbits for the majority of electrons terminate on the segment of lower potential, irrespective of the segment toward which they start. These electrons, being driven against the RF component of the field, give energy gained from the DC field to the RF field.

In Fig. 6 are shown the paths, plotted by Kilgore,[7] of two electrons starting initially toward opposite segments but both striking the segment of lower potential. Each path is completely traversed in a time during which

[2] The magnetron oscillator discussed by Hull, in which the magnet winding is coupled to the plate circuit, is not considered as it is essentially an audio frequency device. K. Okabe in his book, "Magnetron-Oscillations of Ultra Short Wavelengths" (Shokendo, 1937), distinguishes five types, but it is not clear just how his types C and E are to be identified.

[3] These oscillations have been called Habann, quasi-stationary, or dynatron oscillations, and correspond to Okabe's type D.

[4] These oscillations have been called electronic oscillations by Megaw, transit time oscillations of the first order by Herriger and Hülster, and correspond to Okabe's type A.

[5] These oscillations are the running wave type discussed by Posthumus, the transit time oscillations of higher order of Herriger and Hülster, and correspond to Okabe's type B.

[6] This type was disclosed by Habann, Zeit f. Hochfrequenz. 24, 115 and 135 (1924).

[7] G. R. Kilgore, Proc. I.R.E. 24, 1140 (1936).

the RF field changes little. Thus it is possible by applying DC potential differences between the anode segments to measure a negative resistance between them. As can be seen from the orbits of Fig. 6, magnetic fields considerably above the cut-off value are used. With magnetrons of this type, power output up to 100 watts at 600 mc/s at an efficiency of 25% has been attained.[7] Oscillations of frequency as high as 1000 mc/s, (30 cm.) have been produced.[8] Because a large number of orbital loops are required, however, making $\omega \ll \frac{eB}{m}$, this type of magnetron oscillator demands the

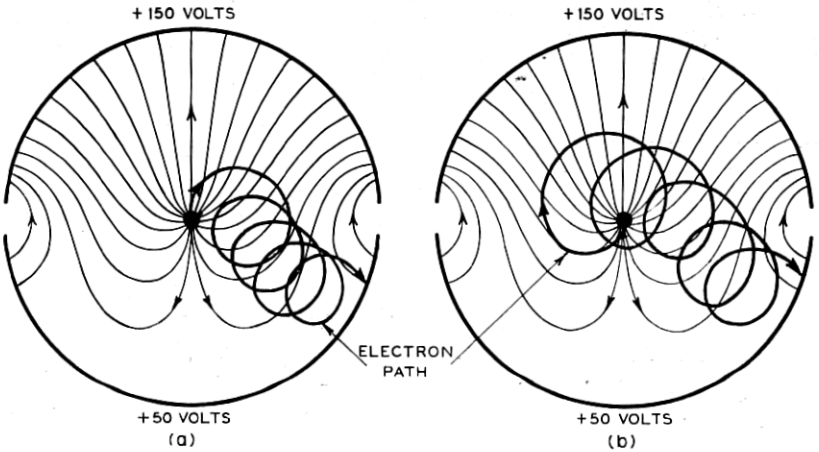

Fig. 6.—Electron paths plotted by Kilgore for the negative resistance magnetron oscillator, Type I. During the time the orbits shown are being executed, the cathode is at zero potential and the anode segments at the potentials indicated. Lines of electric force on an electron are plotted in this figure. The two orbits are those of electrons which start initially toward opposite anode segments. It should be noted that in either case the electron is driven to the segment of lower potential against the RF field component.

use of high magnetic field in the centimeter wave region and is thus less desirable than other types.

2.3 *The Cyclotron Frequency Magnetron Oscillator—Type II:* Not long after the invention of the DC magnetron, oscillations between anode and cathode were found to occur near the cut-off value of magnetic field.[9] These were found to be strongest for wavelengths obeying a relation of the form:

$$\lambda = \frac{\text{constant}}{B}. \tag{9}$$

[8] E. C. S. Megaw, Journ. I.E.E. (London) 72, 326 (1933).
[9] A. Zacek, Cos. Pro. Pest. Math. a Fys. (Prague) 53, 578 (1924). A summary appeared in Zeit. f. Hochfrequenz. 32, 172 (1928).

Later, it was shown that the oscillation period is equal to the electron transit time from the vicinity of the cathode to the vicinity of the anode and back. This made it possible to calculate a value for the constant in the above equation in good agreement with experiment.[10] The oscillation frequency is that of the rotational component of the electronic motion, that is, approximately the cyclotron frequency of equation (7).

The mechanism must be explained in terms of electrons moving in the DC radial electric and axial magnetic fields and the superposed RF radial electric field. This may be done as follows: An electron leaving the cathode in such phase as to gain energy when moving from the cathode toward the anode will also gain energy during its return, striking the cathode with more energy than it had when it left. There, such an electron is stopped from further motion during which it would continue to absorb energy from the

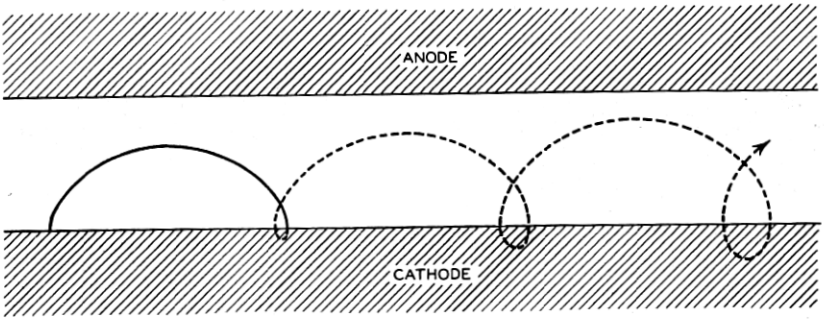

Fig. 7.—An approximate orbit of an electron which gains energy from the RF field in a cyclotron frequency or Type II magnetron oscillator, shown for the plane case. The orbit is continued as a dashed line indicating how it would be traversed were it not stopped by the cathode. The DC electric force on the electron is directed from cathode to anode.

RF field at the expense of the oscillation. The electron will execute an orbit something like that of Fig. 7 for the plane case. An electron leaving the cathode in the opposite phase, on the other hand, loses energy when moving toward the anode and again on its return toward the cathode. As is shown in Fig. 8, it reverses its direction after the first trip without reaching the cathode surface and starts over on a second loop of smaller amplitude, remaining in the same phase and continuing to lose energy to the field. This process continues until all the energy of the rotational component of the electron's motion has been absorbed by the RF field. If the electron is not removed at this stage, in its subsequent motion the rotational component will build up, extracting energy from the RF oscillation. Means such as tilting the magnetic field or placing electrodes at the ends of the tube have been used to remove the electrons from the interaction space when all the

[10] K. Okabe, Proc. I.R.E. 17, 652 (1929).

rotational energy has been absorbed. It is possible to maintain the oscillations and extract energy from them because electrons which give energy to the field can do so over many cycles, whereas electrons of opposite phase can gain energy over only one cycle before they are removed.

Magnetrons oscillating in this manner have been built with split anodes.[10,11] Here the RF field with which the electron interacts is more tangential than radial but the criterion for oscillation is the same, namely, resonance between the field variations and the rotational component of the electron's motion. Operating efficiencies of 10 to 15% have been obtained. It was with a magnetron of this type having an anode diameter of 0.38 mm. that radiation of wavelength as low as 0.64 cm. was generated.[12]

The cyclotron frequency magnetron oscillator has been almost entirely superseded by the traveling wave magnetron oscillator as a generator of

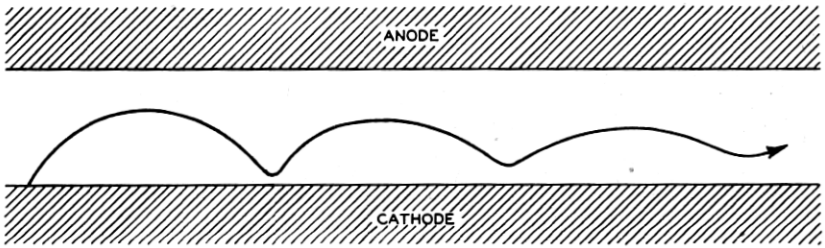

Fig. 8.—An approximate orbit of an electron which loses energy to the RF field in a cyclotron frequency or Type II magnetron oscillator, shown for the plane case. If the electron after losing all its rotational energy remains in the interaction space, it gains energy from the RF field, and its orbit builds up cycloidal scallops in a manner directly the reverse of that shown here. The DC electric force on the electron is directed from cathode to anode.

centimeter waves. In the main this is the result of the impossibility of removing electrons emitted from an extended cathode area from the interaction region at the proper stage in their orbits. This inherent drawback is not shared by the traveling wave magnetron oscillator which may be operated at higher efficiency without critical adjustment of orientation in the magnetic field or of the potential of auxiliary electrodes.

2.4 *The Traveling Wave Magnetron Oscillator—Type III:* Oscillations have been found to occur in the magnetron which are independent of any static negative resistance characteristic and which can occur at frequencies widely different from the cyclotron frequency. In 1935[13] the electronic mechanism of these oscillations was correctly interpreted as an inter-

[11] H. Yagi, Proc. I.R.E. 16, 715 (1928).
[12] C. E. Cleeton and N. H. Williams, Phys. Rev. 50, 1091 (1936).
[13] K. Posthumus, Wireless Engineer 12, 126 (1935).

action of the electrons with the tangential component of a traveling wave whose velocity is approximately equal to the mean translational velocity of the electrons. Later[14] the role of the radial component of the rotating electric field in keeping the electrons in proper phase was recognized. Magnetrons of wavelength as short as 75 cm., operating at better than 50% efficiency, were built prior to 1940, but performance such as was later to be attained with this type of magnetron at much shorter wavelengths was not attained then, perhaps primarily because of the lack of a good resonator. It was a magnetron of this type which the British brought to the United States in 1940. The British magnetron was a 10 cm. oscillator, intended for pulsed operation, having a tank circuit consisting of eight resonators built into the anode block as shown in Fig. 1.[15]

3. The Electronic Mechanism

3.1 *Electronic Interaction at Anode Gaps:* The electrons in the interaction space of the magnetron oscillator are the agents which transfer energy from the DC field to the RF field. As such, they must move subject to the constraints imposed by the DC radial electric and DC axial magnetic fields, considering, for the moment, the RF fields to be small. Under these conditions, as has been seen for the DC cylindrical magnetron (see Fig. 4 for $B > B_c$), electrons follow approximately epicycloidal paths which progress around the cathode. The mean velocity of this progression, that of the center of the rolling circle, depends upon the relative strengths of the electric and magnetic fields [see equation (5) for the plane case]. By proper choice of DC voltage, V, between cathode and anode and of magnetic field, B, the mean angular velocity of the electrons may be set at any desired value.

The RF electric fields in the interaction space, with which the electrons moving as described above must interact, are the electric fields fringing from the slots in the anode surface. These fields are provided by the N coupled oscillating cavities of which the magnetron resonator system is composed. As will be discussed in more detail later, such a system of resonators may oscillate in a number of different modes in each of which the oscillations in adjacent resonators, and thus the fields appearing across adjacent anode slots, bear a definite phase relationship. For a system of N resonators it will be seen that the phase difference between adjacent resonators may assume the values $n\frac{2\pi}{N}$ radians, n being the integers 0, 1, 2, $\cdots$, $\frac{N}{2}$.

Adopting another point of view, one may consider the potentials placed upon the anode segments by the resonators. The variation of the potential

[14] F. Herriger and F. Hülster, Zeit. f. Hochfrequenz, 49, 123 (1937).

[15] The use of such internal resonators is reported in the literature by N. T. Alekseieff and D. E. Maliaroff, Journ. of Tech. Phys. (U.S.S.R.) 10, 1297 (1940); republished in English, Proc. I.R.E. 32, 136 (1944). A. L. Samuel has obtained U. S. Patent #2,063,342 Dec. 8, 1936, for a similar device.

from one segment to the next depends upon the mode of oscillation of the system as a whole. The restriction on the phase difference stated above requires the sequence of anode segment potentials at any instant to contain

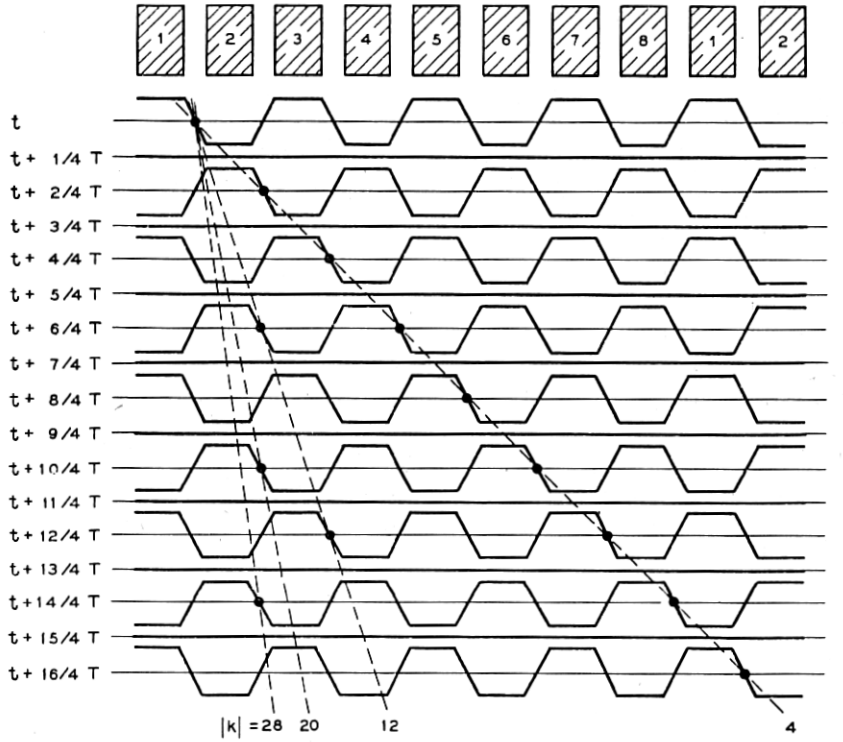

Fig. 9.—A plot showing the π mode anode potential wave at several instants in an eight resonator magnetron and the mean paths of electrons which interact favorably with the RF field. The plot is developed from the cylindrical case, the shaded rectangles at the top representing the anode segments. The anode potential variation is a standing wave, shown here for a sequence of instants one quarter period ($T/4$) apart. Note that the potential is constant across the anode surfaces and varies linearly between them. Electrons interacting favorably with the RF field cross the anode gaps when the field there is maximum retarding as indicated by the filled circles. The lines for $|k| = 4, 12, 20, 28, \cdots$ represent mean paths of electrons traveling with mean angular velocities $\frac{2\pi f}{4}, \frac{2\pi f}{12}, \frac{2\pi f}{20}, \frac{2\pi f}{28}, \cdots$ around in the interaction space. Since the field is a standing wave, it is clear that electrons possessing these velocities in either direction may interact favorably with the RF field.

n complete cycles in one traversal of the cylindrical anode, n still denoting the integers $0, 1, 2, \cdots, \frac{N}{2}$. In general, these anode potential waves may be standing waves or waves traveling around the anode structure in either direction with angular velocity $\frac{2\pi f}{n}$ radians per second, where f is the RF

frequency. For the two modes in which adjacent resonators are in phase ($n = 0$) and π radians out of phase ($n = \frac{N}{2}$, the so-called π mode), however, only standing potential waves on the anode are possible. As examples of

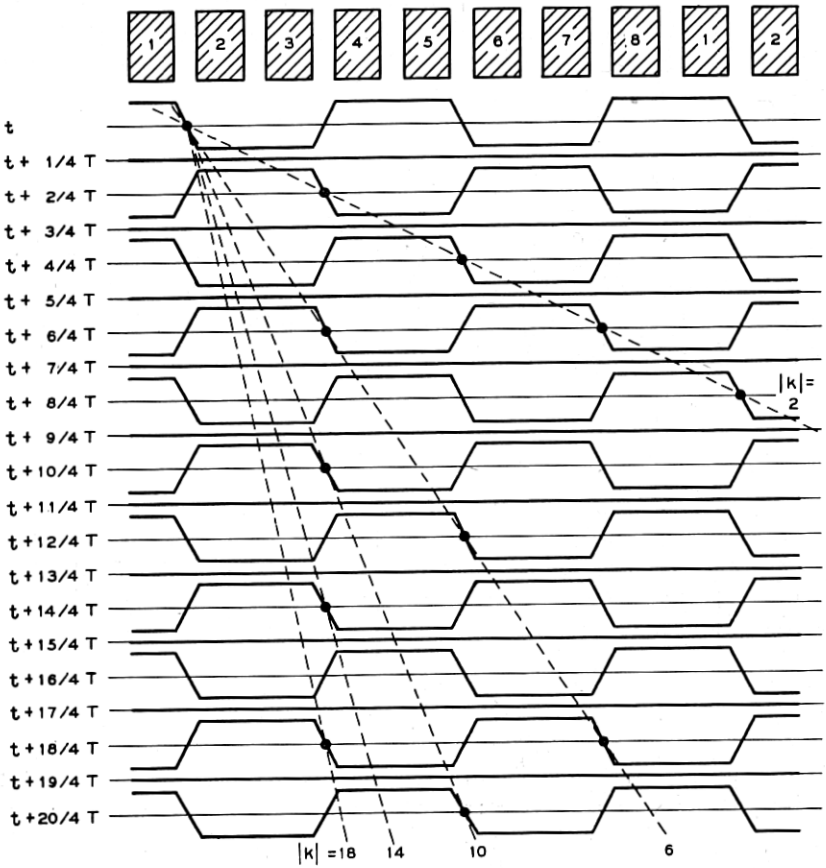

Fig. 10.—A plot similar to that of Fig. 9 for the standing wave component of anode potential of periodicity $n = 2$ in a magnetron having eight resonators. Electrons which interact favorably have mean angular velocities $\frac{2\pi f}{2}, \frac{2\pi f}{6}, \frac{2\pi f}{10}, \frac{2\pi f}{14}, \cdots$ in either direction in the interaction space.

standing and traveling anode potential waves in an anode structure having eight resonators ($N = 8$), the standing wave for $n = 4$ and standing and traveling waves for $n = 2$ are shown in Figs. 9, 10, and 11 respectively.

From what has been said about the RF field and the electronic motion in the interaction space of the magnetron oscillator of Type III, it is possible

to understand its fundamental electronic mechanism. As in any oscillator, the criterion for oscillation is that more energy shall be transferred to the RF field by electrons driven against it than is taken from the RF field by electrons accelerated by it. This can be accomplished in the traveling wave

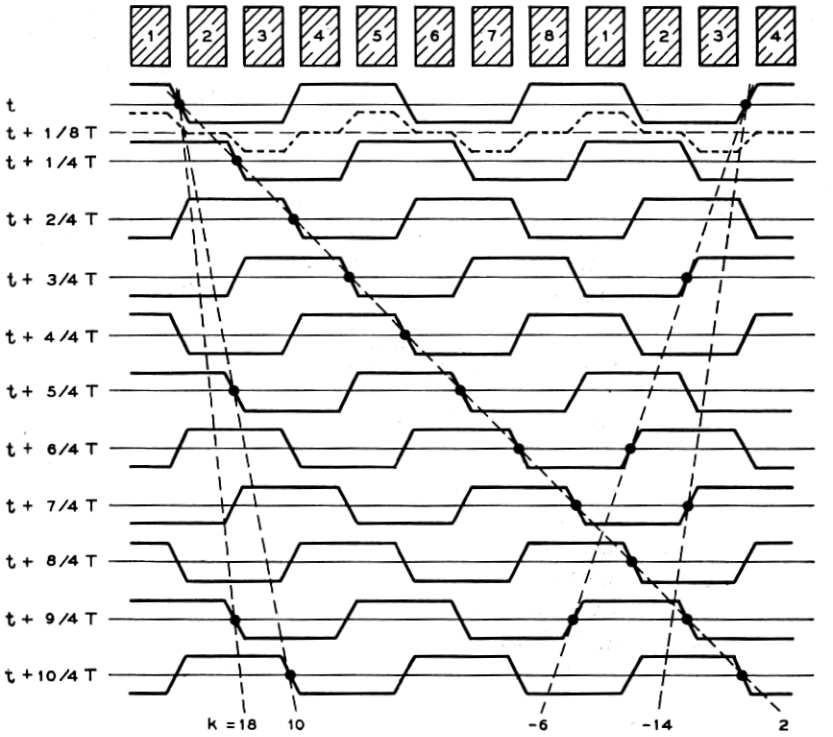

Fig. 11.—A plot similar to those of Figs. 9 and 10 for the rotating wave of anode potential of periodicity $n = 2$ in a magnetron having eight resonators [see equation (13) in the text]. The field at the instant $t + \frac{1}{8}T$ is plotted as a dashed line to show that the traveling wave does not preserve its shape at all instants. Whereas the wave travels in one direction with the angular velocity $\frac{2\pi f}{2}$, electrons which travel with velocities $\frac{2\pi f}{2}, \frac{2\pi f}{10}, \frac{2\pi f}{18}, \cdots$ in the same direction or with velocities $\frac{2\pi f}{6}, \frac{2\pi f}{14}, \cdots$ in the opposite direction interact favorably with the RF field. Directions of electron motion must now be distinguished. Electrons whose velocity is opposed to that of the rotating field are said to be driving a "reverse" mode.

magnetron oscillator only if the mean angular velocity of the electrons is such as to make them pass successive gaps in the anode at very nearly the same phase in the cycle of the RF field across the gaps. Then it is possible for an electron which leaves the cathode in such phase as to oppose the tangential component of the RF field across one anode gap, to continue to

lose energy gained from the DC field to the RF field at successive gaps. Electrons which gain energy from the RF field are driven back into the cathode after only one orbital loop and are removed from further motion detrimental to the oscillation. This process of selection and rejection of electrons forms the groups of bunches, shown in Fig. 2(c), which sweep past the anode slots in phase to be retarded by the RF field component. The criterion that the electron drift velocity shall be such as to keep these bunches in proper phase is analogous to the condition that the drift angle in a velocity variation oscillator [Fig. 2(b)] be such as to cause the bunches to cross the gap of the second or "catcher" cavity in phase to lose energy to the RF field across the gap.

The condition placed upon the mean angular velocity of the electrons may be discussed more readily by reference to Figs. 9, 10, and 11. Consider first, however, only Fig. 9 for the standing potential wave of the $n = 4$ mode, and focus attention on an electron which crosses the gap between anode segments 1 and 2 at the instant t when the RF field is maximum retarding, that is, the potential on segment 1 is maximum and on segment 2 minimum. It is clear that this electron can cross the next gap in the same phase if the time required to reach it is $(|p| + \frac{1}{2})\ T$, in which p is any integer and T is the period of RF oscillation. In Fig. 9, four lines are drawn representing the mean paths of electrons moving with such velocities as to make $p = 0, 1, 2,$ and 3. Each line crosses a gap when the RF field is maximum retarding, that is, when the potential has the maximum negative slope at the center of the gap. As will be seen later, a more convenient parameter, to be called k, is that whose absolute magnitude, $|k|$, specifies the number of RF cycles required for the electron to move once around the interaction space. $\frac{|k|}{N}$ is then the number of cycles between crossings of successive anode gaps, which for the π mode of Fig. 9 must take on the values:

$$\frac{|k|}{N} = |p| + \frac{1}{2}, \qquad p = 0, \pm 1, \pm 2, \cdots,$$

or the values given by the more general expression, applicable to any mode:

$$\frac{|k|}{N} = |p| + \frac{n}{N}, \qquad p = 0, \pm 1, \pm 2, \cdots.$$

In this expression, $\frac{n}{N}$ is the phase difference between adjacent resonators, expressed as a fraction of a cycle. k may thus assume the values given by

$$\left.\begin{aligned} k &= n + pN, \\ p &= 0, \pm 1, \pm 2, \cdots. \end{aligned}\right\} \quad (10)$$

The mean angular velocity which the electrons must possess is then given by

$$\frac{d\theta}{dt} = \frac{2\pi}{kT} = \frac{2\pi f}{k}, \tag{11}$$

in which θ is the azimuthal angle.

For the π mode ($n = \frac{N}{2}$) it is seen that the negative integers, p, give the same series of values for $|k|$ as do the positive integers including zero. The sequence is $|k| = 4, 12, 20, 28, \cdots$. Reference to Fig. 9 indicates that electrons may travel in either direction around the interaction space and interact favorably with the RF field, provided their mean angular velocity is given by equation (11) with values of k specified by equation (10). That this should be so is clear from the fact that the anode potential wave is a standing wave with respect to which direction has no meaning. Fig. 9 also makes clear how an electron moving with velocity different from that corresponding to the lines shown, will fall out of step with the field, and on the average be accelerated as much as it is retarded, thus effecting no net energy transfer.

In Figs. 10 and 11, diagrams for the $n = 2$ mode similar to that of Fig. 9 for the π mode are shown. Fig. 10 is for electronic interaction with a standing wave of periodicity $n = 2$ and Fig. 11 for a traveling wave of the same periodicity. Again, as in the case of the π mode, the values of k for favorable electronic interaction are given by equation (10).

The sequence of positive integral values of p (including zero) and the sequence of negative integral values of p do not each give the same sequence of values for $|k|$ as was the case for the π mode. For $p \geqq 0$, $|k| = 2, 10, 18, \cdots$, and for $p < 0$, $|k| = 6, 14, 22, \cdots$. For the standing potential wave (Fig. 10) each of these values of $|k|$ does specify the velocity of possible electron motion in *either* direction for favorable interaction with the field. For the traveling potential wave (Fig. 11), on the other hand, only the positive values of k ($p \geqq 0$) correspond to electron motion in the same direction as the traveling wave, the negative values of k ($p < 0$) corresponding to electron motion in the direction opposite to the traveling wave. The sign of k has significance. If the electrons are moving with velocities specified by equation (11) with the negative values of k from equation (10), and are thus moving counter to the traveling RF field wave, the electrons are said to be driving a "reverse" mode.

The actual electron orbits do not correspond to simple translation but, as has been discussed, to rotation superposed on translation. The epicycloid-like scallops in the orbit are of no significance to the fundamental electronic mechanism. It is the mean velocity of the electron motion around the interaction space, specified by the relative values of V and B, that is of importance. The magnetron may operate, for example, at such

high magnetic field, provided V has the proper value, that the scallops became relatively small variations in an otherwise smooth orbit (see Fig. 18).

In the cylindrical magnetron, the radial variation of the DC electric field, resulting in a decrease in the mean angular velocity of the electrons as they approach the anode, would make it impossible for an electron to keep step with the fields across the anode gaps were not a mechanism of phase focusing operative. That such focusing is inherent in the interaction of electrons and fields will be seen later.

3.2 *The Interaction Field:* The electronic mechanism which has been discussed in terms of electron motions through the fields at the gaps in the multisegment anode, may also be discussed in terms of the traveling waves of which the RF interaction field may be considered to be composed. The RF interaction field corresponds to anode potential waves like those plotted in Figs. 9, 10, and 11. The interaction fields for the several modes of oscillation of the resonator system are thus to be distinguished by the number, n, of repeats of the field pattern around the interaction space. Since the potential at the anode radius is nearly constant across the faces of the anode segments and varies primarily across the slots, the azimuthal variation of the field cannot be purely sinusoidal but must involve higher order harmonics.

For a mode of angular frequency $\omega = 2\pi f$, corresponding to a phase difference between adjacent resonators of $n\frac{2\pi}{N}$, the anode potential wave is of periodicity n around the anode and may be written as a Fourier series of component waves traveling in opposite directions around the interaction space:

$$V_{RF} = \sum_k A_k e^{j(\omega t - k\theta + \gamma)} + \sum_k B_k e^{j(\omega t + k\theta + \delta)}, \qquad k = n + pN, \quad p = 0, \pm 1, \pm 2, \cdots. \tag{12}$$

Note that the summations are taken over all integral values of k given by equation (10).

The interaction field for any mode of periodicity n is thus represented by two oppositely traveling waves, whose fundamentals are moving with angular velocities $\frac{\omega}{n} = \frac{2\pi f}{n}$, and whose component amplitudes, A_k and B_k, in general are not equal. γ and δ are arbitrary phase constants. The expression (12) may be reduced to the form:

$$V_{RF} = \sum_k (A_k - B_k) \cos(\omega t - k\theta + \gamma) + \sum_k 2B_k \cos\left(\omega t + \frac{\gamma + \delta}{2}\right) \cos\left(k\theta - \frac{\gamma - \delta}{2}\right), \qquad k = n + pN, \quad p = 0, \pm 1, \pm 2, \cdots, \tag{13}$$

which shows that the complete field pattern may be considered to consist of a rotating wave superposed on a standing wave, each having a fundamental component of periodicity n.

The fact that the periodicities, k, of the harmonics in the expressions (12) or (13) are those for which k has the values given by (10) may be determined from a Fourier analysis of the complete anode potential waves like those of Figs. 9, 10, and 11. Only those harmonics which specify the same pattern of potentials at the centers of the anode segments as the fundamental are admitted in the analysis.

As has been mentioned before, the complete field patterns for $n = 0$ and $n = \frac{N}{2}$ are standing waves. Thus for these modes of oscillation $A_k = B_k$ in the expressions (12) and (13). For the other modes, $n = 1, 2, 3, \cdots, \frac{N}{2} - 1$, the electrons may interact with the traveling field component of expression (13) or with the standing field components which, in case $A_k = B_k$, is the only component present (see Figs. 10 and 11 for the case $n = 2$, $N = 8$).

The terms in expressions (12) and (13) for which $| k | = n$ are the fundamental components; those for which $| k | \neq n$ are called the Hartree harmonics. The components of field strength corresponding to these harmonics in the interaction field pattern fall off in intensity from anode to cathode more rapidly the higher the value of k. The variation with radius is of the form $\left(\frac{r}{r_a}\right)^k$. Thus the farther from the anode one samples the field, the more like the fundamental sinusoidal pattern it appears.

For each value of k in expression (12), whether or not $A_k = B_k$, there are two oppositely traveling sinusoidal wave components of periodicity k. Since each requires k cycles of the RF oscillation to complete one trip around the interaction space, the linear velocity at the anode surface is $\frac{2\pi f r_a}{k}$ corresponding to an angular velocity of $\frac{2\pi f}{k}$. Thus, as seen in Fig. 11 for the instant $t + T/8$, the change of shape of the total traveling wave indicates that the components of which it is composed travel with different velocities. In Fig. 23 are shown instantaneous RF interaction field patterns for the fundamental components ($p = 0$) of the $n = 1, 2, 3$, and 4 modes of an anode block having eight resonators.

3.3 *The Traveling Wave Picture:* It is instructive to discuss the operation of the Type III magnetron oscillator in terms of electron interaction with the traveling wave components present in the interaction field. This might at first appear to be difficult in view of the many components of several possible modes. By mode frequency separation, as discussed later, it is

generally possible, however, to restrict oscillation to only one mode, usually the π mode. Further, the fact that the electronic motion in crossed DC electric and magnetic fields results in a mean drift of electrons around the interaction space, enables one to restrict his attention to a single traveling wave corresponding to the fundamental or a single Hartree harmonic of the field of this mode; for it is possible, in principle at least, by proper adjustment of V and B to equate the mean angular velocity of the electrons to the angular velocity, $\frac{2\pi f}{|k|}$, of *any* one of the traveling field components. When this is true, only the field of this component has an appreciable effect upon the electron's motion. With respect to the fields of the oppositely traveling component of the same harmonic (same k), and the components of all other harmonics (different k), the electron finds itself drifting rapidly through regions of accelerating and decelerating field with no net energy transfer. From the point of view of the electron, the fields of the other components vary so rapidly as to average out over any appreciable interval of time. The only exception to these statements occurs when a harmonic of periodicity k' of another mode of frequency f' has the same angular velocity as the harmonic of periodicity k, that is, when $\frac{2\pi f'}{|k'|} = \frac{2\pi f}{|k|}$. The effect on magnetron operation of this coincidence of angular velocities will be discussed further in a later section. In the calculation of electron motions, the restriction to the field of a single traveling wave component has been called the rotating field approximation.

The consideration of the electronic mechanism has thus been reduced to that of the motion of electrons under the combined influence of the radial DC electric field, the axial DC magnetic field, and a sinusoidal field wave traveling around the interaction space. From what has been said thus far it is clear that for energy to be transferred to the RF field it is necessary that the mean electron velocity very nearly equal that of the traveling wave. Then an electron leaving the cathode in such phase as to find itself moving in a region of decelerating tangential component of the RF field, may continue to move with this region and lose energy to the field. In contrast to the Type II magnetron oscillator, the energy transferred to the RF field in this case is the potential energy of the electron in the radial DC electric field. The energy in the rotational component of the motion remains practically unaffected and the electron orbit from cathode to anode looks something like that plotted in Fig. 12 for the case with plane electrodes. On the other hand, an electron which leaves the cathode in such phase as to gain energy in a region of accelerating tangential RF field, is removed at the cathode after only one cycle of the epicycloid-like motion. If this did not occur, the electron would continue to move with the field and absorb energy. An approxi-

mate orbit is shown in Fig. 13. It is instructive to compare the orbits of the two categories of electrons in the traveling wave magnetron oscillator with the orbits of corresponding electrons in the cyclotron frequency type of magnetron oscillator (Figs. 7 and 8). In each case, it is the fact that "favorable" electrons may interact for a considerably longer time than "unfa-

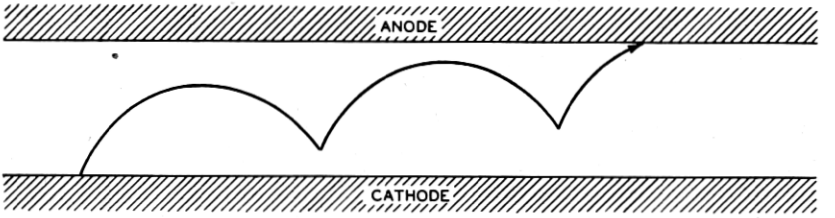

Fig. 12.—An approximate orbit of an electron which is losing energy to the RF field in a traveling wave or Type III magnetron oscillator, shown for the plane case. Here the energy loss is potential energy of the electron in the DC field. Compare this with the orbit in Fig. 8 where the energy loss is rotational energy of the electron. The DC electric force on the electron is directed from cathode to anode.

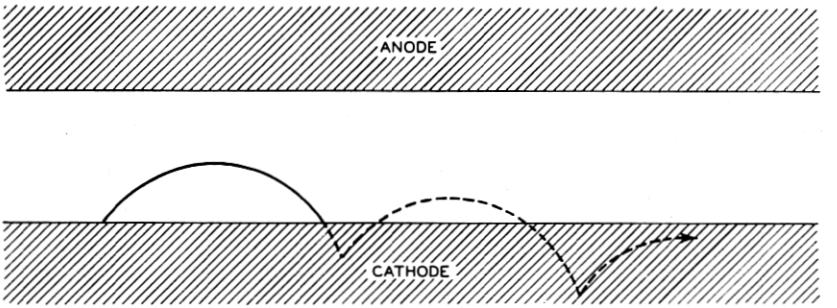

Fig. 13.—An approximate orbit of an electron which gains energy from the RF field in a traveling wave or Type III magnetron oscillator, shown for the plane case. The orbit is extended as a dashed line as though the cathode were not there. The energy gained is potential energy of the electron in the DC field. Compare this with the orbit in Fig. 7 where the energy increase is in the rotational energy of the electron. The DC electric force on the electron is directed from cathode to anode.

vorable" electrons which makes possible a net energy transfer between the DC and RF fields.

One may now compare the traveling wave picture of the electronic mechanism with that presented earlier in which the motion of electrons past the gaps in the anode structure is considered. An electron moving so that $\frac{|k|}{N} = |p| + \frac{n}{N}$ cycles of the RF oscillation elapses between its crossing of two successive anode gaps, is thus moving around the interaction space in synchronism with a traveling component of the *kth* harmonic of the inter-

action field. Both points of view are of value. That involving the motion of electrons past the anode gaps is more fundamental physically. That in terms of a traveling wave component, on the other hand, is more convenient in calculations of electron orbits including space charge effects, where by transformation to a coordinate system rotating with the field it is possible to treat of motions in static fields.

3.4 *Phase Focusing:* It has been seen from two points of view how groups of electrons which move around the interaction space of the magnetron oscillator are formed by a process of selection and rejection of electrons by the tangential component of the RF field. However, space charge debunching and the discrepancy at all but one radius between the mean velocity of translation of the electrons and the velocity of the interaction field would tend to disperse these groups and prevent efficient interaction, were it not for the phase focusing provided by the radial component of the RF field.

The mechanism of the phase focusing may be discussed either in terms of the interaction of electrons with the actual fields existing at the anode gaps or in terms of the traveling wave picture of the electronic mechanism. The fundamental mechanism involved depends upon the effect of the radial component of the RF field in aiding or opposing the radial DC field in determining the mean drift velocity of the electron around the interaction space. If the radial RF field increases the net radial field in which the electron finds itself at any instant, the mean velocity of the electron increases as can be seen from equation (5) for the plane case. Similarly, a decrease in the net radial electric field, caused by the RF radial component, results in decreased electron translation velocity. These changes in the electron's velocity operate so as to keep the electron near the position in which it can interact most favorably with the tangential component of the RF field.

Consider an electron which crosses an anode gap at the instant the RF field there is maximum retarding, that is, an electron which is to be found on the plane marked M in Fig. 14 at this instant. It experiences about as great an increase of velocity by virtue of the radial component aiding the DC radial field before crossing the gap as decrease by virtue of the radial component opposing the DC radial field after crossing the gap. Another electron which is lagging behind the electron just considered is to be found opposite a positively charged anode segment, as at P in Fig. 14, when the RF field passes through its maximum value. Since the RF field component decreases with time after this instant, the effect of the radial component of the field on the electron's velocity after crossing the gap will be less than its effect before crossing the gap, the net effect being one of increasing the mean velocity of translation, bringing the electron more nearly into the proper phase. An electron which leads the electron first considered, on the other

hand, will be found opposite the negatively charged anode segment beyond the gap when the RF field is maximum, and for it the net effect of the radial component is to reduce the mean velocity of the electron, bringing it also more nearly into the proper phase.

In discussing the mechanism of phase focusing from the traveling wave point of view, the field lines of Fig. 14 may be considered to be those of the traveling wave component with which the electrons are interacting. Then the whole field pattern indicated moves to the right as shown by the arrow above the plane of maximum retarding tangential field at M. An electron

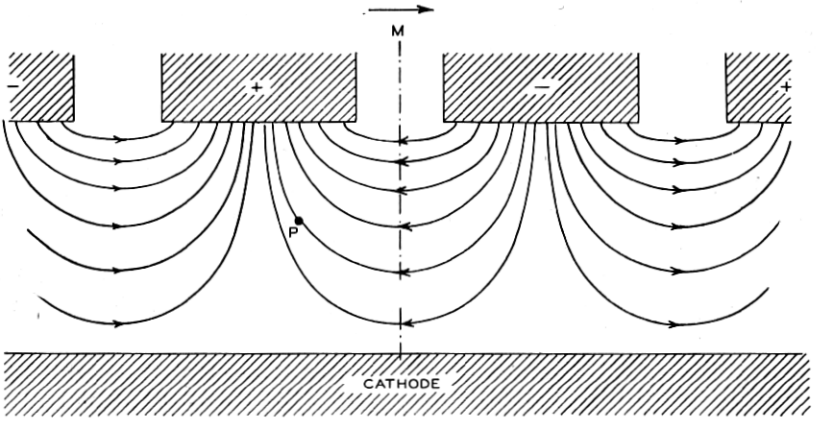

Fig. 14.—A plot of lines of electric force on an electron (drawn for the plane case) for the fundamental of the π mode. It is shown for the purpose of explaining the phase focusing property of the radial field component. The plane of maximum opposing force on the electron intersects that of the figure along the line M. The arrow shown above the line M indicates the direction of electron motion. The force on the electron due to the DC electric field is directed from cathode to anode. The force lines shown may be considered to be those of the total fundamental field component at the instant the field is maximum. Then an electron at the point P will cross the center of the anode gap after the instant of maximum retarding force. Or the lines shown may be considered to be those of the traveling component of the fundamental moving in the same direction as the electrons. In this case an electron at the point P is lagging behind the maximum of the retarding tangential field.

which falls behind the position M to the point P, for example, finds itself in a stronger net radial electric field which increases its mean translational velocity tending to bring it back to the position M. The reverse holds for an electron which runs ahead of the plane M.

3.5 *Space Charge Configuration:* The over-all picture of the electronic mechanism in the Type III magnetron oscillator thus presents a spoke-shaped space charge cloud of electrons wheeling around the cathode in synchronism with the anode potential wave, each spoke in a region of maximum retarding field. This picture of what is happening has been very handsomely confirmed by actual orbital calculations taking account of

space charge. The calculations have been carried out by the so-called self consistent field method using the rotating field approximation mentioned earlier. In this method, orbits of electrons are calculated in an assumed field, and the space charge due to these electrons determined. The field calculated on the basis of this space charge distribution may then be compared with that assumed. This cycle of calculations is repeated, each time using the calculated field of the previous cycle as that in which the electrons move, until a field is obtained which is consistent with that used in calculating the electron orbits. This method will be recognized as that used in the calculation of electron orbits about the nucleus in atoms.

The result of one such calculation is shown in Fig. 15. The orbits of four electrons which were emitted from the cathode in different phases are plotted in a set of coordinates rotating with the RF field component. One electron is returned to the cathode, and the other three reach the anode. The boundaries of the space charge cloud are shown as dashed lines. The spoke-shaped structure is clear, and its position with respect to the rotating anode potential wave is as expected. The number of spokes of the cloud is equal to the periodicity of the component of the mode with which the electrons are interacting. In the case of Fig. 15 there are four spokes, since the magnetron is operating in the fundamental of the $n = 4$ mode ($k = 4$, $p = 0$).

3.6 *Induction by the Space Charge Cloud:* Another view of the mechanism by which the electrons drive the resonator system may be obtained by considering the effect of the space charge spokes in inducing current flow in the anode segments themselves. For example, the oscillation of the resonator block in its π mode corresponds to the periodic interchange of electric charge from each anode segment, around a resonating cavity to the next anode segment. This oscillation is maintained, much in the manner of a pendulum escapement drive, by the space charge spoke appearing in front of an anode segment at that instant in the oscillation cycle when it can aid in building up the net positive charge on the segment. At the same instant, the adjacent segments, being opposite a "gap" in the space charge wheel, may build up a negative charge.

The RF current, I_{RF}, induced in the anode structure, thus results from the motion of the spoke-shaped space charge cloud in the interaction space. It is not to be confused with the total circulating RF current in the resonator system. Whereas I_{RF} must be in a phase with the space charge cloud it need not be in phase with the RF voltage, V_{RF}, between the anode segments. In terms of the electron motions, this means that the spokes of the space charge cloud may lead or lag the maxima in the tangential field. In general, the electronic admittance defined by the ratio of I_{RF} to V_{RF} may thus include a susceptance as well as a conductance. The product of V_{RF} and the in-phase component of I_{RF}, integrated over a period of one cycle of RF

oscillation, equals the energy per cycle which is delivered to the load. This amount of energy is twice that transferred in the half cycle during which the spokes of space charge move against the field from positions in front of one

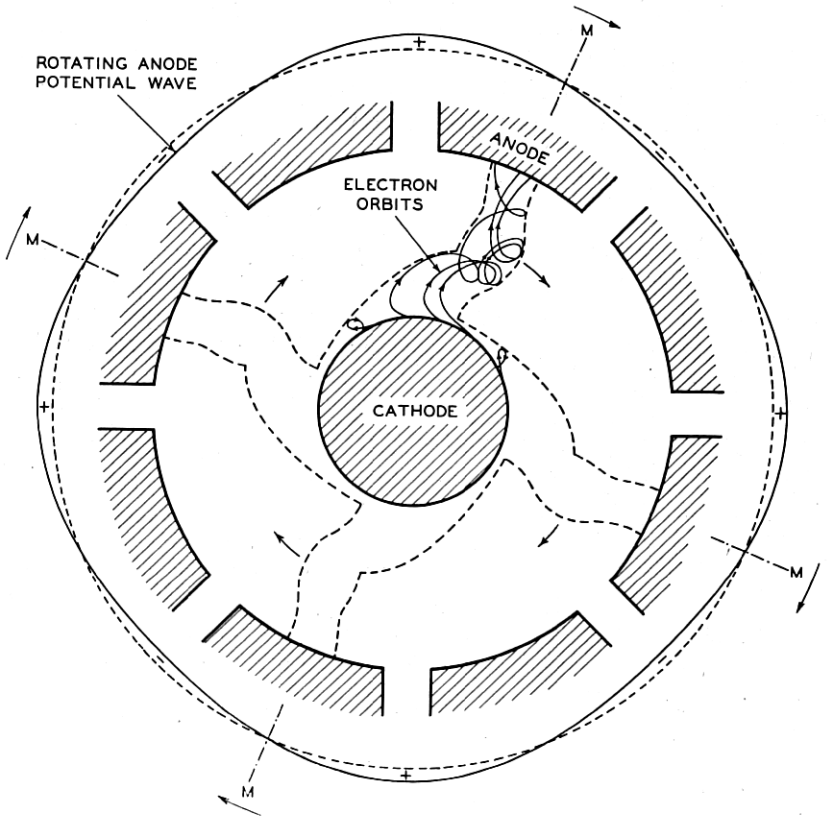

Fig. 15.—The orbits of four electrons which left the cathode in different phases, plotted in a coordinate system rotating with the anode potential wave. These orbits have been calculated by the self consistent field method which includes space charge effects. In this frame of reference the orbits exhibit loops whereas in a stationary frame they would more nearly exhibit cusps. The dashed lines inclose the orbits of the electrons and hence delineate the boundaries of the space charge cloud which rotates around the cathode in synchronism with the anode potential wave. Planes of maximum retarding tangential field are represented by the lines M (see Fig. 14). This figure is reproduced by courtesy of the British Committee on Valve Development (CVD) and is taken from the CVD Magnetron Report No. 41.

set of alternate anode segments to similar positions in front of the adjacent anode segments.

In each spoke of the electron space charge cloud, individual electrons progress from cathode to anode. The DC current, I, passed by the magnetron is made up of electrons which strike the anode from the ends of the space charge spokes. Quite apart from its dependence on other parameters,

this DC current is directly proportional to anode length, h. If the magnetron is driven at greater DC current, the space charge in the interaction space increases but the phase of its structure with respect to the traveling anode wave does not change to a first approximation. Thus both the in-phase and quadrature components of I_{RF} increase with no change in electronic admittance. The second order effects which do arise from small shifts in the phase of the rotating space charge structure are discussed in Section 10.4 *Electronic Effects on Frequency.*

4. Conditions Relating Measurable Parameters

4.1 *Necessary Conditions for Oscillation:* After having discussed the electron motions in the interaction space of the Type III magnetron oscillator, the viewpoint will now be changed to that looking from the outside in, so to speak, and it will be asked what conditions relating measurable parameters are imposed by the nature of the electronic mechanism. Beyond the geometrical parameters of cathode and anode radii, r_c and r_a, one can determine the DC voltage, V, applied between cathode and anode; the magnetic field B, in which the magnetron is placed; the DC current, I, drawn by the anode; the frequency of oscillation, f; and, from impedance measurements, the RF load, $Y_s = G_s + jB_s$, presented to the electrons by the resonator, output, and load.

Perhaps the most fundamental condition for oscillation of the traveling wave magnetron is that imposed by the requirement of synchronism between the electron drift and the RF field. As has been indicated, the angular velocity of a rotating component of a Hartree harmonic of the interaction field, of order k, is $\frac{2\pi f}{|k|}$. An approximate expression for the mean angular velocity of the electrons may be determined by neglecting the variation of electric field with radius and calculating the angular velocity midway between cathode and anode, thus:

$$\frac{v}{(r_a + r_c)/2} = \frac{E/B}{(r_a + r_c)/2} = \frac{V/(r_a - r_c)B}{(r_a + r_c)/2} = \frac{2V}{(r_a^2 - r_c^2)B}.$$

Equating this to the angular velocity $\frac{2\pi f}{|k|}$, one obtains the relation:

$$V = \frac{\pi f}{|k|} r_a^2 B \left[1 - \left(\frac{r_c}{r_a}\right)^2\right]. \tag{14}$$

In this derivation it should be recognized that the angular velocity $\frac{2\pi f}{|k|}$ may be considered either to be that of a traveling component of the RF field with which the electron interacts or the mean angular velocity which the

electron must have to maintain proper phase with the total RF fields existing across the anode gaps.

Posthumus[13] derived an expression, assuming negligible cathode diameter, which is similar to equation (14). By the same method as that used above, Slater has derived an expression differing from (14) by a term which results from the use of a more accurate value for the electron's translational velocity at the midpoint between cathode and anode in cylindrical geometry. Slater's expression is:

$$V = \frac{\pi f}{|k|} r_a^2 B \left[1 - \left(\frac{r_c}{r_a}\right)^2\right] - 2\frac{m}{e}\left(\frac{\pi f r_a}{|k|}\right)^2 \left[1 - \left(\frac{r_c}{r_a}\right)^2\right]. \quad (15)$$

Hartree has derived an expression from a consideration of the conditions under which electrons are just able to reach the anode with infinitesimal amplitude of RF voltage in the k^{th} harmonic. It is:

$$V = \frac{\pi f}{|k|} r_a^2 B \left[1 - \left(\frac{r_c}{r_a}\right)^2\right] - 2\frac{m}{e}\left(\frac{\pi f r_a}{|k|}\right)^2. \quad (16)$$

In a sense this condition represents a cut-off relation for the oscillating magnetron analogous to Hull's cut-off relation for the DC magnetron [equation (8)].

Plotted on a V-B graph, the expressions (14), (15), and (16) represent parallel straight lines. The line of equation (14) passes through the origin; the so-called Hartree line of (16) is tangent to the DC cut-off parabola; the so-called Slater line of (15) lies above the Hartree line but below the line of expression (14). Each of the above expressions indicates that the electrons will drive a given harmonic of the RF interaction field in a type III magnetron oscillator only at values of DC voltage and magnetic field which bear a definite relation. This relation expresses the fact that V/B is very nearly constant [equation (14)].

In Fig. 16 are plotted as an illustration, the Hartree lines for the fundamentals ($p = 0$) of the $n = 1, 2, 3$, and 4 modes and for the $k = -5$ harmonic ($p = -1$) of the $n = 3$ mode of a 10 cm. magnetron with eight resonators.[16]

[16] This magnetron, used as an illustrative example in Part I, has the following characteristics:

Number of resonators, N = 8.
Cathode radius, r_c = 0.3 cm.
Anode radius, r_a = 0.8 cm.
Anode length, h = 2.0 cm.
Anode to end cover distance = 0.6 cm.
Frequency (π mode), f = 2800 mc/s.
Wavelength (π mode), λ = 10.7 cm.
DC operating voltage, V = 16 kv.
Operating magnetic field, B = 1600 gauss.
Typical operating peak current, I = 20 amps.
Over-all efficiency, η = 42%.
Peak power output, P_o = 135 kw.
Pulse duration, τ = 1 microsecond.
Pulse repetition frequency = 1000 pps.

Since the operating voltage is found to increase with increasing current, oscillation at a constant anode current takes place along a line, such as the Slater line for example, lying slightly above and parallel to the Hartree line (see Fig. 16). The separation of the operating line from the Hartree line increases with increasing DC current.

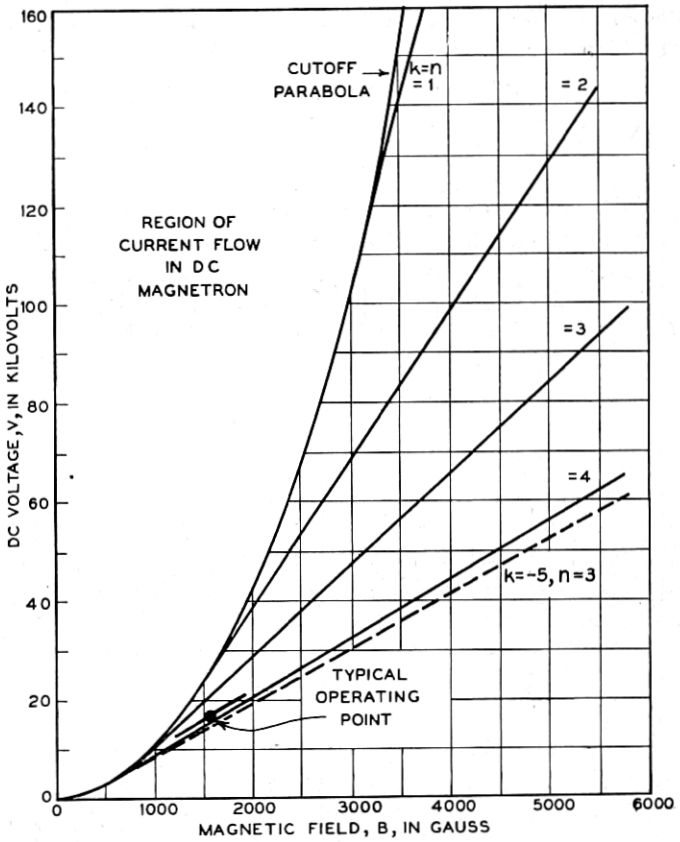

Fig. 16.—A *V-B* plot for a magnetron having eight resonators (see footnote 16) showing the cut-off parabola and Hartree lines for several rotating field components. The ranges of DC voltage and magnetic field have been extended considerably beyond values ever applied to such a magnetron to show the lines for the fundamentals of all of the modes. The typical operating point plotted is that specified in footnote 16 and plotted in Fig. 17.

The necessary conditions for oscillation discussed above have been of great value in the identification of the modes of operating magnetrons and as the starting point in the design of new magnetrons for given wavelength, magnetic field, and voltage.

4.2 *The Performance Chart:* Another fundamental performance char-

acteristic of the operating magnetron is the *V-I* plot or performance chart. In Fig. 17 such a chart is plotted for the same magnetron[16] used as the example for Fig. 16. In it are plotted contours of constant magnetic field, RF power output, and over-all efficiency. The fact that the constant mag-

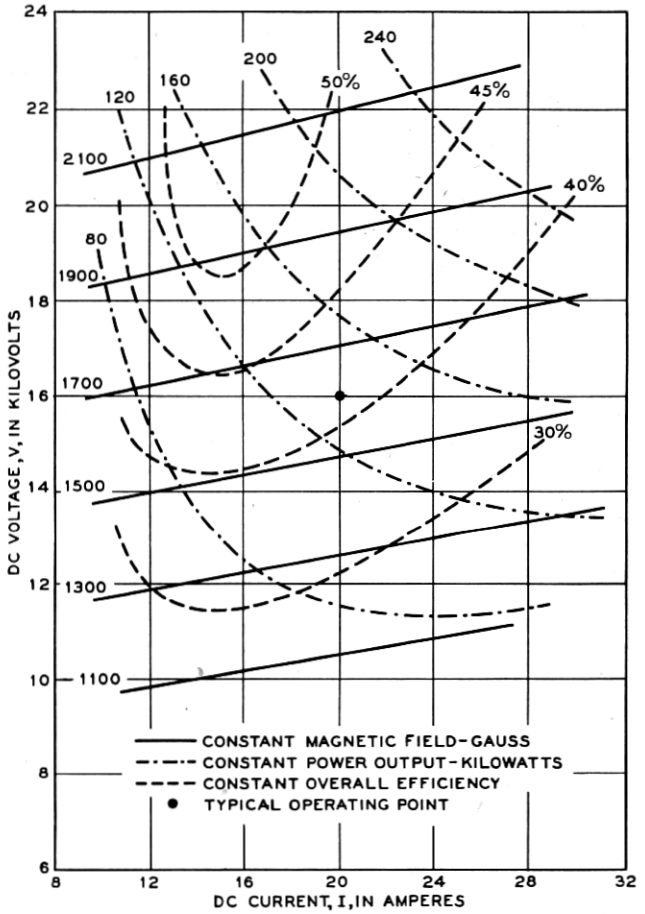

Fig. 17.—A *V-I* plot or performance chart for a magnetron having eight resonators (see footnote 16). Contours of constant magnetic field, power output, and over-all efficiency are shown. The typical operating point plotted is that specified in footnote 16 and plotted in Fig. 16.

netic field contours are nearly horizontal and spaced as they are is a manifestation of the oscillation conditions of equations (15) and (16). The increase of voltage with current is an effect, attributable to the space charge, quite independent of the condition of synchronism between field and elec-

trons. For if the magnetron is to deliver more power at a given magnetic field, the induced RF current must increase. This entails increased space charge and a greater DC current flow. To maintain the increased space charge additional DC voltage is required.

4.3 *The Electronic Efficiency:* The performance chart also shows the not too surprising fact that more power may be drawn from the magnetron as the voltage and current are increased. More interesting are the increase of the over-all efficiency with voltage and the maximum through which the efficiency passes with increasing current. This variation of over-all efficiency, η, is to be attributed to changes in the electronic efficiency, η_e, since the other factor involved in the over-all efficiency, the circuit efficiency, η_c, is essentially constant over the diagram ($\eta = \eta_e\eta_c$).

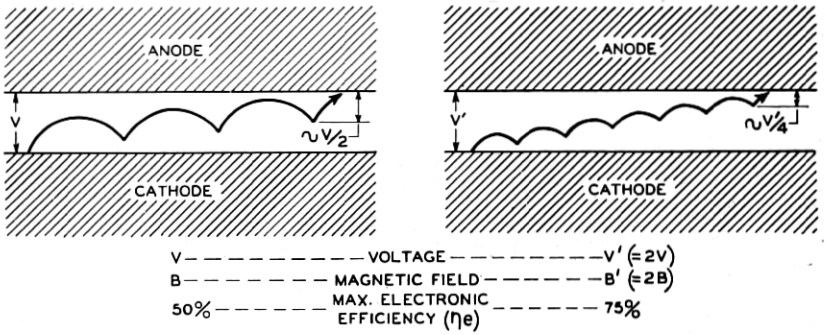

Fig. 18.—Approximate orbits of electrons which transfer energy to the RF field, plotted for operation of a plane magnetron at two different magnetic fields. It is shown how the relative kinetic energy gained beyond the last cusp and dissipated at the anode decreases as the magnetic field and voltage of operation are increased, resulting in increased efficiency of electronic conversion of energy from the DC field to the RF field. The two illustrative cases differ by a factor two in DC voltage and hence by the same factor in magnetic field and diameter of the rolling circle.

The increase of electronic efficiency with voltage, and hence magnetic field, may be explained by the picture of electron motions in the interaction space. The highest electronic efficiency is attained when the electrons reaching the anode do so with least kinetic energy. For the approximate orbit of Fig. 12, the energy lost at the anode per electron is that gained as kinetic energy beyond the last cusp. Bringing the last cusp closer to the anode, corresponding to a reduction of the amplitude of the rotational component of the electron motion, reduces the ratio of kinetic energy lost at the anode to the potential energy possessed by the electron at the cathode. Thus, according to equation (6) for the radius of the rolling circle, this fractional energy loss should vary as V/B^2 or, since V/B is approximately constant, as $1/B$, η_e increasing with B. In terms of the approximate electron orbits for a plane magnetron, Fig. 18 shows how increase in voltage

and magnetic field increases the electronic efficiency. The dependence of electronic efficiency on B predicted by this simple picture is in accord with the dependence predicted by more sophisticated theories.

In all probability the decrease of electronic efficiency toward low and high currents is, in part at least, the result of decrease in the phase focusing action. This occurs as a result, on the one hand, of low RF field strength in the proper mode when the current and RF oscillation are small, and, on the other hand, as a result of space charge debunching when the current and space charge become very large. In addition, at low currents the leakage to the anode of electrons which are not effective in interaction with the RF field, assumes a more dominant role, reducing the effective electronic efficiency. These electrons are no doubt those emitted near or at the ends of the cathode.

Of importance to the motion of electrons near the ends of the interaction space, and thus to the electron leakage, are the configurations of the DC electric and magnetic fields there. These depend upon the geometry of the cathode ends and surrounding walls and of the magnetic pole pieces. The electrons are largely confined to the interaction space by the axial force, directed toward the center of the interaction space, produced by the non-uniformities in the electric and/or the magnetic fields. For uniform magnetic field, the desired focusing action on the electrons may be achieved by disks at cathode potential which are mounted at each of the cathode and extend beyond the cathode surface over the ends of the interaction space as may be seen in Fig. 1. In other cases, distortion of the magnetic field in the end spaces of the magnetron, in addition to cathode end disks, has been used to produce the same effect.

Although the dependence of operation of a magnetron oscillator on load is primarily a circuit problem, detailed discussion of which will be delayed until the RF circuit has been discussed, there is one feature of the dependence on load and circuit characteristics which may properly be discussed now. This is the dependence of the electronic efficiency, η_e, on the circuit conductance, G_s, presented to the electrons. The plot in Fig. 19 is a typical example and shows an optimum value of conductance, to each side of which η_e decreases. With decreasing G_s the RF voltage increases. Whereas initially the increase of V_{RF} with decreasing G_s increases the phase focusing properties, it results eventually in such strong RF field that electrons are drawn more or less directly to the anode where they arrive with considerable kinetic energy. On the other hand, the decrease in V_{RF} with increasing G_s eventually will result in an RF field too weak to produce the necessary amount of phase focusing. The value of G_s presented to the electrons depends not only upon the output circuit properties and load but also upon the parameters of the resonator itself. The dependence of electronic efficiency upon G_s is a

good example of how intimately the electronics and circuit of the magnetron oscillator are associated.

4.4 *Scaling:* Once an efficient design has been achieved for a given wavelength, voltage, current, and magnetic field, one is interested in reproducing it at other values of these parameters. In doing this, use is made of the theory of scaling. For cases where the interaction space remains geometrically similar and the magnetron operates in the same mode, the same efficiency is presumably achieved when it is arranged that the electron orbits remain similar. Directly from dimensional arguments applied to Maxwell's equations for the electromagnetic field and to the equations of

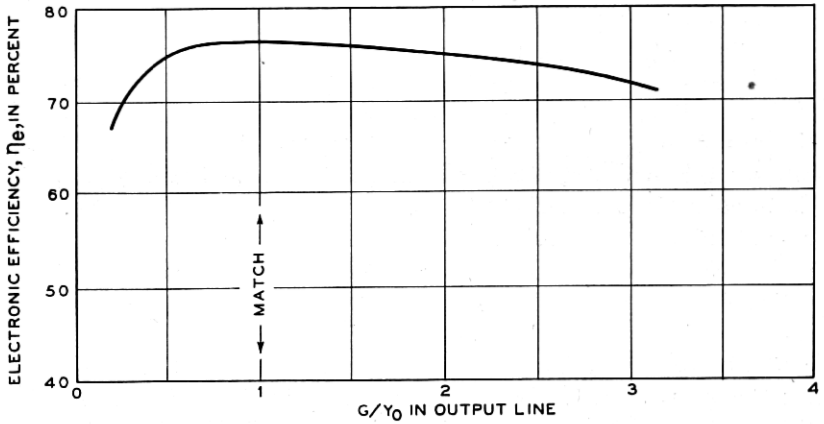

Fig. 19.—A plot of electronic efficiency as a function of load conductance. The conductance G/Y_o in the output line is related to that presented by the circuit to the electrons, G_s, directly through the magnetron resonator and output circuits. The magnetron with which these data were obtained is a 3.2 cm. magnetron having sixteen resonators.

motion of the electrons, it can be shown that the orbits and operation will be equivalent for all conditions for which the loading and the quantities

$$\lambda B, \quad (\lambda/r_a)^2 V, \quad \text{and} \quad (\lambda^3/r_a^2 h) I$$

remain invariant.

It would perhaps be of interest to consider, as a simple example, the case for which all the linear dimensions of a given magnetron are changed by a factor α. The new resonant wavelength, λ', is equal to $\alpha\lambda$ since the new resonator is α times the size of the original, while the new frequency is $f' = f/\alpha$. The new anode radius, cathode radius, and anode length scale directly so that

$$r'_a = \alpha r_a, \; r'_c = \alpha r_c \text{ and } h' = \alpha h$$

Since λB, $(\lambda/r_a)^2 V$, and $(\lambda^3/r_a^2 h)I$ must remain invariant,

$$\lambda' B' = \lambda B \text{ or } B' = B/\alpha,$$

$$(\lambda'/r'_a)^2 V' = (\lambda/r_a)^2 V \text{ or } V' = V,$$

and

$$(\lambda'^3/r'^2_a h')\, I' = (\lambda^3/r_a^2 h)\, I \text{ or } I' = I.$$

Thus the magnetic field changes by $1/\alpha$ and the operating voltage and current remain unchanged.

The idea of scaling has been extended to magnetrons of varying r_c/r_a and N by the introduction of sets of reduced variables for V, B and I involving r_c/r_a and N, in terms of which the performance may be expressed independently of the exact nature of the magnetron.

4.5 *Effect of Other Components in the Interaction Field:* In the discussion of the traveling wave magnetron oscillator, it has been considered that the electrons interact with a single traveling RF field component, generally a component of the fundamental of the π mode. The justification for this, as has been stated, is that from the point of view of the electron the fields of all other Hartree harmonics of the π mode vary so rapidly that their effects average out over an appreciable number of RF cycles. This is generally true, as well, for the harmonics of other modes which may be excited. The fact has been mentioned that it is possible for the values of V and B for oscillation in the π mode very nearly to satisfy equation (16) for oscillations in a harmonic of another mode. Then the angular velocity, $\frac{2\pi f'}{|k'|}$, of the harmonic very nearly equals that of the π mode, $\frac{2\pi f}{N/2}$, and the Hartree line of the harmonic lies very close to that of the π mode (see Fig. 16). The effect of this situation on magnetron operation will be discussed in connection with the problem of "moding" in Section 10.6 *Oscillation Buildup—Starting.*

Of particular interest is the presence in the interaction space, in addition to the π mode field, of an RF field component which is independent of angle. Such a component appears, for example, as an inherent contamination in the interaction field of the so-called "rising sun" type resonator system to be described later. Generally, this component is of no concern because the electrons interact with the π mode component throughout a time interval covering several cycles, during which the effect of the contamination averages out. The exception to this occurs when the frequency of the rotational component of the electron motion, approximately the cyclotron frequency, resonates with the RF frequency as in a Type II magnetron. From equation (2) this occurs for the plane case when $f = c/\lambda = eB/2\pi m$, from which $\lambda B = 2\pi cm/e = 10{,}700$ gauss-cm. For a typical cylindrical case the constant is somewhat greater, being about 12,500 gauss-cm. When λB has this

value, perturbation of the electron motion occurs, decreasing the efficiency of interaction with the traveling wave and manifesting itself on the perform-

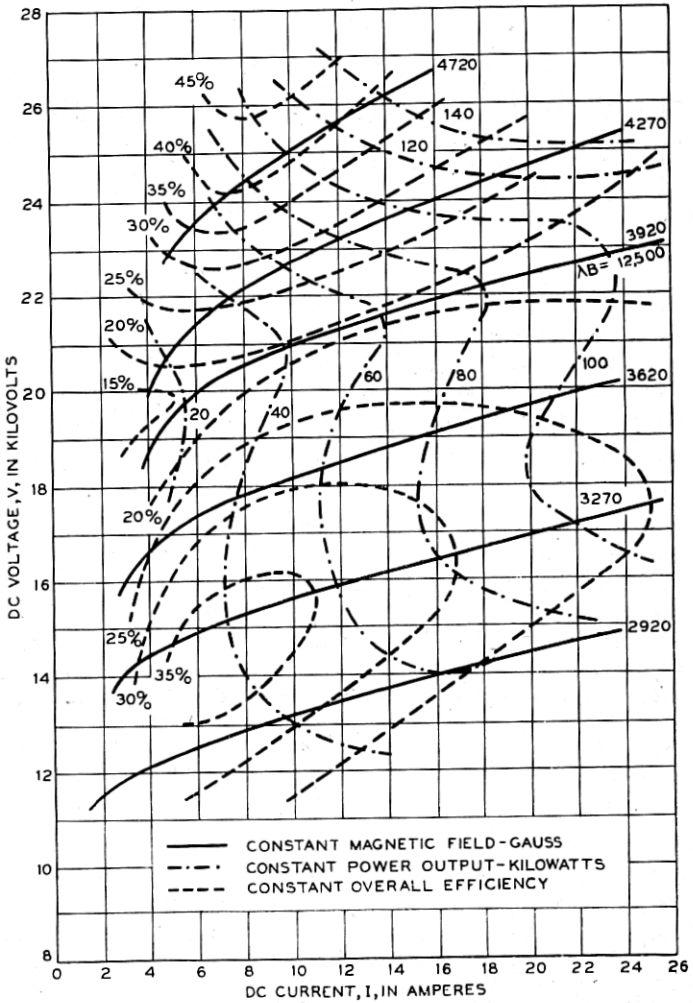

Fig. 20.—A performance chart for a magnetron which has present in its interaction field a contaminating component independent of azimuth. Note the efficiency "valley" appearing along the line $B = 3920$ gauss (compare with Fig. 17). The wavelength of the magnetron being 3.18 cm., λB along the efficiency "valley" is 12,500 gauss-cm. The data were obtained on a magnetron having a "rising sun" type resonator system and are reproduced here through the courtesy of the Columbia Radiation Laboratory.

ance chart as a "valley" in operating efficiency appearing along the constant B line for which $\lambda B = 12{,}500$ gauss-cm. In Fig. 20 is plotted the performance chart of a magnetron, having a "rising sun" type anode structure which

exhibits this kind of behavior. In general, it would be preferable to operate this magnetron at magnetic fields above the "valley," but considerations having to do with available magnetic fields, in some cases may make it necessary to operate near the efficiency maximum at lower magnetic fields.

5. The RF Circuit of the Magnetron Oscillator

5.1 *General Considerations:* The discussion to this point has presented a picture of how the multicavity magnetron oscillator works from the point of view of its electronics; how in this respect it is related to other types of magnetron oscillators; and how, on the basis of the picture of the electronic mechanism, some of its fundamental operating characteristics are to be accounted for. In the same manner the RF circuit of the magnetron oscillator, comprising the resonator system, the output circuit, and the load, will be discussed. The importance of this part of the magnetron is apparent. It provides the RF fields with which the electrons interact. To do this, electromagnetic energy must be stored in the cavities of the resonator, which reservoir in turn is tapped to deliver energy through the output circuit to the useful load. The detailed manner in which these functions are performed has a bearing, not only on such circuit characteristics as circuit efficiency or on the effect of load on frequency, but, as has been seen, on the electronic efficiency as well. Furthermore, the circuit analysis of the magnetron oscillator enables one to explain the remaining important operating characteristic, the so-called Rieke diagram, which describes the operational dependence on load.

The type of resonator system used in the magnetron oscillator of concern here has already been indicated in Fig. 1. It is a resonator system comprising a number of cavities spaced equally about the cylindrical anode. This general shape is dictated by the slotted anode cylinder upon which the RF interaction field is set up. To be sure, other types of resonators have been devised which contrive to place π mode potentials on the anode segments of a cylindrical magnetron. Here, however, except for brief references, the discussion will concern itself with the multicavity resonator system of the general type shown in Fig. 1. Although the individual cavities have not been limited to hole and slot geometry like those shown in Fig. 1, and other features have been added, a resonator system consisting of a system of cavities, arranged around the anode in the manner of Fig. 1, has been used in the majority of magnetron oscillators developed for centimeter wave generation since 1940.

5.2 *Simple Single Frequency Resonator:* The fact that the magnetron resonator system has a number of cavities electromagnetically coupled together makes it multiresonant. What has been learned about the various modes and their electromagnetic field configurations, and how they may in a sense be controlled to improve magnetron operation must be discussed in some detail. Before this is done, however, it would be well to refresh one's memory as to the fundamental ideas concerned with a single electromagnetic

resonator like one of the magnetron cavities.[17] This is important not only because the magnetron resonator system comprises a number of such cavities but also because the resonator system as a whole may under certain circumstances be considered to resonate at but one frequency, in which case it behaves like a simple single frequency resonator.

Concerned with the simple electromagnetic resonator are the fundamental ideas of a natural frequency of resonance, of the rate of energy loss or the sharpness of resonance, and of the characteristic admittance or the energy storage capacity. The electromagnetic resonator, whether it has lumped or distributed constants, consists of a device in which energy is transferred between electric and magnetic fields cyclically in a manner entirely analogous to the transfer of energy between potential and kinetic in the simple swinging pendulum. Each of these oscillations, electromagnetic or mechanical, is described by a second order differential equation in terms of a parameter such as voltage or current on the one hand, and angular displacement of the pendelum bob on the other. The solutions represent simple harmonic oscillations, the one for the simple electrical circuit having the frequency,

$$f_0 = \frac{\omega_0}{2\pi} = \frac{1}{2\pi\sqrt{LC}}. \tag{17}$$

This occurs when the susceptances of the two components of the circuit, L and C, are equal, or when

$$\frac{1}{\omega_0 L} = \omega_0 C. \tag{18}$$

The fact that a finite time is required to transfer the energy between the electric and magnetic fields is a lumped constant circuit is not surprising since a finite time is required for a condenser to charge or discharge, and for a current to build up or decay in an inductance.

5.3 *The Q Parameters:* The type of oscillation of the simple L-C circuit discussed above is its natural or free oscillation, not constrained by the ap-

[17] In the next sections of this paper, material has been drawn from the theory of a single resonant circuit having either lumped or distributed constants, the theory of coupled circuits, and the theory of centimeter wave transmission in coaxial lines and wave guides, treatments of which are to be found in the following representative texts:

L. Page and N. I. Adams, *Principles of Electricity*, D. Van Nostrand Co., New York (1931).

E. A. Guilleman, *Communication Networks*, Vols. I and II, John Wiley and Sons, New York (1931).

J. G. Brainerd, G. Koehler, H. J. Reich, and L. F. Woodruff, *Ultra-High Frequency Techniques*, D. Van Nostrand Co., New York (1942).

J. C. Slater, *Microwave Transmission*, McGraw-Hill Book Co., New York (1942).

R. I. Sarbacher and W. A. Edson, *Hyper and Ultrahigh Frequency Engineering*, John Wiley and Sons, New York (1943).

S. A. Schelkunoff, *Electromagnetic Waves*, D. Van Nostrand Co., New York (1943).

plication of any external driving force. It is the sort of oscillation the circuit would undergo were it left to itself after being excited or started initially. Such an oscillation, once started, does not continue indefinitely because the energy put into the circuit initially, dissipates itself in resistive losses in the circuit components and in a load which may be coupled electromagnetically to the circuit. The exponential rate at which the original energy is dissipated is a very important characteristic of the circuit. It is usually specified by a parameter Q, defined as 2π times the ratio of the energy stored in the circuit to the energy dissipated per cycle of the oscillation.[18] Thus a circuit always loses a certain fraction of its energy per cycle independent of how great this energy may be. In the exponential decay of oscillations in a resonator from which the drive has been removed, $Q/2\pi$ is the number of cycles of oscillation, required for the stored energy to decay to $1/e$ of its initial value. Similarly, in the buildup of oscillations in a resonator to which is fed a constant amount of energy per cycle, $Q/2\pi$ is the number of cycles required for the stored energy to buildup to $(1 - 1/e)$ of its final equilibrium value.

It is possible to define several types of Qs for a circuit, depending upon the nature of the energy dissipation being considered. If one considers only the energy lost in the resistance of the circuit components themselves, one defines the so-called unloaded Q, Q_o. If the circuit is coupled electromagnetically to a resistive load, the Q defined in terms of the energy dissipated in the load and internal resistance is called the loaded Q, Q_L. Finally, for some purposes it is convenient to consider the ratio of energy stored to that dissipated in the external load only. This defines the external Q, Q_{ext}. It is clear that both Q_L and Q_{ext} are functions of the degree of coupling between the oscillating circuit and the resistive load.

The Q parameters, however, tell one more than the rate at which energy is dissipated in a circuit oscillating at its natural frequency. The admittance of the circuit, measured as a function of the frequency of an external driving source, passes through a minimum at the natural frequency of oscillation of the circuit. The sharpness of the dip in the admittance curve is determined by the Q_L of the circuit in such a manner that the sharper the dip, the higher the Q_L. In passing through resonance the susceptance of the circuit changes sign from inductive for frequencies below the frequency of resonance, to capacitive, for frequencies above the frequency of resonance. The rate at which the susceptance varies with frequency is another measure of the sharpness of resonance and of the Q_L of the circuit.

5.4 *Energy Storage and Loss:* The remaining ideas concerned with a simple L-C circuit of lumped constants which should be mentioned here are the characteristic admittance of the circuit, the energy storage capacity,

[18] As will be seen in the subsequent discussion the factor 2π is included here so as to simplify the definition in terms of admittance.

and how these are related to each other and to the concepts already mentioned. For this purpose it is convenient to consider the circuit shown in Fig. 31 (c). Across the terminals AB is connected the L-C circuit in which the resistive losses are represented by the circuit conductance G_c. The circuit is loaded by the admittance $Y_L'' = G_L'' + jB_L''$.

Looking into the circuit at the terminals AB one sees the admittance:

$$Y_s = G_c + jB_c + Y_L'' = G_c + \frac{1}{j\omega L} + j\omega C + Y_L''$$

which may be rewritten:

$$\begin{aligned} Y_s &= G_c + j\sqrt{\frac{C}{L}}\left(\frac{\omega}{\omega_0} - \frac{\omega_0}{\omega}\right) + Y_L'' \\ &\cong G_c + 2j\left(\frac{\omega - \omega_0}{\omega_0}\right) Y_{0c} + Y_L'', \end{aligned} \tag{19}$$

where $\omega_0 = \frac{1}{\sqrt{LC}}$ and $Y_{0c} = \sqrt{\frac{C}{L}}$.

The expression $\sqrt{\frac{C}{L}}$, having the dimensions of an admittance, is by definition the characteristic admittance of the circuit, Y_{0c}. Its relation to the energy stored in the circuit, and through this to the various Qs defined above, may be seen from the following: Using the root mean square value of voltage, the energy stored in the circuit is CV_{RF}^2. This can be reduced by the use of the definition of the resonant frequency and by differentiation of the expression (19) for the admittance, thus:

$$CV_{RF}^2 = \frac{Y_{0c}}{\omega_0} V_{RF}^2 = \frac{1}{2}\left|\frac{dB_c}{d\omega}\right|_{\omega=\omega_0} \cdot V_{RF}^2 . \tag{20}$$

Thus, at a given frequency ω_0, the energy stored in the circuit for unit voltage applied to it may be specified either by the characteristic admittance of the circuit, Y_{0c}, or by the rate of change of susceptance with frequency at the resonant frequency, $\left|\frac{dB_c}{d\omega}\right|_{\omega=\omega_0}$.

The loss of energy per cycle in the circuit itself, that is, in the shunt conductance G_c, is the power loss in the circuit divided by the frequency, $\frac{V_{RF}^2 G_c}{\omega_0/2\pi}$. From this and equation (20) the unloaded Q is seen to be:

$$Q_0 = 2\pi \frac{\frac{Y_{0c}}{\omega_0} V_{RF}^2}{\frac{V_{RF}^2 G_c}{\omega_0/2\pi}} = \frac{Y_{0c}}{G_c}. \tag{21}$$

Similarly, for the loaded and external Qs:

$$Q_L = \frac{Y_{0c}}{(G_c + G_L'')}, \tag{22}$$

$$Q_{\text{ext}} = \frac{Y_{0c}}{G_L''}. \tag{23}$$

It follows that the Qs are related thus:

$$\frac{1}{Q_L} = \frac{1}{Q_0} + \frac{1}{Q_{\text{ext}}}. \tag{24}$$

The efficiency of the circuit, defined as the fraction of the energy which reaches the useful load is then:

$$\begin{aligned} \eta_c &= \frac{G_L'' V_{RF}^2}{G_L'' V_{RF}^2 + G_c V_{RF}^2} = \frac{G_L''}{G_L'' + G_c} \\ &= \frac{\frac{Y_0}{Q_{\text{ext}}}}{\frac{Y_0}{Q_{\text{ext}}} + \frac{Y_0}{Q_0}} = \frac{1}{1 + \frac{Q_{\text{ext}}}{Q_0}} = \frac{Q_L}{Q_{\text{ext}}}. \end{aligned} \tag{25}$$

5.5 *Resonators with Distributed Constants.* The individual cavities of the magnetron oscillator, however, are circuits in which the parameters are distributed and not lumped. They may be considered to be "strip-type" resonators, three forms of which generally used in magnetrons, are shown in Fig. 21 (a), (b), and (c). Type (a) has been called the slot type resonator; (b), the vane type, deriving its name from a common method of fabrication in which rectangular plates are disposed around and brazed to the inside of a cylindrical cavity; and (c), the hole and slot type resonator. The forms of these resonators, especially the parallel strip form of Fig. 21 (a), suggest that the resonators may be considered as sections of terminated transmission lines.

Voltage and current waves traveling down a section of uniform transmission line, terminated at one end by a short circuit and driven by a sinusoidal voltage at the other end, are reflected at the shorted end. The interference of the incident and reflected waves results in standing waves of voltage and current along the line. Since the voltage and current waves suffer phase changes on reflection differing by π radians, the corresponding standing waves are shifted by $\pi/2$ radians relative to one another. Thus the input admittance of the section of line is a periodic function of the distance, ℓ, to the shorted end. For a lossless line, this admittance is given by the expression:

$$Y = -jY_0 \cot \frac{2\pi\ell}{\lambda} = -jY_0 \cot \frac{2\pi f\ell}{c}. \tag{26}$$

In (26), Y_o is the characteristic admittance of the line. For a line of given length, this expression gives the input admittance as a function of frequency. When the frequency is $c/4\ell$, the line is a quarter wavelength long, and the

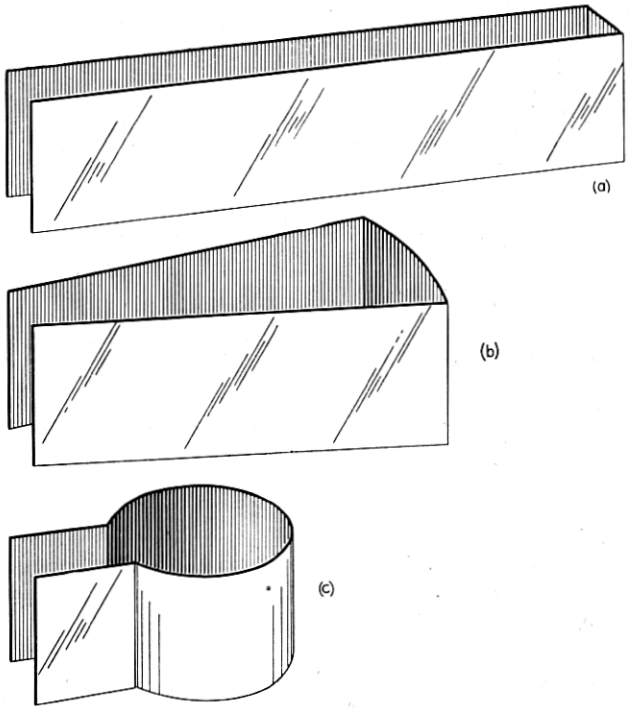

Fig. 21.—Three "strip type" cavities commonly used in magnetron resonator systems, each resonant at the frequency c/λ. Type (*a*) is essentially a quarter wavelength ($\lambda/4$) section of uniform transmission line. It should be noted how types (*b*) and (*c*) are physically shorter than type (*a*) by virtue of the greater relative capacitive loading near the open ends.

input admittance, if the line is lossless, is zero. In other words, the section of line resonates at this frequency.[19] In a quarter wavelength resonator of

[19] The frequency of resonance, $f = c/4\ell$, is the fundamental or lowest frequency of an infinite series of resonant frequencies for which the line length is $(2q - 1)\lambda/4$;

$$f_q = (2q - 1)c/4\ell, q = 1, 2, 3, \cdots.$$

These frequencies may be specified by considerations of the phase relationships which must

uniform geometry, the voltage is maximum at the input end and the current is maximum at the shorted end, each varying sinusoidally to a node at the other end of the line.

The frequency of resonance of a section of terminated uniform line is thus determined by its length. If the geometry of the line is nonuniform, the frequency of resonance may be determined by the solution of Maxwell's equations with the appropriate boundary conditions. In general, this procedure is involved and tedious, however. One may get a reasonable idea of the values of ω_0 and Y_0 by assuming the half of the resonator near the open end to be capacitive only, the half near the closed end inductive only, and calculating C and L by application of elementary formulas to an equivalent parallel plate capacitance and a single turn sheet inductance of height h and proper cross sectional area. In the case of geometry like that of Fig. 21 (c), the division of the resonator on this basis is obvious.

A line of physical length ℓ', less than $\lambda/4$, may be made to resonate at the frequency c/λ by connecting across its input end a lumped capacitive susceptance, of magnitude, ωC, equal to that of the inductive susceptance of the line, $Y_0 \cot \frac{2\pi\ell'}{\lambda}$ [see equations (18) and (26)]. In like manner, resonators like those of Fig. 21 (b) and (c), whose physical length is less than $\lambda/4$, may be considered to be made up of an inductive section of uniform line across which additional capacitance has been inserted near the open end, bringing the frequency of resonance to c/λ. In Fig. 21, the three resonators of different physical lengths all resonate at the same frequency.

In addition to the resonant frequency of a resonator of distributed constants, one may define its Qs and characteristic admittance and link these to the rate of change of susceptance and energy storage capacity at resonance as was done for the circuit of lumped constants. Resonators of different geometry but of the same resonant frequency differ in characteristic admittance and loss conductance and hence in the Qs and the amount of energy which can be stored with unit voltage impressed across the input end. Of the resonator types shown in Fig. 21, the slot type has the largest admittance, the vane type, the smallest admittance, with the hole and slot type intermediate.

6. Resonator Systems

6.1 *Two Coupled Resonators:* The resonator system of the magnetron oscillator consists of a number of individual resonators of distributed parameters, machined into the anode block. As the simplest case of a system of coupled resonators, consider that having two resonators which are coupled

exist between oppositely traveling waves on a lossless line for constructive interference. These considerations are similar to those employed later in the discussion of the modes of oscillation of the magnetron resonator system as a whole.

only by the mutual linkage of magnetic lines and which resonate at the same frequency, ω_0, when uncoupled.

When such a coupled system is shock excited it is observed that the oscillation amplitude in either of the circuits is modulated at a so-called beat frequency, ω_B. A fraction or all of the energy in the system, depending on the initial conditions, surges back and forth at this frequency between the circuits similar to the manner in which the energy of motion is exchanged between two coupled pendulums. The total energy in the system is constant, the beats differing in phase by $\pi/2$ radians between the circuits.

The observation of beats is a manifestation of the fact that the two coupled resonators form a complex system oscillating simultaneously in its two modes for which the frequencies are $(\omega_0 + \omega_B)$ and $(\omega_0 - \omega_B)$. The oscillation in either circuit results from the superposition of the two component oscillations in this manner:

$$A \cos (\omega_0 + \omega_B)\, t + B \cos [(\omega_0 - \omega_B)\, t + \delta] =$$

$$(A - B) \cos (\omega_0 + \omega_B)\, t + 2B \cos\left(\omega_B t - \frac{\delta}{2}\right) \cos\left(\omega_0 t + \frac{\delta}{2}\right), \tag{27}$$

with a similar expression for the case when $A < B$. The oscillation may be predominantly of one frequency, that is, almost entirely in one mode, if, for example, $A \gg B$. In general, the oscillation is a superposition of a steady oscillation in the predominant mode $[(\omega_0 + \omega_B)$ if $A > B]$ and an oscillation whose amplitude varies with the beat frequency, ω_B. In the special case, when the component oscillations are of equal intensity, $A = B$, the amplitude of the resultant oscillation in either circuit goes to *zero* periodically at the frequency ω_B. This represents the case for which all the energy present in the system is transferred back and forth between the circuits.

The frequency separation of the two modes arises from the coupled effect of the oscillation in each of the circuits on the oscillation in the other. Thus, in the mode of lower frequency, $(\omega_0 - \omega_B)$, the two circuits oscillate in phase and the self induction effect in each circuit is aided by the mutual induction, each circuit behaving as though it were oscillating freely with a greater value of self inductance and hence at lower frequency [equation (17)]. For the mode of higher frequency, $(\omega_0 + \omega_B)$, the reverse is true. Here the two circuits oscillate out of phase by π radians, the mutual induction opposing the self induction and the circuits oscillating as though uncoupled with a smaller value of self inductance and hence at higher frequency.

If instead of shock exciting the system of two coupled resonators it is forced to oscillate by applying to it a sinusoidal voltage of variable frequency, the admittance of the system is found to pass through minima at the mode frequencies $(\omega_0 + \omega_B)$ and $(\omega_0 - \omega_B)$. Thus it is possible to drive the system and store energy in either of the two modes. For each mode of

the coupled circuit system, as for the simple single frequency resonator, Q parameters and a characteristic admittance may be defined which specify sharpness of resonance and energy storage capacity, respectively.

6.2 *The Multicavity Anode Structure:* As an introduction to the discussion of the multicavity resonator system of the magnetron oscillator having cylindrical symmetry, consider the system of a series of resonators machined side by side in a linear block as shown in Fig. 22. One may consider such a linear array either to be infinite in extent or to be terminated in some manner at the ends of a string of N identical resonators.

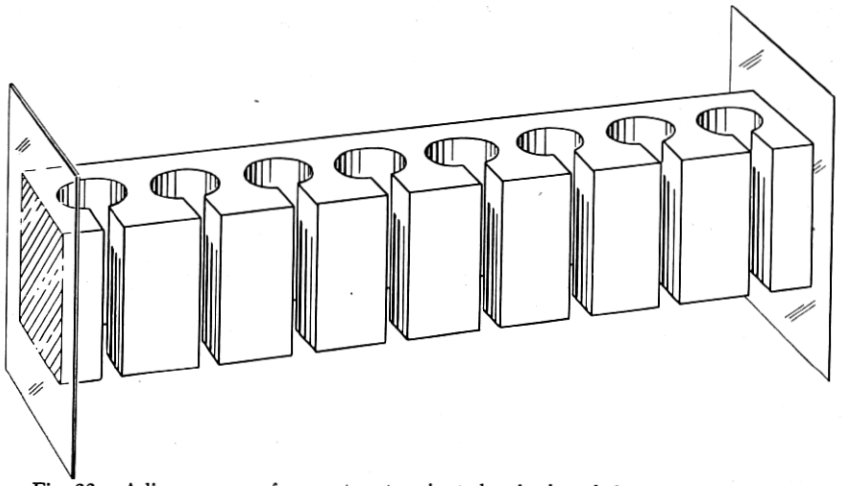

Fig. 22.—A linear array of resonators terminated at both ends by generalized terminations represented by planes. The figure is meant also to indicate the nature of the infinite array of resonators referred to in the text.

The oscillation in each resonator of the array of coupled resonators is specified by a differential equation in terms of a variable, such as current or voltage, the constants of the circuit itself, and the mutual interaction between the circuit and its neighbors. Each solution of the set of simultaneous differential equations for all the resonators involved corresponds to a definite phase shift between adjacent resonators. The allowed values of this phase shift depend upon the boundary conditions imposed on the string of resonators. If the block is infinitely long, all values of phase shift are allowed. In terms of the electromagnetic field pattern formed on the front surface of the block by the fringing fields of the individual resonators, this means that traveling wave solutions representing waves of any velocity, traveling over the surface of the block in directions normal to the slots, are possible. If the block is terminated, on the other hand, the boundary

conditions restrict the phase shift between resonators to a set of specific values. These correspond to the traveling waves which on reflection at the terminations constructively interfere.

The cylindrical magnetron anode structure is a series of N resonators connected in a ring. It may be thought to be a section of a linear array of resonators rolled into a cylinder. The boundary condition imposed is that of connecting together the resonators at the ends of the string. Under these circumstances only those modes of oscillation are possible for which the total phase shift around the ring is $2\pi n$ radians, n being any integer including zero. The oscillations in adjacent cavities then differ in phase by $\frac{2\pi n}{N}$ radians. Again this means that only those waves traveling around the anode block which constructively interfere are possible solutions. These are waves which, after leaving an assumed starting point and traversing the anode once, arrive back in phase with the wave then leaving in the same direction. The anode potential waves and the RF interaction fields in the interaction space to which they correspond have already been discussed in connection with equations (12) and (13). In these electromagnetic field patterns, the electric and magnetic field components are displaced both in space and time phase by $\pi/2$ radians relative to one another, similar to the manner in which voltage and current on a terminated transmission line are related.

6.3 *The Modes of the Resonator System:* It has been seen that the modes of oscillation of a magnetron resonator system are characterized by definite values of the phase shift between adjacent resonators specified by $\frac{2\pi n}{N}$, in which the parameter n may assume only integral values including zero. Each such mode of oscillation has a frequency different from the frequency of any other mode and from the frequency of one of the N resonators oscillating freely and uncoupled from its neighbors. In the general case of N coupled resonators, as in the case of two coupled resonators previously discussed, the modes of oscillation have different frequencies because of the effect of the mutual coupling between the resonators. For $N = 2$, the oscillations in the two resonators are either in phase or π radians out of phase, the induction in one circuit by the other either directly adding to or subtracting from the self induction. In the case of the multiresonator system the mutual induction effect may bear phase relations to the self induction other than 0 and π radians. Thus not only the magnitude of the coupling but also this phase relationship determines the magnitude of the effect of the mutual induction and hence the amount of deviation of the

mode frequency from that of a single uncoupled resonator. If the coupling between resonators were in some way gradually reduced, all mode frequencies would converge to the value for a single uncoupled resonator.

The complete anode potential wave for a mode specified by the parameter n has been given in equation (12). Each of its traveling components is represented by a fundamental of periodicity n and a series of so-called Hartree harmonics of periodicities $k = n + pN$, $p = 0, \pm 1, \pm 2, \cdots$. Any sinusoidal component for which the number of complete cycles around the anode is greater than $\frac{N}{2}$ is thus a harmonic of the complete field pattern for one of the modes whose fundamental is of periodicity $n = 1, 2, \cdots, \frac{N}{2}$. Physically distinguishable modes of oscillation exist only for the values of n less than or equal to $\frac{N}{2}$, including zero. However, this accounts for only $\frac{N}{2} + 1$ of the N modes of oscillation which one expects a system of N resonators to possess. The reason for this is that in general the frequency of a mode specified by the parameter n (except for the values 0 and $\frac{N}{2}$) is a double root for a perfectly symmetrical anode structure. The mode is thus a doublet and is said to be degenerate. One would expect this on mathematical grounds from the fact that the general solution of expression (12) has four arbitrary constants, whereas a singlet solution of the system of second order differential equations specifying the oscillations should have no more than two.

The nature of the degeneracy of the modes of the resonator system is perhaps most clearly seen by investigating what happens when the symmetry of the system is destroyed by the presence of a disturbance or perturbation at one point, a coupling loop in one of the cavities for example. Such a disturbance provides the additional boundary condition needed to remove the degeneracy.

Consider the effect of the perturbation on the nth mode. It represents an admittance shunted across the otherwise uniform closed ring of resonators. This shunt admittance may be represented by ϵY_0, ϵ being a complex number, taken to be small for simplicity, and Y_0 the characteristic admittance of the closed resonator system. In such a system, a potential wave incident upon the disturbance ϵY_0, having an amplitude a at the disturbance, breaks up into a reflected wave and a transmitted wave which, if ϵ is small, have the amplitudes $-\frac{\epsilon}{2}a$ and $\left(1 - \frac{\epsilon}{2}\right)a$, respectively [see equation (30)

for the reflection coefficient on a transmission line]. In passing across the disturbance, a wave undergoes a small phase shift $\delta\phi(\omega)$. Since the total phase shift around the entire system must remain $2\pi n$, one may write: $\phi(\omega) + \delta\phi(\omega) = 2\pi n$, in which $\phi(\omega)$ is the phase shift around the system not including the disturbance. If there is no disturbance, $\omega = \omega_n$ (ω_n is used here for the ω_0 of the nth mode), $\delta\phi(\omega) = 0$, and $\phi(\omega_n) = 2\pi n$. For waves incident upon ϵY_0 from either direction, the respective amplitudes a and b at ϵY_0 must satisfy the equations:

$$a = \left[-\frac{\epsilon}{2} b + \left(1 - \frac{\epsilon}{2}\right) a\right] e^{j\phi(\omega)}$$

$$b = \left[-\frac{\epsilon}{2} a + \left(1 - \frac{\epsilon}{2}\right) b\right] e^{j\phi(\omega)}.$$

Writing $2\pi n - \left|\frac{\partial\phi}{\partial\omega}\right|_{\omega_n} \cdot (\omega - \omega_n)$ for $\phi(\omega) = 2\pi n - \delta\phi(\omega)$ in these equations and keeping only first order terms, one obtains the following pair of homogeneous linear equations for a and b:

$$\left[j\left|\frac{\partial\phi}{\partial\omega}\right|_{\omega_n} \cdot (\omega - \omega_n) - \frac{\epsilon}{2}\right] a - \frac{\epsilon}{2} b = 0$$

$$-\frac{\epsilon}{2} a + \left[j\left|\frac{\partial\phi}{\partial\omega}\right|_{\omega_n} \cdot (\omega - \omega_n) - \frac{\epsilon}{2}\right] b = 0.$$

These equations have a solution if and only if the determinant of the coefficients vanishes, that is, if:

$$j\left|\frac{\partial\phi}{\partial\omega}\right|_{\omega_n} \cdot (\omega - \omega_n)\left[j\left|\frac{\partial\phi}{\partial\omega}\right|_{\omega_n} \cdot (\omega - \omega_n) - \epsilon\right] = 0.$$

The two solutions are thus: $\omega = \omega_n$, for which $a = -b$, and $\omega = \omega_n - \frac{j\epsilon}{\left|\frac{\partial\phi}{\partial\omega}\right|_{\omega_n}}$ for which $a = b$.

From these facts concerning the amplitudes, namely, that at the disturbance ϵY_0 the amplitudes of the two oppositely traveling waves must either be equal or equal and opposite in sign for all time, one may conclude that the waves are of equal amplitude and that the standing waves resulting for each frequency must have a node at the disturbance for the $\omega = \omega_n$ solution and an antinode there for the $\omega = \omega_n - \frac{j\epsilon}{\left|\frac{\partial\phi}{\partial\omega}\right|_{\omega_n}}$ solution.

What this means in terms of the general solution for the degenerate mode

of periodicity n of equation (13) may now be seen. Expression (13) may be rewritten in terms of θ measured from the disturbance ϵV_0 in this way:

$$V_{RF} = \sum_k (A_k - B_k) \cos(\omega t - k\theta + \gamma) + \sum_k 2B_k \cos\left(\frac{\gamma - \delta}{2}\right) \cos\left[\omega t + \left(\frac{\gamma + \delta}{2}\right)\right] \cos k\theta + \sum_k 2B_k \sin\left(\frac{\gamma - \delta}{2}\right) \cos\left[\omega t + \left(\frac{\gamma + \delta}{2}\right)\right] \sin k\theta. \quad (28)$$

When the degeneracy is removed, the first summation representing the traveling wave vanishes since the amplitudes A_k and B_k are equal for the reasons indicated. Furthermore, the second term involving cos $k\theta$ terms is then the component of the doublet whose frequency changes, and the third term involving sin $k\theta$ terms is the component of undeviated frequency. For the latter component the disturbance appears at a node and hence has no effect. The reverse holds for the cos $k\theta$ solution. For it, the frequency deviation depends on the magnitude of the disturbance through the quantity ϵ. The disturbance caused by the coupling loop in an actual magnetron resonator system is sometimes sufficient to split the components into distinguishable resonances.

Thus an unsymmetrical multicavity resonator system in general has two modes of different frequency for each value of n. With respect to the asymmetry as origin, one of these modes has a cosine-like field pattern, the other a sine-like field pattern. This is true for $n = 1, 2, \cdots, \frac{N}{2} - 1$, contributing $N - 2$ modes. The remaining two modes of the resonator system, for which $n = 0$ and $\frac{N}{2}$, are singlet modes even in the symmetrical anode. This may be seen from the analysis demonstrating the splitting of the nth mode into two components. For the $n = 0$ mode, since the anode potential wave is independent of azimuthal angle, the solution $\omega = \omega_n$ for which $a = -b$ represents the trivial case of zero amplitude at all points. Similarly, for the $n = \frac{N}{2}$ mode (the π mode) the $\omega = \omega_n - \frac{j\epsilon}{\left|\frac{\partial \phi}{\partial \omega}\right|_{\omega_n}}$ solution for which $a = b$ yields a cosine-like pattern giving zero potentials at each anode segment, an equally trivial case. Thus each of the N modes of the multicavity resonator system have been accounted for.

As an example, plots of the field configurations for the modes of a magnetron having eight resonators are shown in Fig. 23. For clarity, only the

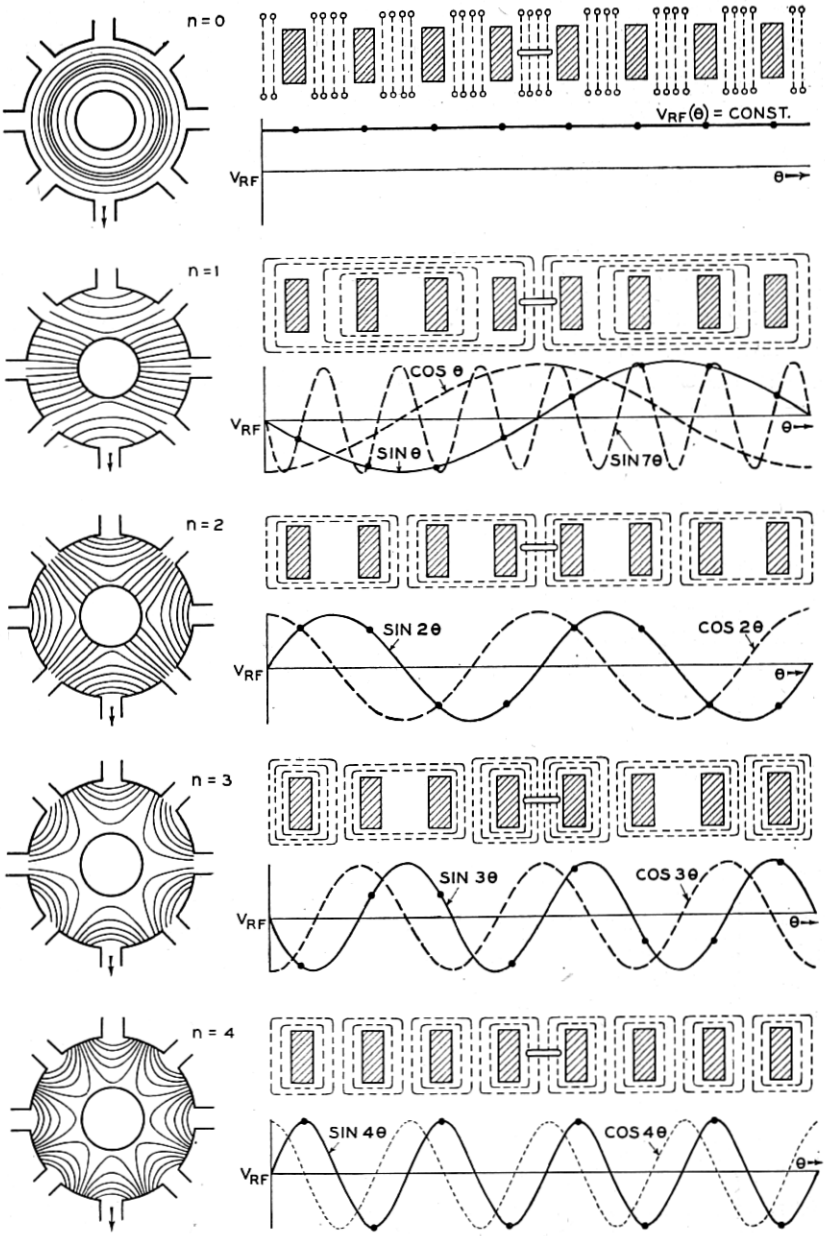

Fig. 23.—Configurations of electric fields, magnetic fields, and anode potentials for the $n = 0, 1, 2, 3$, and 4 modes of a resonator system having eight resonators. For each field pattern of periodicity n, the configuration of the electric lines of force in the magnetron interaction space is shown at the left, the configuration of the magnetic lines threading the resonators is shown at the upper right, and anode potential waves are shown at the lower

electric field lines of the fundamental component ($p = 0$) of each mode are shown in the interaction space. Only the magnetic field lines are shown in the resonators. Below these is plotted the distribution in potential for each of the fundamentals, sin $n\theta$ and cos $n\theta$, $n = 0, 1, 2, 3,$ and 4. For the $n = 0$ mode the magnetic flux threads through all the resonators in the same direction and returns through the interaction space. That all the segments are in phase and the interaction space field is independent of angle may be seen. That there is but one π mode is also seen from the fact that the cos 4θ term corresponds to zero potential on all the anode segments. The first Hartree harmonic for the $n = 1$ mode, namely that for which $p = 1$, having seven repeats ($k = 7$) or a total phase shift of 14π radians around the anode, is also plotted in Fig. 23 in addition to the fundamental. The fact that it yields the same variation of anode segment potential around the anode as the fundamental is apparent.

If the system of N resonators were shock excited it would oscillate in all of its modes simultaneously, producing beats in a manner analogous to but considerably more complicated than that for the system of two resonators already discussed. Furthermore, if the system were forced to oscillate by an external drive whose frequency can be varied, the admittance of the system would go through a minimum at each of the mode frequencies. With each such resonance there are associated values of the Qs, characteristic admittances, energy storage capacities, and the like.

The loading of the two modes of the same value of n by the output circuit of the magnetron depends on the position of the output loop relative to the respective standing wave patterns. If the output coupling loop forms

right. The interaction field plots represent only the fundamental components in each case. The higher harmonics would affect the fields as plotted most radically near the slots in the anode surface. The arrow shown in one of the slots in each case indicates the resonator which is coupled to the output circuit. The field lines in each plot are spaced correctly relative to one another but not relative to those in any other plot. In the plot of magnetic field lines in the resonator system (shown as dashed lines), the anode is developed from the cylindrical case, the anode segments being represented by the shaded rectangles. At the center is a representation of the output loop. The magnetic lines for the $n = 0$ mode thread through each resonator in the same direction and back through the interaction space in the opposite direction as indicated by the open circles at the ends of the lines. For each mode the magnetic lines are shown for the instant when RF current flow is maximum and all anode segments are at zero potential. In the plots of anode potential, the full lines represent the potential variations with azimuthal angle θ of the fundamental components sin $k\theta$, $k = n$. θ is measured from the position of the output coupling loop. The full circles on these curves indicate the potentials of the anode segments. The dashed lines represent the cos $k\theta$, $k = n$, modes. It should be noted that the cos 4θ configuration is trivial as it yields zero potential on each anode segment at all times. The cosine curves may also be taken to represent the azimuthal variation of magnetic field intensity which is in time quadrature with respect to the corresponding sine curves of potential. Similarly, the sine curves may represent magnetic field intensity corresponding to the cosine curves of potential. For the $n = 1$ mode the potential variation for the second Hartree harmonic ($n = 1$, $p = -1$) is also plotted (actually sin 7θ is plotted instead of sin -7θ for comparison with sin θ). It is to be noted that it corresponds to the same anode segment potentials as its fundamental.

the asymmetry discussed above, one of the modes is strongly coupled and the other weakly coupled. The strongly coupled mode is that for which the anode potential wave is sine-like with respect to the cavity containing the output coupling loop as origin. In this mode the current and hence the magnetic flux in the output cavity is maximum. The fact that one of the modes of periodicity n is weakly coupled may be of significance in magnetron operation. As will be discussed later, oscillation in a loosely coupled mode, having a high Q by virtue of its being damped only by losses in the resonator system itself, may build up more rapidly under electron drive than that of the π mode. Then it is possible for the magnetron to oscillate either steadily under certain conditions, or intermittently, in an unwanted mode. For this reason it is usually necessary to provide a second asymmetry in the anode structure so as to shift the standing wave patterns of the two modes of same n most likely to offend and in this way to equalize their coupling to the output circuit.

6.4 *Higher Order Modes:* To this point in the discussion the RF circuit of the magnetron has been assumed to behave like a string of N lumped circuits coupled together in a ring, each circuit having only one natural frequency of resonance. This structure, as has been seen, has N modes of oscillation. Actually the multicavity resonator, since its constants are distributed, has an infinite number of modes of oscillation. They are to be distinguished by the nature of the variation of the RF field along the axis of the resonator system and radially in the individual resonators. Thus there may be nodal planes passing through the resonator system normal to its axis, or nodal cylinders, concentric with the axis of the system, passing through the resonators. The modes may be classified as symmetric or antisymmetric depending on whether the two ends of the system are in phase or π radians out of phase. The variation of RF voltage along the anode length is a circular sine or cosine function if the mode frequency is greater than the resonant frequency of the unstrapped resonator system and is a hyperbolic sine or cosine function if the mode frequency is less. The fundamental multiplet of N modes discussed above are symmetric modes corresponding either to no variation or to a hyperbolic cosine variation of RF voltage along the length. In these modes of the resonator system the cavities, considered as radial shorted transmission lines, resonate in their fundamental modes. Generally the frequencies of the higher order modes of the resonator system are quite far removed from those of the fundamental multiplet and only rarely need be considered.

6.5 *Other Types of Resonators:* As alluded to earlier, other types of magnetron resonators have been devised which can supply the proper alternate π mode potentials to the segments of a multisection anode. Two of these which have received some consideration by magnetron designers

but which have not come into general use will be mentioned in passing. One, the so-called "serpentine" anode structure, consists of a single slot, cut into the anode body, which winds up and down the anode length and around the interaction space. It is essentially a "half-section" wave guide, closed on itself, oscillating in its fundamental at the cut-off wavelength. As one passes along the resonator, the field for this mode is uniform, but, by virtue of the geometrical arrangement, the field it supplies to the interaction space is π radians out of phase from gap to gap. Other modes correspond to integral numbers of wavelengths along the length of the "serpentine" resonator. The separation in frequency between the fundamental and the next highest harmonic generally is not as great as is desirable.

The other magnetron resonator system to be mentioned involves the use of a single toroidal cavity of rectangular cross section whose inner cylindrical surface has been removed. Across this opening are placed the anode segments, adjacent ones being connected to opposite sides. The fundamental of this cavity corresponds to the cut-off wavelength as in the "serpentine" structure. This cavity has been mentioned in the literature[20] and has received some attention during the war. It is most useful in low voltage CW magnetrons where the small interaction space makes possible a resonator with sufficiently great mode separation between the fundamental and the first harmonic.

7. Separation of Mode Frequencies

7.1 *Necessity and Means:* The frequencies of the modes of the magnetron resonator system near that of the π mode would ordinarily be closely grouped were not steps taken to separate them. Curve (a) of Fig. 25 shows the distribution of mode wavelengths for a typical 10 cm. resonator system like that of Fig. 1. It is not easy to account for the exact nature of this curve. By virtue of the fact that the mutual induction effects between circuits bear different phase relations to the self induction effects for different modes one would expect the mode frequencies to differ. However, the conditions at the ends of the resonator block, in which region the flux lines link the resonators, are extremely important and affect frequency in a way not completely explained as yet. That the end regions should have an effect is understandable since they contribute capacitance and inductance as does any other part of the resonating cavity in which there are electric and magnetic field lines. Furthermore, as might be expected, it has been demonstrated that the end conditions have a greater effect on mode frequency the lower the mode number n. This results from the fact that the field strength in a mode of periodicity n falls off inversely as rapidly as the nth power of the distance from the resonator block.

From the point of view of the electronics of the magnetron, one might

[20] This resonator is the so-called "turbator" discussed by F. Lüdi, Bull. Schweiz. Elektrotechn. Verein, Vol. 33, No. 23 (1942).

think proximity of mode frequencies to be no problem because the different modes, even if of the same frequency, generally require different conditions relating the operating parameters V and B for oscillation [see relation (14)]. From the circuit point of view, however, close proximity of the mode frequencies is clearly undesirable, for under such conditions it is possible that a second mode may be excited by the electronically driven mode which is usually the π mode. The π mode oscillation, coupled to the second mode through some asymmetry in the resonator system, under these conditions sets up forced oscillations in the second mode. The interaction field pattern of the second mode then appears as a contamination of the π mode pattern, adversely affecting the electronic interaction with the π mode.

The mode frequency separation in magnetron resonator systems generally has been accomplished by two methods which bear an instructive relation to the means by which the mode frequencies of two coupled resonators may be separated. In the two resonator system, it is clear that the mode frequency separation can be increased by increasing the coupling since the difference in mode frequencies is brought about by the mutual coupling between the circuits, as has been explained. On the other hand, mode frequency separation may also be accomplished by detuning the individual resonators relative to one another. In either case the mode frequencies separate. Under shock excitation of the system, the beat frequency, equal to half the difference in the two mode frequencies, increases, corresponding to the greater rate of interchange of energy between one resonator and the other.

In the multicavity resonator system of the magnetron these means correspond, on the one hand, to the increase of coupling by conductive connections between the resonators, or so-called straps, and, on the other hand, to the use of cavities tuned alternately to different frequencies. This latter method has been used in the so-called "rising sun" anode structure to be discussed presently.

7.2 *Strapping of the Resonator System:* The idea of strapping a magnetron anode appeared in a British attempt to lock the oscillation of the resonator system into the π mode by connecting alternate anode segments together with wire straps. Although the number of modes of such a strapped structure is not changed, since its N-fold symmetry remains, the so-called "mode-locking straps" did succeed in separating the modes and making for easier oscillation in the π mode alone. The frequency separation of the modes is not infinite, however, because the straps are not of negligible length compared to a wavelength and thus have appreciable impedance between points on the structure to which they are connected. In most magnetron resonator systems today, straps of some form or other are employed.

In Fig. 24 are shown four types of strapping including the early British

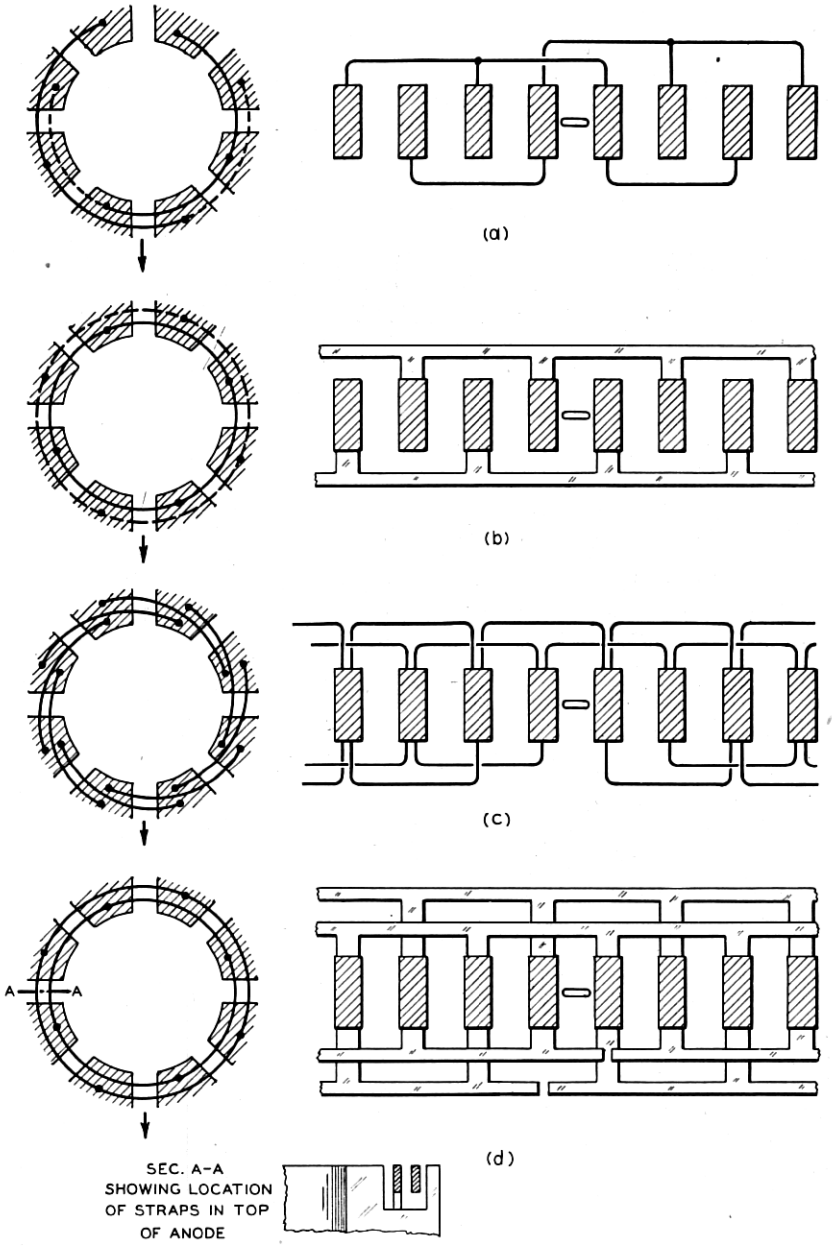

Fig. 24.—Schematic diagrams of four strapping schemes used in magnetron resonator systems. End views are shown on the left, and views rolled out as in Fig. 23 are shown on the right. (*a*) represents the early British type of unsymmetrical wire strapping, (*b*), a single ring type, (*c*), the so-called echelon type of wire strapping, and (*d*), the double ring type. In types (*a*) and (*b*) the straps on each end are at the same radius except where they overlap but are shown separated on the left-hand diagram for clarity. In types (*c*) and (*d*) the straps on the same end are at the same height and are shown as in the right-hand diagrams for clarity. The section *A*–*A* through type (*d*), shown below, indicates how the straps may be recessed into the resonator structure for shielding. The nature of the strap breaks introduced into types (*c*) and (*d*) are seen. In type (*c*) two links are removed and in type (*d*) actual breaks are made in the otherwise symmetrical rings. The breaks, shown here adjacent to the output coupling loop, are usually placed diametrically opposite.

type. In Fig. 25 are shown the distributions of mode frequency for a typical resonator system unstrapped, and strapped with three of the types of strapping shown in Fig. 24.

It is possible to account, in quite simple terms, for the shift which takes place in the mode frequency distribution when the anode is strapped. For this purpose consider a double ring strapped system like that of Fig. 24 (d). The role of the straps in determining mode frequency depends upon the relative magnitudes of their shunt inductive and capacitive effects. The

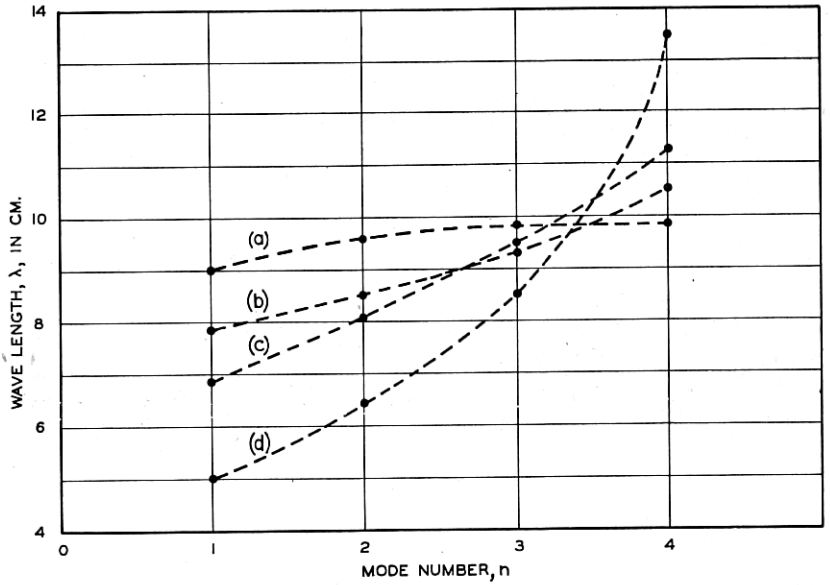

Fig. 25.—Plots of the variation of mode wavelength with mode number for a resonator system, unstrapped, or strapped in different ways. Curve (*a*) is for the unstrapped anode structure. Curve (*b*) is for the same structure strapped as shown in Fig. 24 (*a*), curve (*c*) for the same structure strapped as shown in Fig. 24 (*b*), and curve (*d*) for the same structure strapped as shown in Fig. 24 (*d*). It is to be noted how the wavelength increases for large n and decreases for small n as the "strength" of strapping is increased.

capacitive effect of the straps for any mode depends upon the amount of shunt capacitance added relative to that already present in the resonators and upon the positions in the system to which they are connected. This latter determines the average phase difference between the rings and thus their potential difference per unit RF voltage excitation. Similarly, the inductive effect of the straps depends upon the magnitude of their shunting inductance relative to that in the resonators. However, the important consideration concerning the points to which the straps are connected is the phase differences between points along the resonator system to which a

given ring is connected. This determines the amount of current which the strap carries.

In the case of the π mode the two straps are π radians out of phase, each strap being connected to points which are in phase and at potential maxima [compare Figs. 23 and 24 (d)]. Their effect is predominantly capacitive. The only currents flowing in the straps are the charging currents of the strap capacitances. If a resonator system having a total capacitance C, a total inductance L, and a π mode angular frequency ω_0, is strapped by a strapping system which adds a total capacitance C_s to the resonator system, the new frequency is

$$\omega_0' = 1/\sqrt{L(C + C_s)} = \omega_0/\sqrt{1 + C_s/C}.$$

The change in frequency is thus specified by the so-called "strength" or "tightness" of the strapping implied in the ratio of strap to resonator capacitance.

For modes of lower pericdicity, $n < N/2$, the average potential difference between the straps and thus their capacitive effect is less because the straps connect points on the resonator structure differing in phase by less than π radians. This corresponds to the shunting of a resonant line by a capacitance nearer the voltage node, at which point it would have no effect. On the other hand, a *given* ring now connects points on the anode whose potentials differ in phase. The ring thus provides additional conducting paths for the circulating RF currents in the resonator system. These paths are essentially shunt inductances across the resonators which reduce the over-all inductance of the resonator system, shifting the mode to shorter wavelength. As mode number decreases the two straps come closer together in potential but each strap connects points of greater potential difference. Thus the capacitive effect decreases, the currents carried by the straps and hence the inductive effect increase, resulting in a progressive depression of mode wavelength.

In Fig. 25 the curves (a), (b), (c), and (d) represent the progression from the unstrapped case, (a), through three successive cases of increasing strength of strapping. This increase in strength of strapping has resulted both in an increase of strap capacitance and a decrease of strap inductance as the increase of π mode wavelength and the decrease of mode wavelengths for smaller n demonstrates. It is accomplished by increasing both the inter-strap and strap-to-body capacitances as well as the cross sectional area of the straps.

The magnitude of the inductance of a strap depends on its physical length between the points on the anode structure to which it is connected. As this length increases, the strap inductance increases and hence has less effect as a shunt path. For this reason, the effectiveness of a given strapping scheme in producing separation of mode frequencies is reduced if the anode

diameter is increased for higher voltage operation or to accommodate a greater number of resonators around the anode periphery.

Finally, it should be pointed out that the location of the straps at the ends of the anode structure causes their effectiveness to reduce with increasing anode length. As anode length is increased, the mode frequency distribution approaches that of the unstrapped resonator system of infinite length.

7.3 *Asymmetries in Strapping—Strap Breaks:* Of very great importance to the operation of a strapped resonator system is the degree of symmetry in the strapping system. The early British strapping is not symmetrical around the anode. The other three types shown in Fig. 24 are symmetrical except for breaks which are usually incorporated at least on one end of the anode. These asymmetries in the strapping provide the most convenient method of incorporating in the resonator system the additional asymmetry needed to orient the standing wave patterns of doublet modes with respect to the output circuit of the magnetron so as to equalize their loading. In addition, the strap asymmetries are arranged so as not to affect the symmetrical distributions of voltage and current in the resonator system for the π mode but to destroy such symmetry to an appreciable extent for other modes. For example, the destruction of the symmetry of the $n = 3$ mode pattern in a system of eight resonators by a single asymmetry in the strapping amounts to its contamination with a field component of periodicity corresponding to $n = 1$. Since the voltage and magnetic field values at which this contaminating component may be driven by the electrons are considerably farther removed from the π mode values than are those of the $n = 3$ mode, one has effectively converted the $n = 3$ mode into another mode less troublesome electronically.

In the echelon strapping of Fig. 24 (c) the asymmetry is produced by removal of two of the connecting links. The breaks in the strip or ring straps of Fig. 24 (d) are located as shown in the center of a link between two strap "feet". The break is thus at a current node in the strap for the π mode and has no effect on the pattern symmetry of this mode. For the other modes, however, the breaks appear at points where currents would normally flow and so represent sharp discontinuities in the structure for these modes.

In connection with strapped resonator systems there are two further points which should be mentioned. The first of these is the necessity in some cases of shielding the straps from the interaction space. The inner ring straps, mounted on the ends of the anode structure, present potentials to the interaction space which are independent of angle. This amounts to a perturbing $n = 0$ like component in the field pattern which is particularly strong near the ends of the anode and which affects magnetron operation adversely

in the manner already discussed in Section 4.5 *Effect of Other Components in the Interaction Field.* It can be removed by shielding the straps as shown for the case of the double ring straps in the section A-A of Fig. 24 (d). The shields, being parts of the anode segments, maintain the proper potential distribution in the interaction space. The echelon straps of Fig. 24 (c), since they overlap, need not be shielded.

Secondly, the location of the straps at the ends of the resonator system has an effect on the amount of variation of RF voltage along the length of the anode in the π mode. For anodes of length approaching a half wavelength or greater, this may become great enough to warrant attention. It is instructive, in this connection, to consider the anode structure as being made up of two circular strip transmission lines, the straps at the ends of the structure, between which there are connected at intervals N "half-section" wave guides, the N resonators of the system. Since the resonant frequency of the system is less than that of an individual resonator, the resonators act as inductances connected across each set of straps and as wave guide connections between the sets of straps operating beyond cut-off, the RF voltage varying hyperbolically along their lengths. Since the two ends of the anode structure are in phase, the mode is symmetric about the median plane and the variation of RF voltage along the axis is expressed by the hyperbolic cosine.

7.4 *The "Rising Sun" Resonator System:* The second type of magnetron resonator system in which the mode frequencies may be separated sufficiently well to allow "clean" operation in the π mode is an unstrapped structure involving the use of resonant cavities of two sizes so arranged that adjacent cavities are alternately large and small. This resonator system, called the "rising sun" system, accomplishes mode frequency separation by a means analogous to the increase in separation of the mode frequencies of a system of two coupled resonators achieved by relative detuning of the individual resonators. At the Columbia Radiation Laboratory during a series of experiments with asymmetries in an unstrapped resonator system, designed to achieve good operation in a harmonic of one of its doublet modes rather than in the π mode, it was observed that as the natural frequencies of the two sets of resonators were separated the mode frequencies diverged in two groups as though each group corresponded to one of the two sets of resonators and that in this configuration the π mode was quite well separated from the other modes. Thus the system appeared to be well suited for π mode operation, providing a means of mode separation without the use of straps. As such it is particularly adaptable to use in magnetrons of short wavelength where straps become very small and extremely difficult to construct.

A "rising sun" resonator system for $N = 18$ is shown in Fig. 26. The distribution of its mode frequencies is shown in Fig. 27, together with distributions for unstrapped and strapped eighteen resonator systems which have the same π mode frequency. It is seen that the modes of the "rising sun" resonator system arrange themselves into two groups or branches. Since the anodes are quite "long" (approximately $3\lambda/4$) the distribution for the unstrapped case having uniform resonator size [curve (a)] approximates the distribution for an anode of infinite length. It is reversed from the

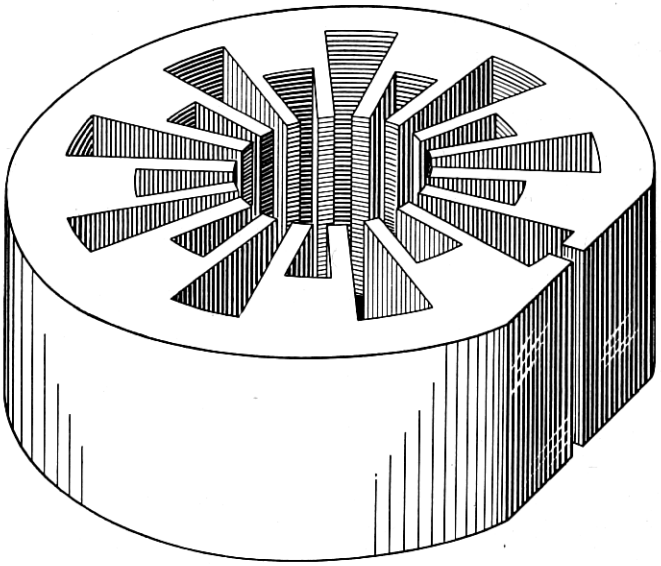

Fig. 26.—A so-called "rising sun" type resonator system having eighteen resonators. The slit at the "back" of the resonator in the right foreground is to be connected to the output circuit (compare Fig. 30).

unstrapped distribution of Fig. 25, curve (a), in which the end effects upon modes of small n are appreciable.

In the system of two coupled resonators, whether or not they are tuned individually to the same frequency, it has been seen that there are two mode frequencies corresponding to oscillations of the coupled system in which the resonators are in phase or π radians out of phase. In the "rising sun" system one observes two *groups* of mode frequencies corresponding to oscillations of the coupled *systems* of resonators in which corresponding

modes of the component systems, that is, modes of the same pattern periodicity, add in phase or π radians out of phase. Thus the modes of a "rising sun" system having eighteen resonators corresponding to $n = 0, 1, 2, \cdots, 8$, and 9 are to be compounded of the two sets of modes for the large and

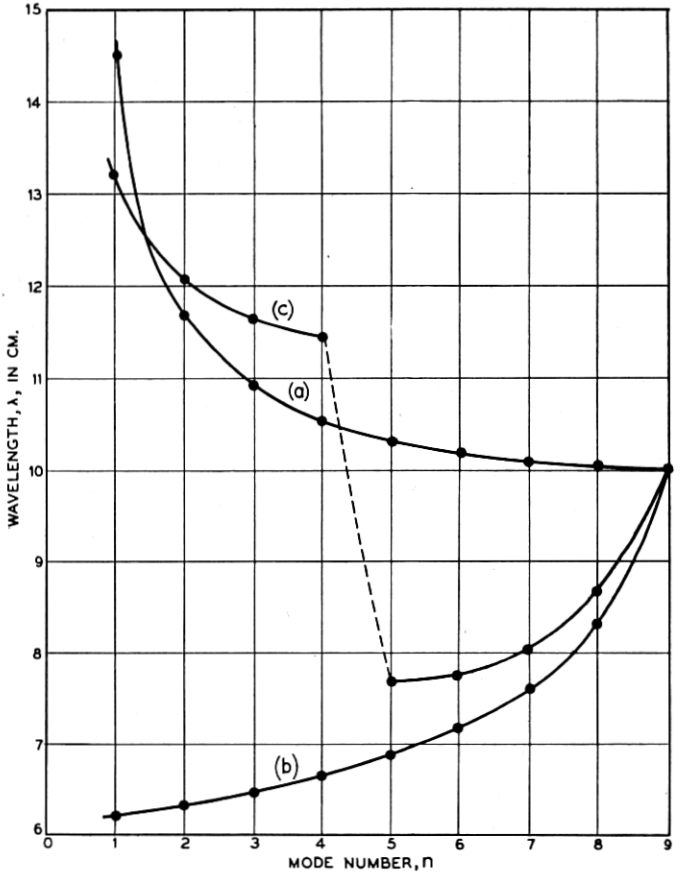

Fig. 27.—Plots of mode wavelength as a function of mode number for three different resonator systems of eighteen resonators having the same axial length and π mode wavelength. Curve (*a*) is for an unstrapped resonator system of identical resonators. Curve (*b*) is for a "heavily" strapped resonator system having identical resonators. Curve (*c*) is for a "rising sun" type resonator system having a ratio of resonator wavelengths of 1.8.

small resonators, each set including modes of periodicities $n' = 0, 1, 2, 3,$ and 4. The two $n' = 0$ modes when added in phase give the $n = 0$ mode of the whole system but when added π radians out of phase give the $n = 9$ or π mode of the whole resonator system. This latter fact is perhaps made more clear by the observation that in the $n = 9$ or π mode all the large

resonators are in phase and π radians out of phase with all the small resonators. Similarly the $n' = 1$ modes of the two component sets of resonators added in phase give the $n = 1$ mode, added π radians out of phase give the $n = 8$ mode. The $n' = 2$ modes yield the $n = 2$ and $n = 7$ modes of the total resonator, and so on. Modes of the component resonator systems of different periodicities do not add as they are uncoupled in the same sense as two modes of a resonator system with resonators all of the same size. The curve showing the distribution in mode frequency from $n = 0$ to $n = 4$ thus has the usual shape for increasing periodicity of the field pattern. The distribution in mode frequency for the remaining modes, however, is reversed in form and, as n goes from 9 down to 5, appears as a distribution should for which the mode periodicity increases. The two branches of the mode frequency distribution curve thus appear as approximate mirror images which are shifted relative to one another along the frequency scale by virtue of the difference in phase of the mutual coupling between the two sets of resonators. As far as frequency is concerned, the π mode of the total system has the characteristics of a mode whose field pattern is independent of angle, and its frequency is well separated from those of other modes.

As in the case of both unstrapped and strapped symmetrical resonator systems, equivalent circuits have also been devised and studied for the "rising sun" structure. Suffice it to say here concerning them that in each case it has been possible to explain and predict the mode frequency behavior to a surprising degree of accuracy.

As a magnetron resonator the "rising sun" system has both advantages and disadvantages. Its most obvious advantages are its lack of strapping with consequent ease of construction for short wavelengths and the ability to make an anode structure of any length with no penalty in mode frequency separation. Although the frequency separation of the π mode from other modes is not as great as is possible in strapped magnetrons, its independence of anode length and the fact that it can be realized at higher values of N are both important for high power magnetrons. Furthermore, the "rising sun" structure, having no strap losses, possesses an inherently higher unloaded Q than strapped resonator systems. This results in an improvement in circuit efficiency by a factor which may be as high as 1.2 at 1.25 cm. wavelength.

The major disadvantage of the "rising sun" resonator system is the presence in its π mode interaction field of a strong admixture of a component independent of angle. How this comes about may be seen from the following considerations: The π mode frequency of the composite resonator system lies somewhere between the free oscillation frequencies of the large and small resonators. When oscillating in the π mode, therefore, the large resonators are longer and the small resonators shorter than an equivalent

quarter wavelength. Said another way, the electrical distance from the back of a large resonator to its opening in the anode, across the segment face, and to the back of the adjacent small resonator is an electrical half wavelength along which the voltage and current vary approximately sinusoidally. For this reason the maximum in the RF voltage and the corresponding current node do not appear at the mouth of either cavity but at a point (M of Fig. 28) somewhat inside the opening of the large cavity. This means that the electric field across the mouth of the larger cavity is greater than that across the mouth of the smaller cavity. The excess, since all the large cavities are in phase, adds up around the anode to form an electric field

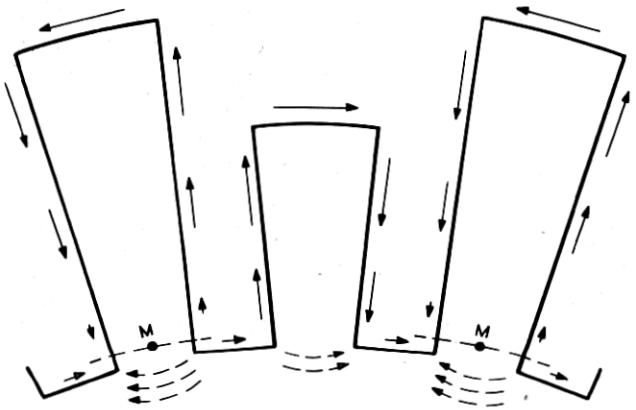

Fig. 28.—A diagram illustrating the origin of the component independent of angle in the π mode interaction field of the "rising sun" resonator system. The length of the arrow lying parallel to and just inside the resonator wall at any point is proportional to the magnitude of the RF current flowing there. The RF current node, and hence RF voltage maximum, occurs at M, inside the mouth of the larger cavity. Note that this gives rise to currents flowing in the faces of the anode segments which are in the same direction around the interaction space and that the RF field strength across the mouth of a larger cavity is greater than that across the mouth of a smaller cavity. This latter is indicated schematically by means of the dashed arrows.

component independent of angle like the $n = 0$ mode field in Fig. 23. Further, it is seen in Fig. 28 that at any instant there are currents flowing across the faces of the anode segments which are all in the same direction around the anode. With this net circumferential current is associated the unidirectional RF magnetic field component parallel to the axis shown also in Fig. 23.

The amount by which the two sets of mode frequencies of the "rising sun" structure are separated increases with increasing ratio of resonator sizes. Corresponding to this, the amount of $n = 0$ like component in the interaction field increases.

The presence of the component independent of angle in the interaction

field is thus an inherent characteristic of the "rising sun" resonator system. One is faced with the problem of designing for sufficient mode separation without unduly increasing this component. How the presence of this component in the interaction field perturbs the electronic interaction with the π mode, resulting in a performance characteristic like that of Fig. 20, has already been discussed.

8. Output Circuit and Load

8.1 *Output Circuit:* In the general physical description of the centimeter wave magnetron whose constituent parts are shown in Fig. 1 there remains the discussion of the output circuit. The output circuit is the means of coupling the fields of the magnetron resonator to the load and as such it must contrive to induce a voltage across a coaxial line or a waveguide to which the load circuit is connected. Several types of coupling are involved in magnetron construction. These are illustrated schematically in Fig. 29. Here the resonator of the magnetron is represented by a simple L—C circuit and any transformer action of the output circuit between the resonator and the load is to be accounted for by the unspecified network T. The scheme of Fig. 29 (a) involves magnetic coupling, that of (b), electrostatic coupling, those of (c) and (d), two forms of direct coupling.

Type (a), it is clear, corresponds to the output coupling accomplished by a loop, like that shown in Fig. 1, feeding a coaxial line. The loop may be placed inside the cavity as in Fig. 1, may be placed above the resonator in the end space as in the case of the so-called "halo" loop, or may be placed with its plane parallel to the axis of the anode between the resonators in the end space. In each case the coupling is effected mainly by linking of magnetic lines of force by the loop. The coupling is not entirely magnetic, however. There is electrostatic induction in the loop by the anode segments near it, corresponding to coupling of type (b) of Fig. 29, and in the case of the third possible placement of the loop listed above, there is involved some direct coupling of the type (c) of Fig. 29 since the loop is terminated on an anode segment on which there is RF potential.

In most cases the coaxial line must expand in dimensions from the loop extremity, pass through the vacuum envelope, and be provided with a means of coupling to the coaxial load line of the system in which the magnetron is used. The output circuit from the loop to the smooth line of the system must provide the transformer action necessary to load the loop by an admittance which gives the desired Q [see equation (23)]. What this admittance must be is dependent, to be sure, on the size and position of the loop, that is, upon the degree to which it couples the magnetic lines in the resonator. Generally, the attempt is made to build the transformer

into the magnetron, preferably inside the vacuum envelope where any large standing waves present are less likely to cause RF voltage breakdown.

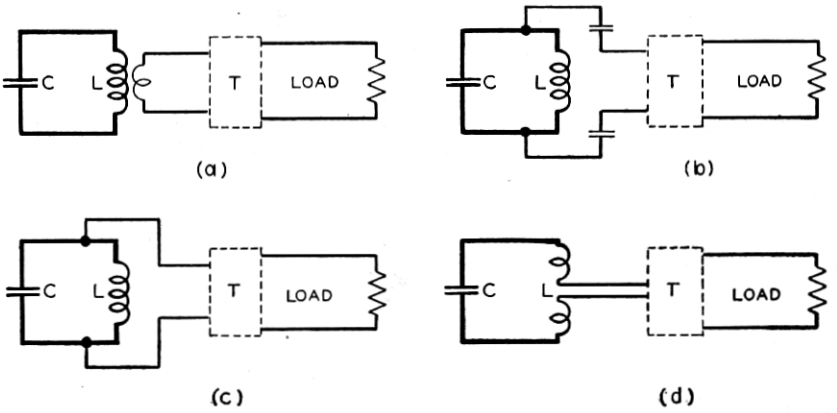

Fig. 29.—Schematic circuit diagrams representing four types of output couplings Type (*a*) is magnetic coupling, (*b*), electrostatic, (*c*) and (*d*), two forms of direct coupling. The unspecified network *T* represents the output circuit between the points where it couples to the resonator system and the load.

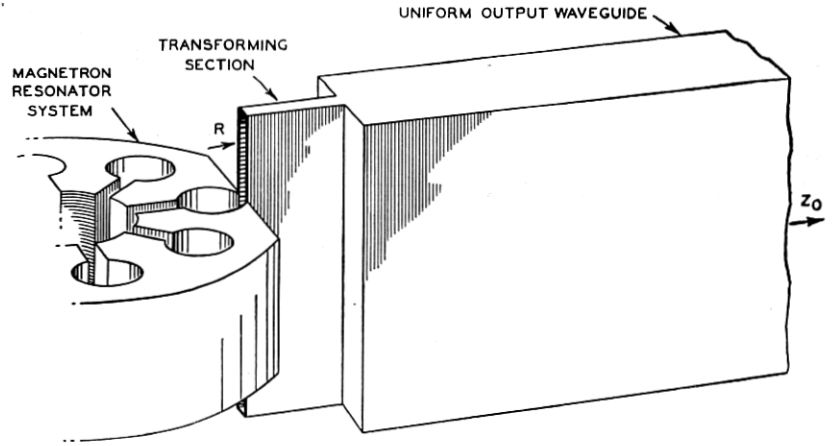

Fig. 30.—An example of a type of waveguide output circuit. It is representative of the type of coupling of Fig. 29 (*d*). Other types of resonator systems may be used (compare Fig. 26), and the transforming section, for example, may be of dumbbell-shaped cross section rather than of rectangular cross section as shown.

The type of magnetron output circuit represented schematically by Fig. 29 (d) is the so-called waveguide output. Here one of the resonators is broken into by means of a slit as shown in Fig. 30. Attached to this slit is a transforming section which feeds directly into the load waveguide. The im-

pedance, R, at the resonator presented by the output circuit must be small. The characteristic impedance, Z_0, of the waveguide is large. The transformer usually consists of a quarter wavelength section of characteristic mpedance equal to the geometric mean of R and Z_0, $\sqrt{RZ_0}$. The vacuum seal is made by a dielectric window in the waveguide. The quarter wave transformer section may be a parallel plate transmission line cut in the resonator block or may be a waveguide line of rectangular or dumb-bell shaped cross section. Here again, the specific amount of its transformer action must be adjusted, usually by variation of the small dimension, until it provides the proper value of Q_{ext}.

Another type of output circuit involves coupling a coaxial line directly onto the straps. This represents practically a pure case of the type of coupling shown in Fig. 29 (c).

8.2 *Load:* The load admittance which the output line presents to the output circuit of the magnetron oscillator depends upon the characteristic admittance, Y_0, of the line and upon the manner in which the line is terminated. In discussing the single resonator of the magnetron resonator system as a section of lossless transmission line terminated by a short circuit, the input admittance and its relation to the standing waves on the line were mentioned. Since the termination reflects all the energy incident upon it in the shorted line, the voltage standing wave ratio, σ, defined as the ratio of the maximum voltage to the minimum voltage along the line, is infinite. The input admittance of a shorted section of length ℓ has been given in equation (26).

In the general case in which the line is terminated by an admittance, Y_T, not all the energy incident upon the termination is reflected, the standing wave, whose position is determinated by the phase of Y_T, has a finite value of σ greater than unity, and the input admittance is given by the expression

$$Y = Y_0 \frac{Y_T + jY_0 \tan \frac{2\pi\ell}{\lambda}}{Y_0 + jY_T \tan \frac{2\pi\ell}{\lambda}}. \tag{29}$$

If the voltage reflection coefficient, $\vec{r}$, is defined as the ratio of the complex voltage amplitudes of the reflected and incident waves, A_R and A_I,

$$\vec{r} = \rho e^{j\phi} = \frac{A_R}{A_I},$$

the standing wave ratio may be written

$$\sigma = \frac{|A_I| + |A_R|}{|A_I| - |A_R|} = \frac{1 + \rho}{1 - \rho},$$

and the input admittance, Y, expressed as

$$Y = Y_0 \frac{1 - \vec{r}}{1 + \vec{r}}.$$

Conversely:

$$\vec{r} = \rho e^{j\phi} = \frac{\sigma - 1}{\sigma + 1} e^{j\phi} = \frac{1 - Y/Y_0}{1 + Y/Y_0}. \tag{30}$$

If the line is matched, that is, terminated in its characteristic admittance, $Y_T = Y_0$, it is clear that the input admittance, Y, is equal to Y_0, the voltage reflection coefficient, $\vec{r}$, is zero and the voltage standing wave ratio, σ, is unity.

These concepts are recalled here because they are used in specifying the magnetron load. The remaining point of interest with respect to admittance relationships on transmission lines is the transformation of admittance which occurs in going through a line of variable characteristics such as the output circuit of the magnetron. Such a section of nonuniform line may in general be considered as a lossless transducer, the admittance transformation through which is expressed as a bilinear form. In terms of the reflection coefficient $\vec{r}_2$ looking into the load at the output terminals of the transducer, the reflection coefficient $\vec{r}_1$, looking into the transducer at its input terminals may be written thus:

$$\vec{r}_1 = e^{-j\vec{\alpha}_{12}} \frac{\beta_{12} + \vec{r}_2 e^{j\vec{\alpha}_{21}}}{1 + \beta_{12} \vec{r}_2 e^{j\vec{\alpha}_{21}}}. \tag{31}$$

In this expression the number β_{12} and the angles $\vec{\alpha}_{12}$ and $\vec{\alpha}_{21}$ are the three parameters completely describing the transducer, which for lossless transducers are real numbers.

9. Equivalent Circuit Theory

9.1 *The Equivalent Circuit:* From time to time in the discussion thus far, reference has been made to a lumped constant circuit or circuits which may be considered to be equivalent to the resonator system, output circuit, and load of the magnetron oscillator. One is now in a position to appreciate the justification for the use of such a simple, singly resonant circuit to represent as complex a device as the magnetron. As has been pointed out, this justification lies in the ability to separate the mode frequencies and to diminish sufficiently well, excitation of all modes except the π mode. Further, in the discussion of the equivalent circuit shown in Fig. 2, it was pointed out how the output circuit and the electronics may be treated by circuit analysis. This particular equivalent circuit will now

be discussed in some detail. From an analysis of this circuit it will be explained how the power which the magnetron delivers and the frequency at which it oscillates depend upon the load attached to it.

Consider now the equivalent circuit shown in Fig. 2, or as repeated in Fig. 31 (a). Since the N cavities of which the magnetron resonator system is composed are essentially in parallel for the π mode, the C of the equivalent circuit is N times the capacitance and the L is $\frac{1}{N}$ times the inductance of a single cavity. G_c is the shunt conductance representing the series resistance

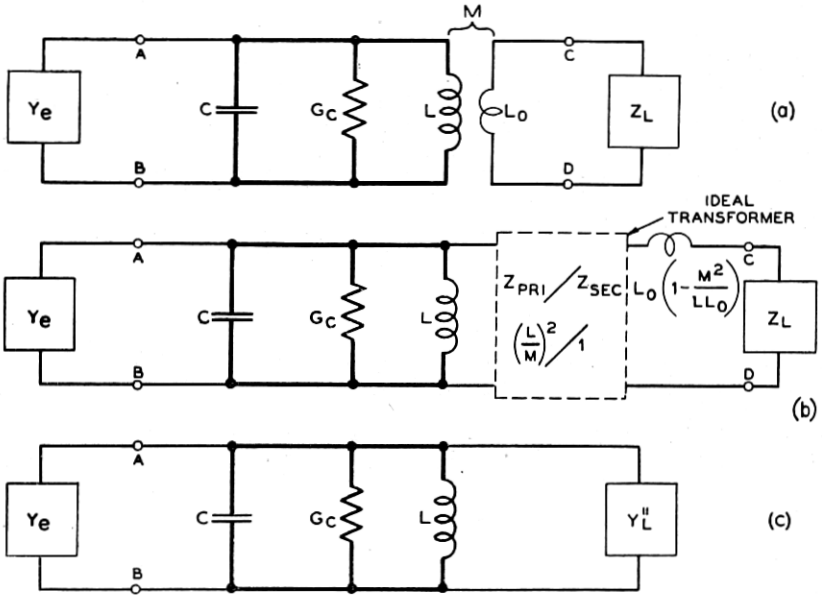

Fig. 31.—A diagram showing an equivalent RF circuit for the magnetron oscillator, (*a*), and how this circuit may be reduced in two steps, (*b*) and (*c*), to a simpler form.

in the copper walls of the resonator system, L_0, the inductance of the output loop which is coupled by the mutual inductance, M, to the lumped inductance of the equivalent resonating circuit. Z_L represents the impedance of the load at the loop terminals. Thus it represents the load impedance to which the magnetron is attached, transformed through the output circuit to the loop terminals.

The first step in understanding the circuit of Fig. 31 (a) is to reduce it to a simpler form. This is done in two steps as shown in Fig. 31. The inductances L and L_o, with mutual inductance M between them, form a transformer through which the impedances in the secondary circuit, $j\omega L_0$ and

Z_L, are reflected into the primary circuit. It may be shown[21] that the circuit of Fig. 31 (b) is the equivalent of that of Fig. 31 (a). The coupling into the primary circuit is represented by an ideal transformer connected across the primary inductance L to the secondary winding of which are connected the load impedance Z_L and a reduced loop reactance

$$X_0 = j\omega L_0\left(1 - \frac{M^2}{LL_0}\right).$$

The ideal transformer effects a voltage transformation of $\frac{L}{M}$:1 or an admittance transformation of $\left(\frac{M}{L}\right)^2$:1 from its secondary to its primary terminals. Thus, the admittance, Y_L'', presented at the primary terminals of the ideal transformer, is

$$\begin{aligned} Y_L'' = G_L'' + jB_L'' &= \left(\frac{M}{L}\right)^2\left(\frac{1}{X_0 + Z_L}\right) \\ &= \left(\frac{M}{L}\right)^2 Y_L' = \left(\frac{M}{L}\right)^2 (G_L' + jB_L') \end{aligned} \tag{32}$$

in terms of the admittance Y_L' at the secondary terminals.

The equivalent circuit has now been reduced to that of Fig. 31 (c) used earlier in the discussion of a single resonator of the magnetron resonator system. Each of the quantities defined or derived for this circuit are now to be applied to the magnetron resonator system as a whole. These include the characteristic admittance of the resonator, Y_0, the unloaded, loaded, and external Qs given by the relations (21), (22) and (23), and the circuit efficiency, η_c, of equation (25).

Looking to the left at the terminals AB into the electron stream one sees the electronic admittance $Y_e = G_e + jB_e$. This is defined in terms of the current, I_{RF}, induced in the anode segments by the electrons moving in the interaction space, and the RF voltage, V_{RF}, appearing across the resonators, that is, across the terminals AB of Fig. 31 (c). Looking into the circuit at the terminals AB one sees the admittance Y_s.

This admittance by equations (19) and (32) is

$$\begin{aligned} Y_s &= G_c + j2Y_{0c}\frac{\omega - \omega_0}{\omega_0} + Y_L'' \\ &= G_c + j2Y_{0c}\frac{\omega - \omega_0}{\omega_0} + \left(\frac{M}{L}\right)^2 (G_L' + jB_L'). \end{aligned} \tag{33}$$

[21] See Guillemin, Communications Networks, Vol. II, p. 154.

The condition for oscillation stated earlier requires that:

$$Y_e + Y_s = 0,$$

or:

$$G_e + jB_e + G_c + j2Y_{0c}\frac{\omega - \omega_0}{\omega_0} + \left(\frac{M}{L}\right)^2 (G'_L + jB'_L) = 0. \quad (34)$$

Separating real and imaginary parts, this reduces to the pair of equations:

$$\left.\begin{aligned} G_e + G_s = 0, \quad \text{or,} \quad G_e + G_c + \left(\frac{M}{L}\right)^2 G'_L = 0, \\ B_e + B_s = 0, \quad \text{or,} \quad B_e + 2Y_{0c}\frac{\omega - \omega_0}{\omega_0} + \left(\frac{M}{L}\right)^2 B'_L = 0. \end{aligned}\right\} \quad (35)$$

Since $\left(\frac{M}{L}\right)^2 G'_L$ is equal to G''_L, one may write the first of equations (35) in terms of the Qs defined by (21), (22), (23) and (24) thus:

$$-G_e = G_s = Y_{0c}\left(\frac{1}{Q_0} + \frac{1}{Q_{ext}}\right) = \sqrt{\frac{C}{L}}\frac{1}{Q_L}. \quad (36)$$

9.2 *The Rieke Diagram:* The electronic conductance and susceptance, being functions of the parameters such as V_{RF}, V, and B which govern the electronic behavior of the magnetron, are not known *a priori* except for the fact that they are undoubtedly slowly varying functions of frequency. The circuit conductance and susceptance are given by equation (33). Equations (35) state that the circuit conductance and susceptance must be the negative of the electronic conductance and susceptance respectively. It is from these relations that the behavior of the oscillator under changes of load is to be inferred.

Suppose now that one were to vary the load in such a way that only B'_L changes, G'_L remaining constant. Then, by the first of equations (35), G_s and hence G_e would not change. If, further, the frequency of oscillation changes such that

$$2Y_{0c}\frac{\Delta\omega}{\omega_0} + \left(\frac{M}{L}\right)^2 \Delta B'_L = 0, \quad (37)$$

by equations (35) B_s and hence B_e remain constant as well and the electronic operation of the magnetron involving the RF voltage, V_{RF}, is undisturbed. Since the power delivered by the magnetron is

$$P = -G_e V_{RF}^2 = G_s V_{RF}^2, \quad (38)$$

contours of constant G'_L on a plot of performance versus load, Fig. 32 (a), are thus contours of constant output power. Along any such constant

power contour the frequency of the magnetron varies linearly with B'_L as equation (37) indicates. Hence any constant frequency contour on the diagram is obtainable from a neighboring contour of different frequency through translation in the direction of B'_L by an amount given by equation (37). The form of the contours of constant frequency depends upon the interdependence of the electronic parameters G_e and B_e. The fundamental electronic performance as a function of load is specified by the conductance G_s presented to the electrons at the anode slots, changes in load susceptance being compensated for by frequency changes and hence susceptance changes in the resonator. As G'_L is varied G_s, G_e, and the output power must vary as well. If B_e is independent of these changes the constant frequency contours will correspond to lines of constant B'_L. Actually it is found that B_e does depend to some extent on G_e, resulting in the constant frequency contours on the $G'_L - B'_L$ plot being approximately straight lines inclined to the constant B'_L lines at a small angle α as shown in Fig. 32 (a).

If the $G'_L - B'_L$ plane is transformed to the reflection coefficient or $\vec{r}$ plane on which the load characteristic is usually plotted, contours of constant G'_L or power become circles tangent to the circle $\rho = 1$ at the same point. Constant B'_L contours form the set of circles orthogonal to these. The contour of constant frequency of Fig. 32 (a) transforms to a circle which intersects all the contours of constant power at the angle α.

Fig. 32 (b) is thus the form of the characteristic depicting the dependence of magnetron performance on load, called the Rieke diagram, plotted for that point in the equivalent circuit where the admittance looking out into the load is $Y'_L = G'_L + jB'_L$. Between this point and a point in the smooth output line, with respect to which the load admittance is usually measured, there is the series reactance X_o and the output circuit of the magnetron, forming a transducer through which the reflection coefficient defining the load admittance may be transformed by the expression (31). In undergoing such a transformation the contours of constant power and frequency plotted on the $\vec{r}$ plane retain their general form although they may be rotated and expanded or contracted. Thus the general form of the Rieke diagram shown in Fig. 32 (b) should be the same as that experimentally determined and plotted on a reflection coefficient plane for a point in the output line. Fig. 33 is such a Rieke diagram and its resemblance to that of Fig. 32 (b) is apparent.

9.3 *Magnetron Circuit Parameters:* The fact that the circuit theory of the magnetron based on the simple equivalent circuit of Fig. 31 (a) explains the nature of the Rieke diagram so well is ample justification for its use. The parameters which specify the equivalent magnetron circuit may be

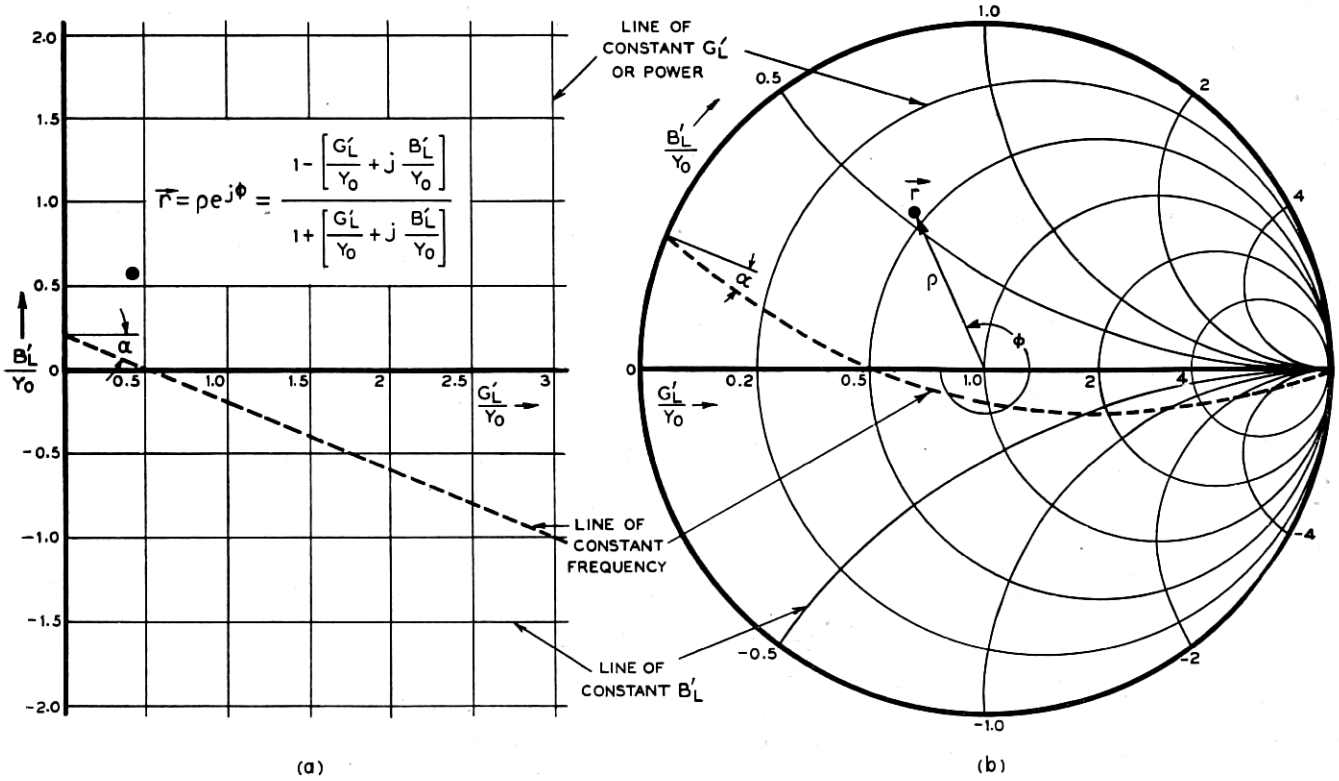

Fig. 32.—Charts showing how the G'_L–B'_L plane of (*a*) transforms to the $\vec{r}$ plane of (*b*) under the bilinear transformation written out in the upper half of chart (*a*). A line of constant magnetron frequency is shown plotted on chart (*a*) and in its transformed position on chart (*b*). Note that all the straight lines of (*a*) becomes circles in (*b*) with angles of intersection preserved. Note also the transformation of the admittance point represented by the filled circle. The configuration of constant G'_L lines, corresponding to constant output power, and constant

determined as a function of frequency by a measurement of the impedance Z_c looking into a non-oscillating magnetron through its output circuit and an independent measurement or calculation of one of the parameters such as C or Y_{0c}. The impedance Z_c in terms of the equivalent circuit is the impedance across the terminals CD in Fig. 31 (a) looking to the left with

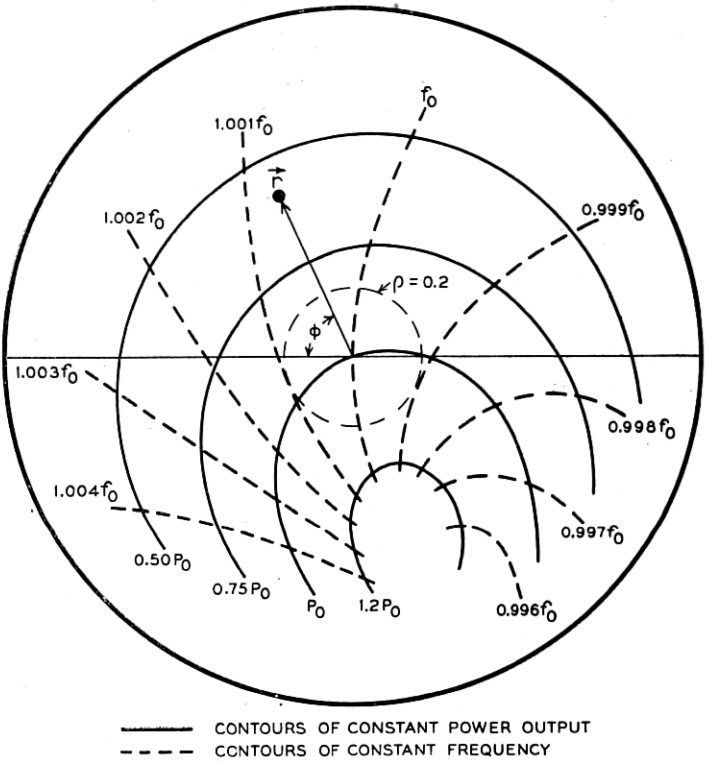

Fig. 33.—A typical experimental Rieke diagram for magnetrons in the centimeter wavelength range. The $\rho = 0.2$ circle indicates a pulling figure of 0.02 f_o *mc/s* for this example. Present practice is to couple long wavelength magnetrons more tightly to the load and short wavelength magnetrons less tightly to the load than this. The rotation of the diagram from the position of the contours of chart (*b*) of Fig. 32 is attributable to the transformer action between the terminals of the ideal transformer of the circuit of Fig. 31 (*b*) and the point in the output line to which the experimental diagram is referred.

the terminals AB open circuited. From the circuit of Fig. 31 (b) this is seen to be

$$Z_c = j\omega L_0\left(1 - \frac{M^2}{LL_0}\right) + \left(\frac{M}{L}\right)^2\left[\frac{1}{G_c + j2Y_{0c}\dfrac{\omega - \omega_0}{\omega_0}}\right] \qquad (39)$$

which, using equation (21), becomes

$$Z_c = jX_0 + \left(\frac{M}{L}\right)^2 \frac{1}{Y_{0c}} \left[\frac{1}{\frac{1}{Q_0} + j2\,\frac{\omega - \omega_0}{\omega_0}}\right] = R_c + jX_c \tag{40}$$

The experimental data may be given in terms of the values of R_c and X_c plotted as functions of ω as shown in Fig. 34. The value of X_0 is deter-

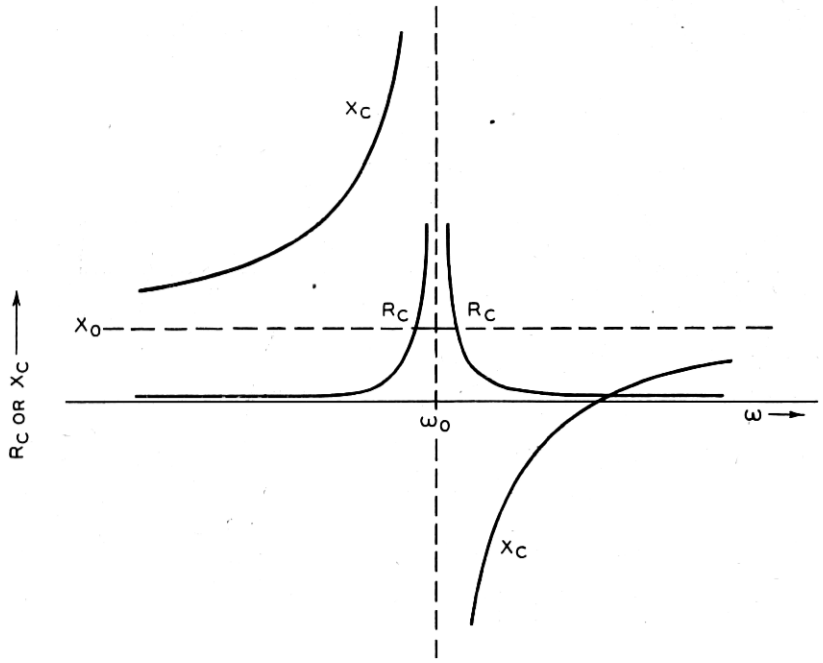

Fig. 34.—A plot of the resistive and reactive components of the impedance $Z_c = R_c + jX_c$, looking into a non-oscillating magnetron through its output circuit [terminals CD of Fig. 31 (*a*)]. Note the symmetry of the reactance about the point (ω_o, X_o) determining the value of X_o, the loop reactance.

mined by the fact that the reactance curve is antisymmetric about the point (X_0, ω_0). When X_0 has been determined one may determine the admittance, $\frac{1}{Z_c - jX_0}$, at the terminals of the ideal transformer of Fig. 31 (b). In terms of the circuit parameters this admittance is

$$\frac{1}{Z_c - jX_0} = \left(\frac{L}{M}\right)^2 Y_{0c}Q_0 + j2Y_{0c}\left(\frac{L}{M}\right)^2 \frac{\omega - \omega_0}{\omega_0}. \tag{41}$$

The conductance term, $\left(\frac{L}{M}\right)^2 Y_{0c}Q_0$, is independent of frequency and the susceptance term, $2Y_{0c}\left(\frac{L}{M}\right)^2 \frac{\omega - \omega_0}{\omega_0}$ varies linearly with frequency. If these quantities are plotted from experimental data as functions of ω, the values of Q_0 and $\left(\frac{L}{M}\right)^2 Y_{0c}$ may be determined. To determine the individual values of the factors in $\left(\frac{L}{M}\right)^2 Y_{0c}$ for a given magnetron, it is necessary to calculate or somehow to measure a value for $Y_{0c} = \sqrt{\frac{C}{L}} = \omega_0 C = \frac{1}{\omega_0 L}$. When used with ω_0 this yields values for L, C, and M. How this is done will not be explicitly discussed here. From the values of Q_0 and Y_{0c}, values of Q_L, Q_{ext}, and η_c may be calculated for any magnetron load G_L'' by the relations (21), (22), (23), and (25). There are other methods of extracting the Q values from the experimental data than that presented above.

When values of the circuit parameters are available one can calculate the values of G_s and B_s from which G_e and B_e are obtained. From the output power the RF voltage is then calculable by equation (38), and from this and the electronic admittance the in-phase and quadrature components of the RF current may be obtained. Using the circuit efficiency, η_c, now determined as a function of load, one can obtain the dependence of the electronic efficiency, η_e, as a function of load conductance from experimental values of the over-all efficiency, η, measured along a constant frequency contour of a Rieke diagram ($\eta = \eta_e\eta_c$). The plot of Fig. 19 was obtained in this way. One is now in possession of values for each of the parameters upon which the electronics of the magnetron depends and may study the relations between them.

9.4 *Pulling Figure:* The Rieke diagram completely specifies the dependence upon load of the magnetron output power and frequency of operation. Nevertheless, it is convenient to be able to specify by a single parameter the dependence of operating frequency on load changes. The preceding discussion has shown that the changes in load conductance reflected into the resonant circuit of the magnetron, that is, specified at either the primary or secondary terminals of the ideal transformer of Fig. 31 (b), vary output power only. Further, if G_e and B_e are unrelated, load susceptance changes specified at the same points vary frequency only. Since G_e and B_e are in fact related, constant frequency contours on the $G_L'-B_L'$ plane, as has been seen, are inclined to constant B_L' lines at the angle α. Thus changes in B_L' are more effective by the factor $1/\cos\alpha$ in affecting frequency

than equation (37) would indicate. The quantity calculated for $\frac{\Delta\omega}{\Delta B_L'}$ from equation (37) multiplied by the factor $1/\cos\alpha$ is a parameter which specifies the dependence of frequency on load. It may be specified at any value of load admittance Y_L', that is, for any position on the ρ plane. Generally, however, one considers the rate of change of frequency with susceptance at matched load, for which Y_L' is equal to the characteristic admittance Y_0' of the output line at the point in question. Using the parentheses $(\ )_0$ to indicate that the quantity enclosed is measured at the match point and incorporating the factor $1/\cos\alpha$, one obtains from (37):

$$\left(\frac{\Delta\omega}{\Delta B_L'}\right)_0 = \frac{1}{2}\left(\frac{M}{L}\right)^2 \frac{\omega_0}{Y_{0c}} \frac{1}{\cos\alpha}. \tag{42}$$

The quantity $\left(\frac{\Delta\omega}{\Delta B_L'}\right)_0$ as it stands is not a convenient one to measure For this reason it is customary to specify the total excursion of frequency, $\Delta f = \frac{\Delta\omega}{2\pi}$, resulting from a standard variation in $\Delta B_L'$, namely, that obtained by the total possible phase variation of a standing wave of 1.5 voltage ratio in the line at the point in question. This is equivalent to traversing the $\rho = 0.2$ circle on the reflection coefficient plane, shown on Fig. 33. It can be shown that such a variation of load admittance results in a variation of susceptance of $\pm$ 0.41 times the characteristic admittance of the line, Y_0', corresponding to a total susceptance variation of 0.82 Y_0'. When determined in this way the total frequency excursion is called the pulling figure, PF. Hence by equation (42)

$$PF = \Delta f = \frac{\Delta\omega}{2\pi} = \frac{1}{2}\frac{2\pi f_0}{2\pi}\left(\frac{M}{L}\right)^2 \frac{.82 Y_0'}{Y_{0c}} \frac{1}{\cos\alpha}$$

$$= 0.41\, f_0 \frac{\left(\frac{M}{L}\right)^2 Y_0'}{Y_{0c}} \frac{1}{\cos\alpha}. \tag{43}$$

Since $Y_0' = (G_L')_0$, the quantity $\left(\frac{M}{L}\right)^2 Y_0'$ in this expression is recognized as $(G_L'')_0$, the load admittance at the primary terminals of the ideal transformer when the line is matched at the point in question, namely, the secondary terminals. Using this fact and equation (23) the pulling figure is seen to be:

$$PF = 0.41\, f_0 \frac{(G_L'')_0}{Y_{0c}} \frac{1}{\cos\alpha} = \frac{0.41\, f_0}{(Q_{ext})_0} \frac{1}{\cos\alpha}. \tag{44}$$

Although this equation was derived for a specific point in the equivalent circuit, it is of general validity at any point in the output circuit or load line of the magnetron, provided the quantity $(Q_{ext})_0$ is properly interpreted as the external Q measured at match in the line at the same point.

10. Special Topics

10.1 *Frequency Stabilization:* The degree of stability of the operating frequency of the magnetron to load changes is specified by the external Q, as equation (44) indicates. The external Q, by equation (23), may be increased either by decreasing the load conductance, G_L'', or by increasing the circuit characteristic admittance, Y_{0c}. The first alternative may be accomplished by reduction of the coupling between the load and magnetron resonator system. Although this results in greater frequency stability, it entails a reduction in output power. Increase of the characteristic admittance of the magnetron resonator system, on the other hand, increases the energy storage capacity as indicated by equation (20) without appreciably changing the output power. Frequency stability may be increased in this way either by redesign of the magnetron resonator system or by coupling to it a tuned cavity of high unloaded Q. In the latter case, the degree of stabilization, defined as the ratio of energy stored in the combination of magnetron resonator system and stabilizing cavity to the energy stored in the magnetron resonator system alone, is the factor by which the external Q is increased and the pulling figure decreased. In actual practice the stabilizing cavity may be coupled into one of the magnetron resonator cavities or may be built into the output circuit.

10.2 *Frequency Sensitive Loads:* In the preceding sections it has been seen how the load admittance, among other parameters, determines the frequency at which the magnetron oscillates. If this load admittance is itself a function of frequency, it may be possible for the condition of oscillation to be satisfied at more than one frequency. This fact makes for an uncertainty of operation, which is to be avoided. Should the load fluctuate for example, as it does in many applications, the oscillation may jump discontinuously from one frequency to another. If the magnetron is pulsed, it may in certain circumstances oscillate at different frequencies on successive pulses. A tunable magnetron operating into a frequency sensitive load exhibits periodic gaps in its tuning characteristic in which the magnetron cannot be made to operate.

The discussion here will be limited to the specific type of frequency sensitive load consisting of a long line terminated in an admittance, assumed to be frequency insensitive, which differs from the characteristic admittance of the line. The input admittance of such a line is represented by a reflec-

tion coefficient of amplitude, ρ, depending only on the termination [see equation (30)], and of phase, ϕ, depending only on the frequency, f, and the line length, ℓ. Thus:

$$\phi = \frac{2\pi\ell}{\lambda/2} = \frac{4\pi\ell f}{c},$$

from which

$$f = \frac{c\phi}{4\pi\ell}. \tag{45}$$

This equation expresses the linear relation between frequency and phase for the load, specified by the reflection coefficient, into which the magnetron operates. The heavy dashed lines in Fig. 35 represent this relation for two particular line lengths, ℓ_1 and ℓ_2, with ℓ_2 very much longer than ℓ_1. The difference in line length, $\ell_2 - \ell_1$, corresponds to an input phase difference of many times π radians. For the case in Fig. 35, however, this is chosen as an integral multiple of π so that the curve, plotted for the fundamental period 0 to π, will lie in the same range.

The variation of operating frequency of the magnetron with variable phase of the load reflection coefficient is a periodic function whose amplitude increases with increasing amplitude, ρ, of the reflection coefficient. This function may be determined graphically from a Rieke diagram of the magnetron, like that shown in Fig. 33, by traversing the appropriate circle concentric with the center of the diagram and plotting the frequency of operation against phase. In Fig. 35 are plotted such curves for two values of ρ corresponding to different terminations at the end of the long line.

A more detailed analysis of the condition of oscillation shows that it is possible for the magnetron to oscillate stably at those intersections of the magnetron and load frequency characteristics at which the slope of the load line is greater than the slope of the magnetron characteristic. Thus, as indicated in Fig. 35, oscillation may occur at only one frequency for the line of length ℓ_1 if $\rho = 0.2$ but at two frequencies if $\rho = 0.5$. In the latter case the middle intersection, indicated by an open circle, does not correspond to stable oscillation. For a line of length ℓ_2, on the other hand, two oscillation frequencies are possible at both $\rho = 0.2$ and $\rho = 0.5$. If in either case the line lengths ℓ_1 and ℓ_2 are increased by only an approximate quarter wavelength, corresponding to a phase change of $\pi/2$ radians, the light dashed lines labelled ℓ_1' and ℓ_2' in Fig. 35 represent the load characteristics, and oscillation can occur at only one frequency with ρ equal either to 0.2 or 0.5.

If one considers the relationships depicted in Fig. 35 it becomes clear that there are two critical relationships between ρ and ℓ. The first specifies the

values of ρ and ℓ which if exceeded makes oscillation possible at more than one frequency at all phases of the load reflection coefficient. The second specifies the values of ρ and ℓ which must not be exceeded if oscillation is to be possible at only one frequency for all phases of the load reflection coefficient. This latter relation between ρ and ℓ is that for which the slope of the load line is equal to the slope of the magnetron characteristic at its point of inflection.

From what has been said it would appear that the use of long load lines is to be avoided if at all possible. If the magnetron is pulsed and the line

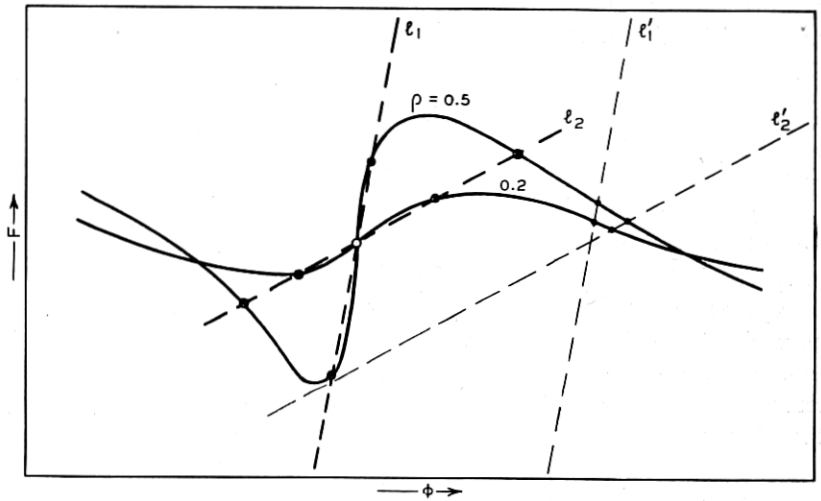

Fig. 35.—Plots of the frequency characteristics of a magnetron and a frequency sensitive load for two magnitudes of reflection coefficient, ρ, and two line lengths, ℓ. The ordinates are frequency and the abscissas are phase angle of the reflection coefficient in the fundamental period 0 to π radians. Stable oscillation occurs at the intersections indicated by filled circles. The open circle indicates a point of unstable operation for the three conditions $\rho = 0.5$ and $\ell = \ell_1$, $\rho = 0.5$ and $\ell = \ell_2$, and $\rho = 0.2$ and $\ell = \ell_2$. In addition, it indicates a point of stable operation for $\rho = 0.2$ and $\ell = \ell_2$. These four points are coalesced on the figure for simplicity. The lines ℓ_1' and ℓ_2' indicate how stable operation at both $\rho = 0.2$ and 0.5 may be attained by an increase of line length of approximately a quarter wavelength.

is sufficiently long, however, it is possible for the oscillation in a pulse to have been completed before any energy reflected from the termination has arrived back at the magnetron. Under these circumstances the magnetron operates into an effectively infinite line which presents its characteristic admittance to the magnetron output. For a pulse of one microsecond duration this would require a line length of about 150 meters. Usually such lengths are not possible or are undesirable by virtue of attenuation, and either the line is made sufficiently short or its length critically adjusted or the standing wave on it reduced so as to cause operation to occur at a single

frequency. Studies have been made of the transient conditions prevailing near the beginning of a pulse when, in establishing the steady state, the successive reflections are returning to the magnetron and, as a consequence, its frequency is changing. Except in a limited region on the Rieke diagram where operation is completely uncertain, it has been shown that the magnetron will settle down to operation at one frequency dictated by the phase of the first reflection, even if oscillation at two frequencies by the previous analysis is possible. Gaps in the tuning curve of a tunable magnetron correspond to the periodic traversal of this uncertain region as the frequency is varied and the load reflection coefficient moves around a constant ρ circle on the Rieke diagram.

10.3 *Magnetron Tuning:* To tune the magnetron oscillator it is necessary to vary a susceptance somewhere in its circuit. It has already been observed how variation of load admittance when reflected into the resonator system as a susceptance change results in frequency pulling. Although for other reasons this variation is usually limited by output circuit design to the order of 0.1% of the operating frequency, it could be increased and used in special instances as a means of tuning the magnetron. Similarly the susceptance of a stabilizing cavity coupled into the resonator system may be varied by tuning the cavity. This method in general enables one to tune over a wider range than does variation of load susceptance since the resonator system is usually more tightly coupled to the stabilizing cavity than it is to the load.

The largest tuning ranges have been attained, however, when it has been arranged to vary one of the frequency determining parameters of the magnetron resonator itself. Schemes have been devised which alter primarily either the inductance or the capacitance of the resonant cavities. Variation of the inductance has been found more convenient at the shorter wavelengths and variation of the capacitance easier at longer wavelengths.

Variation of the inductance may be accomplished by the insertion of a conducting pin into each resonator where the RF magnetic lines of force are concentrated. In a system of hole and slot type resonators it is arranged to move the pins in and out along or near the axes of the holes. Such an arrangement is shown schematically in Fig. 36 (a). As the pins are inserted they reduce the volume available for the magnetic flux, thus reducing the inductance and increasing the frequency. Tuning ranges as great as $\pm 7\%$ of the mean frequency have been attained by this means. In spite of the fact that the ratio of strap to resonator capacitance remains nearly constant, the separation of mode frequencies, as might be expected, decreases with increasing frequency because of the increase in strap inductance resulting from increase of its electrical length. The effect is not so large,

however, that with reasonable tightness of strapping difficult is encountered with mode frequency separation.

Variation of the capacitance may be accomplished by moving a member in the vicinity of the region of large distributed capacitance of the resonators. One such tuning scheme is that shown in Fig. 36 (b) in which a member shaped like a "cookie cutter" is moved in and out of annular grooves in one end of the resonator block, the other end of which is usually strapped. As the member is inserted the mode frequencies decrease. The frequency range available for π mode operation is limited by the fact that the fre-

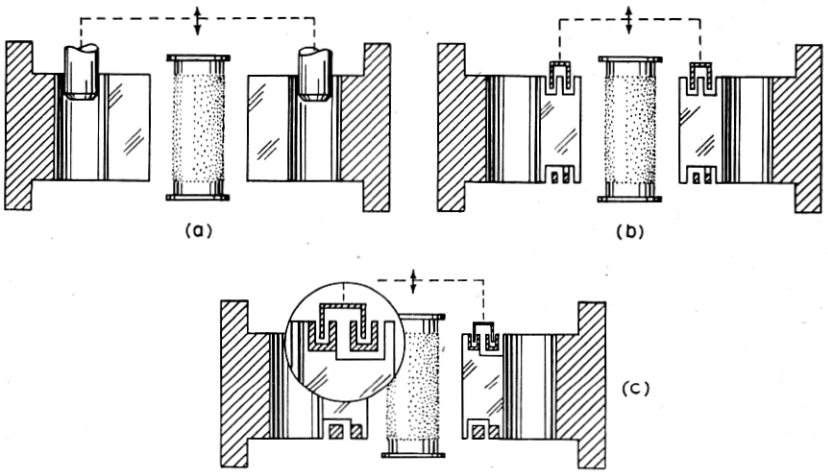

Fig. 36.—Schematic diagrams showing three types of tuning schemes which have been used in magnetron resonator systems. The views represent sections on a diametral plane through the anode structure. The cathode is shown in the center of each part of the figure. The resonators are of the hole and slot type. (*a*) shows the scheme involving variation of the inductance by means of tuning pins, (*b*), the scheme involving variation of resonator capacitance, and (*c*), that involving variation of strap capacitance. Each of the last two schemes is accomplished with a "cookie cutter" shaped member.

quencies of modes of smaller n, which are normally higher than that of the π mode, change faster and eventually cross the π mode frequency.

To understand what determines the frequency of resonance in any mode, it is sufficient to consider the inductances and capacitances present in the average sector of the resonator system across which there is a half wavelength azimuthal variation of RF potential with an extremum at either end. In the π mode of an $N = 8$ resonator system, one may thus consider one eighth of the system, namely, a single resonator; in the $n = 1$ mode, one may consider half of the resonator system. In the case of the half wavelength sector for the $n = 1$ mode, across which the potential varies monotonically (see Fig. 23), the four resonators may be considered as connected essen-

tially in series, making up an equivalent resonator oscillating at the $n = 1$ mode frequency. If one considers further, for the sake of argument, that there is no coupling between resonators, all the modes would have the same frequency but the net inductance and capacitance of the equivalent resonator for each mode of periodicity n, would be proportional to $N/2n$ and $2n/N$, respectively. Thus for the $n = 1$ mode, the equivalent L is four times and the equivalent C is one quarter of the respective values for the π mode. The tuner capacitance added to the equivalent resonator for the $n = 1$ mode, on the other hand, may be considered to be approximately a series-parallel arrangement of capacitances each of which is that between the tuner and one anode segment, C_T : the two parallel capacitances at the positive anode segments connected in series through the tuner ring with the two parallel capacitances at the negative anode segments, the combination having a net capacitance C_T. For the π mode, the net tuner capacitance added per half wavelength potential variation is made up of two capacitances each of magnitude one half of that between the tuner and one anode segment, connected in series through the tuner; the net tuner capacitance is thus $C_T/4$.

By similar reasoning for any mode, one may conclude that the added tuner capacitance per half wavelength sector increases as n decreases, while the net resonator capacitance across which the tuner is shunted decreases as n decreases. In this way the increased effectiveness of the tuner in varying the mode frequencies of the low periodicity modes is accounted for. In actuality the resonators in the half wavelength variation of RF potential are not in simple series connection because of the phase relations between them; the approximation improves for smaller n. Also because of the phase relation between adjacent resonators, the adjacent tuner to segment capacitances are not charged to the same potential and so are not actually in simple parallel connection. Furthermore, the coupling between resonators is important. These considerations modify the above argument somewhat but do not affect the conclusions reached as to the trend of tuning for the different modes. In all the tuning schemes described, second order effects come in through change in the electrical lengths of the straps and tuner as the frequency is varied.

If one arranges to vary the characteristics of the straps by means of a movable tuning member as in the scheme of Fig. 36 (c), considerably greater tuning ranges may be achieved than by the means just described. In this instance, the straps are enlarged to channels of U-shaped cross section, in and out of which the tuning member of "cookie cutter" shape is driven. The effect of insertion of the tuning member is to increase the capacitance per unit length of the strap system by increasing the interstrap capacitance and to decrease the inductance per unit length by effectively increasing the

cross sectional area of the straps. The effects of these changes upon the mode frequencies may be seen from the considerations of the effect of straps on the mode frequencies of the unstrapped resonator system already discussed. The increase in strap capacitance increases the wavelength of the π mode; the decrease in strap inductance decreases the wavelength of modes of smaller n. As the tuning member is inserted, the mode frequencies separate, and no limitation on the range of operation in the π mode is imposed by interference from other modes. This means has been used for tuning ranges of better than $\pm 6\%$, but there is nothing inherent in the scheme to prevent its use for ranges considerably in excess of this value.

Tuning of the magnetron resonator system by any of the means described above alters its characteristic admittance, $Y_{0c} = \sqrt{\frac{C}{L}}$, and hence the stored energy. For fixed output coupling and load admittance this amounts to a variation of the effective loading as specified by the external Q. In some cases, attempts have been made to compensate for this by designing into the output circuit a frequency characteristic which keeps the external Q, and hence the pulling figure, more nearly independent of frequency.

Each of the tuning schemes described above is adaptable to precise and specific frequency adjustment or to frequency variation at a slow rate. For tuning over small ranges it is possible to vary the magnetron frequency electronically, enabling one to frequency modulate its output at a high rate. Of the schemes tried for this purpose there may be mentioned that in which an intensity modulated electron beam of a specific velocity is shot parallel to a superposed DC magnetic field through one of the magnetron resonators or a closely coupled auxiliary cavity.

Concerning the variation of magnetron operating frequency will be mentioned finally the shifts which are brought about by temperature variations of the resonator block. Since the resonator system is generally constructed entirely of copper, it expands or contracts uniformly with temperature and the frequency shifts are those attained by a uniform scaling of the resonator system by a very small factor. The temperature coefficient of frequency may readily be seen to equal the negative of the linear coefficient of thermal expansion of copper.

10.4 *Electronic Effects on Frequency:* In Section 3.6 *Induction by the Space Charge Cloud* it has been seen that the electrons moving in the interaction space of the magnetron oscillator contribute an admittance Y_e connected to the resonator system. The magnitude of the negative electronic conductance determines the energy delivered to the circuit and thus the amplitude of oscillation. The electronic susceptance, arising from the phase relation between the space charge spokes and the maximum of the tangential

retarding field, affects the frequency of oscillation. Under equilibrium conditions the magnitude of the current, I_{RF}, induced in the anode segments, its phase relative to the RF voltage between the segments, and the operating frequency adjust themselves such that this admittance, $Y_e = I_{RF}/V_{RF}$, equals the circuit admittance Y_s. The induced RF current and its phase relative to the RF voltage both depend upon the parameters such as V and B, governing the electronic operation of the magnetron. The frequency change at constant load arising from changes in V or B when divided by the change in the DC current, I, drawn by the magnetron, is called the frequency "pushing" and is measured in mc/s per ampere.

A further effect of the electronic susceptance is the shift of the resonant frequency between the oscillating and non-oscillating conditions of the magnetron. In general the oscillating frequency is lower than the resonant frequency of the non-oscillating magnetron. Thus the electronic susceptance is capacitive with the space charge spokes moving somewhat ahead of the field maxima during oscillation. This shift in the resonant frequency is important in pulsed radar systems where the same antenna is used for both receiving and transmitting. An echo of the transmitted pulse on its return then encounters a high, off-resonance impedance at the magnetron which absorbs very little of the returned energy. Most of the received pulse energy is consequently made available to the receiver. For some magnetrons the shift off resonance is not sufficient and other means such as the use of the so-called ATR box are required to divert the received pulse energy into the receiver.

10.5 *Frequency Spectrum of a Pulsed Magnetron:* Only if a generator operates for an infinitely long time is its output "monochromatic", that is of a single frequency. The period of operation of a CW oscillator is generally long enough to make any deviations from this unobservable.

If, however, the oscillation is modulated as in the case of pulsed magnetrons for which the pulse duration is of the order of one microsecond, it is readily detectable that the output is "polychromatic" with the energy distributed throughout a band of frequencies. The plot of the distribution in frequency of the energy generated is called the frequency spectrum.

This state of affairs is perhaps made plausible if one considers pulsing the magnetron to be a very drastic means of amplitude modulating its output. Already, in connection with the case of two coupled circuits, it has been seen how amplitude modulation of an oscillating system in time has associated with it the distribution of the energy over more than one frequency. In an analogous but more complicated manner, a sinusoidal oscillation which is amplitude modulated by a nonsinusoidal pulse shape like that of Fig. 37 (a) is compounded of frequencies not now discrete but

distributed continuously throughout a band, Fig. 37 (a′). The energy distributions in time and frequency are related mathematically by the Fourier transform.

The breadth of the frequency distribution is inversely proportional to the modulating pulse width as shown in Fig. 37. The spectrum widths of operating magnetrons may exceed the theoretical width by a factor of not more than two for reasons not altogether clear.

10.6 *Oscillation Buildup—Starting:* Of importance in the design and operation of pulsed magnetrons are the phenomena associated with the buildup of oscillation when the voltage is applied. Here will be discussed briefly what is known about the problem, the factors upon which the rate of buildup of oscillation in the circuit depends, how this is related to the rate

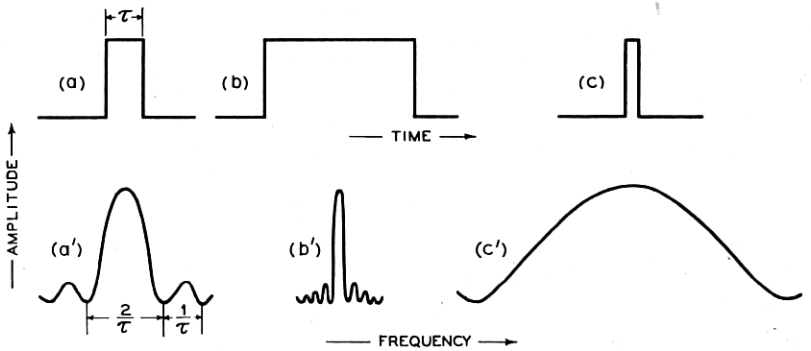

Fig. 37.—Plots of DC voltage pulse shapes (*a*), (*b*), and (*c*) and the frequency spectra (*a′*), (*b′*), and (*c′*) resulting from each, respectively. These are shown for the idealized case of perfectly rectangular voltage pulse shapes.

of voltage buildup and to pulser characteristics, and how these factors result in various types of magnetron starting behavior.

The rate of buildup of oscillation in the magnetron depends not only upon the circuit characteristics but also upon the electronic behavior with increasing DC and RF voltages. Because of the nonlinear nature of the electron interaction, the amount of energy fed to the circuit per cycle is dependent upon the amplitude of the oscillation. Considering the condition for oscillation given by the first of equations (35) and expanding it to include during buildup a term to account for the energy being stored in the resonators, one may derive a simple expression for the rate of increase of RF voltage amplitude. The energy stored in the circuit at any instant being $W = CV_{RF}^2$, the rate at which energy is being stored is $\frac{dW}{dt} = 2CV_{RF}\frac{dV_{RF}}{dt}$.

This corresponds to a conductance term, G, obtained by equating $\frac{dW}{dt}$ and GV_{RF}^2:

$$G = 2C \frac{dV_{RF}}{dt} \frac{1}{V_{RF}}. \tag{46}$$

The necessary condition for oscillation during buildup is thus:

$$G_e(V_{RF}) + G_s + G = 0, \tag{47}$$

from which one obtains

$$G_e(V_{RF}) + G_s + 2 \frac{C}{V_{RF}} \frac{dV_{RF}}{dt} = 0. \tag{48}$$

Since oscillation in the magnetron does in fact build up, $| G_e(V_{RF}) |$ must be greater than G_s when oscillation starts. When equilibrium is reached, $G_e(V_{RF}) + G_s = 0$. Thus $| G_e(V_{RF}) |$ must be a decreasing function of V_{RF} crossing the value G_s at the operating point. By equation (48), V_{RF} thus builds up rapidly at first and then more slowly as $| G_e(V_{RF}) |$ approaches G_s.

Increase in load, resulting in an increase of G_s, decreases the rate of oscillation buildup.[22] The dependence on the total resonator capacitance indicates that for magnetrons of different sizes related by a simple scale factor, G_e and G_s under such scaling presumably remaining invariant, the rate of buildup decreases with increasing wavelength. Unknown in relation (48) is, to be sure, the exact transient dependence of G_e on RF and DC voltages, magnetic field, and interaction space geometry. It is known, however, that an increase of cathode diameter, although it is accompanied by a decrease in electronic efficiency, does reduce the difficulty with "modding" resulting from failure to start in the π mode.

Associated with the rate of buildup of RF oscillation in determining magnetron starting behavior is the rate at which the DC voltage is applied. From the discussion of the electronics of the magnetron it is clear that oscillation is not possible at all values of V but only for a limited range near that which provides synchronism between the electron motion and the rotating field pattern. If the pulser can apply a voltage which rises to a value in this region and which can remain at substantially this value regardless of the current drawn, no difficulty is encountered. However, should the pulser regulation be such that to secure operation at a given voltage

[22] This is directly the opposite of the behavior with respect to load variations of a circuit being driven in such a way that a constant amount of energy is fed in per cycle, in which case the rate of buildup is inversely proportional to Q.

and current it is necessary to apply a voltage which on no load would rise to a value considerably higher than the operating value, the rate at which the voltage passes through the range of possible operating values and the relation of this rate to that of RF buildup are extremely important. Should the pulse voltage rise so rapidly as to pass through the region where oscillation is possible before the RF oscillation can build up and cause the magnetron to pass current, which by modulator regulation keeps the DC voltage from rising further, the magnetron fails to start. Clearly, the more rapid the oscillation buildup the more rapid a voltage rise is permissible. Conversely, for a given rate of DC voltage rise, failure to start should appear at greater load and longer wavelength as relation (48) implies. Experience has corroborated both of these conclusions. It is also clear by equation (48) that the equalization of loading of the doublet modes of the same periodicity, which is achieved by proper location of strap asymmetries, equalizes their starting times and makes possible interference with π mode starting less likely.

When oscillation in the π mode fails, the magnetron may fail to oscillate at all or may oscillate in another mode for which the operating voltage in a harmonic is higher than but close to that of the π mode. In this case, as has been seen, $\frac{2\pi f'}{|k'|} > \frac{2\pi f}{N/2}$, and the Hartree line of the "second" or "primed" mode lies just above that of the π mode. This case in which oscillation in the π mode is skipped for oscillation in another mode represents the most common type of "moding" encountered in pulsed magnetrons. If, on the other hand, $\frac{2\pi f'}{|k'|} < \frac{2\pi f}{N/2}$, and the Hartree line of the harmonic of the "second" mode lies just below that of the π mode, as in Fig. 16, the magnetron is observed to oscillate first in the "second" mode before oscillation at low currents in the π mode commences. When the mode driven during the interval at the top of the pulse is the π mode, oscillation in the "second" mode occurs only momentarily on the rise and fall of each pulse as the voltage passes through the range of operating values for this mode.

The starting behavior of pulsed magnetrons may be shown by the so-called dynamic performance chart or V-I plot on which the course in time of the voltage and current is shown. In Fig. 38 are shown three V-I plots of this type. The initial current rise is the charging current of the cathode to anode capacitance. The current rise when oscillation commences is very rapid and is shown as a dashed line. After remaining for the major part of the pulse at the operating point, indicated in Fig. 38 by a large dot, the current and voltage fall during which they follow closely a constant B line of the static performance chart (see Fig. 17).

In Fig. 38 (a) is shown the dynamic V-I plot for normal operation in the

π mode. In Fig. 38 (b) is shown a dynamic plot after the voltage control has been raised above the point of π mode failure. Here the magnetron does not oscillate at all. As seen in Fig. 38 (c), further increase of the voltage control of the pulser makes possible oscillation in the $k = -5$ ($p = -1$) harmonic of the $n = 3$ mode ($N = 8$). In both (b) and (c) of Fig. 38 it is of interest to note how the magnetron tries to oscillate in the π mode as the voltage at the end of the pulse falls through the range of permissible values. These attempts at oscillation are indicated by the magnetron drawing in this region small amounts of current which vary from pulse to pulse.

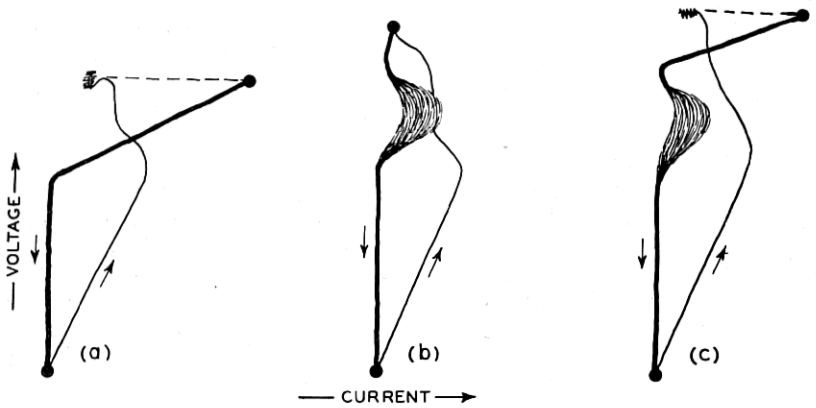

Fig. 38.—Three so-called dynamic V-I plots or dynamic performance charts illustrating the mode skip phenomenon. The plots are copies of presentations obtained with an oscilloscope whose vertical deflection is proportional to DC voltage and whose horizontal deflection is proportional to DC current. On any plot the heaviness of the lines is roughly inversely proportional to the rate at which the coordinates are traversed, and the large dot at the upper extremities represents the operating point at the top of the pulse. (*a*) shows shows normal operation in the π mode. (*b*) shows failure to oscillate in any mode, the π mode being skipped. (*c*) shows oscillation in a harmonic of a mode of smaller n.

10.7 *Magnetron Cathodes:* One important component part of the magnetron oscillator which to this point has not been discussed in detail, but which has been assumed present and operating satisfactorily, is the cathode. Its duty is to supply the electrons which serve as the intermediaries between the DC and RF fields. In terms of the usual requirements of vacuum tube cathodes, the number of electrons demanded of a magnetron cathode is little short of prodigious. Magnetron cathodes may be required to deliver current densities of the order of 50 amperes per square centimeter as contrasted with the 0.5 amperes per square centimeter emitted by oxide cathodes in high vacuum tubes normally.

How oxide surfaces are capable of emitting such enormous currents is

not yet entirely clear. It is certain, however, that the RF oscillation in the magnetron is responsible for the fact that such currents may be attained. This is made evident experimentally by measuring the current that may be drawn when the magnetic field is reduced so that oscillation is impossible and comparing it with the current drawn during oscillation. At temperatures even in excess of the operating temperature such pulsed emission currents of excellent magnetrons may run as low as 1% of the currents flowing during oscillation. Furthermore, the fields at the cathode during these measurements may actually exceed those present during oscillation because of the absence of the dense space charge clouds in the interaction space.

In the process of phase selection of electrons, as previously discussed, those electrons starting from the cathode in a phase such as to gain energy from the RF field are removed from the interaction space and driven into the cathode. They impart to the cathode the energy they have gained, causing secondary electrons to be emitted and the cathode temperature to increase. In most magnetrons the amount of this returned energy is about 5% of the input, though in some cases it may become as high as 10%. This means that the average energy of back bombardment may run as high as 75 watts per square centimeter of cathode surface. This amount of energy must be dissipated under equilibrium conditions by radiation and conduction. In general, the short wavelength magnetrons are run with no heater power supplied to the cathode, the cathode temperature being maintained by back bombardment. In many cases, cathode overheating by this process is actually the limitation on the operating capabilities of the magnetron.

There is some experimental evidence that the large current drawn from the magnetron cathode is not primarily made up of secondary electrons but may result from an "enhanced" primary emission. This is supported by the fact that the secondary electrons emitted at the return to the cathode of the "out of phase" electrons are themselves, assuming negligible emission time, largely "out of phase" electrons later to return to the cathode. However, the emission of large numbers of secondary electrons may lead to an "enhanced" primary emission by a process not now understood. As possible processes may be mentioned field emission or an actual lowering of the cathode work function, each brought about by the fields in the cathode coating which result from the charge loss attendant upon the secondary emission. Ionic conduction or electrolytic action in the coating may also contribute in some manner to a lowered work function and to the "enhanced" emission, although such ionic processes would generally involve time intervals longer than a microsecond. The actual mechanism involved, however, is still speculative.

A word about the relation of magnetron scaling to magnetron cathode

problems will here be in order. It has been seen earlier that, in scaling all magnetron dimensions by a factor α, the magnetic field changes by a factor $\frac{1}{\alpha}$ while the current and voltage remain unchanged. That this places severe requirements on the cathode may be seen by considering the scaling of a 10 cm. magnetron down to 1 cm. The operating current may be 20 amperes in both cases. If this corresponds to a current density of 5 amperes per sq. cm. at 10 cm., 500 amperes per sq.cm. will be required at 1 cm. What is more, the back bombardment in watts per sq. cm. is increased by a factor of 100. Both of these requirements are completely unreasonable and preclude direct scaling in this instance. Consequently, an attempt is made in such cases to decrease the current density by increasing both the cathode length and diameter. Increasing the latter usually involves increasing the anode diameter and the number of resonators. Even so, current densities may exceed 50 amperes per sq. cm., as stated earlier.

The pulsed magnetron cathode at the shorter wavelengths (less than 10 cm.) in the centimeter band is a limiting factor in magnetron design. In CW magnetrons the small size of the interaction space has made the cathode an important and difficult design problem throughout the centimeter wavelength region. Considerable effort has been expended in a number of laboratories not only to understand the physics of the operation of the magnetron cathode but to find suitable materials and constructional designs. It has become clear that a good magnetron cathode which will meet the special conditions of high current density and high voltage gradient and the considerable electron back bombardment are these: (1) sufficient primary emission to enable the magnetron to start and to supply a part of the required operating current; (2) sufficient secondary emission to supply the remainder (it may be practically all) of the required current density through whatever mechanism is involved; (3) sufficient active material to permit satisfactory life; (4) some mechanical means of holding the active material on the cathode surface; (5) sufficiently low electrical resistance of the coating to permit large bursts of current without undue local heating and high back bombardment without excessive coating temperature; and (6) satisfactory over-all heat dissipation characteristics, conductive and/or radiative, to keep evaporation of active material to a minimum.

In pulsed magnetrons of wavelength 10 cm. or greater it has generally been possible to use plain oxide coated cathodes. Nickel base material is generally used and the active material is the usual double carbonate coating (reduced to the oxides during activation). At wavelengths of 3 cm. and shorter the development of satisfactory pulsed magnetrons would have been impossible without the development of special cathodes. In the main,

these have been aimed at meeting requirements (3) to (5) above. The constructions have made use of wire meshes and of sintered nickel matrices both to reduce the coating resistance and to hold sufficient material on the cathode in a manner such that it may be dispensed gradually during life.

10.8 *The Magnetic Circuit:* The magnetic field required for operation of the magnetron oscillator is generally obtained, except in laboratory experiments, by means of a permanent magnet. At long wavelengths and in early models at shorter wavelengths, the magnetron and permanent magnet are separable. Building the magnetic pole faces into the magnetron structure itself and attaching the magnetic material to it has made possible the reduction of the over-all magnet gap, and hence total magnet weight, as well as the use of mechanically superior axial cathode mountings. The resulting so-called "packaged" magnetron design has been used at shorter wavelengths where the magnetic fields are high but need not extend over a large area. The total magnet weight under these conditions is much less than that required in a separate magnet. Needless to say, the possession of good permanent magnet material and the work done on magnet design have contributed materially to the success of the centimeter wave magnetron.

10.9 *Magnetron Measurements:* The fundamental measurements made on the magnetron oscillator have already been discussed or alluded to where the performance characteristics of the magnetron and its circuit theory are described. Here will be described briefly the technique of measurement.

Magnetron measurements are of two general types. One is made on the oscillating magnetron and the other on the non-oscillating magnetron. The latter may be made at any stage in the fabrication of the magnetron after its anode structure and output circuit are completed. Figs. 39 and 40 illustrate schematically the apparatus employed in these tests.

Perhaps the best way of describing the techniques of magnetron measurements is to list all of the parameters, quantities, or characteristics associated with such measurements and for each to give the definition, method of measurement or calculation, or the way it is put together from other data, as the case may be. In any event, the list given below permits of ready reference. Although the text applies directly to pulsed magnetrons the simplifications for CW magnetrons are obvious.

The *DC magnetic field*, B, in which the magnetron operates is generally supplied in the laboratory by an electromagnet, the field in the gap generally being calibrated in terms of the current passed through the magnet coils.

The *peak DC voltage*, V, applied to the magnetron cathode is measured by means of a peak voltmeter or by observing a known fraction of the voltage

pulse on the calibrated screen of an oscilloscope. In a simple but suitable peak voltmeter it is arranged to charge a condenser through a diode to the peak voltage which may then be measured with a high resistance DC voltmeter.

The *peak DC current*, I, drawn by the magnetron is measured by passing the current through a known resistance, usually one or two ohms, and determining the peak voltage developed across the resistance by means of a peak voltmeter or calibrated oscilloscope.

The *average DC current* drawn by the magnetron is the current measured on a DC meter connected in one leg of the pulsing circuit, as shown in Fig. 39.

The *pulse duration*, τ, as its name implies, is the length of the time during which the voltage, usually measured near the top of the pulse, is maintained across the magnetron. It may be determined from the pulse presentation on an oscilloscope having a calibrated sweep or it may be calculated as indicated below when other parameters are known.

The *pulse recurrence rate*, *pps*, is the repetition frequency at which the voltage pulse is applied and is determined by the frequency of the calibrated primary oscillator driving the pulser or modulator circuit.

The *duty cycle*, defined as the fraction of time the pulsed magnetron operates, may be determined as the ratio of average to peak DC current or as the product of the pulse duration and the pulse recurrence rate.

The *peak input power* is the product of the peak DC voltage and the peak DC current.

The *average input power* is the product of the peak input power and the duty cycle.

The *voltage and current pulse shapes* as observed with oscilloscopes are of importance in studying the spectrum and moding characteristics of the magnetron under test.

The *dynamic V-I plot*, or *dynamic performance chart*, is viewed on an oscilloscope in which at any instant the vertical deflection is proportional to peak DC voltage and the horizontal deflection proportional to peak DC current. Three such plots are shown on Fig. 38 and their usefulness is indicated in the corresponding text.

The *average output power* is the average centimeter wave power delivered to the useful load. The simplest and most foolproof method of measuring this power is to absorb the energy in a column of water. From a determination of the rate of water flow and its temperature rise the power may be calculated readily. The water column terminating the coaxial line or wave guide of the test apparatus is made reflectionless either by tapering it or preceding it by a quarter wavelength matching plate of proper dielectric constant, analogous to the optical quarter wave plate.

The *peak output power* may be calculated as the average output power divided by the duty cycle.

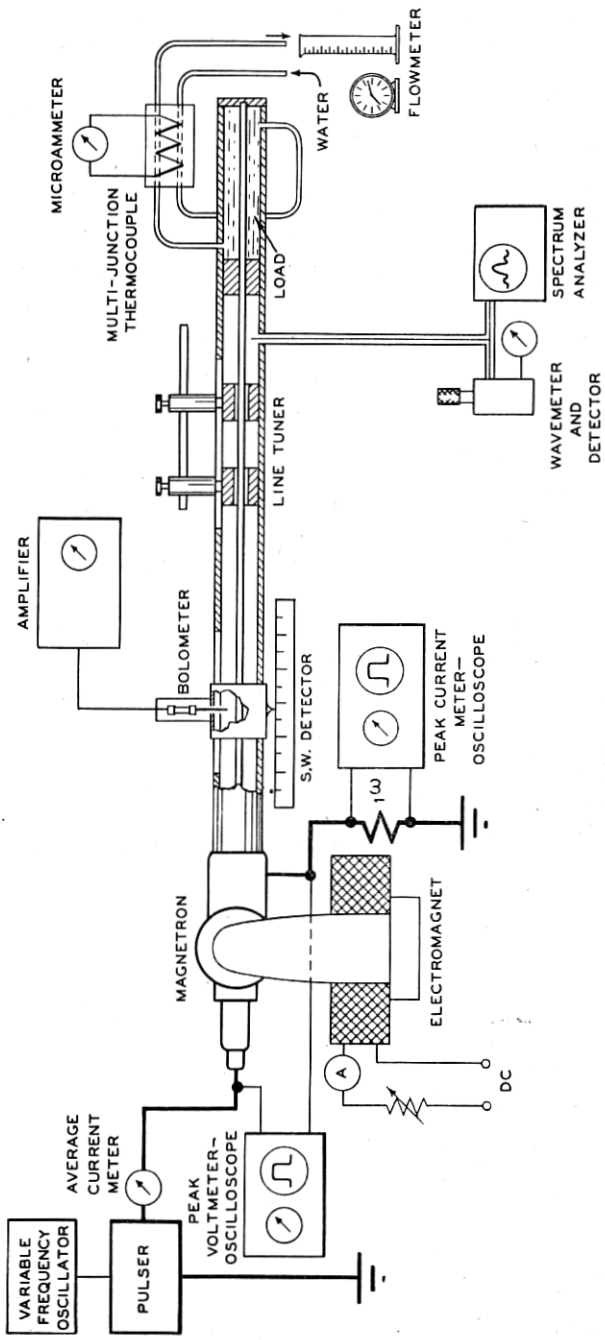

Fig. 39.—A schematic diagram showing the arrangement of apparatus generally used in making measurements on an operating magnetron in the laboratory.

The *over-all efficiency* of operation is the ratio of the peak output to peak input powers or the ratio of average output to average input powers.

The *frequency of oscillation* of the magnetron is determined by feeding a small amount of the RF power into a calibrated variable frequency resonant cavity of high Q and by means of a detector observing the frequency at which the cavity absorbs or passes power.

The *load impedance* into which the magnetron operates is determined by measurement in the output line of the voltage standing wave and its phase with respect to some previously chosen reference point. This measurement is made with a *standing wave detector* in which it is arranged to move an electrostatic probe along a section of slotted line in which it samples the RF energy in the line. The energy picked up by the probe is detected after sufficient attenuation either by a crystal or by a small bolometer whose resistance is a function of the energy fed into it. The voltage standing wave

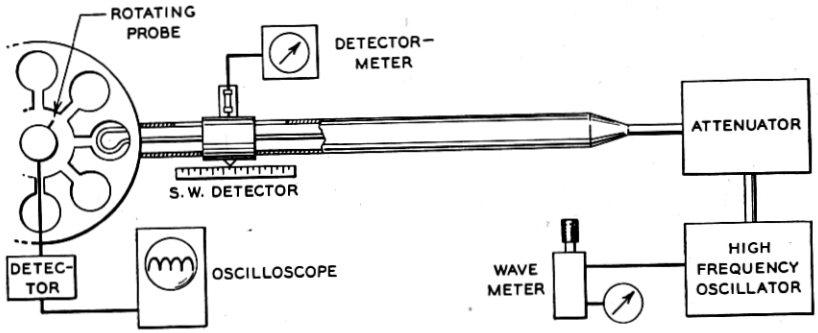

Fig. 40.—A schematic diagram showing the arrangement of apparatus used in making measurements on a non-oscillating magnetron or magnetron resonator block.

ratio and its phase may be translated into impedance, admittance, or reflection coefficient in the manner already discussed. The magnetron load impedance may be varied from the match presented by the terminating water column by means of a *line tuning section* or *tuner*. In one such line tuning section, two sleeves constituting in effect quarter wavelength lines of low characteristic impedance may be moved relative to one another to vary the magnitude, and moved together to vary the phase of the standing wave.

The *Rieke diagram*, is a plot of constant output power and frequency on a reflection coefficient plane. Its construction thus involves the measurement of output power, frequency, and load impedance as the line tuners are moved over a wide range of positions. The operating parameter maintained constant is usually chosen to be the peak DC current. Such a diagram is shown in Fig. 33.

The *pulling figure, PF*, defined as the maximum frequency excursion of the magnetron as the load reflection coefficient traverses the $\rho = 0.2$ circle, may be obtained from the Rieke diagram. It may be measured directly by two simple wavemeter measurements taken at the frequency extrema occuring as the standing wave of 1.5 voltage ratio is moved up and down the line. Various types of *standing wave introducers* have been devised to produce a reflection coefficient of $\rho = 0.2$ for the specific measurement of pulling figure.

The *performance chart* is a plot of constant magnetic field, peak output power and over-all efficiency contours on a *V-I* plane. Its construction thus involves the measurement of peak DC voltage, peak DC current, and peak output power at several magnetic fields. Sometimes frequency, pushing figure, and spectrum appearance are also determined. Figs. 17 and 20 are examples of this chart.

The *frequency spectrum* is the distribution of energy with frequency for a pulsed magnetron and is displayed on a so-called *spectrum analyzer.* This analyzer is a very narrow band tunable radio receiver whose pass band is varied periodically twenty or so times per second over several *mc/s*. The response of the receiver to the frequency distribution of energy appears on an oscilloscope whose sweep is synchronized with the pass band frequency variation.

The *pushing figure* is the instantaneous frequency change in *mc/s* per ampere change in peak DC current at constant load. It may be obtained by measuring the frequency shift on a spectrum analyzer as the pulse current is changed by a known amount. The current change must be executed rapidly enough to avoid frequency shifts arising from temperature changes.

Impedance measurements on the non-oscillating magnetron involve the use of a variable frequency RF oscillator feeding power through an attenuator and a standing wave detector into the output circuit of the magnetron (see Fig. 40). These measurements determine as a function of frequency the impedance Z_c discussed in the text.

Mode frequencies are determined from the impedance measurements on the non-oscillating magnetron by noting the frequencies at which the input standing wave is observed to go through a minimum. They may also be determined by the observation of energy maxima with a pickup loop or probe placed in the resonator system.

Mode identification is made by observing the periodicity of RF field in the interaction space of the resonator system. This is done by sampling the field with a rotating RF probe placed in an axial cylinder corresponding to the cathode as shown in Fig. 40. The probe response is detected and displayed on an oscilloscope with sweep synchronized to the rotation of the probe.

PART II

DEVELOPMENTAL WORK ON THE MAGNETRON OSCILLATOR AT THE BELL TELEPHONE LABORATORIES, 1940–1945

11. General Remarks

IN THE first part of this paper the fundamentals of the theory of the magnetron oscillator have been discussed. The objective has been to establish for the reader a general picture of the nature of the electronic mechanism and of the role played by the RF circuit and load.

In the second part of the paper is traced the research and development work done at the Bell Telephone Laboratories on the magnetron oscillator during the war years, 1940–1945. The effort was directed, for the most part, toward the development of magnetrons to meet definite radar needs.

Fifteen different types or families of magnetrons were developed at the Bell Laboratories during the war. Included among these are some 75 separate Western Electric Company or RMA code numbers. It has been found most convenient to discuss the work done on each type of magnetron as a unit, although, to be sure, there has been considerable interplay between projects. Something is said of the origin of each type, of the problems encountered in its development, and of the solution of these problems, in some cases involving studies and experiments of general interest. Special characteristics and general performance data for each type of magnetron discussed are given. Included also is a general discussion of the work done on magnetron cathodes, which, although carried out on specific magnetrons, has been of general applicability to all.

Before proceeding with the detailed discussion, it would be well for the reader to recognize the general scope of the work to be described and the general nature of the problems encountered. The work of the Bell Laboratories in the development of pulsed magnetrons for radar use has extended over practically the whole range of effort surveyed in the Introduction. Work has been done throughout the range of wavelengths from 45 cm. to 1 cm. and on magnetrons capable of developing over one megawatt peak RF power. It has included work on such features as tuning, coaxial and wave guide outputs, several types of resonator systems and strapping schemes, and on the incorporation of the magnetic circuit into the magnetron structure in so-called "packaged" types.

The scope of the developments to be described may be judged from Figs. 41, 42, 43, and 44. That part of a magnetron oscillator which perhaps best gives one an idea of size and wavelength range is the resonator block. In Fig. 41 is shown a series of resonator blocks ranging in resonant fre-

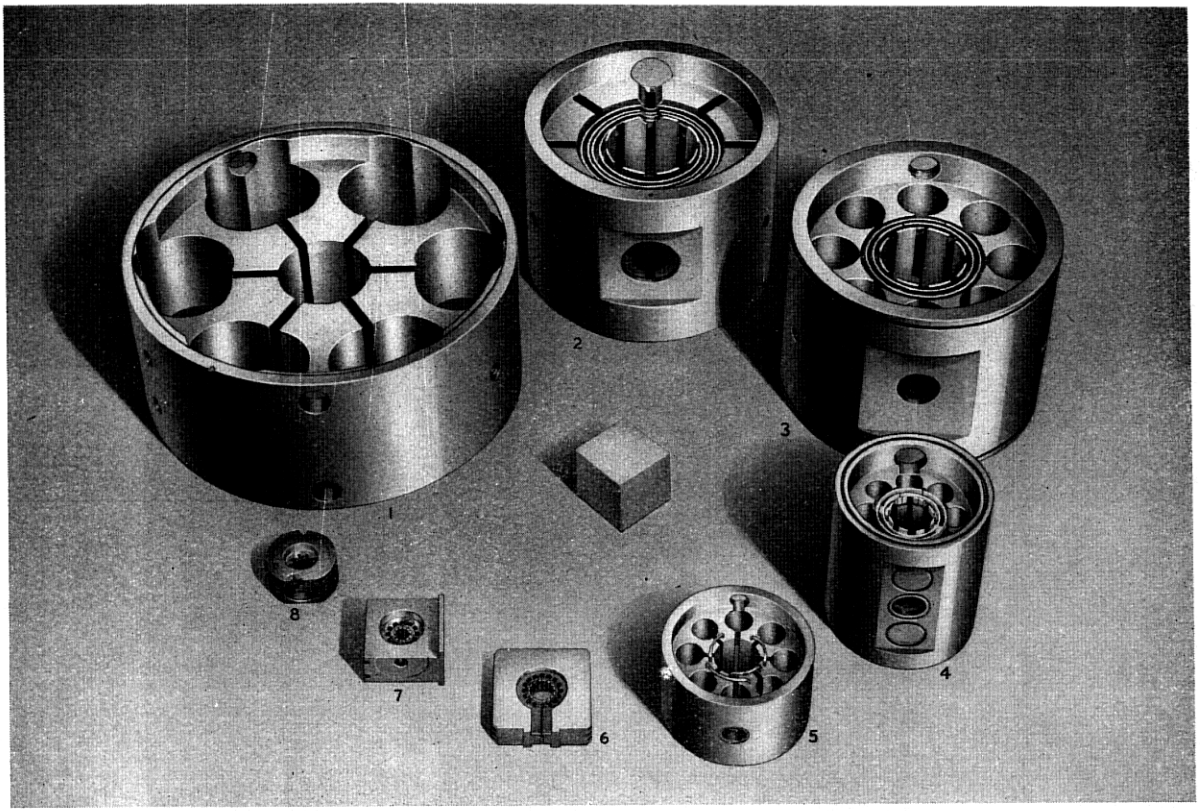

Fig. 41—Resonator blocks of centimeter wave magnetrons developed at the Bell Telephone Laboratories. From the largest to the smallest these resonator systems are those of: (1) the 700 A-D magnetrons of fixed frequencies near 700 mc/s; (2) the 5J26 magnetron, tunable over the frequency range 1220 to 1350 mc/s; (3) the 4J21-30 magnetrons of fixed frequencies near 1280 mc/s; (4) the 720A-E magnetrons of fixed frequencies near 2800 mc/s; (5) the 706AY-GY magnetrons of fixed frequencies near 3000 mc/s; (6) the 4J50 magnetron at 9375 mc/s; (7) the 725A magnetron at 9375 mc/s; and (8) the 3J21 magnetron at 24,000 mc/s. Note the hole and slot type resonators of (1), (3), (4), (5), (6), and (7); the slot type resonators of (2); and the vane type reson-

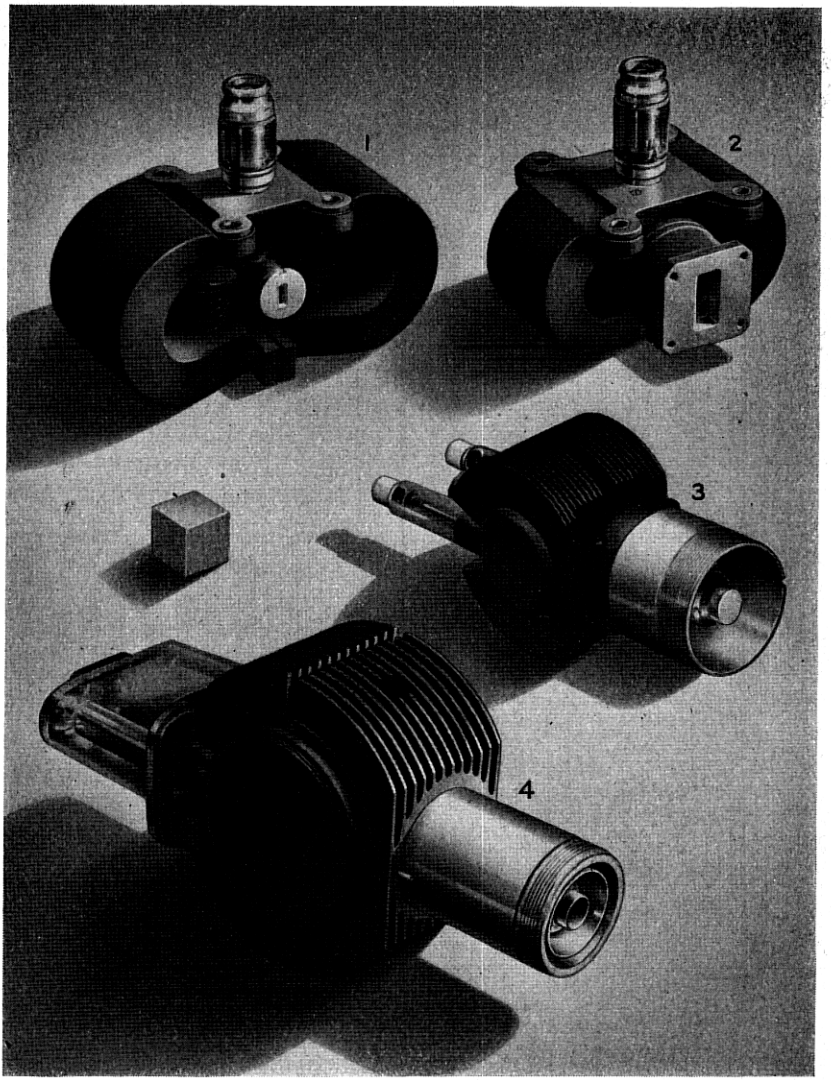

Fig. 42—Four fixed frequency magnetron oscillators. They are: (1) the 3J21 magnetron (60 kw., 24,000 mc/s); (2) the 4J52 magnetron (100 kw., 9375 mc/s); (3) the 720A-E magnetron (1000 kw., ~2800 mc/s); (4) the 4J21-30 magnetron (600 kw., ~1280 mc/s). Note the two types of output circuit, coaxial and waveguide; the use of packaged magnets; and the two types of input leads.

quency from 700 mc/s to 24,000 mc/s.[23] In Fig. 42 is shown the external view of four magnetrons of operating frequencies distributed over the range

[23] In this and other photographs of PART II either a one inch cube or a line of length one inch has been included for size reference.

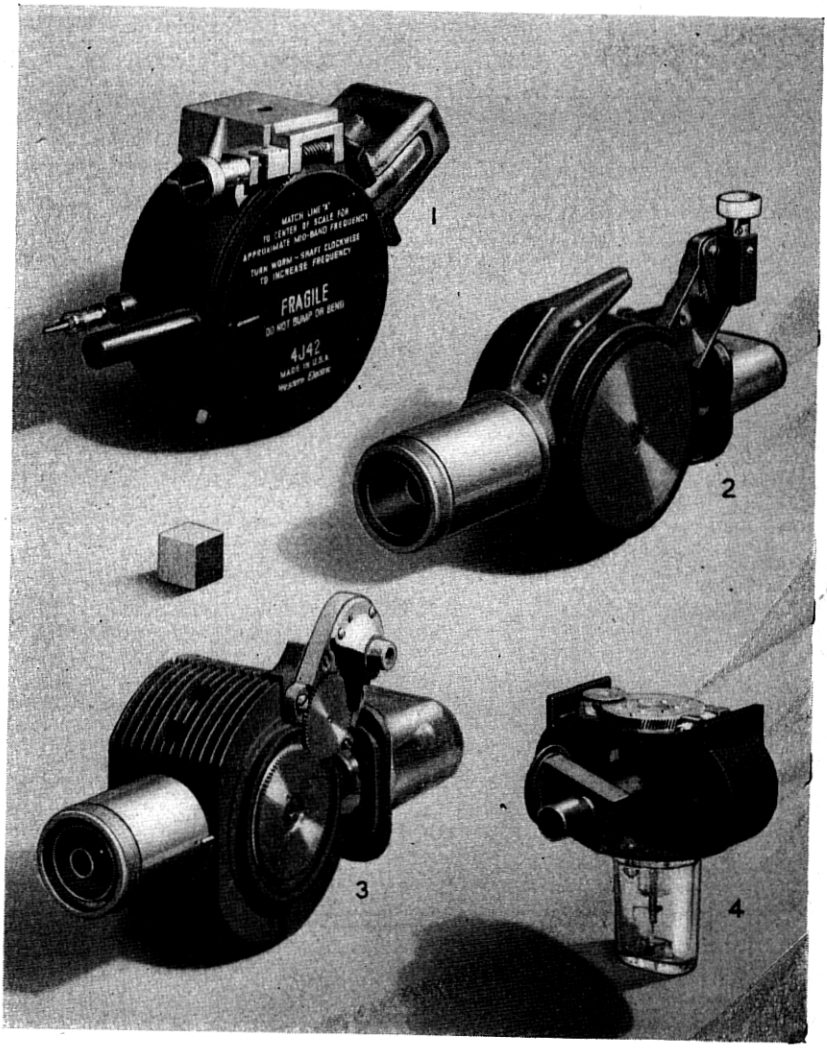

Fig. 43—Four tunable magnetron oscillators. They are: (1) the 4J42 magnetron (40 kw., 660 to 730 mc/s); (2) the 4J51 magnetron (275 kw., 900 to 970 mc/s); (3) the 5J26 magnetron (600 kw., 1220 to 1350 mc/s); and the 2J51 magnetron (55 kw., 8500 to 9600 mc/s).

in which work has been done. It illustrates both the coaxial and waveguide types of output circuits, the use or not of attached magnets, and the two types of input leads and cathode supports. In Fig. 43 is shown the group of tunable magnetrons developed as replacements for fixed frequency models with which they are electrically and mechanically inter-

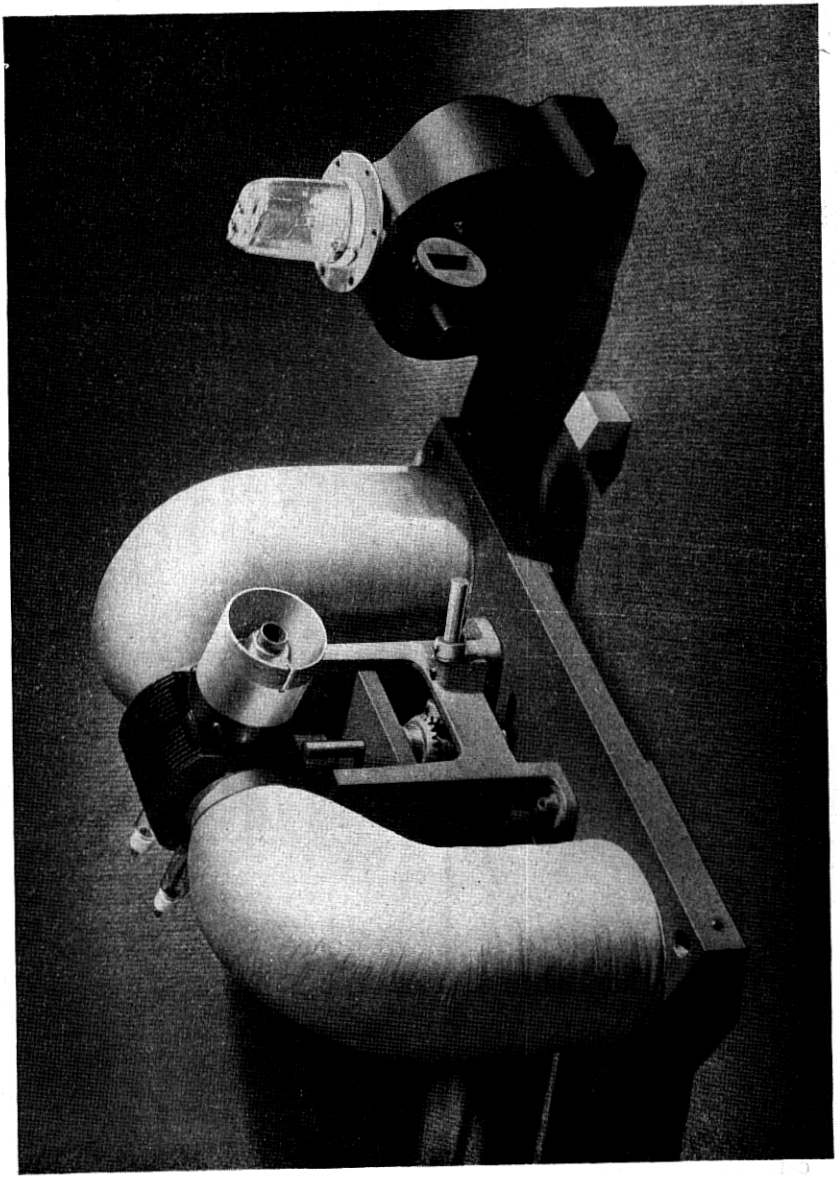

Fig. 44—The 720A-E (1000 kw., ~2800 mc/s) and the 725A (55 kw., 9375 mc/s) magnetrons, shown at the left and right respectively, each mounted in its magnet.

changeable. Finally, in Fig. 44 are shown two magnetron oscillators, the 720A and 725A, mounted in their magnets. By comparison with Fig. 42, the space and weight saved by packaging may be seen. A fair comparison is that between the 725A and magnet of Fig. 44 and the 4J52, number 2 in Fig. 42. Both are 3.2 cm. models, the latter, moreover, being capable of generating higher power.

The designer of a magnetron oscillator is faced with a variety of tasks. If the magnetron is to be used in a specific application he has at his disposal data concerning the amount of power available to drive the magnetron, the nature of the pulsing if such is to be used, the frequency of operation, mechanical features having to do with form and weight, and an idea of what the user hopes or expects to obtain in the way of output power, frequency stability, and operating efficiency. It is the problem of magnetron design to arrange the resonator system, output circuit, cathode, magnetic circuit, and mechanical features to meet these requirements if possible.

In the design of the resonator system it must be arranged to achieve the proper frequency of operation, proper characteristics regarding modes, the proper size of interaction space, and other characteristics which have a bearing on the electronic operation. In special cases a tunable resonator system must be provided.

In the design of the output circuit it is necessary to arrange the type of coupling to the resonator system, the necessary impedance transformation from resonator to load, the type of external coupling, a vacuum seal, and generally to take into account the possibility of electrical breakdown when the power delivered is high.

In the design of the magnetron cathode, attention must be paid to its surface and how it is equipped to meet the rigorous demands made of it. The cathode mounting and input leads must be designed for proper geometry at the cathode ends, heat dissipation, mechanical strength, and DC voltage breakdown strength.

The requirements placed on the magnetic circuit of a magnetron must be borne in mind throughout the design of the magnetron itself. Considerable effort may be expended in arranging for the magnet gap, and hence the required magnet, to be as small as possible. In "packaged" magnetrons the magnet pole pieces, which are built into the magnetron structure, must be designed to produce a field of proper configuration and to make the necessary external magnets feasible.

Generally, the design of the mechanical features of a device as complicated as the multiresonator magnetron oscillator is extremely important and must provide for structural strength under a variety of conditions, as well as cooling facilities and external protection of relatively fragile parts.

12. Reproduction of the British Magnetron

The problem undertaken at the Bell Telephone Laboratories immediately after the visit of the British delegation in October 1940 was the reproduction of the 10 cm. magnetron for study and for general radar use at the Bell Laboratories and the Radiation Laboratory at the Massachusetts Institute of Technology. The data available were contained in a drawing of a magnetron having six resonators and in an X-ray photograph of the magnetron used in the demonstration at the Whippany Laboratory, described in the Introduction. The X-ray photograph, reproduced in Fig. 45, showed a

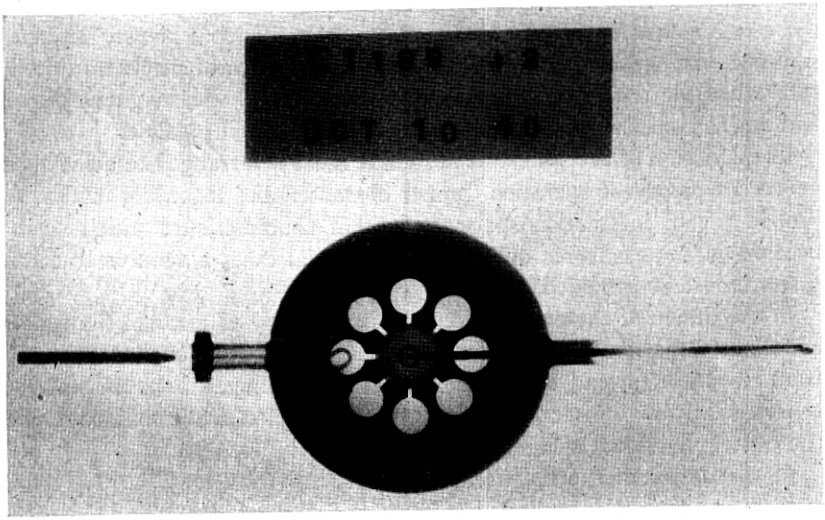

Fig. 45—An X-ray photograph of the 10 cm. magnetron oscillator brought to America by a British delegation in October 1940 and copied at the Bell Laboratories. It is the prototype of most magnetron oscillators in the centimeter wave region developed in Great Britain and the United States during the war.

resonator system having eight resonators. Since this arrangement was known to operate, it was adopted as the starting point for the work here.

In its first tests at Whippany, the British magnetron was pulse operated at about 10 kv. and 10 amps. peak current. The pulses were of 1 microsecond duration and recurred 1000 times per second. The magnetic field required was about 1100 gauss. The magnetron was loaded with a simple radiating antenna of unknown load impedance. Under these conditions the magnetron generated RF power estimated at the time to be greater than 10 kw.

The eight hole and slot type resonators of the British magnetron were spaced around an anode of 0.8 cm. radius. The resonator system, machined in a block of copper, was 2 cm. long. It was unstrapped, strapping

not being known at the time, and in its general features was much like that shown schematically in Fig. 1.

The output circuit of the British magnetron was also similar to that of Fig. 1. It had no particular transformer properties designed into it. The vacuum seal, made of copper, glass, and tungsten, was incorporated in the output coaxial line in very much the same manner as that shown in Figs. 60 and 61.

The cathode was a plain, oxide coated, nickel cylinder, 0.3 cm. in radius. It had nickel end disks of 0.5 cm. radius and was mounted on radial leads passing through glass vacuum seals like those shown in Fig. 61. The leads are placed diametrally across the resonator hole to minimize RF flux linkage to the cathode structure. Preliminary British results indicated that the cathode could be activated properly and would possess a reasonable lifetime under the original operating conditions.

The British magnetron had been designed for use with a magnet having a gap of about 1.75 in. and a pole face diameter of 1.25 in., producing a magnetic field of about 1500 gauss.

Several of the constructional features of the British magnetron were new. The cylindrical block of copper into which the resonator system was machined was used as the vacuum envelope. It was closed at either end by copper disk cover plates. The vacuum seal was made during the pumping and baking process by the alloying at the baking temperature of gold rings between the cover plate and block. The alloying was done at high pressure provided by a clamp bolted across the magnetron. Although no getter was used, satisfactory vacuum conditions could be maintained after seal-off.

By mid-November of 1940, a number of working reproductions of the British magnetron had been supplied in our Laboratories and to the Radiation Laboratory at M. I. T., and a program of study of the magnetron oscillator commenced. The work thus started was continued, on the one hand, to put the new magnetron into production, and on the other hand, to attempt to understand it, improve upon it, and extend its range of usefulness.

13. Magnetrons for Wavelengths of 20 to 45 Centimeters

13.1 *The 700A-D Magnetrons:* After the British 10 cm. magnetron had been successfully reproduced and an emergency program of research and development of multicavity magnetron oscillators commenced, the question immediately was asked: Can a multicavity magnetron be designed to operate near 40 cm. in the pulsed radar set under development in the Whippany radio laboratory? Clearly there now existed the possibility of much greater power than was possible with triodes at this wavelength with reasonable

life expectancy. The modulator of the radar set provided pulsed input power to the oscillator at about 12 kv. and up to 10 amps. peak current.[24]

The performance of the 10 cm. multicavity magnetrons appeared to make the development of such a generator at 40 cm. feasible. A straightforward enlargement of the 10 cm. magnetron by a factor of four was out of the question, however, as it resulted in a magnetron entirely too bulky, requiring a prohibitively large magnet. The development of the 700 mc/s magnetron oscillator thus involved departures from the British design. In particular it was found necessary to reduce the axial length of the resonator system to a considerably smaller fraction of a wavelength than in the 10 cm. design. The development involved design of the interaction space for maximum operating efficiency, the resonator system, for which both eight and six resonator structures were employed, and the output circuit for coupling into the existing radar system.

An early 700 mc/s multicavity magnetron design employed eight resonators of axial length less than one tenth wavelength; the 10 cm. design was about one fifth wavelength long. Operating models initially produced approximately 10 kw. of RF power near the desired frequency. It was found, however, that a smaller and lighter magnetron could be made to operate at the same voltage if the number of resonators were reduced from eight to six, permitting smaller anode and cathode radii [equation (16) in PART I]. The weight and over-all diameter was further reduced by use of elongated holes in the hole and slot resonators. This change resulted in the resonator system used in the 700A-D magnetrons (see Figs. 41 and 46). Each hole is made by boring two intersecting cylinders in the resonator block as may be seen in Fig. 46. No difficulty was encountered in achieving the desired frequency. The frequency differences between the four coded magnetrons near 700 mc/s were achieved by variation of the resonator slot width.

The separation of mode frequency between the $n = 3$ mode (π mode) and the nearest other mode is of the order of 3 per cent. Although this is small compared to that obtainable in strapped magnetrons, it is greater than that for the early unstrapped magnetrons near 10 cm. This is reflected in greater operating efficiency.

The cathode in the 700A-D magnetrons is supported, as in the British magnetron, by radial leads extending across the center of one of the hole and slot resonators. The cathode diameter was varied in an experiment designed to determine the value for maximum operating efficiency. Early experiments of this type involving measurements of output power and efficiency were quite crude and conclusions from their results were by no means as significant as those based on measurements of frequency. The primary

[24] This radar development is discussed in: W. C. Tinus and W. H. C. Higgins, "Early Fire Control Radar for Naval Vessels," *Bell Syst. Tech. Jour.*, 25, 1 (1946).

difficulty lay not in the actual measurement of power or voltage but in the fact that the magnetrons were not loaded in a reproducible fashion. It was considerably later that load impedance measurements were made and used in evaluating magnetron performance. In many early studies the effect of load on operation was not sufficiently disentangled from the effects of other things. In spite of these inadequacies, however, it was generally possible to distinguish a good design change from a bad one, and much of value was gained in early work.

The cathode diameter used in the 700A-D magnetrons is given in TABLE I along with other data on these and other magnetrons in the 20 to 45 cm.

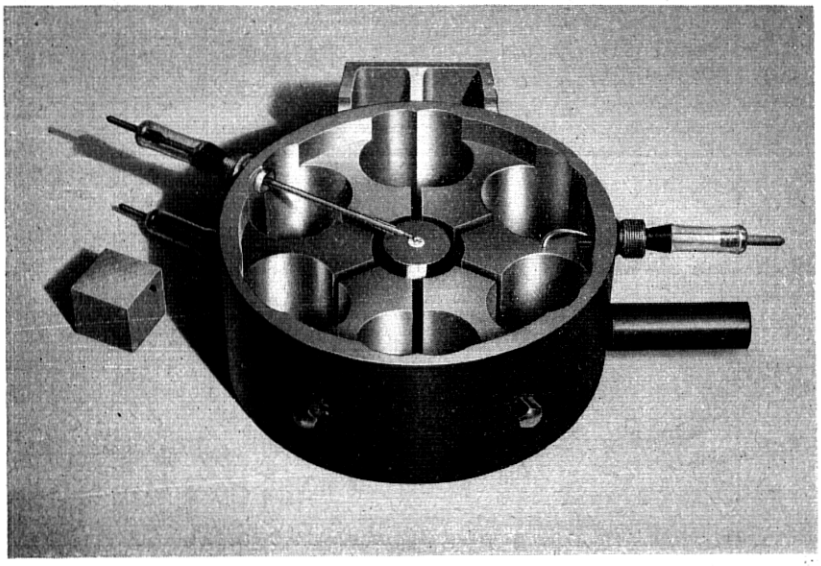

Fig. 46—An internal view of a 700A-D magnetron (40 kw., ~700 mc/s) showing the unstrapped resonator system of six hole and slot circuits, the cathode, the cathode end disks and support leads, and the output coupling loop and lead.

wavelength range. It should be noted that the optimized ratio r_c/r_a is 0.300 as compared to 0.375 in the British magnetron having eight resonators. Plain oxide coating is used on the cathode. Life expectancy is thousands of hours.

As may be seen in Fig. 46, the output coupling is accomplished by means of a loop in the end space of the structure. The loop is connected to an anode segment. It is driven by direct coupling to the anode segment and by coupling to the magnetic flux linking the two adjacent resonators. The output circuit was not designed to operate into a matched output line, however, and external impedance transformation must be incorporated into the load line.

TABLE I

MAGNETRONS FOR WAVELENGTHS OF 20 TO 45 CENTIMETERS

	700A-D Unpackaged	728A-J Unpackaged			5J23 Unpackaged			4J21-25 Unpackaged			4J26-30 Unpackaged			4J42 Unpackaged Tunable	4J51 Unpackaged Tunable	5J26 Unpackaged Tunable	
N	6	8			8			8			8			6	8	8	
r_c (in.)	0.160	0.266			0.266			0.218			0.230			0.199	0.266	0.375	
r_a (in.)	0.689	0.687			0.709			0.582			0.612			0.689	0.687	0.687	
h (in.)	1.576	1.716			2.360			1.940			2.040			1.451	1.500	1.940	
Magnet gap (in.)	2.980	3.290			3.990			3.540			3.640			2.983	3.290	3.640	
Weight (lb.)	12.5	13.0			16.5			15.0			15.0			16.5	14.5	18.5	
Resonators	hole and slot	hole and slot			hole and slot			hole and slot			hole and slot			hole and slot	hole and slot	slot	
Unstrapped λ (cm.)	43.0	~26.0			~21.5			~18.0			~19.0			~38.0	~23.5	10.3	
Straps	none	double ring			echelon wire			double ring			double ring			wire	double ring	double channel	
λ (cm.)	43.0	32.1			28.6			22.8			24.0			43.0	32.1	23.4	
f (mc/s)	720–680	970–900			1056–1044			1350–1280			1280–1220			670 to 730	900 to 970	1220 to 1350	
Nearest mode	$n = 2$	$n = 3$			$n = 3$			$n = 3$			$n = 3$			$n = 1$	$n = 1$	$n = 3$	
λ separation (%)	−3	~−30			~−20			−20			−20			−16	+4	~−60	
Tuning	—	—			—			—			—			resonator capacitance	resonator capacitance	strap capacitance	
Δλ (%)	—	—			—			—			—			10.2	7.5	10.3	
Tuner travel (in.)	—	—			—			—			—			0.100	0.080	0.154	
Q_o	>5000	~4500			~3200			2800			2800			1600→2500	3500→4500	700→1800	
Q_{ext}	~280	170			150			170			180			285	215	210	
η_c (%)	~95	~96			~95			94			94			87	95	82	
Output circuit	coaxial	coaxial			coaxial			coaxial			coaxial			coaxial	coaxial	coaxial	
V (kv.)	12	19.0	21.0	24.5	16.5	19.0	24.5	15.5	22.0	26.5	16.5	23.0	27.0	12.0	23.0	27	27
I (amps.)	10	19	20	28	20	24	33	25	40	48	25	40	46	9	20	46	46
B (gauss)	650	1000	1100	1200	800	900	1100	900	1200	1400	900	1200	1400	650	1100	1400	1400
τ (μs)	2	1	1	1	1	1.5	1	1.5	1	5	1.5	1	5	1.5	1	1	5
pps	1000	1000	1000	1000	2000	1000	1000	1000	1000	200	1000	1000	200	2000	1000	1000	200
P_o (kw.)	40	210	260	400	170	250	475	175	440	640	200	470	700	30	285	600	600
η (%)	33	58	62	58	55	55	59	45	50	50	48	51	56	28	62	48	48
η_c (%)	~35	~61	~65	~61	~58	~58	~62	48	53	53	51	54	60	32	65	58	58
PF (mc/s)	~1.2	2.5	2.5	2.5	3.0	3.0	3.0	3.4	3.4	3.4	3.0	3.0	3.0	1.2	1.9	3.0	3.0

In mechanical construction the 700A-D magnetrons involved techniques like those described above. The input and output leads included copper to glass to tungsten seals much like those in the reproductions of the British magnetron. The end covers were sealed to the resonator body by means of the gold ring technique employed in the British magnetron.

The 700A-D magnetrons are limited in frequency to the four 10 mc/s bands between 680 and 720 mc/s, respectively. These magnetrons operate at 12 kv. and 8 amps. peak current input at a magnetic field of 650 gauss. Over-all efficiency ranges between 30 and 40%, which is better, as has been explained, than that attained with unstrapped 10 cm. magnetrons. Other data of interest are given in TABLE I.

One feature which is immediately apparent from the rated operating conditions of the 700A-D magnetrons is the fact that the ratings are not nearly as high as one might expect from the size of the magnetron. Back bombardment of the cathode at considerably greater input power could easily be handled. The difficulty lay in the fact that it was impossible to drive the magnetrons in the π mode to much greater currents than the rated currents. If the attempt is made to drive the magnetron harder it either refuses to oscillate at all or oscillates in another mode. This phenomenon has been the single deterrent in the development of higher power magnetrons at wavelengths greater than 20 cm. It is now recognized as a starting time phenomenon having to do with the rate at which oscillation builds up and the rate at which pulse voltage is applied (see Section 10.6 *Oscillation Buildup—Starting*). What has been done in studying the phenomenon and in magnetron design to circumvent it will be discussed in some detail in connection with the 5J26, the tunable replacement for the 4J21-30 series.

In quantity production the 700A-D magnetrons presented new problems, all of which arose because of its size. The oxide coated cathode, having a relatively large surface area, gave off a considerable quantity of gas during cathode activation. In as much as the massive copper anode could be outgassed only by a long baking process at temperatures below the softening point of the glass parts, difficulty with magnetrons "going soft" after seal-off was encountered initially.

The development of the 700A-D magnetrons was carried on simultaneously with early studies at 10 cm. and with the early attempts to produce power at 3 cm. A number of auxiliary experiments were undertaken which, although they were not a part of the specific magnetron development, contributed results of considerable value complementary to those obtained at the shorter wavelengths. In particular, these experiments had to do with the technique of measurement and of magnetron scaling.

Before the invention of straps the 700A-D magnetrons were scaled to 10 cm. to explore the possibilities of a more efficient magnetron design at this wavelength. Straps were introduced before the completion of the experiment. The resultant strapped magnetron having six resonators was very efficient—60 per cent—but required a high magnetic field as can be seen by referring to equation (16) of PART I. Like other magnetrons, the 700A-D became much more efficient when strapped. At the normal test point the efficiency ranged around 50 per cent, while at higher magnetic field and voltage, 75 per cent over-all efficiency was achieved. The introduction of straps into the manufactured design was not undertaken.

One further experiment of interest arose during the development of the 700A-D magnetrons from the desire to measure the gas pressure in a sealed-off magnetron. The non-oscillating magnetron itself was used as an ionization manometer. With the magnetic field set at a high value above cutoff and under conditions of no RF oscillation, electrons which arrive at the anode can do so only after having lost energy by collision with a gas molecule. Under these conditions the anode current is directly proportional to the pressure.

Although by present standards the 700A-D magnetrons might appear somewhat crude and inadequate, they nevertheless have an important place in the story of wartime magnetron development. They filled an immediate need in the radar system for which they were designed, providing the U. S. Navy with a radar set which saw service in a number of crucial engagements. Furthermore, the development of the 700A-D magnetrons provided invaluable experience.

13.2 *The 728A-J Magnetrons:* The 728A-J magnetrons were developed for fire control and search radar systems to supersede those which had used the 700A-D magnetrons In these n w systems a magnetron generator was to be required which could deliver 200 kw. peak output power in the frequency range 920-970 mc/s (later extended to 900 mc/s).

In an ear'y design, the resonator system had eight resonators and was strapped with wire straps in the early British configuration [see Fig. 24(a) of PART I]. The anode length was 4 cm., the same as was used in the 700 A-D, which on a wavelength basis was about 2/3 that used in the British 10 cm. magnetron. The first models were designed for operation at pulse voltages of about 27 kv. When, subsequently, it was decided to reduce this voltage, a redesign involving a reduction of size of the interaction space became necessary. Since more had been learned about the technique of strapping in the meantime, it was decided that straps of the double ring type [see Fig. 24(d) of PART I] should be used in the new design. At first, the straps were set on the ends of the anode structure projecting into the end spaces but were later recessed into channels cut into the copper resonator

structure for the purpose of electrostatic shielding from electrons in the interaction region. The frequency range required was spanned by the use of anode structures having three different slot widths for the primary frequency separation, small additional frequency shifts being obtained by small distortions of the straps. Resonant frequencies of magnetron resonator systems were now being determined prior to sealing for pumping by measurements like those described in PART I, during which any necessary strap adjustment could be made.

The cathode was a plain, oxide coated, nickel cylinder much like that used in the 700A-D magnetrons. The heater inductance was considerably higher than that of any previous cathode assembly. It was found that sudden and severe transient conditions, such as those imposed by a momentary internal arc between cathode and anode, would cause relatively high voltages to develop between the cathode and the open end of the heater. This could break down the heater insulation and cause either open or short circuits. This difficulty was minimized by incorporating in the driving equipment a condenser across the heater and an RF choke in series with the heater. Before final design specifications were submitted, the input leads and cathode structure were completely redesigned to provide greater rigidity and strength. To withstand violent shock and vibration, the structure was designed to have as high frequencies of mechanical resonance as possible. The structure looked much like that to be seen in the 5J23 magnetron of Fig. 49. Direct mechanical injury to the input leads is prevented by the use of a heavy glass housing.

The output circuit in early experimental models was a coaxial type fed by a loop in one of the resonators. The central conductor was a tungsten rod to which the glass seal was made and to which the inner conductor of the load coaxial was clamped. When the resonator system was redesigned for lower voltage, a new design of output circuit was made in which was used a choke or contact-free load coupling like that designed for the 720A-E. This removed the possibility of stress being applied to the glass of the output seal at either the inner or outer conductors. Except for the critical dimensions determined by frequency, the output circuit is identical to that used on the 5J23 shown in the photograph of the cut-away model of Fig. 49.

In Fig. 47 is shown a schematic diagram of this type of coupling. On both inner and outer conductors an electrical short circuit is produced at the gap between magnetron and load coaxials by folded low impedance coaxial sections incorporated into the bodies of the conductors. In the outer conductor a half wavelength section folded once is employed. In the section shown at (a), the joint is made at the current node in the choke section by the outer of two cylinders which project from the load end of the coupler

into the magnetron lead. In the partial section shown at (b), this outer cylinder is not used and the joint occurs at the end of the section where there is a current antinode. In this method there exists the greater possibility of sparking should the coupling not be clamped tightly. A folded quarter wavelength section is built into the inner conductor. If the wavelength is short enough, as in the 5J26 and the 720A-E (see Figs. 58 and 63), this section need not be folded, the inner post on the magnetron center conductor can be eliminated and replaced by a solid center conductor on the load side.

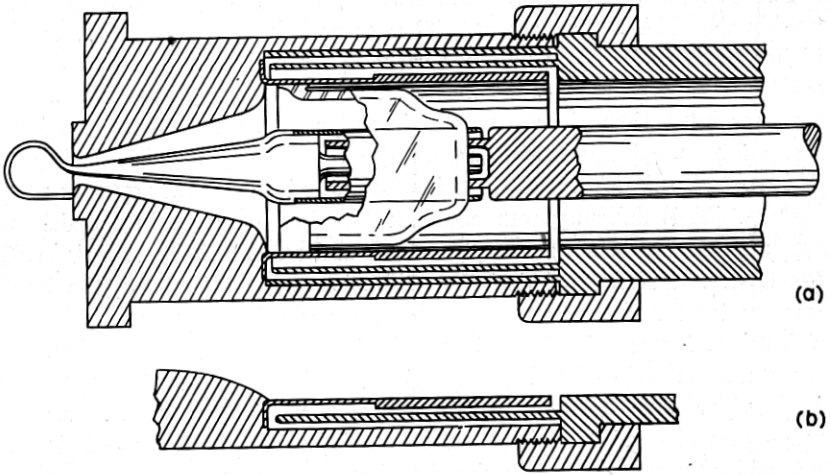

Fig. 47—A schematic diagram of the type of coaxial output circuit used in a number of magnetrons of wavelength 10 cm. or greater. Of particular interest are the means of contact-free or "choke" coupling employed in the inner and outer conductors, consisting of a folded concentric line section which presents zero impedance at the gap in the conductor. (a) and (b) represent two variations of the "choke" in the outer conductor as explained in the text.

The more recent designs of magnetrons for wavelengths greater than 10 cm. have some form of this coupling.

The impedance required at the output coupling to load the 728A-J magnetrons for sufficient power output necessitated a rather high standing wave in the output line. This standing wave was provided by a transformer built into the radar system to which the magnetron was attached. This caused no trouble since the output power was below the point where RF voltage breakdown in air in the line or coupling would occur. The press of time necessitated the adoption of this output circuit although "preplumbing" by incorporation inside the vacuum of the necessary transformer action for coupling directly to a matched load line would have been preferable. Such a design was executed but its completion came too late for its incorporation into the manufacturing specifications.

Ten different magnetrons, coded the 728A-J, were put into manufacture. These covered the frequency range from 900 to 970 mc/s, a 7 mc/s range being allotted to each code type. The operating characteristics of the final design together with other pertinent data are tabulated in TABLE I. An external view of the magnetron is shown in Fig. 48. A maximum current limitation for satisfactory operation in the π mode was also encountered in this magnetron but at current values above the 20 ampere operating point

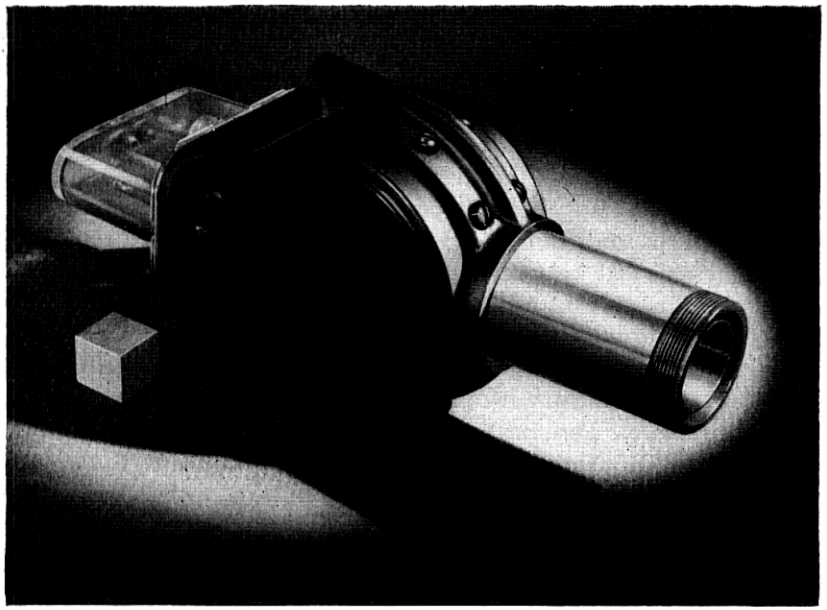

Fig. 48—An external view of a 728A-J magnetron (275 kw., ~930 mc/s). The concentric cylindrical sleeve to be seen inside the output circuit coupling, from which the magnetron is supported, is a part of the "choke" (see Fig. 47). Note the heavy glass protective housing over the input leads.

at which the required output power was attained. Because of the shorter wavelength, the current limitation was not as severe as that encountered in the 700A-D.

The 728A-J magnetrons were driven by a spark wheel, line type modulator. The greater tendency of the driving voltage to overshoot with this modulator, by virtue of the slowness of buildup of RF oscillation, was reduced by the use of a series resistance and capacitance network coupled across the magnetron input like that used earlier with 720A-E magnetrons at 10 cm.

13.3 *The 5J23 Magnetron:* The request for the Laboratories to develop

a semiportable radar pack set and a searchlight control radar involved the design of a new magnetron in the frequency range 1050 to 1110 mc/s to operate at a maximum pulse voltage input of 25 kv. with power output of at least 200 kw. Since these requirements, except for frequency, were essentially those of the 728A-J magnetrons already under development, the new work closely paralleled that already in progress.

Because of the maximum current limitation being encountered in the development of longer wavelength magnetrons, a relatively longer anode was designed for the new magnetron, coded the 5J23, thus insuring satisfactory operation at higher current and input power. The resonator system was "heavily" strapped with echelon wire straps [see Fig. 24(c) in PART I]. Coarse frequency variation was accomplished by the use of straps at different heights above the surface of the anode block. Finer frequency adjustments were made in "pretuning" the structure, before sealing, by small displacements of the wire straps already in position.

Output circuit work on the 5J23 was done together with that on the 728 A-J magnetrons and went through the same series of developments. The output circuit used in the manufacturing design is identical with that of the 728A-J except for the dimensions critical to wavelength.

For operational reasons, only one magnetron, the 5J23, in the frequency range 1074 to 1086 mc/s, was coded. Fig. 49 shows a cut-away view of its internal structure. Performance characteristics and other data are to be found in TABLE I. Note that the 5J23, by virtue of its greater anode length and higher frequency, has a higher critical current, I_c, above which π mode operation fails, than do the 700A-D or 728A-J magnetrons.

13.4 *The 4J21-30 Magnetrons:* When development work on the 5J23 had just been completed, an international agreement on frequency allocation made the frequency range of the 5J23 unavailable for radar purposes at some future date. Consequently the work was to be redone for operation in the band 1220 to 1350 mc/s. The 5J23 and the equipment in which it was used were to continue in manufacture and be used in the period necessary for the development of the new equipment and magnetrons. In addition to the frequency change, power output demands on the magnetron were raised considerably, it being required that the new magnetrons produce at least 500 kw. output power. Although the maximum current limitation had seriously affected maximum output power capabilities of the magnetrons in this wavelength range, it appeared that the new high power demands were within reach by virtue of the higher frequency at which the new magnetrons were to operate.

The new assignment came just upon completion of the 5J23 and made it necessary to build or acquire new laboratory equipment, CW oscillators,

wavemeters, output couplings, and loads. On the other hand, the new development did provide the opportunity to make use of new ideas and developments, some of which, although already completed, could not be used in magnetrons then in manufacture.

When work on this new series of magnetrons was commenced, the art of magnetron development had reached the stage where for the first time it was possible to make a reasonably satisfactory approach to the problem of a new design. The principles of magnetron scaling had been worked

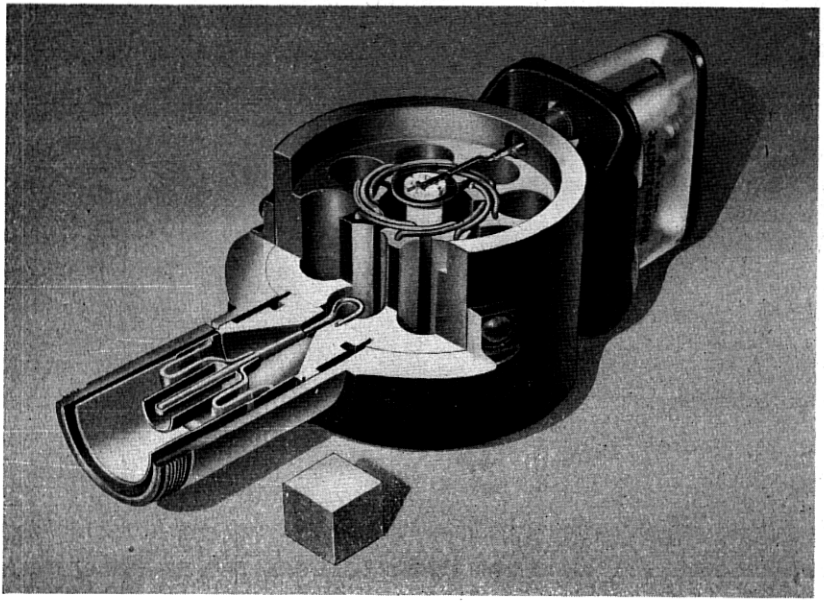

Fig. 49—A sectioned 5J23 magnetron (275 kw., ~1050 mc/s) showing, among other things, the echelon type of wire strapping and coaxial output circuit with contact-free load connector.

out and tested in detail, enabling one to make use of results obtained or verified at different frequencies. The mode frequency spectrum of a magnetron resonator system was now understood and the means of controlling it by strapping were in use. The problem of the output circuit was in hand. Magnetrons were being "preplumbed" and the problems of reproducibility were being solved. Furthermore, the method of studying each of these magnetron characteristics by CW measurements on resonator blocks and output circuit models had advanced to the point where it was possible to complete a design in detail before an operating magnetron had been constructed. Such a procedure was adopted for the new series of

magnetrons, coded the 4J21-30, in the band 1220-1350 mc/s. A satisfactory resonator system giving proper operating voltage, π mode frequency, and mode frequency separation was designed prior to and incorporated in the first operating model. Similarly, a satisfactory output circuit for proper loading over the broad band of frequencies and the design of mechanical features involved in the cathode, cathode mount, cooling facilities, output circuit, straps, and resonator system were provided.

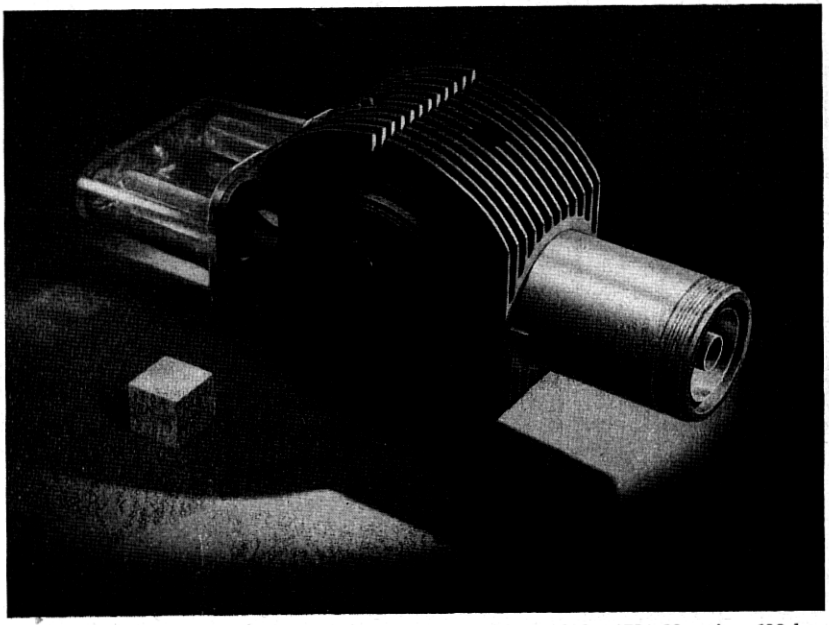

Fig. 50—An external view of the 4J28 magnetron (one of the 4J21-30 series, 600 kw., ~1280 mc/s). Note the cooling fins attached to the magnetron body.

The new interaction space and resonator system were scaled from a compromise between the 728A-J and the 5J23 designs. Shielded, double ring straps like those of the 728A-J were adopted. Two anode structures differing somewhat in resonator dimensions and size of interaction space were used, one for the short wavelength half of the band (4J21-25), the other for the long wavelength half of the band (4J26-30). The different frequencies within each of these groups were attained by the use of straps of different widths.

A single design of output circuit for the entire frequency range necessitated making the transformer properties as independent of frequency, or as broad band, as possible. The output circuit has three parts. At the outside of the

magnetron is the choke or contact free coupling to the load coaxial. The general type of design used in previous magnetrons was followed here. The transformation from the load coaxial to the coaxial which breaks into the resonator at the coupling loop was made by use of a tapered line in which the characteristic impedance was kept constant. The proper loading was accomplished by adjustment of the loop size. It was found possible to achieve a sufficiently low loaded Q in this way within the bounds of a satisfactory geometrical arrangement. Each of these design procedures was

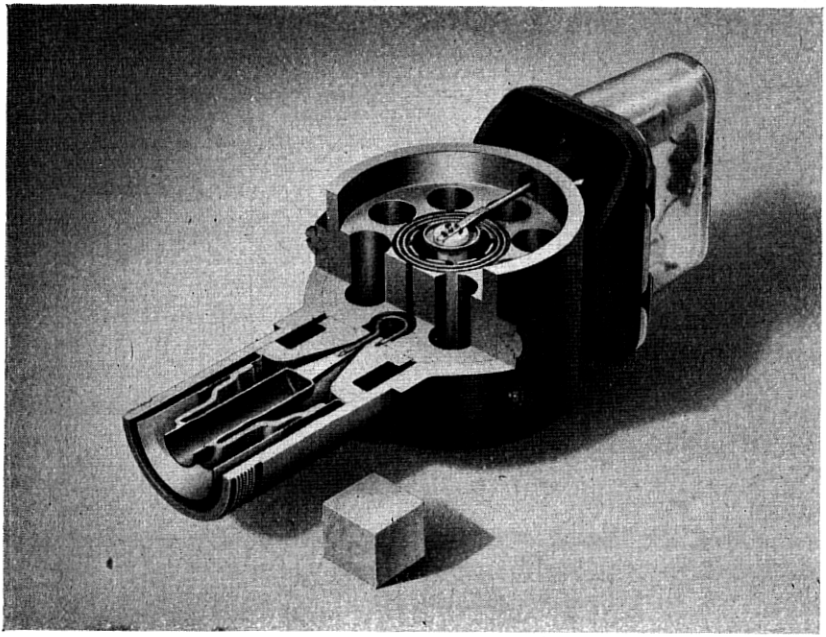

Fig. 51—An internal view of a 4J21-30 magnetron (600 kw., ~1280 mc/s). Of special interest are the recessed double ring straps and the output circuit in which the characteristic impedance of the coaxial line from loop to load is approximately constant.

carried out by CW measurement of impedance, looking into a model through the output circuit. Special models of the tapered line and choke coupler were also studied.

When operating magnetrons were constructed, except for minor changes, no redesign was necessary. The first working models performed satisfactorily at the required pulse voltage, current, magnetic field, power output, and pulling figure. It was possible to get more than 750 kw. output at better than 50 per cent efficiency from these magnetrons.

An external view of the final design may be seen in Fig. 50 and a photograph of a cut-away model in Fig. 51. Operational and other data are given

in TABLE I. A typical performance chart of one of the series is shown in Fig. 52. The maximum current boundary limits the output to values well below those at which other factors, such as cathode dissipation, become restrictive.

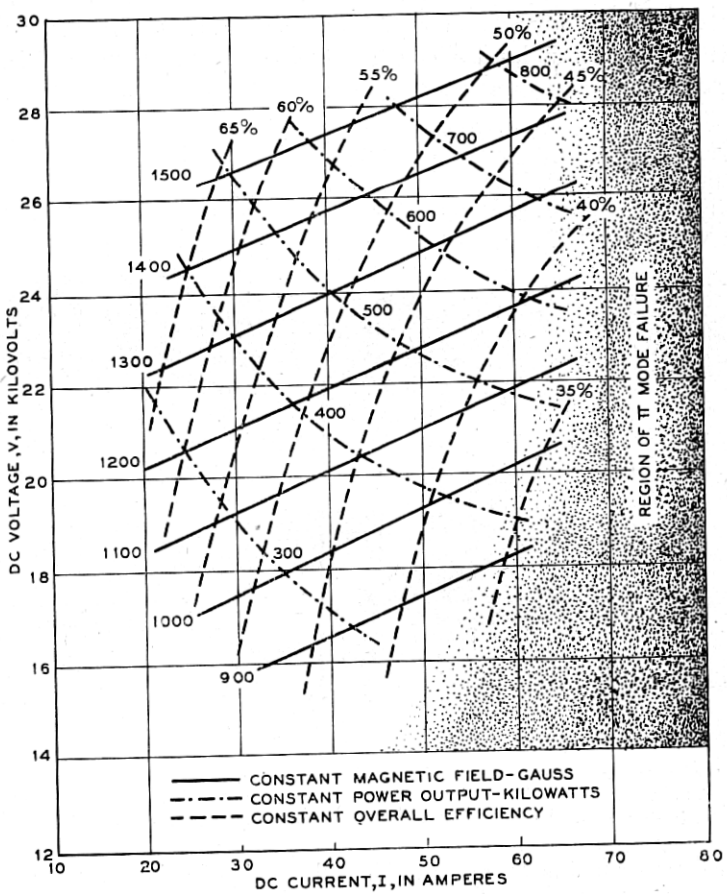

Fig. 52—A typical performance chart of a magnetron of the 4J21-25 series (~1315 mc/s).

During operation in the high power, spark gap, line type modulator with which the magnetron was to be used, it was found that the pulse voltage applied to the cathode input leads was sometimes sufficient to cause flash-over. If the arc persisted, vacuum failure from cracking or puncturing of the glass resulted. The external flash-over was accompanied by internal arcs between cathode and anode which were injurious to the life of the

magnetron. To circumvent this difficulty, the input leads and their glass housing were redesigned. The glass of the leads was lengthened and folded to provide a greater surface distance over which the arc must strike. Although the redesign was limited somewhat by the space available in the transmitter unit, it was possible to make leads which could stand 60 cycle peak voltages of almost twice the normal pulse voltage applied to the magnetron. This step all but eliminated flash-over in operation. To take care of the occasional flash-over, a spark gap across which the breakdown could occur was added in the equipment.

The 4J21-30 magnetrons are illustrative of carefully designed nontunable magnetrons of wavelengths 20 to 30 cm. developed at the Bell Laboratories. They were the first magnetrons designed here completely on the basis of CW impedance measurements.

14. Tunable Magnetrons for Wavelengths of 20 to 45 Centimeters

14.1 *General:* As fixed frequency magnetrons became available in the various frequency bands designated for radar use, the interest quite naturally turned to the development of tunable magnetrons. The operational reasons for this were to enable one to set the frequency of a radar system at will, thus avoiding interference between sets in a large group of aircraft on naval vessels, to enable one to vary the frequency at will from time to time or as the need arises to avoid jamming, and to permit the stocking of fewer magnetrons to cover a given frequency band.

Early work on tunable magnetrons at the Bell Laboratories was done with 10 cm. models. Although no such developments were carried to the stage of production, the ideas and techniques evolved were used at other frequencies. Somewhat later the Bell Laboratories committed itself to a program of development of tunable magnetrons for pulsed radar use in the 20 to 45 cm. wavelength range.

The program initially was not directed toward the goal of some particular magnetron of fixed specifications. Rather, it was the intention to explore the field of possible tuning methods and to find that one which appeared both electrically and mechanically to be best suited for large magnetrons. Work in this initial stage was done on anodes of the 4J21-30 series and may be divided into two main channels characterized by the degree of symmetry involved in the tuning scheme. In one, the tuning of the entire anode block is accomplished by modification of a single one of the resonators and may thus be characterized as unsymmetrical tuning. In the other, each resonator of the multiresonator block is tuned in a symmetrical fashion.

Among the unsymmetrical types studied were those employing an auxiliary loop in one resonator connected to a reactive element which could be either a

coaxial line terminated in a plunger or a variable capacitance, or a coaxial to wave guide junction with movable plungers in the wave guide. Another form involved the deformation of one of the resonators itself to accommodate a prism shaped tuning element which was moved from outside the vacuum through a diaphragm arrangement.

Although considerable effort was expended in the study of unsymmetrical tuning schemes and much learned about them in the course of this work, they have two rather fundamental drawbacks which caused them to be replaced by the symmetrical types in which these defects could be eliminated. In the first place, it is difficult by this means to obtain the desired range of frequency change. Secondly, by virtue of asymmetry, operation in other modes is difficult to avoid except over rather narrow frequency ranges. Those types in which part of the tuning circuit is outside the vacuum envelope have the additional drawback of bringing high RF voltages into structures in air where very high standing waves are necessary and breakdown difficult to avoid.

It was found possible to circumvent each of these difficulties by using symmetrical tuners. Some such tuners were like those tried on 10 cm. models and involved spider-like straps connecting alternate segments to two common points on the axis of the tube. These points in turn were connected to the center and outer conductors of a coaxial line. After passing through a vacuum seal, this coaxial line connected to a reactor like those used in the unsymmetrical schemes.

In the general arrangement finally used, a tuning member was mounted in the end space. The structure included a vacuum diaphragm mounted in the end cover of the magnetron. The tuning was effected by variation of the capacitance between the resonator system and the tuning member.

In unstrapped magnetrons, the tuning was accomplished by moving a tuning member of the general shape of a "cookie cutter" in a single groove cut into the slotted portion of the anode structure. Later, this range was increased by using two slots and a tuning member having two concentric rings. This type of tuner was used on both the 4J42 and 4J51 magnetrons to be discussed. It is the first of the two types of tuning by variation of capacitance discussed in PART I of this paper. Considerable effort was expended to extend the frequency range of tuning by strapping the untuned end of the resonator system and by variations of the resonator dimensions on which relative mode frequencies depend. It was found possible to obtain a tuning range of better than ± 5 per cent, but it appears quite difficult to exceed this amount appreciably in high voltage magnetrons using this tuning means.

In the strap tuning scheme, use was made of straps of channel or U-shaped cross section, inside which the double rimmed "cookie cutter" element is moved. The tuning arrangement of the 5J26 magnetron is of this type. It is the second of the two types of tuning by variation of capacitance discussed in PART I.

Quite early in this program of development it became apparent that the armed services would require all these tunable magnetrons to be mechanical and electrical replacements for existing fixed frequency magnetrons, interchangeable in all respects. This requirement, in addition to the facts of electrical design, indicated that the "cookie cutter" type of tuner represented the line of attack most likely to succeed. The capacitance in the anode structure or in the straps is the frequency determining circuit parameter most easily varied, as it is the most accessible in these large size magnetrons. The tuning element may be moved conveniently by a mechanism, compact in the axial dimension, mounted in the end space and cover of the magnetron. These are factors of prime importance in "unpackaged" magnetrons where over-all axial length is important. Magnetrons in this wavelength range are sufficiently large to make such a mechanical design feasible.

The magnetrons of wavelength 20 to 45 cm. for which tunable replacements were designed were: the 700A-D series (680-720 mc/s), the 728A-J series (900–970 mc/s), and the 4J21-30 series (1220-1350 mc/s). Although it was preferable to span the 4J21-30 band with one tunable replacement, the use of two tunable replacements, each covering half the band, would have been satisfactory had it been necessary. In the development of each of the tunable replacements, improvements and modernizations which could be incorporated within the limitations of mechanical and electrical interchangeability were made.

14.2 *The 4J42 Magnetron:* The tunable replacement for the 700A-D series is the 4J42. It covers an increased frequency band of 660 to 730 mc/s. The tuning is accomplished by variation of the intersegment capacitance of the anode structure itself, the first of the two capacitance tuning methods listed above. Frequency varies nearly linearly with displacement of the tuning member. The tuning range, although adequate for the purposes of the 4J42, is limited by interference of other modes as was discussed in PART I. In this respect it is not a great deal better than can be attained by unsymmetrical means. The advantages of symmetrical capacitance tuning enumerated above made it the logical choice nevertheless. A satisfactory tuning range of the π mode without interference from other modes was achieved by strapping the end of the magnetron opposite that at which the tuning mechanism is mounted. This necessitated changes in the resonator

dimensions of the 700A-D magnetrons to obtain the frequency range desired. The cathode structure was improved, making use of later developments. Its diameter was changed from 0.8 cm. to 1.0 cm. in order to increase the maximum current to which operation in the π mode is possible. The anode diameter was retained; the operating conditions were not appreciably affected. It was necessary to retain the original form of output circuit.

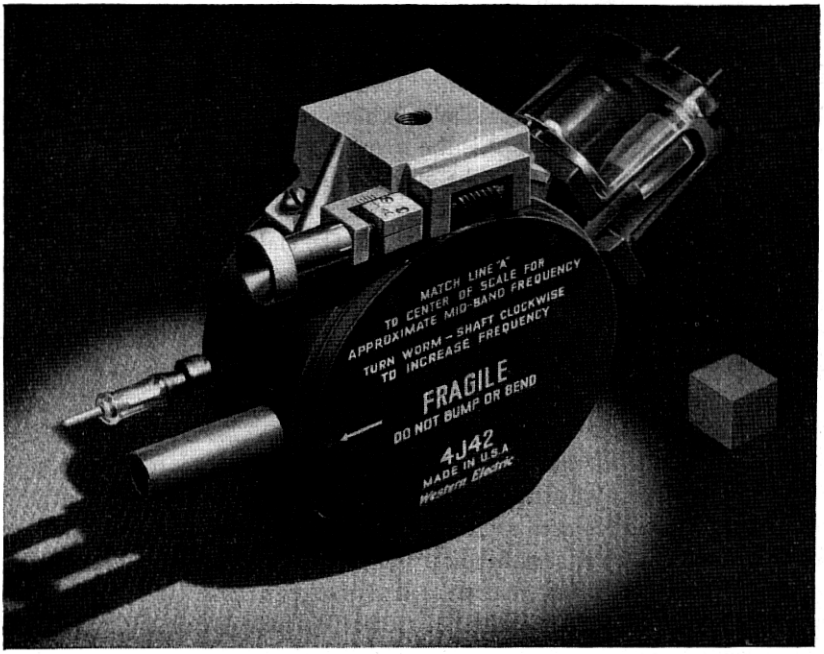

Fig. 53—The 4J42 tunable magnetron (40 kw., 660 to 730 mc/s)—the tunable replacement for the 700A-D magnetrons. The worm drive in the mounting bracket operates the tuning mechanism enclosed in the end cover of the magnetron. Note the improved input leads and protective housing (see Fig. 46).

In Fig. 53 is shown an external view of the 4J42. In TABLE I are given operational data and other characteristics. The performance of the 4J42 is as good or better than that of the corresponding magnetron in the 700A-D series.

14.3 *The 4J51 Magnetron:* The 728A-J series of fixed frequency magnetrons was replaced by the 4J51, covering the frequency band of 900 to 970 mc/s. An external view of the magnetron is shown in Fig. 54. As in the 4J42, the resonator system is a modification of that used in the fixed frequency prototype, strapped on the untuned end by double ring strapping. Satisfactory mode frequency separation is maintained by increasing the

strap capacitance of the single pair of rings to approximately twice that of one pair in the 728A-J. The tuning scheme is the same as that used in the 4J42. It may be seen in the photograph of a cut-away model in Fig. 55.

The output circuit of the 4J51 incorporated the broad band transformer properties developed for the output circuit of the 4J21-30 series. This necessitated a larger loop size in the 4J51 than was used in the 728A-J.

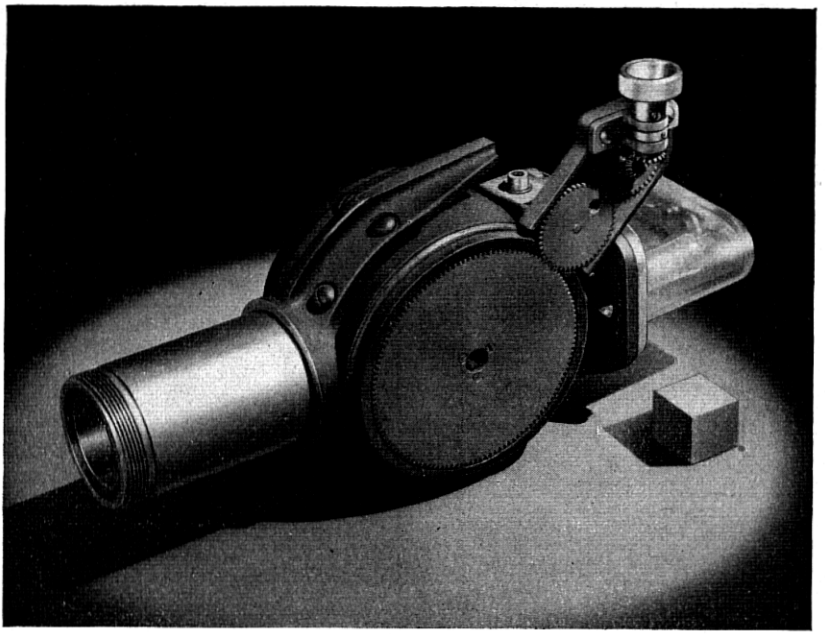

Fig. 54—The 4J51 tunable magnetron (275 kw., 900 to 970 mc/s)—the tunable replacement for the 728A-J magnetrons.

These features may be seen in Fig. 55. The output circuit was designed for coupling to a matched load line.

TABLE I includes relevant data on the 4J51 magnetron. In Fig. 56 are shown power output and mode frequency tuning curves for the magnetron. Fig. 56 may be taken as representative of the type of tunable magnetron in which the intersegment capacitance of the resonator system is varied. The frequency range is limited by the crossing of the π mode frequency curve by those of other modes. The power output is reduced appreciably at the crossing point of the $n = 3$ mode component. Throughout its tuning range, indicated in Fig. 56, the 4J51 magnetron operates as well or better than its fixed frequency predecessors.

14.4 *The 5J26 Magnetron:* Replacement of the 4J21-30 series of mag-

netrons with a tunable equivalent necessitated a tuning range which was found to be unattainable with the scheme used in the 4J42 and 4J51 magnetrons. Two tunable replacements employing the "tuned segment" type of tuning, each spanning half the band, were constructed as "insurance" should the efforts to develop a single replacement having the required range fail. However, it was found that by tuning the straps as has been described in PART I a single tunable magnetron for the entire 4J21-30 series covering the band from 1220 to 1350 mc/s could be provided. An external view of the resulting magnetron, coded the 5J26, is shown in Fig. 57 and an internal view in Fig. 58.

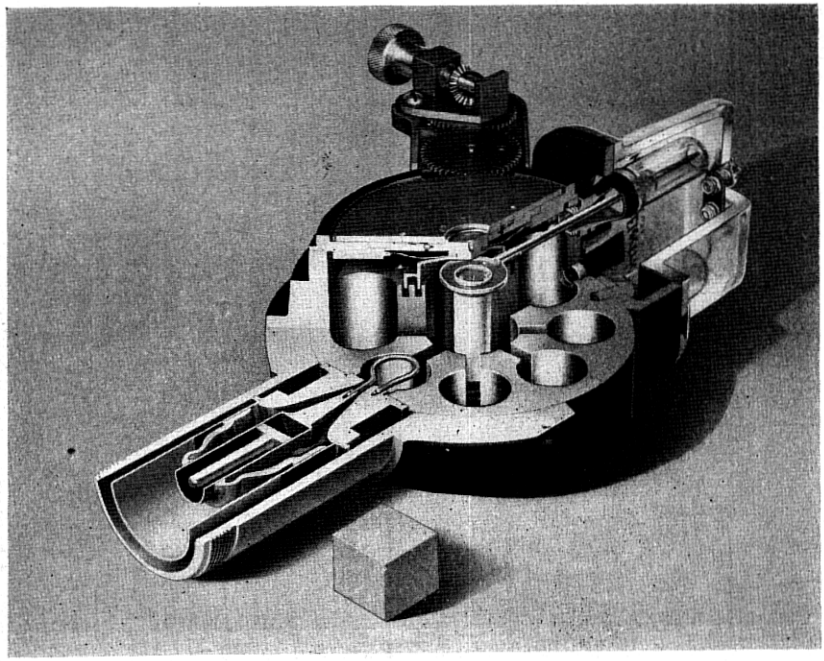

Fig. 55—A view of a cut-away 4J51 tunable magnetron (275 kw., 900 to 970 mc/s). Note the tuning member consisting of two concentric rings which are moved up and down in the grooves in the segments of the anode structure. The details of the tuning drive mechanism, including the flexible vacuum diaphragm, the axial screw, the nut and ball bearing, and the gear drive are to be seen. The resonator system is strapped on the end not seen in the figure.

As can be seen in Fig. 58, the 5J26 magnetron includes radical departures in design in addition to the tuning scheme. Slot type resonators are used in the resonator system, and the anode and cathode diameters, as well as their ratio, are considerably larger than those used in previous designs for the same operating voltage and magnetic field. These features of the design

resulted from a systematic study of the causes of and possible cures for the maximum current limitation encountered in long wavelength magnetrons. The difficulty had been particularly noticeable in the 4J21-30, which on

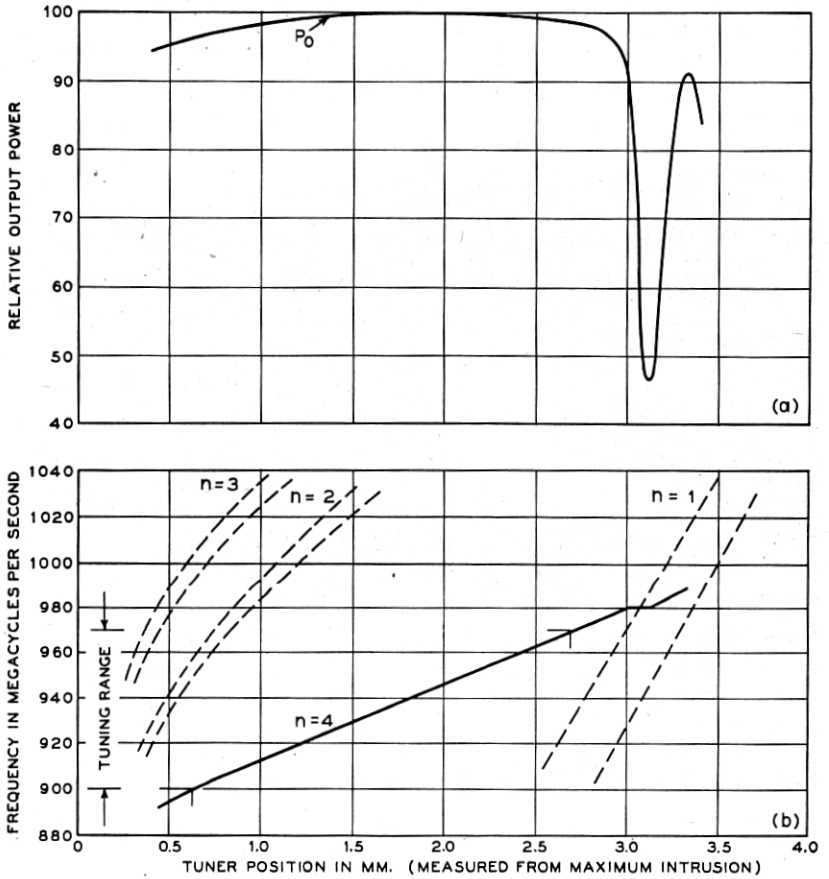

Fig. 56—Typical experimental curves of power output and mode frequency variation with tuner position in the 4J51 magnetron. The following points of interest are to be noted: the relatively more rapid tuning for modes of small n than for the π mode ($n = 4$); the drop in output power at the coincidence of the frequencies of the π mode and one of the components of the $n = 1$ mode; the limitation on the tuning range in the π mode imposed by the crossing of mode frequency curves of other modes; the fact that the $n = 1$, 2, and 3 modes are doublets and the π mode a singlet.

hard tube modulators were able to pass the required current before π mode failure with little margin. For some reason the performance of the early experimental models of the tunable replacement was considerably inferior in this respect and would not meet the specifications for which the magnetron was being designed. Thus a study of the phenomenon was imperative. It

resulted in the 5J26 magnetron. It dictated the nature of the interaction space and resonator system and thus the cathode size and output coupling loop. Initial experiments were performed with a vane type resonator system [see Fig. 21(b)] having channel straps and an interaction space of approximately the size used in the 4J21-30 series.

From studies of dynamic *V-I* plots on the experimental tunable models and other magnetrons under a variety of operating conditions, it became clear that the phenomenon had to do with the rate of buildup of RF oscilla-

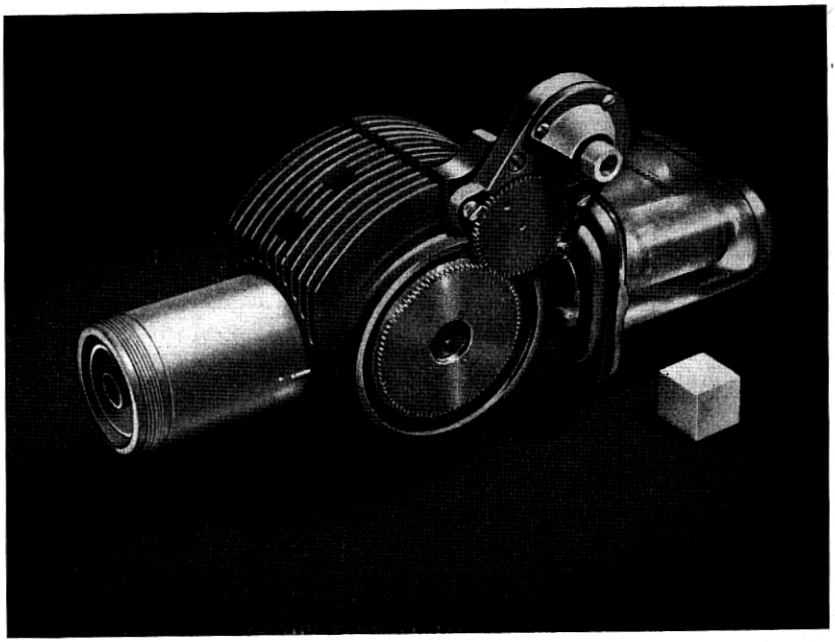

Fig. 57—The 5J26 tunable magnetron (600 kw., 1220 to 1350 mc/s)—the tunable replacement for the 4J21-30 magnetrons.

tion in the π mode and with the rate of rise of the applied DC voltage. The "mode skip" shown in the sequence of *V-I* plots of Fig. 38 and discussed in PART I is an example of the behavior of one of the experimental models used in this work when failure to oscillate in the π mode occurs.

Thus at constant magnetic field there appears to be a maximum DC voltage above which π mode oscillation is impossible. This voltage is presumably that beyond which the mean angular velocity of the electrons around the interaction space becomes enough greater than that of the traveling field component for the phase focusing to fail to maintain synchronism. The term "maximum current limitation" is thus in a sense a misnomer as Fig. 38(b) indicates. Here, π mode oscillation fails even to start and does not

fail at a maximum current on each pulse. The point at which π mode oscillation fails thus has to do with the relation of the rate of rise of DC voltage through the range of permissible values to the rate of buildup of RF oscillation. As one attempts to drive the magnetron harder by applying greater peak voltages to it, the rate of voltage rise in this region becomes greater, finally exceeding that which the rate of RF voltage buildup will permit.

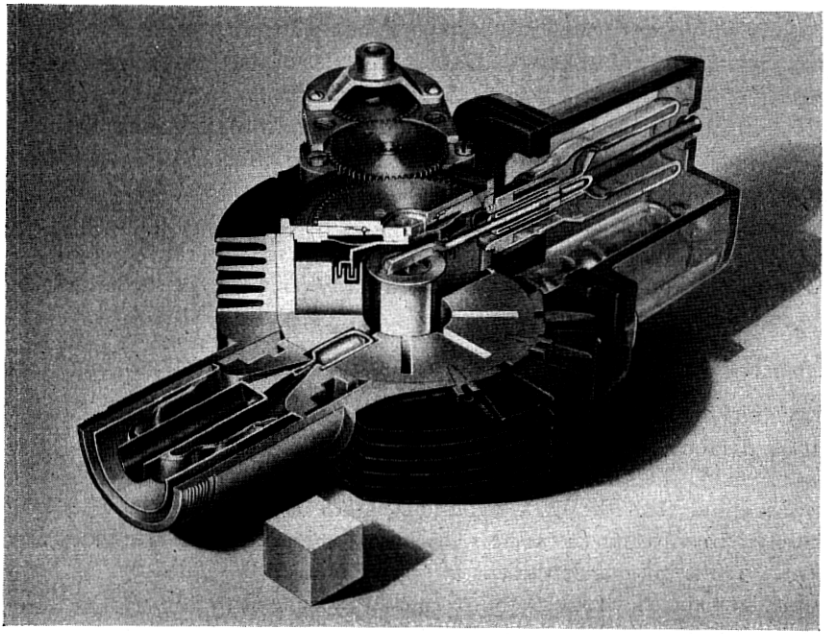

Fig. 58—A view of a sectioned 5J26 tunable magnetron (600 kw., 1220 to 1350 mc/s). Note that the tuning member, consisting of two concentric rings, is moved up and down inside the two recessed channel straps by a mechanism like that in the 4J51 magnetron (see Fig. 55). Compare the interaction space geometry and shape of resonators with those of the fixed frequency 4J21-30 magnetrons (Fig. 51), the changes having been made to achieve better starting characteristics as explained in the text. Note also the enlargement of the output resonator to accommodate the coupling loop, the RF chokes incorporated in the cathode support leads, and the large input lead construction to prevent external flashover.

The phenomenon of π mode failure was studied as a function of five parameters:

1. magnetic field, B;
2. frequency, f;
3. ratio of cathode to anode radii, $\frac{r_c}{r_a}$;
4. load conductance, G_s;
5. rate of DC voltage rise, $\frac{dV}{dt}$.

The results were found to fit well into the picture of starting time behavior discussed in PART I. Thus, increase of frequency and decrease of load both result in a greater rate of RF voltage buildup and permit a greater rate of rise of DC voltage through the range where oscillation starts. The magnetron may thus be driven harder and more current passed. In agreement with these results, changes in the rate of voltage rise applied by the pulser, accomplished by changing its characteristics, also permitted oscillation to continue to higher current and voltage values. The dependence on B and r_c/r_a presumably are to be accounted for by the dependence of $G_e(V_{RF})$ on these quantities. It appears that $G_e(V_{RF})$ increases with both B and r_c/r_a.

Empirical relations of the critical current, I_c, and the electronic efficiency, η_e, at which π mode failure occurs, to the load conductance, G_s, were obtained.[25] Whereas I_c decreases with increasing G_s, η_e decreases.

Since the work was done at different frequencies and interaction space geometries, it was found convenient and instructive to express voltages, currents, and conductances as reduced variables of the type introduced by Slater, that is, as ratios to the voltage, V_o, and current, I_o, at the intersection of the Hartree line and the cutoff parabola, and the conductance, $G_o = \frac{I_o}{V_o}$, respectively. I_o and V_o may be determined from the expressions for the cut-off parabola and the Hartree line [expressions (8) and (16) of PART I, respectively]. Plotted in terms of the reduced variables I_c/I_o and G_s/G_o, it was found that the data relating I_c/I_o to G_s/G_o and η_e to G_s/G_o predicted approximately the same relationship independent of frequency and r_c/r_a. Thus, quite independent of the fundamental significance of these particular reduced variables to the functional dependence of the quantities involved, it appeared that they would be useful in the design of a new magnetron whose design parameters would lie in or near the range for which data were available.

The purpose of the work was to produce a tunable magnetron which would operate satisfactorily to currents in excess of those needed to meet the power output specifications. It was hoped to do this by redesign of the magnetron itself. This course rejected as unsatisfactory the alternative of limiting the rate of voltage rise on each equipment with which the magnetron would be used. The general goal of the proposed changes in magnetron design were to increase the rate of buildup of RF oscillation while at the same time keeping the electronic efficiency at a reasonably high value. These goals are not independent but oppose one another as has been seen. Thus, if r_c/r_a is increased, I_c increases, but η_e decreases. If G_s is increased to increase η_e, I_c drops. The hope of success in the venture lay in the prob-

[25] G_s was determined from the relation $G_s = \frac{Y_{OC}}{Q_L} = \frac{1}{\omega_L Q_L}$ [see equation (36) of PART I], using a calculated value for the total resonator inductance and the measured value of the loaded Q.

ability that these effects do not exactly cancel one another and that a net improvement in performance could be effected.

The design of the 5J26 was accomplished in the following way: The slot type resonator was chosen as it possesses a low value of inductance needed to give a high value of G_s for a given value of loaded Q.[25] The number of resonators was chosen to be eight, the anode length of the 4J21-30 retained, and the design carried out at $Q_L = 150$ and $f = 1220$ mc/s. The empirical relations used were that relating I_c/I_o to G_s/G_o, that relating η_e to G_s/G_o, and the equation of a constant B line on the performance chart obtained for the 4J21-30. In addition to the definitions of G_s, V_o, I_o, and G_o, there were to be met the operating conditions of $V = 27$ kv., $I = 46$ amps., and $B = 1400$ gauss, as well as a maximum value for the over-all diameter of the resonator system dictated by interchangeability. The value of resonator inductance was calculated for a terminated parallel plate line. With the choice of $I_c = 60$ amps., the above mentioned conditions could be solved numerically to give a definite set of design parameters. The anode and cathode radii, resonator length, and thus unstrapped wavelength were determined. The straps were designed to achieve the proper frequency and to provide sufficient tuning range with the tuning means employed. The ratio r_c/r_a was determined as 0.546, considerably in excess of the value 0.375 in the 4J21-30 magnetrons.

The output circuit of the 5J26 magnetron was similar to that used in the other tunable magnetrons of long wavelength. It employed the broad band design of external coupling and transition section to the coupling loop. The size of the loop was dictated by the coupling required to provide a Q_L of approximately 150. It may be seen in Fig. 58.

The input leads of the 5J26 magnetron were of new design, incorporating chokes in the leads to prevent leakage of RF energy picked up on the cathode, and large size center conductor to minimize RF voltage breakdown on the input leads.

The significant design and operating data for the 5J26 magnetron are included in TABLE I. This magnetron design provided a single tunable replacement of superior performance for the entire 4J21-30 series. In Fig. 59 are shown curves of mode frequency tuning throughout the π mode tuning range, indicating that in the strap tuning method difficulties with mode frequency interference are avoided.

15. MAGNETRONS FOR WAVELENGTHS NEAR 10 CENTIMETERS—UNDER 200 KILOWATTS

15.1 *The 706A-C and 714A Magnetrons:* The work in the wavelength region near 10 cm., described in Section 12, was continued in the study of variations from the British design. For the most part these early studies

had to do with the electron interaction space and the resonator system. Later, when driving equipment became available, life studies were started. In the main this work showed the British design to be a very nearly optimum as an unstrapped magnetron. Consequently the series of magnetrons

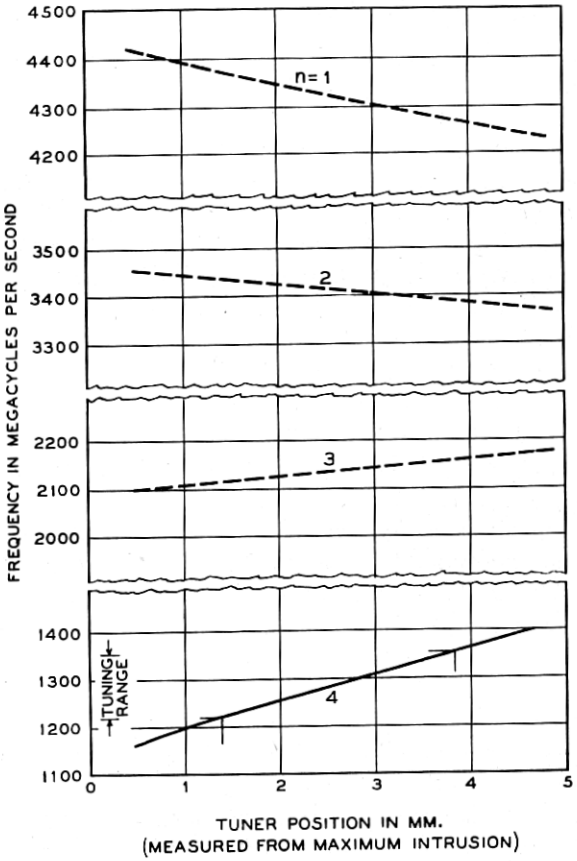

Fig. 59—Curves of mode frequency variation with tuner position in the 5J26 magnetron. The curve for $n = 4$ is experimental, those for $n = 1, 2$, and 3 have been calculated from an equivalent circuit theory of the resonator system (doublet structure not shown). Note the large mode frequency separation and the complete freedom of the π mode from interference by other modes (compare Fig. 56).

having wavelengths near 10 cm. which were coded for American manufacture were similar to the British prototype. The experiments and calculations which had been made constituted a body of valuable information to be used later in departing from the original design.

The variations in the resonator system of the British magnetron were made primarily for the purpose of studying the parameters affecting frequency of operation. Magnetrons were built incorporating such variations as dimensional changes in the hole and slot resonators; the use of other forms of resonators such as slot resonators; and variations of factors affecting the coupling between adjacent resonators, as, for example, the volume of the end space region between the ends of the resonator system and the end covers of the magnetron. A series of magnetrons was built having from four to ten resonators, including odd numbers, but the majority of the experimentation was done with eight resonators as in the original system.

Besides affecting frequency, most of these resonator changes markedly affected the electronic operation as well. Undoubtedly this was the result of changes occurring in the mode frequency distribution. At the time, the significance of this distribution to magnetron operation was not fully appreciated nor, indeed, was it known for these magnetrons. As discussed in PART I in connection with curve (a) of Fig. 25, it was later found that the frequencies of several modes including the π mode were very nearly equal, making the electronic operation quite sensitive to the exact nature of the frequency distribution. This made the experiments difficult to interpret. None of the resonator systems, involving only changes in anode length and diameter with corresponding changes in the cathode, appeared to be appreciably better than that in the British magnetron.

In one rather important experiment the cathode diameter, and thus r_c/r_a, was varied to determine the value for optimum efficiency using the British anode dimensions. The result, confirmed later by comparison with British work, showed the original dimensions to be very nearly optimum.

Some variations of the output coupling to the resonator system were also tried. In one such variation the coupling loop was placed in the end space of the magnetron between two resonators. In this position the loop was coupled magnetically by the flux linking the two adjacent resonators, as well as directly by virtue of the fact that the end of the loop is fastened to the anode segment (see the discussion of output coupling in PART I). It will be recognized that this type of coupling is that used later in the 700A-D magnetrons. The output circuits in the first American 10 cm. magnetrons were like those in the British design.

The constructional techniques used in the British magnetron were followed with some variations. The most bothersome technique was that of making the vacuum seals between the end covers and the body of the magnetron. This was done by means of tin plated gold ring seals between the members. Little difficulty was encountered with this seal in production, however, and it was used throughout the production at the Western

Electric Co. of 10 cm. magnetrons under 200 kw. output power.

The first unstrapped magnetrons coded for manufacture by the Western Electric Co. were the 706A-C for frequencies near 3060 mc/s (9.8 cm.). The frequency differences were achieved by small changes in the resonator slot widths. Another magnetron, the 714A, oscillating at 3300 mc/s (9.1 cm.) was also coded at this time. It differed from the others in having slightly smaller resonator holes. These magnetrons were used in some of the earliest American ship and airborne radar systems. A set of typical operating data is included in TABLE II.

The improvement in measured over-all efficiency to approximately 25 per cent was undoubtedly the result of improvements in the technique of operation and of measuring the output power. Unlike the measurement of frequency, for which good techniques were already available, the measurement of output power initially was crude and unreliable. At first, estimates of power were based on the heating of resistors to incandescence, with no assurance that all the power was being dissipated in this load. The production of corona has always been spectacular evidence of RF power. Later, when water load techniques were used, all the power could be absorbed and measured. Means of line tuning permitted the adjustment of the magnetron load impedance to the point of maximum output power even though the impedance itself was unknown.

Some preliminary studies of magnetron tuning were made as auxiliary experiments. With one or more extra coupling loops terminated externally in adjustable coaxial tuners, tuning ranges of 2 to 4 per cent were achieved.

15.2 *The 706AY-GY, 714AY, and 718AY-EY Magnetrons:* A significant improvement in the multiresonator magnetron was the method of strapping, used by the British as a means of achieving mode frequency separation (see discussion in PART I). When used in the resonator system of the 706A-C magnetrons, the early British "mode locking straps" increased the π mode wavelength from 9.8 cm. to 10.7 cm. and resulted in an increase in operating efficiency by about a factor of two with much more freedom from "moding" difficulties. Here was a really worthwhile advance and no time was lost in making use of it. The resultant strapped magnetron, oscillating at 10.7 cm. wavelength, was used directly as the basis for a new family of magnetrons of wavelength near this value. These were coded as the 718AY-EY series. The cathode, output circuit, and general mechanical features of the 706A-C were adopted essentially without change. Experiments like those done on the original British design, when repeated on strapped magnetrons, indicated the design parameters still to be close to optimum. The cathodes used were plain, oxide coated, nickel cylinders.

TABLE II

MAGNETRONS FOR WAVELENGTHS NEAR 10 CENTIMETERS

	706A-C Unpackaged	714A Unpackaged	706AY-GY Unpackaged			714AY Unpackaged			718AY-EY Unpackaged			720A-E Unpackaged			4J45-47 Unpackaged		
N	8	8	8			8			8			8			8		
r_c (in.)	0.119	0.119	0.110			0.100			0.119			0.107			0.107		
r_a (in.)	0.315	0.315	0.295			0.270			0.315			0.283			0.283		
h (in.)	0.788	0.788	0.788			0.788			0.788			1.576			1.576		
Magnet gap (in.)	1.480	1.480	1.490			1.490			1.490			2.750			2.750		
Weight (lb.)	2.1	2.1	2.1			2.1			2.1			4.9			4.9		
Resonators	hole and slot	hole and slot	hole and slot			hole and slot			hole and slot			hole and slot			hole and slot		
Unstrapped λ (cm.)	9.8	9.1	~8.9			~8.3			9.8			~8.0			~8.0		
Straps	none	none	British wire			British wire			British wire			double ring			double ring		
λ (cm.)	9.8	9.1	9.8			9.1			10.7			10.7			10.7		
f (mc/s)	3100–3019	3320–3280	3100–2914			3320–3280			2890–2720			2890–2720			2855–2750		
Nearest mode	$n = 3$	$n = 3$	$n = 3$			$n = 3$			$n = 3$			$n = 3$			$n = 3$		
λ separation (%)	−1	−1	−11			−11			−11			−10			−10		
Q_0	>1500	>1500	~1000			~1000			~1000			1500			1500		
Q_{ext}	<100	<100	~120			~120			~120			130			130		
η_c (%)	~93	~93	~89			~89			~89			93			93		
Output circuit	coaxial	coaxial	coaxial			coaxial			coaxial			coaxial			coaxial		
V (kv.)	11.0	11.0	11.4	18.5	20.9	11.6	17.7	19.5	11.9	17.9	20.0	21.0	24.0	27.0	21.0	27.0	23.0
I (amps.)	12.5	12.5	12.5	16	20	12.5	16	20	12.5	16	20	45	53	65	45	65	45
B (gauss)	1300	1300	1300	1900	2100	1500	2100	2250	1300	1800	1950	2300	2600	2900	2300	2900	2550
τ (μs)	1	1	1	1	1	1	1	1	1	1	1	1	1	1	1	1	5
pps	1000	1000	2000	1000	1000	2000	1000	1000	2000	1000	1000	1000	650	500	1000	500	120
P_0 (kw.)	25	22	40	146	206	40	125	165	45	136	193	550	800	1100	550	1100	650
η (%)	18	16	28	49	49	28	47	42	30	47	48	58	63	63	58	63	63
η_e (%)	~19	~17	~31	~55	~55	~31	~53	~47	~34	~53	~54	62	68	68	62	68	68
PF (mc/s)	~15	~16	11	11	11	12	12	12	11	11	11	10	10	10	10	10	10

No particular precautions were taken to protect the active coating. Even so, lives both in the laboratory and in the field were shown to be well over 2000 hours. Much later, the mechanical structure of the cathode and its support was improved and a heavy glass protective housing designed to cover the input leads. The performance chart of Fig. 17 in PART I is that of one of the 718AY-EY series. Other data concerning these magnetrons are given in TABLE II.

Quite early in the study of the multicavity magnetron it had been realized that the mode frequency distribution of the resonator system is very important to efficient operation. Evidence had accumulated which indicated that something needed to be done to suppress all but one mode of oscillation. Attempts at influencing mode frequency separation were made in which fluxbarriers or partitions, either complete or partial, were used in the end spaces of the resonator system. These included what was essentially the distortion of the structure into the form of the so-called "serpentine" mentioned in PART I. Although striking changes in operation were produced, supporting the basic contention that there are more ways of doing a thing wrong than right, worthwhile improvements were not achieved.

Following the confirmation, here and elsewhere, of the British results with strapping and the coding of the series of 718AY-EY magnetrons, intensive work was started in the general investigation of the modes of the magnetron resonator system and their relation to the various possible methods for strapping. This work involved the determination of the mode patterns for mode identification, the technique for which was consequently developed. Various strapping schemes were devised, built into magnetron resonator systems, and studied. Among these were the echelon strapping also used by the British, single and double ring strapped systems, and diametral straps which were adaptable to external tuning of the magnetron. The importance of strap shielding and strap assymmetries discussed earlier were brought out in these studies. The effects of end space volume and anode length on mode frequency distribution for given strapping systems were also studied.

Strapping made possible greater tuning ranges with tunable magnetrons. Efficient magnetrons having broken echelon strapping on one end and diametral straps on the other, connected through a glass seal to an external coaxial tuner were built. Tuning ranges of over ± 5 per cent were achieved in this way. There was no demand at the time for tunable magnetrons.

Following the introduction of the 718AY-EY magnetrons, their properties were reproduced at an extended range near the wavelengths of the 706A-C and at the wavelength of the 714A. The designs for these were arrived at by scaling the 718AY-EY to the appropriate wavelengths. The principles

of scaling discussed in PART I had been studied in connection with the extension of magnetron frequencies into the 20 to 45 cm. and 3 cm. wavelength ranges and were fairly well understood by this time. These new strapped magnetrons were coded as the 706AY-GY and the 714AY. The frequency variation over the 706AY-GY band was accomplished by variation of the resonator slot width. The characteristics of these magnetrons, apart from frequency, are essentially the same as those of the 718AY-EY series (see TABLE II). External and internal views of the 706AY-GY type are shown in Figs. 60 and 61. The strapping scheme to be seen in Fig. 61 is the early British system depicted schematically in Fig. 24(a).

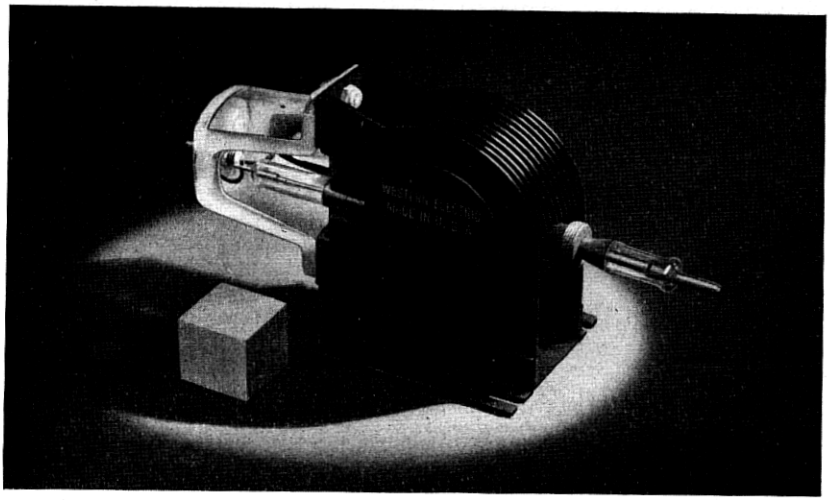

Fig. 60—An external view of a 706AY-GY magnetron (150 kw., ~3000 mc/s).

The means of fabricating the anode block in manufacture is also of interest. This had to be inexpensive and fast. As worked out by Western Electric engineers, it consisted of boring the interaction space hole first and turning the end spaces into the solid copper block. This was followed by two operations in a multiple spindle drill press in which the eight resonator holes are drilled to size. Following this, a broach consisting of eight tapered series of projecting cutting edges, spaced equally around the main shaft, was drawn through the interaction space hole, cutting the eight slots to size in a single operation.

Although more powerful magnetrons were subsequently developed, these 10 cm. magnetrons of power output below 200 kw. are still considered to be highly satisfactory designs. Together with similar designs in Great Britain, they have been produced by several manufacturers in large quantity and

have seen extensive use in many forms of pulsed radar systems. They have also served as the basis for much of the subsequent magnetron design work.

16. Magnetrons for Wavelength near 10 Centimeters—200 Kilowatts to 1 Megawatt

16.1 *The 720A-E Magnetrons:* A natural outgrowth of the early magnetron experimentation was the effort to generate higher power. Since the earliest magnetrons were unstrapped there was much to be hoped for in

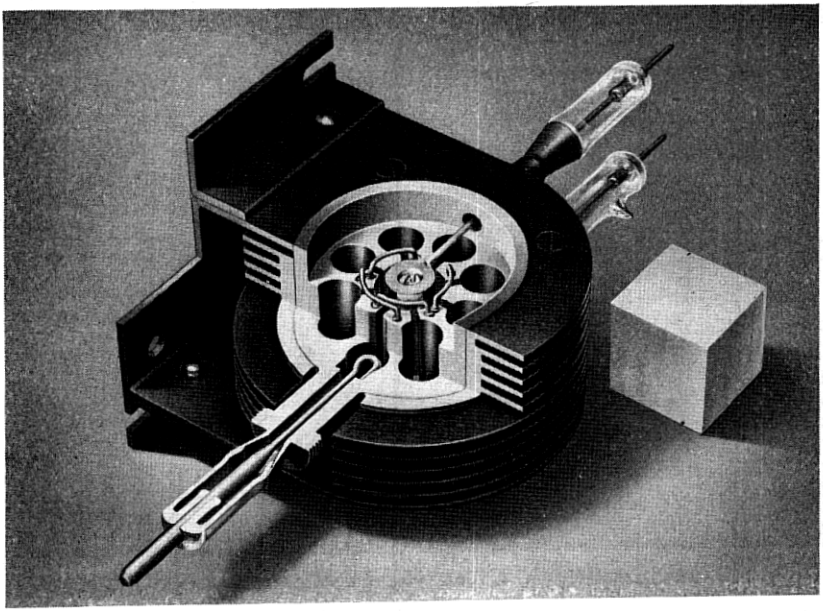

Fig .61—An internal view of a 706AY-GY magnetron (150 kw., ~3000 mc/s). Note the type of wire strapping [compare Fig. 24(a)] and the simple coaxial output circuit.

improved efficiency. Higher power magnetrons would have to be designed to operate at voltages above 20 kv. and currents of greater than 50 amps. To accomplish these objectives, the interaction space was enlarged, in some designs involving a greater number of resonators, and the anode length increased by two or even three times. Although it was possible to develop over 200 kw. with magnetrons of eight, ten, and twelve resonators, efficiencies were poor, seldom exceeding 20 per cent at maximum loading. This was even poorer than unstrapped 10 cm. magnetrons like the 706A-C. The reduction in mode frequency separation attendant upon increases in anode length and number of resonators was later found to be the cause.

Following their first use in the 718AY-EY magnetrons, straps were in-

corporated in the high power designs with immediate improvement in performance. The output circuits used were simple loop to coaxial lead combinations like those in use on the 706A-C.

Radar needs for higher power near 10 cm. had developed to the point of a specific requirement for a magnetron of not less than 350 kw. output. Since it was believed that the best one could obtain from the 718AY-EY was 250 kw. even at the risk of shortened cathode life, the requirement made necessary a new design. In the work on higher power magnetrons, better than 300 kw. had been obtained at efficiencies greater than 50 per cent at maximum loading with what was essentially a double length 718AY-EY

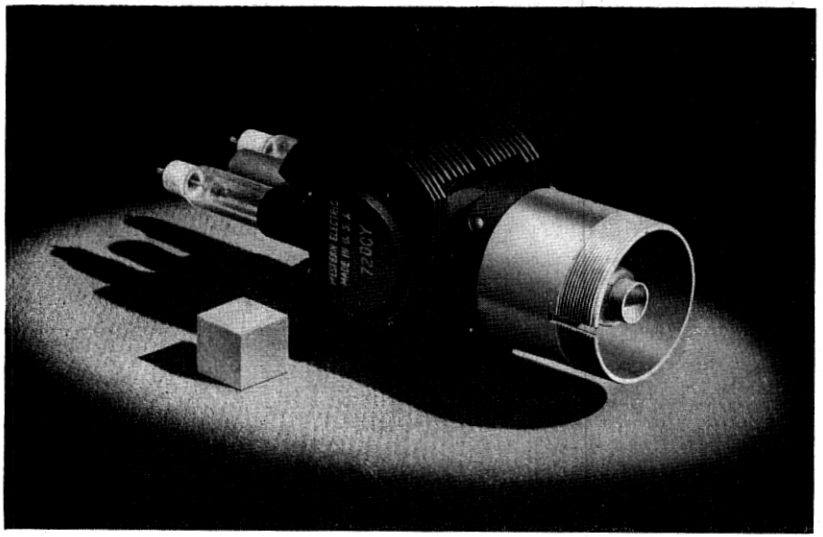

Fig. 62—An external view of a 720A-E magnetron (1000 kw., ~2800 mc/s).

type. Thus it appeared that the new power requirement could be met with such a design. The press of time made it necessary to concentrate further efforts on improving this design, with not much if any time to be devoted to further experimentation along other lines. The chief drawback of the double length magnetron was the large magnet it required. Several months later an equally efficient magnetron, shorter, and having a larger number of circuit elements might have been produced, but the original program had advanced beyond the stage at which it could be changed. The improvements in design of the double length 718AY-EY type magnetron resulted in the 720A-E series.

An external view of the 720A-E magnetron is shown in Fig. 62. A cutaway model is shown in Fig. 63 in which may be seen the nature of the

resonator system, straps, cathode, and output circuit. In TABLE II are given dimensions and other data concerning these magnetrons.

The resonator system has eight hole and slot type cavities. Its anode length is 4 cm., double that of the 706AY-GY. It is strapped with double ring shielded straps of special design which could be stamped out of sheet copper and oven brazed in position in a wide ledge trepanned around the interaction space into the ends of the anode block. These straps were easier to control in dimensions than the echelon straps, used in early experimental models, which had made necessary the development of a pretuning

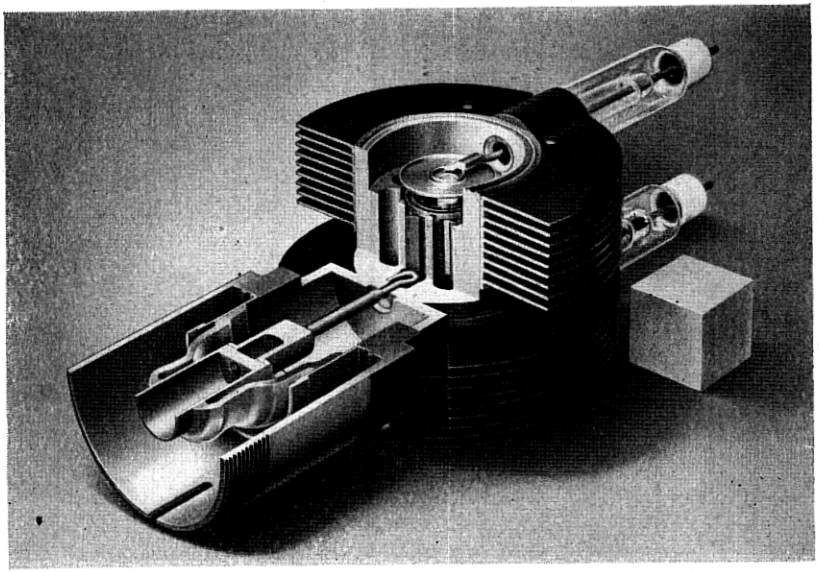

Fig. 63—A view of a cut-away 720A-E magnetron (1000 kw., ~2800 mc/s) showing the large cathode end disks and the impedance transformer sections in the output circuit.

technique. The large number of wire straps used had made it impossible to predict from visual inspection that a given anode would eventually oscillate at a specified wavelength. The straps were adjusted manually to bring the frequency of resonance determined before sealing and pumping into the required range. These heavily strapped models operated at efficiencies up to 65 per cent, but their initial operating wavelengths were near 13 cm. The high operating efficiency was achieved at the required wavelength by scaling the structure. The increase in magnetic field required by the scaling was achieved without increase in magnet size by incorporation of steel disks in the end covers of the magnetron. The new stamped straps required considerably less manipulation during pretuning than the echelon straps.

The five wavelength groups of the 720A-E employ straps of different height.

The cathode was similar to that of the 706AY-GY but longer and with different end disk design. The surface was a plain oxide coating on the nickel cylinder base. Adequate life under the most stringent of its operating conditions was obtained (see TABLE II). The radical departure in cathode end disk design was necessitated by the pickup of RF energy by the cathode. This was aggravated by the length of the cathode. An end disk of conventional size, being closer to the inner strap than to the outer strap, is more influenced by its potential. Since the inner straps are π radians out of phase and the cathode approximately a half wavelength long, conditions were quite right for considerable induction of RF potential on the cathode. Considerable RF power was radiated by the cathode leads. Measurements on a non-oscillating magnetron indicated that cathode pickup could be neutralized very nearly by increasing the end disk diameter. If the end disk completely covered both straps, the charge induced on it by one strap was essentially balanced by that induced by the other strap. The 720A-E with large cathode end disks radiates very little RF energy from its cathode leads.

The greater power which the 720A-E produced made it necessary to redesign the output circuit to include the transformer inside the vacuum. Voltages in the external transformer had been sufficiently high to break down the line. The redesign was carried out empirically by a substitution method. A replica of the output circuit was constructed and terminated in the impedance required to load the magnetron properly. In this replica the loop was replaced by a coaxial line and standing wave detector through which CW power was fed. In this way one could determine the impedance at the loop terminals necessary for proper loading. Then with a specially constructed output circuit, in which the dimensions between the glass seal and the loop terminals could be varied, the dimensional changes necessary to achieve the required impedance at the loop with match in the output load coaxial was determined. The dimensions determined in this way provided the final design. The 720A-E was one of the early "preplumbed" magnetrons.

A coaxial lead coupling using chokes instead of contacts was developed for the output circuit and used not only at 10 cm. but on all the later magnetrons of longer wavelength as has been described. The centrifugal glass seal at the outer conductor is to be noted (see Fig. 63). The original tungsten center conductor to which an external "thimble" was soldered (similar to that in the 5J23, see Fig. 49) was replaced by a Kovar cup to which the glass was sealed directly. Greater strength, better cooling, and elimination

of the high voltage gradient in air which had existed at the small diameter tungsten rod resulted.

In Fig. 64 is shown a typical performance chart for the 720A-E series. Other performance data are given in TABLE II. In Fig. 44 is shown one of the 720A-E magnetrons mounted in its magnet.

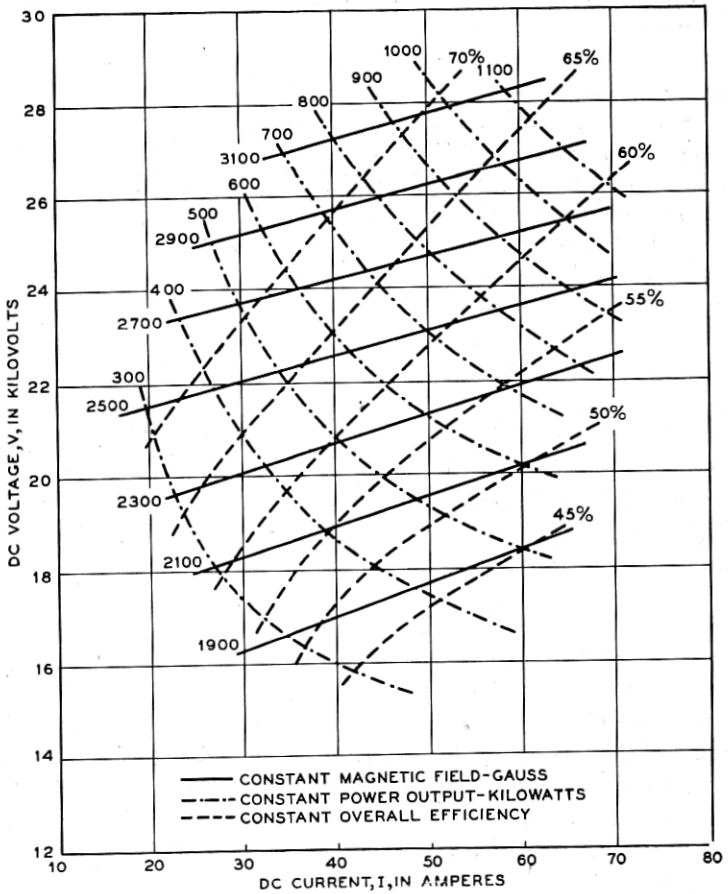

Fig. 64—A typical performance chart of the 720A-E magnetrons (~2800 mc/s).

In the use of the 720A-E on line type modulators the difficulty with what was then called voltage "overshoot" was first encountered. It is the result of the finite buildup time for the RF oscillation during which the pulse voltage rises to values higher than required for π mode operation. It is particularly aggravated on line type modulators for which the magnetron, before it oscillates and draws current, presents a mismatch to the line network causing the voltage to rise to a much higher value. The difficulty was

circumvented by connecting across the modulator network a condenser in series with a resistance equal to the characteristic impedance of the network. The condenser is of low impedance for rapid voltage changes, terminating the network properly during the voltage rise. The condenser, however, stores some energy which must be dissipated at the end of the pulse. The discharge of this energy through the magnetron causes very weak oscillations to occur following the main pulse. This condition somewhat lengthens the interval of time following the pulse during which the radar receiver may not detect an echo.

16.2 *The 4J45-47 Magnetrons:* For the extension of radar range it had been found desirable to use pulses of longer duration with consequent increase in total energy radiated per pulse. As indicated in PART I, the longer the pulse, the narrower the frequency spectrum. A long pulse consequently makes possible a narrower receiver band width, an improved receiver signal to noise ratio, and greater range. Although it was necessary to reduce the peak power somewhat in operating the 720A-E at a pulse length of 5 microseconds, a substantial increase in range could still be effected. The Radiation Laboratory at M. I. T. proposed to use 720A-E type magnetrons on long pulse operation and performed many tests of these magnetrons under these conditions. Many 720A-E magnetrons performed satisfactorily under these long pulse conditions. However, arcing both internally between cathode and anode and externally across the input leads deteriorated the performance and made the life expectancy of the magnetron questionable.

To meet the new demands a new series of magnetrons, the 4J45-47 was developed by making two design changes in the 720A-E. The plain, oxide coated cathode was replaced with a cathode of the "mesh" type to be described in Section 21. MAGNETRON CATHODES. The "mesh" cathode proved to be more rugged, involved less arcing, was longer lived, and required a minimum of changes in internal structure.

External arcing at the input leads was minimized by lengthening the glass section, accomplished by increasing the over-all lead length and shortening the metal section of the lead at the magnetron body, and by enclosing the leads in housings filled with a silicone anticorona compound. These changes were limited by the requirement of interchangeability with the 720A-E.

The modified 720B-D magnetrons were coded the 4J45-47. Operating characteristics are given in TABLE II. These magnetrons were used with long pulses and in the usual service for which the 720A-E had been designed.

17. MAGNETRONS FOR WAVELENGTHS NEAR 3 CENTIMETERS—UNDER 100 KILOWATTS

17.1 *The 725A and 730A Magnetrons:* As the antenna size of a radar is reduced, it is necessary to reduce the operating wavelength to maintain

the same width of radiated beam and resolving power. To meet the needs for aircraft and submarine radar and other applications in which antenna size must be small, shorter wavelength magnetrons were essential. The development of magnetrons of frequency near 10,000 mc/s (3 cm. wavelength) was part of the expanding program of magnetron research and development which grew out of the earliest experiments. The work was concentrated at 3.2 cm., roughly a factor of three below the initial 10 cm. work. From the earliest 3 cm. magnetron developments was evolved an efficient 3.2 cm. magnetron, the 725A, requiring roughly the same driving conditions as were used in the first 10 cm. magnetron applications.

An operating 3 cm. magnetron was built in the summer of 1941. The crude techniques then in use in the 10 cm. wavelength range were adapted to the 3 cm. range, and 5 kw. peak power from this magnetron was measured in a coaxial water load. This design involved an unstrapped resonator system having eighteen quarter wavelength slots. The choice of so many resonators was made in order that large cathode and anode dimensions could be used, later shown to be unreasonable for the voltage range employed. In addition the design suffered from a confusion of many modes of the resonator system and from an inadequate output circuit.

A later design, similar in some respects to one upon which work was done at the M. I. T. Radiation Laboratory, made use of a resonator system having twelve slots. This design operated in a mode other than the π mode, probably that for which $n = 3$ or $n = 4$. The M. I. T. version, the 2J21, was the first 3 cm. magnetron to be manufactured in quantity. Its power output was about 15 kw., generated at an efficiency of from 12 to 15 per cent. Many variations of this design were made without major success in an attempt to obtain efficient and reliable operation.

Prior to the introduction of straps, attempts were made to adapt 10 cm. magnetron designs to 3 cm. While none came up to the 10 cm. operating efficiencies, one such, having an unstrapped resonator system of eight hole and slot resonators, was used extensively in systems experimental work in our Laboratories.

By this time it was realized that some fundamental reason existed for the failure of these 3 cm. magnetrons to reach efficiencies comparable with those obtained at 10 cm. The resonator systems were unstrapped at 3 cm., and they operated in a mode other than the π mode. However, this did not fully explain their failure. Attempts were made to operate strapped 3 cm. magnetrons in the π mode, but they still did not result in the desired or expected improvements. The trouble lay not only in the mode frequency distribution of the resonator system but also in the size of the interaction space. Prior to this time, 3 cm. magnetrons were made with larger inter-

action spaces than direct scaling from 10 cm. would indicate. This had been done to achieve greater cathode size and smaller operating magnetic field. It appeared that 3 cm. magnetrons had been suitable only for operation at high voltage and high magnetic field and were being operated far below their range of maximum efficiency or even of reasonable operation. A decisive step forward was taken when a strapped magnetron was built which was rigorously scaled, according to the scaling principles discussed in PART I, from 10 cm. designs of the same operating voltage and current as that desired at 3 cm.

The first such magnetrons were scaled from the 10.7 cm. strapped magnetrons having eight resonators, the 718AY-EY, with only minor changes being made in the resonators for mechanical reasons. The results obtained were very encouraging although they were erratic for a variety of reasons. Mechanical construction was difficult and not reproducible before newer tools and techniques for making and assembling small parts were introduced. Output circuit variations in many cases completely masked good electronic operation, and it was not until a carefully considered and executed study of the output circuit design was instituted that consistent results were obtained. However, the results were such that it was decided to shift all emphasis in 3 cm. magnetron development at the Bell Laboratories to strapped designs scaled from 10 cm. magnetrons.

This was by no means an easy decision to make. For example, it meant the use of very small parts and clearances, of order 0.010 in., and very close tolerances. That such a magnetron would be feasible for large scale production was by no means obvious. A cathode, 0.100 in. or less in diameter, which must deliver a considerably higher current density than any previous magnetron cathode, would be necessary. Whether such a cathode, at the expected operating conditions, would have any appreciable life was not known. Furthermore, a scaled 3 cm. magnetron would require a much higher magnetic field than previous 3 cm. designs, a demand which might increase the magnet weight.

On the other hand, it was possible that the improved electronic efficiency of the scaled magnetron would result in less rigorous treatment of the cathode in spite of its small size. In spite of the increase in magnetic field, the decrease in anode length of the scaled magnetron made possible the reduction of the magnet gap to a point where it was conceivable that no greater magnetomotive force and size of magnet would be required than in previous 3 cm. designs. Greater stability and freedom from mode troubles could be expected.

Early strapped magnetrons having eight resonators had anode diameters of order 0.175 in. and cathode diameters of order 0.065 in. Magnetrons of

over-all efficiency better than 45 per cent at a pulling figure of 15 mc/s were made.

The cathode life in these magnetrons was very short—10 to 30 hours. Reduction of the severity of the demands made of the cathode was necessary. Strapped magnetrons having twelve resonators and larger cathodes were designed and a few built with promising results.

The 3 cm. magnetron development program was later broadened by the inclusion of personnel from the NDRC Radiation Laboratories at the Massachusetts Institute of Technology and at Columbia University. Effort on magnetrons having twelve resonators was expanded and prosecuted vigorously along with the work on the eight resonator types. Somewhat later the effort was concentrated solely on the twelve resonator magnetron. The design which was made shortly thereafter became, with only minor changes, the 725A.

Experience gained with previous magnetrons at all wavelengths enabled one to design a mechanically feasible resonator system with proper strapping to give the desired RF characteristics and π mode resonant frequency. The interaction space, on the basis of previous work and Hartree's oscillation condition, was designed to meet the specification of 12 kv. and 12 amps. input. The design was complicated both mechanically and electrically by the requirement of interchangeability with the 2J21. Thus good operation at 10 kv. and 10 amps. input was necessary.

The resonator system of the 725A is machined into a separable "anode insert" which, when completed, is brazed into position in the so-called "shell" carrying the leads and cooling fins. The straps are placed in a channel for shielding from the interaction space and are broken on one end.

The first cathodes were the ordinary, nickel sleeve type with double carbonate coating sprayed onto its surface. Not long after the start of the 3 cm. magnetron development, it was recognized that the cathode development problem would be a large part of the over-all project. Indeed, the 725A proved to be an excellent magnetron for cathode development work. Many of the cathode improvements and new designs developed for it have been used successfully in other magnetrons. The cathode as finally developed for the 725A was a nickel blank, complete with end disks and heater chamber turned out of nickel rod. Over the cylindrical portion was welded or sintered a fine nickel mesh in the interstices of which the active coating was applied. This is shown in Fig. 79 and will be described more fully with other cathode developments in Section 21. MAGNETRON CATHODES. Under normal operating conditions the cathode heater is turned off, the necessary heat being provided by electron back bombardment.

Considerable effort was expended in the design of a satisfactory and repro-

ducible output circuit for the 725A. The requirement of interchangeability with the 2J21 restricted the output wave guide flange in its position relative to the axis of the anode and the mounting flange. Previous 3 cm. magnetrons having hole and slot resonators utilized coaxial output circuits coupled to the resonator system by a loop located in the median plane of one of the resonators as in Fig. 1. Although it was recognized that a wave guide output for a small magnetron of this type would be more elegant and reproducible than a coaxial output, difficulty in twisting the plane of polarization from the resonator to the output wave guide flange, involved in the interchangeability requirement, and the lack of experience with such outputs made necessary the choice of an output for the final design similar to the original. To obviate the removal of a large portion of one resonator to accommodate the output and to make the loop easily accessible for inspection and adjustment, it was placed in the end space directly over the circular hole of one of the resonators. This so-called "halo" type loop is shown in Fig. 66. The coaxial line was terminated, as in previous 3 cm. magnetrons, in a junction to wave guide, fabricated as part of the magnetron. The output circuit was designed around a matched junction which, it was hoped, would have the best electrical breakdown strength at the reduced pressures of high altitude operation, would be frequency insensitive, and would avoid adjustment of the junction on individual magnetrons. The entire antenna of the junction was enclosed in the vacuum envelope of the magnetron as may be seen in Fig. 66.

The method of attack on the output circuit problem from this point on may be summarized as follows: First, a matched junction from coaxial to wave guide such that it could be applied to the final over-all design, had to be achieved. Then, for a given choice of loop size and position relative to the resonator, it was necessary to obtain the transformer properties of the coaxial line immediately adjacent to the loop so that the proper over-all coupling from magnetron resonator to wave guide load was achieved. Here again the mechanical restriction on the distance between the resonator and wave guide axes was found to be cumbersome. Two loop sizes were tried, that requiring the higher standing wave in the coaxial transformer to couple it properly being later discarded. At any given stage in the development, the procedure consisted of finding the impedance to be presented to the loop by the coaxial output. This was done by transforming through the entire output circuit to the loop terminals, the impedance needed in the output wave guide for proper loading, using the transformer parameters measured on a simulated output circuit. This impedance at the loop terminals was obtained by variation of the transformer properties of the coaxial line between the loop terminals and the coaxial to wave guide junction. The

change of diameter of the coaxial center conductor at a critical distance from the loop terminals is to be seen in Fig. 66. The height of the output loop above the resonator end surface was a convenient variable upon which the over-all output coupling depended. This was not without disadvantages, however, since its value for reproducibility had to be held to within 0.001 in. Its nominal height above the anode is 0.011 in.

While the scaling of 10 cm. magnetrons to 3 cm. demanded higher magnetic fields than had previously been used at 3 cm., the magnet size was

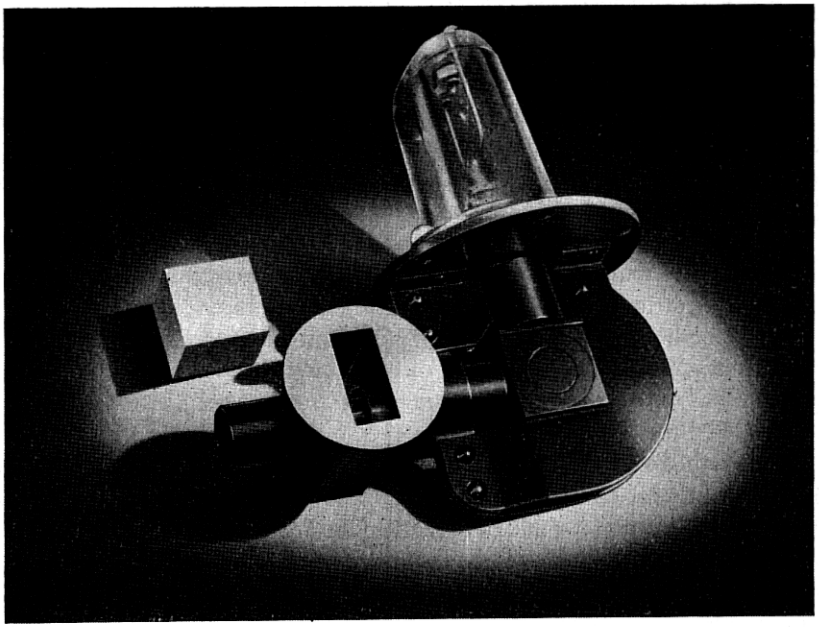

Fig. 65—An external view of the 725A magnetron (55 kw., 9375 mc/s), showing the attached coaxial to wave guide junction in the output circuit.

kept down by the reduction of the magnet gap made possible in the scaling of anode length. A further reduction in effective magnet gap was made by the inclusion of steel disks in the end covers of the magnetron. With these changes, the magnetomotive force required to supply the field for the 725A was almost identical to that required by the 2J21 and no extensive magnet redesign was necessary.

The requirement of interchangeability with the 2J21 made it necessary to place the input and output leads of the 725A at right angles (see Fig. 65). Along with the 725A, there was developed a version, coded the 730A, with input leads mounted directly opposite to the output in a so-called "straight

TABLE III

MAGNETRONS FOR WAVELENGTHS NEAR 3 CENTIMETERS

	725A, 730A Unpackaged			2J48-50 Unpackaged			2J55-56 Packaged	2J51 Packaged Tunable			4J50, 4J78 Packaged			4J52 Packaged	
N	12			12			12	12			16			16	
r_c (in.)	0.051			0.051			0.062	0.062			0.104			0.104	
r_a (in.)	0.102			0.102			0.125	0.125			0.159			0.159	
h (in.)	0.250			0.250			0.250	0.250			0.250			0.250	
Magnet gap (in.)	0.625			0.625			0.384	0.384			0.380			0.380	
Weight (lb.)	1.5,1.1			1.5			3.8	4.6			9.5			5.5	
Resonators	hole and slot			hole and slot			hole and slot	hole and slot			hole and slot			hole and slot	
Unstrapped λ (cm.)	2.3			~2.3			~2.3	~2.6			2.46			2.46	
Straps	double ring			double ring			double ring	double ring			double ring			double ring	
λ (cm.)	3.2			3.22, 3.3, 3.4			3.2, 3.24	3.33			3.2, 3.3			3.2	
f (mc/s)	9375 ± 30			9315 ± 5, 9080 ± 80, 8825 ± 75			9375 ± 30, 9245 ± 55	8500 to 9600			9375 ± 30, 9080 ± 80			9375 ± 30	
Nearest mode	$n = 5$			$n = 5$			$n = 5$	$n = 5$			$n = 7$			$n = 7$	
λ separation (%)	−16			−16			~−16	~−16			−14			−14	
Tuning	—			—			—	resonator inductance			—			—	
$\Delta\lambda$ (%)	—			—			—	12.1			—			—	
Tuner travel (in.)	—			—			—	0.110			—			—	
Q_0	680			680			680	630–460			850			850	
$Q_{ext.}$	280			280			290	290			350			350	
η_c (%)	71			71			70	65			71			71	
Output circuit	coaxial-wave guide			coaxial-wave guide			coaxial-wave guide	coaxial-wave guide			wave guide			wave guide	
V (kv.)	10.0	12.0	13.0	10.0	12.0	13.0	12.0	11.0	12.0	14.3	22.0	22.0	22.0	15.0	15.0
I (amps.)	10	10	12	10	10	12	12	11	12	14	27	27	27	15	13.5
B (gauss)	4500	5400	5650	4500	5400	5650	3350	3050	3350	4000	6900	6900	6900	4950	4950
τ (μs)	1	1	1	1	1	1	1	1	1	1	1	2	5	1	5.5
pps	1000	1000	1000	1000	1000	1000	1000	1000	1000	1000	1000	500	200	1000	200
P_0 (kw.)	31	44	56	31	44	56	50	33	40	60	280	280	280	110	95
η (%)	31	37	36	31	37	36	35	27	28	30	47	47	47	49	47
η_e (%)	44	52	51	44	52	51	50	42	43	46	66	66	66	69	66
PF (mc/s)	13.5	13.5	13.5	13.5	13.5	13.5	12	12	12	12	12	12	12	12	12

through" design. Experimental models were released for systems tests and the need developed for such magnetrons to be used in some special radar systems. The 730A is identical to the 725A except for external mechanical details. An external view is shown in Fig. 67.

Details of the final design of the 725A (and 730A except for the mechanical differences noted) may be seen in Fig. 66. Data on these magnetrons and their performance are given in TABLE III. A typical performance chart

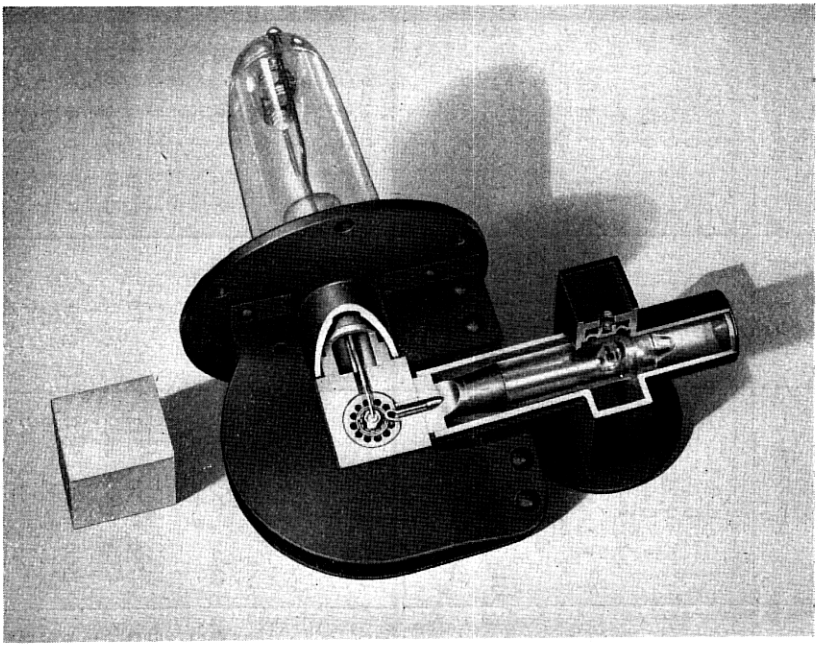

Fig. 66—A view of a cut-away 725A magnetron (55 kw., 9375 mc/s). Note the breaks in the double ring straps, the so-called "halo" loop above the hole of the output resonator, the step in the center conductor of the output coaxial providing the necessary impedance transformation, and the details of the coaxial to wave guide junction.

is shown in Fig. 68. Experience has indicated that it is entirely adequate for 150 kw. input at duty cycles up to 0.001 and, with later cathode designs, at pulse lengths up to 5μs. The RF spectrum is satisfactory even under rather extreme conditions of mechanical vibration and shock, and the operation under a variety of conditions is remarkably free from "moding". Difficulties have been encountered in attempts to push its power input with 5μs pulses much above 175 kw. although with short pulses at lenient duty cycle operation with as much as 300 kw. peak input power has been achieved.

Many difficulties were encountered in the early stages of production above those of training personnel to handle small parts and to perform new types of operations. Maintenance of cathode centering through all operations had to be rigidly supervised since off-center cathodes resulted in poor operation. The size and position of the output loop were very sensitive variables directly affecting output power and pulling figure. The latter were also marked functions of variables in the transformer of the output circuit. It was found, for example, that variations in the glass, and particularly in the bead supporting the center conductor, were causing considerable

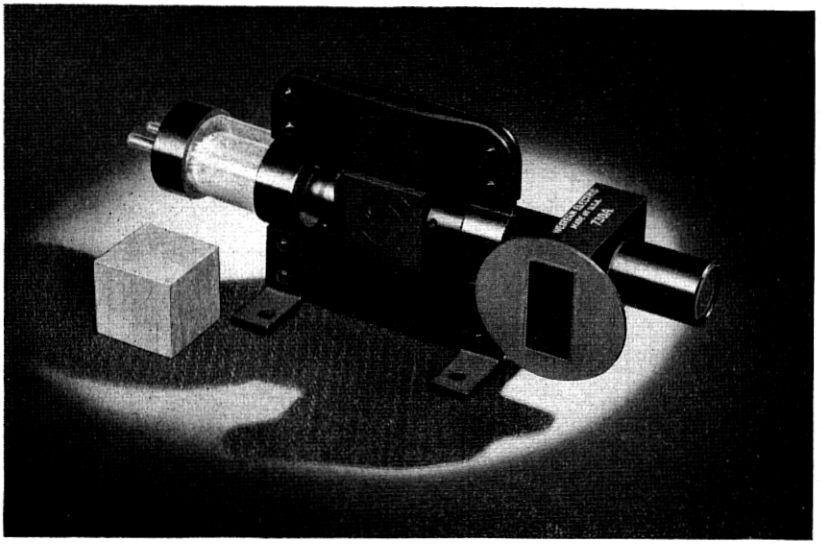

Fig. 67—The 730A magnetron (55 kw., 9375 mc/s)—the "straight through" version of the 725A.

spread in characteristics. Closer tolerance on the glass, involving the use of a molded bead, greatly improved this situation.

With the very narrow limits specified for the operating frequency of the magnetron, it was essential that the anode pretuning be done very precisely. Here, considerable difficulty was encountered with a pretuning arrangement in which the indication of resonance depended on the equivalent line length of the output circuit between the anode block and the detector in the wave guide. Variability in this electrical length caused the actual resonance to vary over a considerably wider range than the required 9375 $\pm$ 30 mc/s. By use of a detector connected at the output loop it was possible to reduce the percentage of magnetrons eliminated for being outside the frequency

limits at final test from more than 50 per cent to less than 1 per cent. At one point in the development, when it appeared that the frequency spread could not easily be reduced, a tuning screw mechanism was designed with which the frequency of the resonator system could be varied by movement

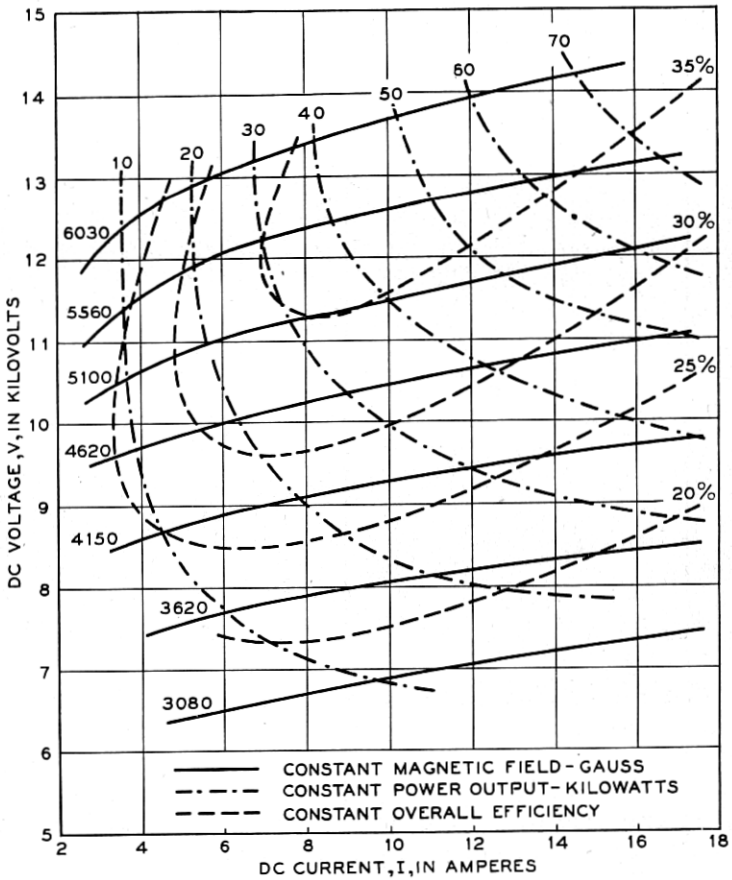

Fig. 68—A typical performance chart of the 725A and 730A magnetrons (9375 mc/s).

of a plug through the side wall of one resonator and which could be adjusted from outside the vacuum envelope at the final acceptance test. Although the mechanism was built, tested, and found to operate satisfactorily, the improvement of the pretuning technique made its adoption unnecessary.

During the initial stages of production it was verified that the pulling figure of the 725A and 730A could be adjusted within limits by variation of the position of the end plate shorting the wave guide section into which the

coaxial output circuit of these magnetrons is terminated. It is possible by a displacement of 0.040 in. of the whole end plate to effect about a 6 mc/s change in pulling figure near the value of 15 mc/s. An end plate consisting of a convoluted diaphragm was constructed which could be adjusted at final test if necessary. By this means it was possible to make the adjustment without disturbing the airtight seal needed in some pressurized installations. The adjustable end plate is to be seen in the cutaway model of Fig. 66.

Despite initial difficulties, it was possible in the first nine months of production to increase the yield of shippable magnetrons meeting all the test specifications from a very low initial figure to over 85 per cent of all those completed and reaching final acceptance tests. Although subsequent tightening of the test specifications, such as the increase of pulse length at test from 1μs at 1000 pps to 2 μs at 325 pps, caused temporary setbacks in the percentage yield, it was nevertheless increased until it ran consistently better than 95 per cent.

Although better magnetrons have since been built in the 3 cm. wavelength range, the 725A occupies a special place in magnetron development at these wavelengths. It represents the first high efficiency, π mode, strapped magnetron for 3 cm. operation, and as such has served as the prototype of most of the subsequent 3 cm. magnetron developments in the United States and Great Britain.

The 725A was manufactured by the Western Electric Co. in this country and the Northern Electric Co. of Canada. The Raytheon Mfg. Co. used Bell Laboratories' design information to produce a 725A magnetron but redesigned the resonator system to use a vane type more adapted to their manufacturing practice. The total number of 725A magnetrons produced in these three plants was over 300,000, indicating the extent to which it was used during the war.

17.2 *The 2J48, 2J49, 2J50, and 2J53/725A Magnetrons:* Following completion of the 725A magnetron at 3.2 cm., requests were made for three similar magnetrons. These were to have the same characteristics as the 725A, differing only in their frequencies of operation.

The 2J48 is an exact duplicate of the 725A but has a narrower spread in frequency, $\pm$ 5 mc/s, around a mean value of 60 mc/s lower than the nominal 725A frequency of 9375 mc/s. The 2J48 was never manufactured by the Western Electric Co.

The 2J49 and 2J50 are 725A types operating at 3.3 cm. and 3.4 cm., respectively. These new wavelengths were met by a new resonator design involving larger resonator holes than in the 725A. The nominal wavelength of the new design was 3.35 cm., tuned either into the 3.3 cm. or the 3.4 cm. band by strap manipulation.

In an effort to get high power from the 725A magnetron operating on long pulses, considerable work was done to build a cathode for a power input of 225 kw. While a few thousand such magnetrons were made and tested at the higher test condition, entirely satisfactory operation was never achieved. Magnetrons tested at 225 kw. input were coded the 2J53/725A but after the first production run were not manufactured again. The 4J50 and 4J52 magnetrons are now available for this range of operating conditions.

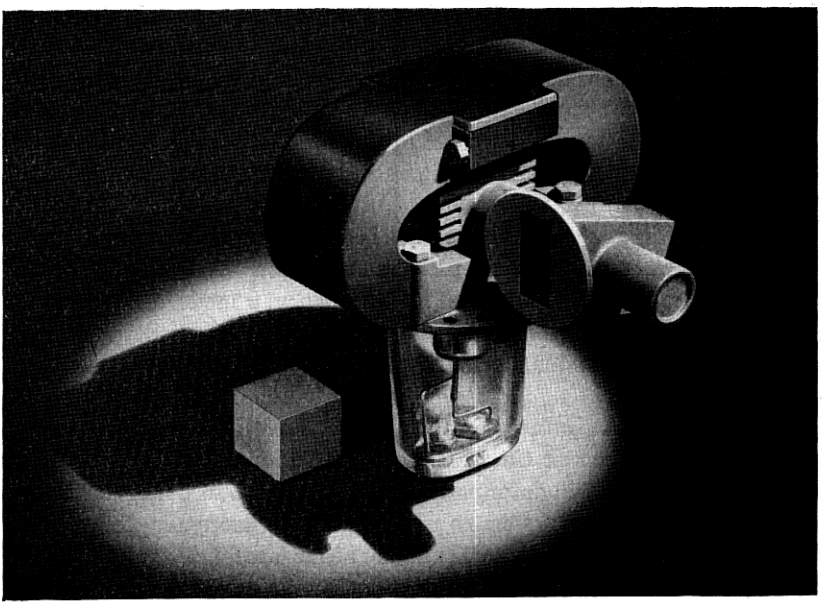

Fig. 69—The 2J55 magnetron (55 kw., 9375 mc/s)—the "packaged" version of the 725A. Compare with the size of the 725A and its magnet shown in Fig. 44.

17.3 *The 2J55 and 2J56 Magnetrons:* The 2J55 and 2J56 are by-products of the development of a tunable 3 cm. magnetron, the 2J51, described below. The 2J51 design, being "packaged" and thus lighter and more compact than the 725A and its magnet, with which it is interchangeable, was ideally suited for conversion into a fixed frequency, "packaged", 3 cm. magnetron. The only design changes required were those associated with the removal of the tuning mechanism and the change in dimensions of the resonator system needed to bring the wavelength to the proper value. The two magnetrons designed in this way for operation at the wavelengths 3.2 and 3.25 cm. were coded the 2J55 and 2J56, respectively. Each weighs 3 lbs. 12 oz. as compared to the weight of 11 lbs. 2 oz. of the 725A magnetron and its magnet.

A photograph of the 2J55 magnetron is shown in Fig. 69 and operating data are included in TABLE III.

18. TUNABLE MAGNETRONS FOR WAVELENGTHS NEAR 3 CENTIMETERS

18.1 *The 2J51 Magnetron:* As in the 20 to 45 cm. wavelength region, the demand arose for tunable magnetron replacements when fixed frequency magnetrons had become available in the 3 cm. band. A significant step toward satisfying this demand was taken at the NDRC Radiation Labora-

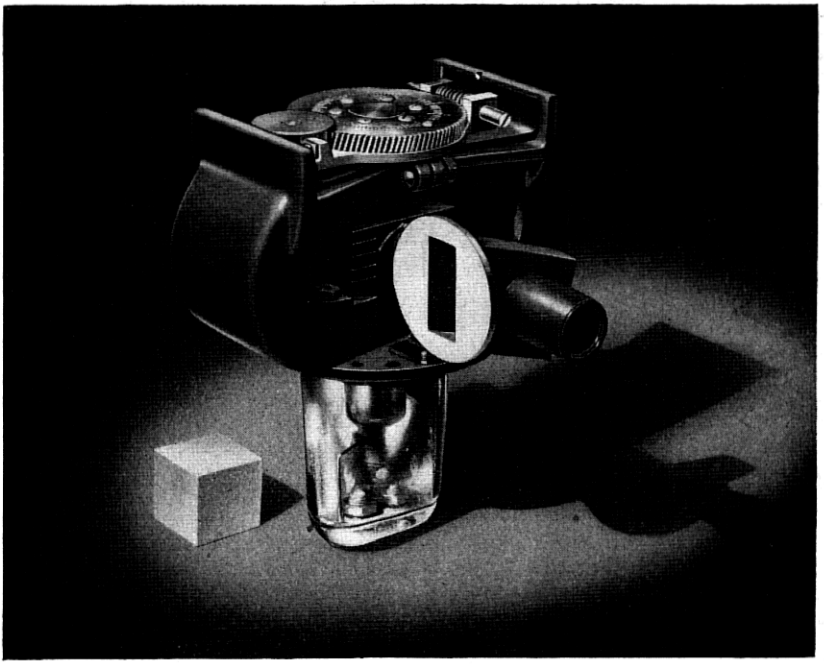

Fig. 70—An external view of the 2J51, tunable, "packaged" magnetron (55 kw., 8500 to 9600 mc/s).

tory at Columbia University in 1943 when a tuned, "packaged" magnetron was built around a 725A anode structure and output circuit. The tuning scheme used was that of variation of resonator inductance, as discussed in PART I, by a so-called tuning head consisting of a set of pins which project into the holes of the resonator system. The mechanism for driving the tuning head is contained inside one of the magnet pole pieces. The other pole piece carries the axial cathode mount. Two magnets are clamped to opposite sides of the pole pieces in the usual "packaged" construction. These and other details are shown in the photographs in Fig. 70 and 71 of complete and cutaway models of the magnetron, coded the 2J51, as it was put into production at the Western Electric Co.

From the inception of the project until the bulk of the work of developing the tunable 3 cm. magnetron was transferred to the Bell Laboratories, a number of problems had been encountered and solved at the Columbia Laboratory. It had been shown that tuning a 725A type magnetron was

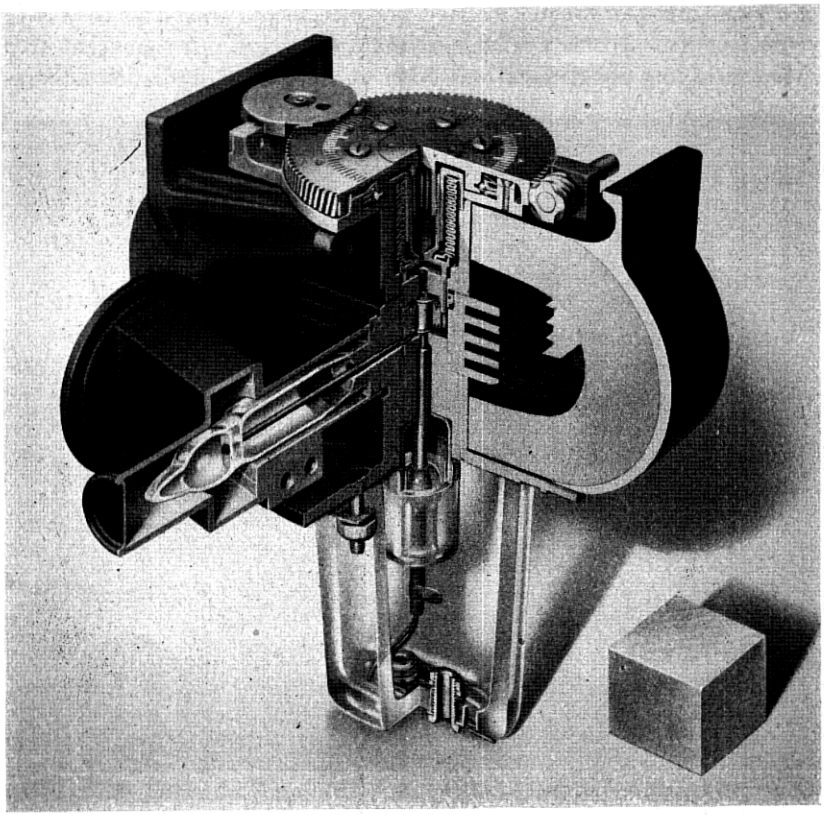

Fig. 71—A view of a sectioned 2J51, tunable, "packaged" magnetron (55 kw., 8500 to 9600 mc/s). Features of interest to be seen are: the tuning pins, the drive mechanism and vacuum bellows, the axial cathode mount, the glass bead support of the center conductor of the coaxial output line, and the sheathed permanent magnet construction.

feasible by the means chosen. The range of wavelength from 3.13 to 3.53 cm. could easily be spanned. The variation in frequency was found to be very nearly linear with position of the tuning pins. It was shown how a spurious resonance of the pin structure occurring within the frequency range could be displaced so as to cause no difficulty. Although no work of revision had been done on the 725A output circuit used in the tunable magnetron, it was demonstrated that tolerably "flat" characteristics of

output power and pulling figure against frequency could be obtained with it. The fundamental mechanical problems of "packaging" the magnetron and providing facilities for driving the tuning head were shown to be feasible and a smooth working and resettable driving mechanism designed and constructed.

The Columbia Radiation Laboratory built a series of these magnetrons, several of which were used in the development of tunable radar systems. The Bell Laboratories had cooperated from the start by supplying 725A magnetron parts, and by making anode inserts of special dimensions to raise the maximum attainable wavelength of the resonator system. It was decided that the Bell Laboratories should take over the main burden of further development of the magnetron for manufacture by the Western Electric Co. By this time its specifications had been quite definitely established. It was to be a magnetron with the general power output capabilities of the 725A, tunable over the frequency range from 8500 to 9600 mc/s (approximately 3.13 to 3.53 cm.). It was to be interchangeable with the 725A magnetron in the sense that it could be installed directly in any radar system using the 725A when the magnetron and its magnet were removed. Interchangeability, as usual, was one of the most annoying requirements. The magnetron was to be "packaged" and provided with magnetic shunts so that the magnetic fields necessary for operation at 10 kv. and 10 amps., 12 kv. and 12 amps., and 14 kv. and 14 amps. could be attained with a single magnet design. No specific requirements on variation of output characteristics were made at that time, but it was understood that only a magnetron whose pulling figure varied by an amount of the order of 3 mc/s or less over the entire frequency band would be acceptable. Similarly, it was understood that the tuning mechanism should provide smooth variation in frequency with a minimum of backlash and of such resettability that the use of a wavemeter would not be required in setting the radar system to a new frequency.

During the course of the development at the Bell Laboratories it became necessary to redesign the magnetron in a number of important respects. The requirement that the magnetron operate at 14 kv. and 14 amps. demanded a magnetic field for which the magnet weight would be prohibitive. Consequently, anode and cathode radii were scaled from those of the 725A magnetron by the factor 1.2. The larger cathode resulting from this redesign made easier the problem of attaining the maximum of 200 kw. peak input power required by the specifications. However, it caused a recurrence of the difficulty with a resonance of the tuning pin structure appearing in the 8500 to 9600 mc/s range. This had been found at the Columbia Laboratory to be a resonance of the capacitance between the pins and anode structure

with the inductance of the end space region through which the pins project from the magnet pole piece into the resonators. As before, the frequency of this resonance was removed by filling the end space with a copper ring or collar.

In the course of study of this resonance and of output circuit characteristics, an extensive program of testing of non-oscillating experimental models, whether operable or not, was carried out to supplement the data of oscillation tests. From these measurements, three important types of data were obtained, namely, the variation of pulling figure with frequency, the amount of RF energy loss introduced by the insertion of the tuning pins, and the variation of frequency with position of the tuning head. The first of these data, combined with measurements of the output circuit transformer characteristics made on simulated and adjustable models, yielded a complete understanding of the functioning of the output circuit. The effect of coupling loop size and of the variation of the dimensions of the coaxial to wave guide junction on the performance of the magnetron over the frequency range were determined. Although other designs of output circuits of the general 725A type were experimented with, it was possible to adjust the parameters of the original 725A output circuit to give a reasonably flat characteristic with frequency. In Fig. 72 are shown the variation of pulling figure and Q_{ext} over the frequency band.

The variation of unloaded Q with frequency, obtained in the above mentioned non-oscillating tests, indicated that stainless steel pins or even such pins copper plated to a considerable thickness were unsatisfactory. It was found that under the heat treatment occurring during brazing operations the copper plate and steel diffused through each other so as to increase markedly the surface resistance of the pins. Copper sheathed pins were found to be satisfactory. Solid copper was finally used as it was found to possess sufficient strength under mechanical shock test. Even so, as Fig. 72 indicates, the Q_o of the resonator system falls off with increasing frequency and pin penetration.

Determination of the variation of frequency with position of the tuning pins dictated the design of the drive mechanism to provide the necessary range of motion. It was found that, with a pin diameter of 0.064 in. moving in resonator holes of 0.088 in. diameter, the frequency band could be spanned in a total travel of 0.110 in. Fig. 72 shows the nearly linear relationship between frequency and pin penetration.

The drive mechanism of the early Columbia models was redesigned to make possible its fabrication by a single brazing operation in a jig and to provide a sleeve rather than a thread bearing. The backlash achieved in the final design is such that one may reset the tuning head for a given frequency

to within 1 mc/s which corresponds to a displacement of the pins of 0.0001 in. and to 0.1 turn of the worm wheel drive. The tuning mechanism is provided with a positive stop at each end of the tuning range. The frequency band is covered in five revolutions of the main drive screw and gear. A flexible vacuum envelope is provided by means of sylphon bellows. Details of the design may be seen in the sectioned model shown in Fig. 71.

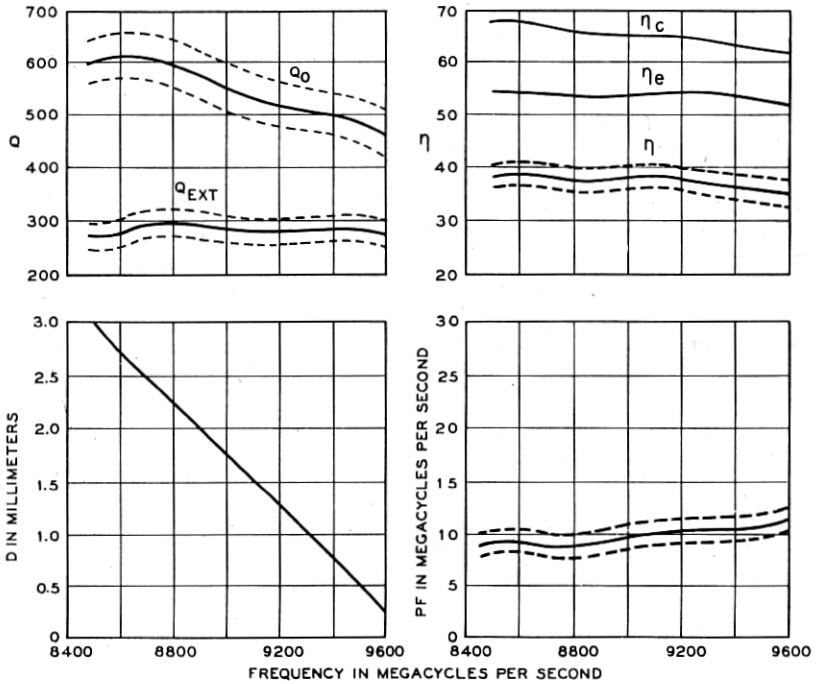

Fig. 72—Smoothed characteristics of the 2J51 tunable magnetron (55 kw., 8500 to 9600 mc/s) throughout its frequency band. Shown is the dependence upon frequency of the unloaded Q, Q_0; of the external Q, Q_{ext}; of the circuit efficiency, η_c; of the electronic efficiency, η_e; of the over-all efficiency, η; and of the pulling figure , PF. Also shown is the dependence of the operating frequency upon position of the tuning pins, D, measured from the position of maximum intrusion. The dashed lines on either side of the experimental curves indicate the range of possible variation of the data. The curves for η_e and η_c have been determined from the experimental results by the use of equation (25) of PART I and the relation $\eta = \eta_e \eta_c$.

The elimination of radial cathode support leads and the use of the magnetic pole pieces as the end covers of the magnetron body made possible a large reduction in the magnet gap and magnetomotive force required to produce the necessary magnetic field. Because of the requirement of interchangeability with the 725A magnetron, a very awkward V-shape magnet design in which the leakage flux was tremendous could not be avoided.

Fortunately, before production commenced, relaxation of the interchangeability requirements made a change in the magnet form possible, and the much more efficient U-shape of those shown in Fig. 70 was adopted.

In performance, the 2J51 magnetron is essentially a 725A capable of operating over a 12 per cent frequency band. TABLE III gives two sets of operating conditions available through the use of the magnetic shunts. Fig. 72 shows several circuit characteristics of the magnetron over the frequency band. Also shown is the variation in over-all operating efficiency. The slight drop in efficiency observed as the frequency increases is due primarily to the decrease in Q_0. The electronic efficiency increases slightly with increasing frequency. The performance chart of the magnetron at its intermediate magnetic field is very similar to that of the 725A at the same field value, as shown in Fig. 68. The performance of the 2J51, when connected to a long, mismatched line exhibits a periodicity in power output, pulling figure, and frequency variation as the tuning is changed. This is expected in such a case because of the resulting changes occurring in the electrical length of the line with changing frequency. If the mismatch is sufficiently great, the condition may exist in which periodic regions of the frequency spectrum are completely unattainable, as discussed in section 10.2 *Frequency Sensitive Loads.*

The 2J51 represents an attempt to design considerable versatility into one magnetron. As has been described in the discussion of the 2J55 and 2J56, the development of the 2J51 provided the opportunity to make available "packaged" magnetrons of fixed wavelengths near 3 cm. by the omission of the tuning mechanism.

19. MAGNETRONS FOR WAVELENGTHS NEAR 3 CENTIMETERS—100 TO 300 KILOWATTS

19.1. *The 4J50, 4J52, and 4J78 Magnetrons:* In the later stages of development of the 725A, it had been demonstrated that a high efficiency scaled magnetron of wavelength near 3 cm. was feasible. It also had become evident that, freed from the hampering restrictions on input power and mechanical interchangeability, a magnetron of considerably greater output power capabilities could be made. The achievement of a magnetron design capable of delivering at least 200 kw. output power at a duty cycle of 0.001 or greater was set as a first objective. This was achieved with a good margin. During its entire course, the program was actively participated in by members of the Radiation Laboratory at M. I. T. working in residence at the Bell Laboratories.

The objective of 200 kw. peak output power at the factory test was not considered to be the maximum obtainable from a 3 cm. magnetron but

was largely determined by the state of development of systems and components when the work began. It was desirable to produce a magnetron which, while marking a very substantial gain over the 725A in power output, should at the same time be of reasonable weight, air-cooled, and capable of operation with a pulser of modest dimensions and of working into the system components in existence or under development.

The design began with the choice of a resonator system having sixteen resonators. The anode diameter was chosen for an operating voltage range of 20 to 25 kv. The increase in number of resonators from twelve to sixteen and operation at higher voltage necessitated a considerable increase in cathode diameter over that of the 725A. The length of the anode was left as before because it was felt that the desired increase in total cathode emission would be available from the increase in cathode area and that the magnet weight ought to be kept as low as possible.

Experimental models incorporating these design changes were built in the 725A type structure with radial cathode mount, "halo" coupling loop and coaxial output terminating in a junction to wave guide. The performance of these early models was satisfactory. Operating efficiency better than that of the 725A mgnetron was achieved over the range of currents from 4 to 40 amps.

However, it was easily to be seen that the 725A type structure was by no means the ideal for a 3 cm. magnetron of increased output power. The output circuit was marginal in its power handling capabilities; it could transmit no more than 300 kw. Furthermore, the opportunity presented itself of eliminating other troublesome features such as the "halo" loop and the coaxial to wave guide junction by designing a wave guide output whose critical dimensions are machined to size. The type of cathode structure of the 725A was limited in its heat dissipation in comparison with the axial type of cathode mount made possible by the use of magnet "packaging". In addition, the axial type cathode mount is superior from the standpoints of DC voltage breakdown and economy of space. Considerations of weight also favored the "packaged" structure, in which the magnet pole pieces form an integral part of the magnetron structure. Many of these first experimental models suffered from a drooping voltage-current characteristic at constant magnetic field in the region of low currents. This effect and its attendant loss of operating efficiency became progressively worse as the magnetron was operated. It was hoped that the parasitic electron emission from the cathode end disks, believed from experiments with non-emissive coating materials to be responsible for the effect, could be eliminated or reduced in an axially mounted cathode.

Accordingly, an entirely new design was undertaken, built around the

sixteen resonator anode structure used in the early work but including the features of "packaging," axial cathode mount, and wave guide output. A number of vexing but nevertheless interesting problems was encountered. Principal among these were the tendency to operate in another mode under certain conditions and the problem of obtaining satisfactory magnetic field uniformity in a design which necessitated the removal of a considerable portion of the center of the magnet pole piece to accommodate the axial cathode mount. Each of these difficulties was surmounted as is described in the detailed discussion later. The resonator system was redesigned quite late in the development to take advantage of the possibility of operating at a lower electronic conductance and hence higher RF voltage for the same output power. The advantages of this step were a reduction in the tendency of the magnetron to "mode" and an increase in unloaded Q.

The development program briefly sketched above resulted in three coded magnetrons, the 4J50, 4J52, and 4J78. The 4J50 and 4J78 magnetrons, identical except for frequency, were built with magnets large enough to permit operation near the maximum power capabilities of the design and with larger input leads to withstand the higher DC voltage required. The 4J52 magnetron, although incorporating the same internal design as the other models, was built with smaller magnets for operation at a set of conditions easily attainable with the higher power design but beyond the reach of the 725A. Developmental work on all three magnetrons was conducted simultaneously.

In the 4J50 magnetron a hole and slot resonator system was adopted. The remarkable freedom of the 725A magnetron from "moding" difficulties had made it appear desirable to retain as large a mode frequency separation as possible. Equivalent circuit theory indicated that to do this the increase in the number of resonators from twelve to sixteen would necessitate about twice the strap capacitance of the 725A. This would have required extremely wide straps for which the recess channel in the anode structure would be very difficult to trepan. For this reason the resonator system was strapped less heavily; the $n = 8$ and $n = 7$ mode frequencies differed by 19 per cent rather than 25 per cent as in the 725A.

In none of the early models built into 725A type structures was any "moding" or "misfiring" observed. When axial cathode and wave guide output were introduced, however, "moding" was experienced both in those with no strap breaks and those with the usual double break at one end of the anode. By enlarging the cathode diameter such that the ratio of cathode to anode radii increased from 0.60 to 0.66, the difficulty was removed in models with broken straps, but it was not possible to eliminate it in those with unbroken straps. Decreasing the r_c/r_a ratio increased the tendency to "mode."

It might be surmised that the trouble in the unbroken strap case was due to a component of $n = 7$ which did not couple to the output circuit. The phenomenon was studied in an operating magnetron with small electrostatic probes built into several resonators. The $n = 7$ components were identified, their relative intensities being approximately those expected. It is of some interest to note that the "moding" encountered here differed from that seen in magnetrons of longer wavelength. The magnetron seemed invariably to start in the π mode, falling into oscillation in the $n = 7$ mode more rapidly as loading increased. As might be expected from this behavior, the mode boundary on a performance chart is little affected by the rate of rise of the pulse as it had been in other magnetrons. Later evidence made it appear that the change in the operating voltage of the $n = 7$ mode brought about by the redesign of the resonator system was a decided improvement.

The necessity of using strap breaks led to an unforeseen difficulty. Under the influence of RF electric forces, the overhanging ends of the straps at the strap breaks moved together and shorted, causing failure after only a few hours of operation. The trouble was eliminated by removing the overhanging portions of the straps with no noticeably harmful effects.

In a 3 cm. magnetron, strapped as heavily as the 4J50, circuit losses become very important in determining the over-all efficiency. A noticeable improvement in unloaded Q was effected when an atmosphere of prepurified N_2 was substituted for the CO_2-alcohol mixture which had previously been used to prevent oxidation during the final brazing. The CO_2-alcohol method had been abandoned for another reason, namely, that chemical analysis showed carbon deposited on the steel pole-pieces underneath the copper plating.

If one determines the circuit efficiency for matched load by impedance measurements on a non-oscillating magnetron [see equation (25) of PART I], one may then calculate its value for any load. From measurements of over-all efficiency as a function of load conductance, the dependence of the electronic efficiency on this conductance may be determined. The curve of Fig. 19 was obtained in this way for the 4J50. The fact that the electronic efficiency, as seen in Fig. 19 is practically independent of load, that is to say, of electronic conductance, together with some observations of the load sensitivity of the "moding" in the 4J52, led to consideration of a new design for the resonator system. It was found invariably that the boundary for mode change in the 4J52 magnetron moved to higher currents as the load impedance was changed to values further removed from the frequency sink and power maximum in any direction on the Rieke diagram. This suggests that, as the circuit conductance [G_s of equation (36)] is

increased, the decrease in RF voltage in the π mode places that mode at a disadvantage in competition with the $n = 7$ mode.

As a result of these considerations, a new resonator system was designed in which the electronic conductance at the normal operating point was to be two thirds of that in the first design. To maintain the pulling figure invariant, it was necessary to reduce the total resonator capacitance. Although all of this capacitance could not be removed from the straps without reducing the mode frequency separation too drastically, a good proportion of it could be. From this, one might expect a gain in unloaded Q since the straps are the lossiest part of the circuit.

The new resonator system is more satisfactory than the old. Mechanically, it is neater in that the outer strap does not extend into the holes of the hole and slot resonators. A definite increase in over-all efficiency attributable to a greater Q_o was observed. The mode separation is 17 per cent, much greater than the expected value. An analysis of data on the $n = 8$, 7, and 6 mode wave lengths, by means of equivalent circuit theory, indicated that this is due to the straps being effectively shorter although their physical length is unchanged in the new design. This is plausible, however, for in the new design the outer strap is connected at a higher voltage point along the resonator.

The cathode structure of the 4J50, 4J52, and 4J78 magnetrons represents a radical departure from previous designs. It was desirable from the production standpoint to be able to build the cathode structure completely as a subassembly before mounting it in the magnetron. This entailed making holes in the magnet pole pieces large enough for the cathode to pass through; these holes were, in fact, made of the same diameter as the anode (0.319 in.). Since no radial cathode support leads were required, it was possible to reduce the end spaces to a height of 0.065 in., making the magnet pole gap 0.380 in. It was recognized that the large hole to gap ratio would result in two bad effects: first, a loss of magnetic field and, second, an antibarreling of the magnetic field which results in an axial force acting on the electrons, directed away from the center of the interaction space. Both of these difficulties were surmounted by the use of cathode end structures made of high Curie temperature permendur (50 per cent iron, 50 per cent cobalt).

The permendur pieces, toroidal in shape, are mounted at the two ends of the cathode (see Figs. 75 and 78). Their cross section and location, necessary for a nearly uniform field over 80 per cent of the gap and a focusing field over the remainder, were determined in electrolytic tank experiments. Since the permendur pieces fill up a part of the hole in the magnet pole piece and have a separation less than the pole gap, they contribute substantially

to the magnetic field in the anode-cathode region. The effective gap is reduced from 0.380 in. to 0.340 in. by their presence, resulting in about a 20 per cent decrease in magnet weight. While their primary function is magnetic, the permendur pieces also serve as normal cathode end disks preventing electrons from reaching the pole pieces. Their smooth contour gives a good DC voltage breakdown condition between anode and cathode. Finally, they are mounted in such a way that there is some thermal isolation from the cathode and that the migration path from cathode to external surface of the permendur is quite long. These features discourage electron emission from the cathode end structures.

Almost any degree of cooling may be obtained with an axially mounted cathode without the attendant disadvantages of the heavy tungsten leads which fill up the end spaces of a magnetron having radial cathode mounting. An upper limit to the cooling is set by the fact that the cathode must be raised to 1050°C in activation, using a heater which can be contained within the cathode sleeve without encroaching too much upon its wall thickness. The high temperature needed during activation sets certain limits upon the materials which may be used in the cathode structure. Since the cathode is mounted from one end only (this being dictated by assembly considerations), mechanical strength is exceedingly important. A cathode, once off center, is subjected to magnetic forces on the permendur ends which tend to pull it further off center. Fortunately, measurement at the magnetic fields used in normal operation shows that these forces are only of the order of one pound for a cathode position 0.015 in. off the axis, increasing to about 3.5 pounds when the permendur is in contact with the wall.

The first cathode surfaces used in these magnetrons were of the "mesh" type. Later, the newly developed, sintered nickel matrix type was used. More recently, considerations of strength have led to the introduction of molybdenum cathodes. The cathode assembly is brazed into a hollow metal cone in the base of which is a receptacle type heater and cathode connection. Because of the length of the supporting structure and the relatively high temperature at which it operates, there is considerable expansion and resultant motion of the cathode in the axial direction. The cathode is offset when cold to correct for this expansion. Performance is not very sensitive to cathode location, but in extreme cases of misalignment moding difficulties may be aggravated. The cathode structure is to be seen in Fig. 78 and is shown mounted in the magnetron in Fig. 75. Attention should be called to the external cathode input lead which is of heavy glass and Kovar construction sufficiently rugged to make unnecessary any protective housing.

In the wave guide output designed for the 4J50 magnetron, the necessary

impedance transformation is accomplished by a quarter wavelength section opening directly into the output wave guide at one end and into the outside wall of one resonator at the other (see Fig. 30 and discussion in PART I). The small height of the resonator system from pole piece to pole piece makes it necessary to use a loaded line, in this case of H-shape cross section. The nature of the output circuit may be seen in the photograph of a cutaway model of the 4J52 in Fig. 75.

The transformation from the wave guide impedance of about 400 ohms through the iris formed by the junction of the H-shape and rectangular wave guides and through the $\lambda/4$ section inserts a resistance of about 2 ohms in series with the resonator to which the output circuit is connected. End effects make the desired transformer length differ slightly from $\lambda/4$. The length necessary to give a pure resistance at the input end was determined by measurements in a 10 cm. model with which the distance from the rectangular wave guide to the first voltage minimum in the H-section could be measured.

The vacuum seal in the wave guide output circuit was made at a circular window sealed in a Kovar cup, mounted between choke couplings as seen in Fig. 75. The diameter of the window and its thickness were chosen so that the reflection coefficient of the window would be quite low over a broad band of wavelengths near 3 cm. Insertion of a dielectric such as the glass window into the wave guide line increases the capacitance per unit length of the line. Compensation for this to bring the characteristic impedance back to the normal value is done by increasing the inductance per unit length over the same region. This may be accomplished by reduction of the long dimension of the wave guide resulting in a nearly square cross section. The circular opening, preferable for glass sealing, is a compromise, the critical diameter being determined by experiment. The relatively large size of the window makes it capable of withstanding RF voltage breakdown even at very high power.

Control of the output coupling is most readily effected by varying the width of the slot in the H-section. The over-all transformation properties of the H-section have been analyzed theoretically and the results confirmed by measurements on output circuit models. By means of this analysis it is possible to estimate fairly well the effect of changes in the slot width upon the pulling figure. To hold the latter within production limits of $\pm$ 2 mc/s, the slot must be held to $\pm$0.001 in.

The output circuit of the magnetron is formed by building up the assembly from sections in what has been called a "sandwich" type construction. The resonator system and the central portion of the output H-section are machined into one slab of copper. The "sides" of the H-section are

milled into this piece on either end. This center slab is "capped" on each end by a slab of copper, in which are contained the magnet pole pieces and appropriate surfaces on which to build the rest of the magnetron. Some of the details of this structure may be seen in the cutaway model of Fig. 75.

Despite the large impedance transformations involved, the output circuit is quite frequency insensitive. As it appeared that these magnetrons might be made tunable, considerable attention was paid to this characteristic. Numerous tests of the output circuit and its component parts were

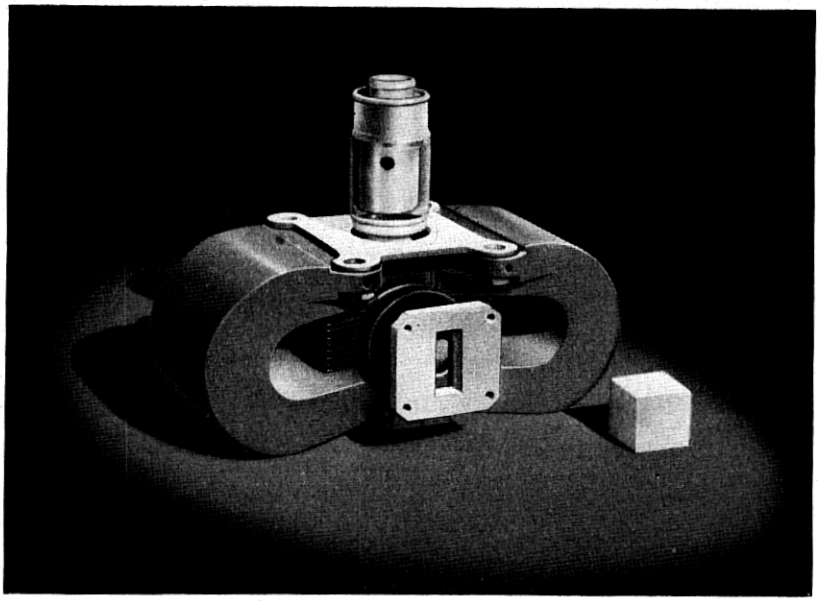

Fig. 73—An external view of the 4J50 "packaged" magnetron (280 kw., 9375 mc/s). Note the circular glass window in the wave guide output circuit and rugged axial input lead which requires no external protecting boot.

made over the 8500–9600 mc/s band. The iris and quarter wave length guide section were studied theoretically in this regard as well. The transformer properties of the window and choke coupling combination is the most frequency sensitive part of the entire output circuit. By adjustment of the distance from the H-section to the window, it was found possible to cancel some of the sensitivity of the two parts.

External views of the 4J50 (4J78) and the 4J52 magnetrons are shown in Figs. 73 and 74 respectively. The internal view of the 4J52 is shown in Fig. 75.

Except for magnet size and cathode supporting structure all three of

these magnetrons are essentially identical. Geometrical and performance data are given in Table III. As may be seen, these magnetrons represent an increase in power capabilities by a sizable factor over the 725A. The 4J52 magnetron has been used extensively under the severe conditions of 5 μs pulse duration, a repetition rate of 200 pulses per second, 15 kv. and 15 amps. input. Under these conditions it has not been possible to eliminate entirely a tendency to arc, although good performance is obtained.

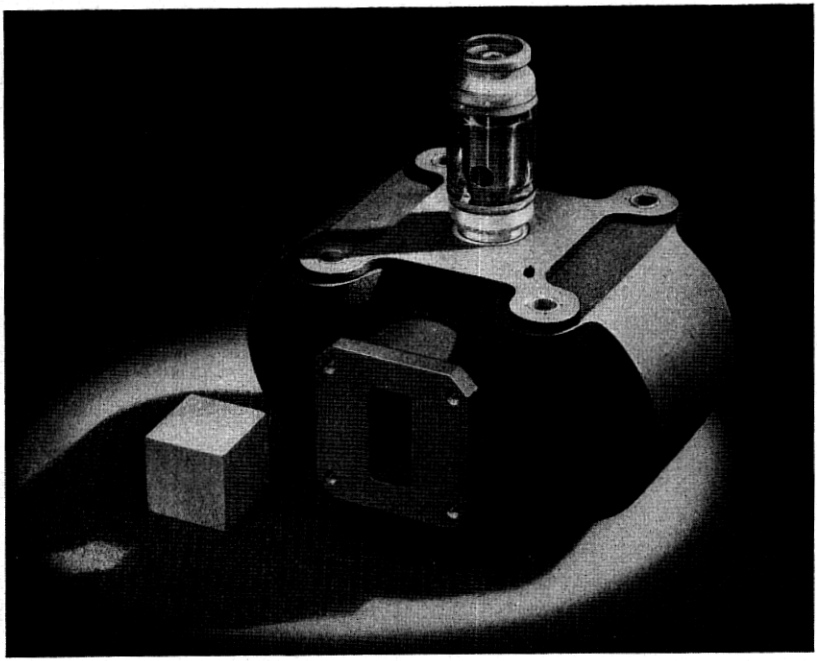

Fig. 74—The 4J52 "packaged" magnetron (100 kw., 9375 mc/s).

In most respects these magnetrons represent the optimum achieved in magnetron design for wavelengths near 3 cm. during the war. Largely because of the lack of hampering electrical and mechanical restrictions, it was possible to make use of all the latest and best techniques in the design of each of its parts. Thus each possesses the desirable features of "packaging," axial cathode mount, wave guide output, and high efficiency at low pulling figure.

20. Magnetrons for Wavelengths near 1 Centimeter

20.1 *Preliminary Work:* Intensive work on magnetrons for wavelengths near 1 cm. began when a joint program with the Radiation Laboratory at

Columbia University was undertaken to prepare for manufacture a variation of a magnetron developed there. Prior to this, some work primarily of an exploratory nature had been done in our Laboratories. When it had been demonstrated that scaling from the 10 cm. range yielded an efficient 3 cm. magnetron, similar attempts were made in scaling to wavelengths of 1 to 2 cm. Magnetrons of such wavelengths, obtained by scaling from eight

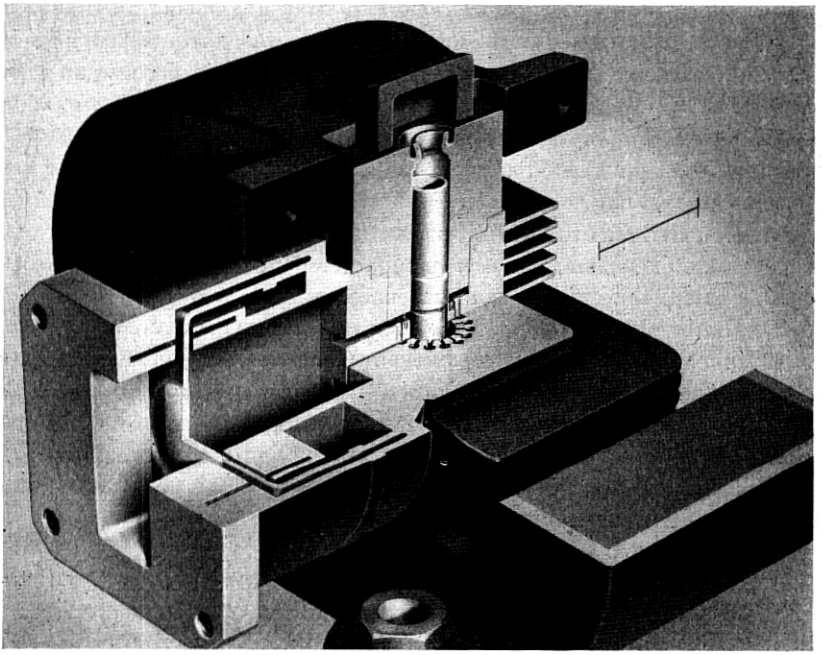

Fig. 75—A view of a cut-away 4J52 "packaged" magnetron (100 kw., 9375 mc/s) which in internal details is essentially like the 4J50 magnetron (280 kw., 9375 mc/s). Of special interest are: the axial cathode construction including permendur end pieces and radiative extension; the quarter wavelength transformer of H-shape cross section (between the output resonator and the line wave guide); and the wave guide window construction with associated chokes.

resonator, 10 cm. models like the 706A-C, were unstrapped while others were strapped with the early British type of strapping and with double ring type strapping. Others were made by scaling from twelve resonator, 3 cm. models and were strapped with both double and single ring straps. The output circuits used were of the loop and coaxial type.

Although some of these magnetrons were faulty, primarily in their output circuits, the majority oscillated. One magnetron of the unstrapped eight resonator variety, the most successful type, was operated over a consider-

able period in our Laboratories. Although no magnetron was developed for manufacture from this work, the experience gained was very useful in the concurrent work at 3 cm. where a similar development program of small magnetrons was under way. Specific developments in this category which should be mentioned are: the use of inserts in which the magnetron resonator system is machined, separable from the rest of the magnetron structure; the use of a double lead cathode input seal to reduce over-all thickness; assembly tools for cathode and strap alignment; and the work with small oxide coated cathodes. The work was discontinued here because of extensive commitments for work at 3 cm. and because an active and successful program of development of magnetrons near 1 cm. wavelength was under way at Columbia University.

The work at the Columbia Radiation Laboratory from the start had been concentrated on magnetrons of very short wavelength. The first Columbia magnetron that was reasonably successful was unstrapped, having a vane type resonator system. It was manufactured in small quantities as the 3J30. Later, the "rising sun" resonator system was discovered there 3J30. Later, the "rising sun" resonator system was discovered as a means of obtaining mode frequency separation. The small scale manufacture was then shifted to the new anode structure, the new magnetron being the 3J31. It was a satisfactory magnetron operating at about 14 kv. and 14 amps., in a magnetic field of 7200 gauss, at a pulling figure of approximately 25 mc/s, and a power output of about 35 kw. The magnetic field was obtained by an external, separable magnet. The cathode was supported by the conventional radial leads.

In addition to the work on the "rising sun" structure, work had continued at the Columbia Laboratory on strapped resonator systems for use at wavelengths near 1 cm. Performance of these magnetrons was quite comparable to that of the "rising sun" variety.

20.2. *The 3J21 Magnetron:* The Bell Laboratories undertook, in collaboration with the Columbia Laboratory, to design a "packaged" version of the 3J31 magnetron for manufacture by the Western Electric Co. At the time, it had not been decided whether the new magnetron should have a strapped or a "rising sun" resonator system. Considerations having primarily to do with manufacturing techniques indicated the latter to be preferable although the former would have been possible. Accordingly, work was started on a "packaged", "rising sun" magnetron to oscillate at 1.25 cm. wavelength (24,000 mc/s). It was to have wave guide output like the Columbia model and axial cathode mount dictated by the "packaged" construction. Operating conditions were to be 15 kv., 15 amps., a pulling figure of 25 mc/s, and as much peak power as could be obtained. It was coded the 3J21.

In the development of the 3J21, the "rising sun" resonator system used by the Columbia Laboratory was adopted practically without change. The ratio of the natural frequencies of the large and small resonators is approximately 1.8. The anode diameter is 0.160 in. and the anode length 0.190 in. The structure is fabricated by the so-called "hubbing" technique,[26] which had been brought to a high state of development at the Columbia Laboratory for the purpose. In this technique, a hardened steel die or hub, machined to be the "negative" of the desired contour, is forced by high hydraulic pressure (of order 250,000 lb./sq. in.) into a copper blank. The hubbed blank, after trimming and turning to size, becomes the resonator system and body of the magnetron. The proper contour to receive the wave guide output circuit is then bored.

The cathode of the 3J21 magnetron has a diameter of 0.096 in. and a length of active coating of 0.165 in. At 15 amps. peak current, the current density at the cathode surface is about 50 amps./sq. cm.—a considerably higher value than that in magnetrons of longer wavelength. Furthermore, the back bombardment of the cathode in this magnetron is about 10 per cent of the input power as compared to the 3 to 6 per cent in longer wavelength magnetrons. For these reasons, the cathode was one of the severest problems of the whole design.

The first axially mounted cathodes were supported on Kovar tubes sealed to the input glass structure. The heater lead was carried down the center of this tube through a glass bead in the input end. The structure resembled that of the 2J51 seen in Fig. 71. Since the hole through the magnetic pole piece was initially 0.100 in. and the cathode end disks 0.130 in. in diameter, the cathode was assembled onto its support after the Kovar tubing was in place. However, in quantity production the cathode could better be assembled as a unit before attachment to the outer glass and pole piece structures. At the expense of magnetic field strength and uniformity, the hole in the pole piece was enlarged to accommodate the entire cathode structure. No ill effects were observed and no special features such as the permendur cathode end structures of the 4J50 magnetron were found necessary.

The problem of the dissipation of the considerable heat of back bombardment was complicated by the necessity of activating the cathode at a temperature of 1050°C. The requirements of heat dissipation and activation oppose one another, one calling for low thermal impedance of the cathode

[26] The technique is here called "hubbing" rather than hobbing for two reasons: The term hobbing has a meaning in machine practice quite apart from the technique in question. The term hubbing is used for processes in which the interior of a piece is removed by forcing a member into it. It presumably arose from the early practice of making axle holes by forcing a hardened steel member through the wrought iron wheel hub. Furthermore, it has an analogous usage in coining.

support, the other, high. To meet each requirement satisfactorily with the first cathode structure was found very difficult if not impossible.

A major step forward was taken in the design of the so-called "soldering iron" cathode in which the heater element is placed in a larger part of the cathode lead, heat being conducted to the cathode surface through a solid rod. The cathode itself is solid, making for greater rigidity and lower thermal impedance. The heater element is placed where it may be made considerably larger and more rugged than if placed inside the cathode, whose diameter is 0.096 in. A view of the 3J21 magnetron cathode structure is to be seen in Fig. 78. The heater is contained within the section of larger diameter immediately adjacent to the cathode.

The "soldering iron" cathode presented more difficult problems of heat conduction and dissipation than the older design. For an operating temperature of 800°C at the cathode surface, it is necessary to heat the heater chamber to about 1000°C, whereas the necessary activation temperature of 1050°C requires the temperature of the heater chamber to be about 1300°C. As a result, rather careful design to provide the proper balance between heat losses by conduction and radiation was necessary. Radiation losses, which are the more important type, are increased by extending the cathode rod considerably beyond the active surface, as seen in Fig. 78. The cathode should also have good thermal conducting properties in this extension, throughout the main cathode body, heater chamber, and support. Under normal operating conditions the heater is turned off, cathode heat being supplied solely by back bombardment.

It is apparent that a cathode design of this type calls for a careful choice of materials. They must be highly refractory as well as of good thermal conductivity and structural strength. Copper, silver, and nickel do not meet all of these requirements. The first cathodes of promise were turned from solid stock of so-called machinable molybdenum, complete with cathode end disks and heater chamber. The heater end was brazed to a Kovar detail, subsequently welded to the support cone of the type developed for the 4J52 magnetron. However, molybdenum machines poorly. The tolerances on size did not permit of large scale production of precision molybdenum parts. Consequently it was proposed to make the cathode of tungsten rod which could be ground to shape even on a production basis. The cathode end disks were to be punched or turned from molybdenum or Kovar and brazed to the tungsten rod. The tungsten rod extends into a hollow molybdenum heater chamber, the dimensions of which are not critical. Inside the heater chamber the heater coil encloses the protruding tungsten rod so that better heat conductivity from the heater to the cathode is provided. The heater is brazed to the cathode at one end in the braze between the tungsten and molybdenum. The other end is spot welded to

a heavy central support lead inside the Kovar cone through a hole provided in the cone. The input end of the heater chamber is flared to accommodate the Kovar support cone to which it is brazed. All of the materials are thus of good structural strength. The tungsten and molybdenum are good thermal conductors, the Kovar not. Some parts of the cathode were grit blasted to increase their radiative emissivity.

The total axial motion of the cathode by thermal expansion from cold start to operation is 0.008 in. The cathode is offset axially by this amount when installed.

The cathode surface consists of a nickel matrix base, like that developed for the 725A magnetron, into which the active coating is impregnated. Attempts were made to increase the thermal conductivity through the 0.008 in. thickness of matrix. Larger particle size was used. Ball milling the nickel powder before sintering resulted in more dense particles. A later improvement was effected by making the matrix oversize by a mil or two, impregnating it with the active coating, and then compressing it to size in a mold. This procedure also resulted in a surface far superior in smoothness and regularity to that previously obtained.

The first output circuit used in the 3J21 magnetron, like that in the Columbia model, involved a quarter wave length transforming section of low characteristic impedance (about 20 ohms), extending from an iris in the "back" of one of the large resonators directly into the output wave guide. This section was 0.350 in. high and about 0.0125 in. wide. It was made by milling a slot into solid bar stock, the top of which was closed by brazing on a copper plate. A quarter wavelength section of this line was brazed between the anode body and the output wave guide piece which carried the choke joints and wave guide window seal. This latter piece was fabricated by hubbing a rectangular wave guide in a copper cylinder into which the circular choke was later turned. The wave guide window consisted of a circular glass disk sealed into a Kovar cup like that used in the 4J50 magnetron (compare Figs. 77 and 75). In the 3J21, as in the 4J50, the external choke facing the wave guide window and a short section of wave guide were later incorporated as part of the magnetron.

Holding the pulling figure of the operating magnetron to a specified value presented a serious problem. The problem was one of securing uniformity of the narrow transformer section and, to some extent, of the resonator to which it is attached. A variation of 1 mil in the width of this transformer produced 3 mc/s change in the pulling figure. Even with an improved mechanical design, the spread in output characteristics was uncomfortably large. Part of the difficulty resulted from the formation of solder fillets in the transformer section during brazing, the size of which could not easily be controlled. A rigid inspection of both electrical and mechanical

properties of each magnetron before sealing and pumping was an absolute necessity to insure reproducibility. The use of an iris coupling between the resonator and the wave guide presented a possible solution. However, the iris required would be too large to be placed directly at the back of the resonator. It was proposed to put a hubbed rectangular resonant iris at the back of the resonator and a decoupling iris a half wave length distant in the wave guide. This construction provided a resonant cavity between the two irises in which the storage of energy would provide some degree of frequency stabilization. The structure of this output circuit may be seen in the photograph of a cutaway model in Fig. 77. Both higher efficiency of

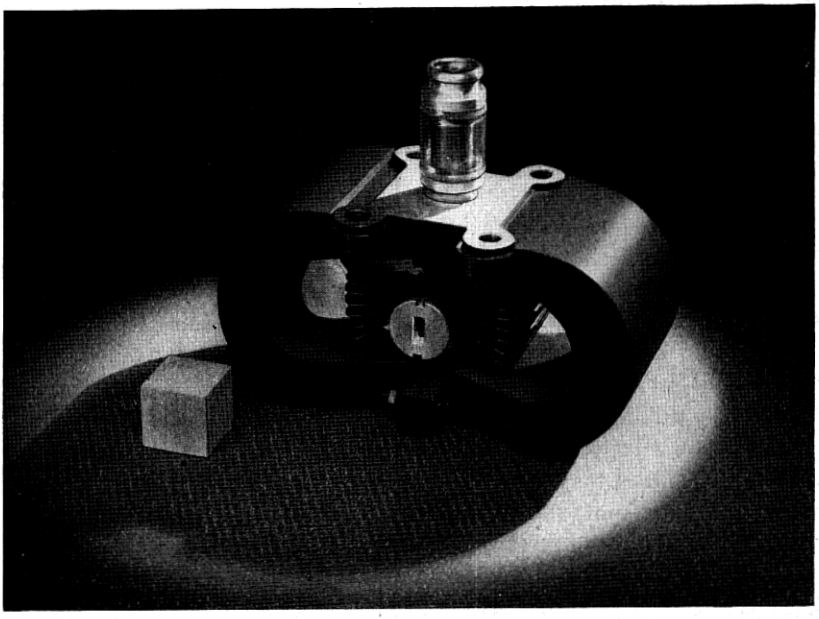

Fig. 76—An external view of the 3J21 "packaged" magnetron (60 kw., 24,000 mc/s).

operation and lower pulling figure than obtained with the earlier circuits resulted. As average values, an increase in over-all efficiency from 24 to 28 per cent and a drop in pulling figure from 25 to 18 mc/s may be cited.

The RF voltage breakdown strength of the wave guide window was marginal. A new design developed at the Columbia and M. I. T. Laboratories, incorporating a larger window and "streamlined" wave guide contours adjacent to it, was modified slightly and used in the 3J21.

The magnetic pole gap was made 0.290 in. This was as small as was felt practical. This and other steps were taken in an effort to save as much as possible on magnet weight.

The mechanical problems connected with the fabrication of the 3J21

magnetron resulted largely from the small tolerances it was found necessary to impose. The tolerance allowed on radial location of the cathode was ±0.002 in.; on transformer slot width (when this output was used), ±0.0005 in.; and on dimensions of the anode structure, ±0.001 in. Deformations, such as those produced by placing a magnetron with slightly misaligned pole pieces on a strong magnet, had to be carefully avoided. The importance

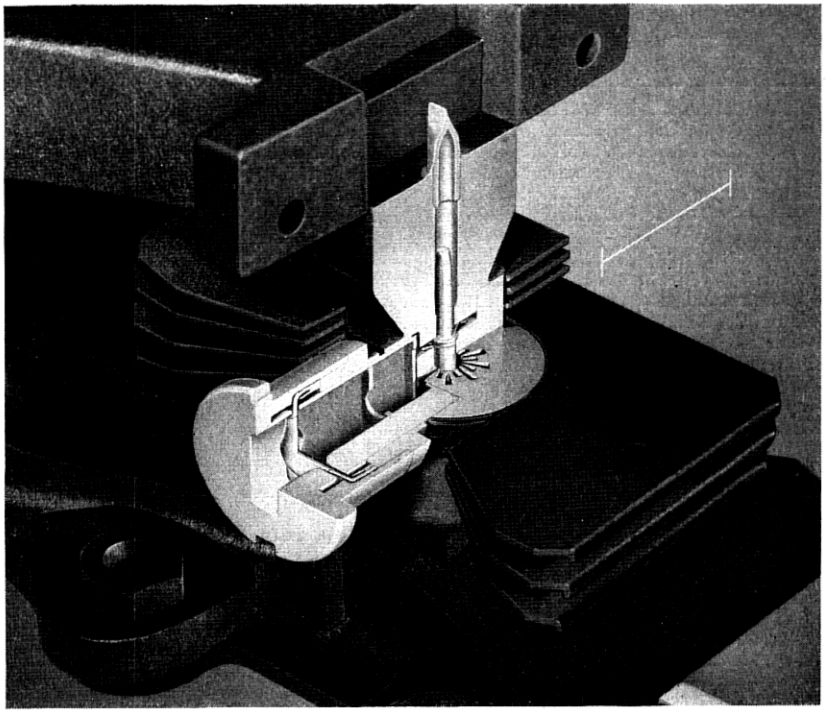

Fig. 77—An internal view of the 3J21 "packaged" magnetron (60 kw., 24,000 mc/s). Note the "rising sun" resonator system, the stabilizing cavity in the wave guide output between a rectangular resonant iris at the "back" of the output resonator and a circular decoupling iris a half wavelength distant, and the beveling of the wave guide edges adjacent to the wave guide window.

of cathode alignment, for example, may be seen from the fact that across the anode-cathode space, which in the 3J21 is only 0.032 in., there is an operating voltage gradient of 165 kv./in. This gradient is doubled in the region where the cathode support passes through the hole in the pole piece, at which point there is a nominal clearance of 0.015 in. Thus the elimination of small burrs and small radii was essential.

An external view of the 3J21 magnetron is shown in Fig. 76, an internal view in Fig. 77. Operational and other data are to be found in TABLE IV.

The principal operational problems encountered in the 3J21 magnetron were the occurrence of so-called "gassy tubes" and some difficulties with "moding." Despite numerous precautions taken during fabrication, gas, identified spectroscopically as hydrogen, was evolved during operation in a discouragingly large number of magnetrons during the developmental work. By the use of a zirconium getter attached to the cathode support cone the difficulty could be circumvented. Also it had been found possible

TABLE IV
THE 3J21 PACKAGED MAGNETRON AT 1.25 CENTIMETERS

N	18	
r_c (in.)	0.048	
r_a (in.)	0.080	
h (in.)	0.186	
Magnet gap (in.)	0.290	
Weight (lb.)	6.6	
Resonator system	"rising sun"	
Resonators	vane type	
Resonator λ ratio	1.8	
λ (cm.)	1.25	
f (mc/s)	23986 ± 240	
Nearest modes	$n = 4$, $n = 8$	
λ separation (%)	+25, −10	
Q_0	1400	
Q_{ext}	580	
η_c (%)	70	
Output circuit	wave guide with λ/2 stabilizing cavity	
Stabilization factor	2	
V (kv.)	15.0	15.0
I (amps.)	15	15
B (gauss)	8000	8000
τ (μs)	0.5	0.25
pps	1000	2000
P_0 (kw.)	60	60
η (%)	26	26
η_e (%)	37	37
PF (mc/s)	17	17

to "clean up" a gassy tube temporarily by running the cathode very hot. This led to a pumping cycle which greatly reduced the occurrence of hydrogen.

Considerable effort was expended in attempting to track down the source of the hydrogen evolution. The iron pole pieces were found to be the major offender, but some hydrogen was evolved from other parts including the cathode. Cleaning and plating solutions release atomic hydrogen which readily permeates the iron pole pieces and other parts. Various

methods of treating the parts, such as preglowing in vacuum, were used. These largely eliminated the difficulty.

An interesting feature of the problem was the relatively infrequent occurrence of hydrogen in magnetrons built at the Western Electric Co. The reason for this was finally traced to the precaution, prescribed by the safety engineers, that the sintering of the copper plate on the pole pieces be done in an atmosphere of 95 per cent nitrogen and only 5 per cent hydrogen. All sintering and brazing operations in our Laboratories had been done in a 100 per cent hydrogen atmosphere. Pole pieces sintered in the predominantly nitrogen atmosphere were found to be nearly as free of hydrogen as the vacuum preglowed parts. However, the use of the zirconium getter was continued in models built at the Laboratories as added insurance against recurrence of the difficulty.

The other operational fault of the 3J21 magnetron was a tendency to oscillate in a mode other than the π mode under certain circumstances. Examination of a large number of magnetrons, opened after operation, showed that the only observable causes were resonator distortion, the presence of brazing flux or other foreign material, and off-center cathode location. As in other magnetrons, the tendency to "mode" was greater when heavily loaded or when operated with a sharply rising voltage pulse. Western Electric engineers concluded, as the result of an extended study of magnetrons in which the cathode position was changed during operation by flexing the input lead, that a cathode position 2 to 3 mils off center toward the output resonator was desirable. A tool was developed with which a permanent change in cathode location could be made on operating magnetrons. By its use many "mody" magnetrons were reclaimed.

An interesting phenomenon, discovered during the development of the 3J21 magnetron, is that known as the "cold start." Whereas most magnetrons may be started with difficulty with a cold cathode, the 3J21 was found to start readily under these conditions over several discrete bands of magnetic field intensity. Although the phenomenon is not well understood, some correlation with the work of Posthumus[13] has been made.

In making tests on the 3J21 magnetron at a duty cycle of 0.001 and a pulse duration of 0.1 μs, the cathode was found to operate at a considerably higher temperature than at 0.5 μs pulse duration and the same duty cycle and average input power. This behavior has since been observed in the 725A and 4J52 magnetrons. It is thought to result from unfavorable conditions during the periods of rise and fall of the voltage pulse, which become a greater percentage of the total pulse duration as the pulse duration is reduced. The effect presumably would not appear if the pulse shape were truly rectangular. With present modulators, however, it

presents a lower limit on pulse duration which may be employed and further complicates the cathode cooling problem.

21. Magnetron Cathodes

From the start of its work with centimeter wave magnetrons, the Bell Laboratories has been engaged in an extensive program of magnetron cathode testing and design. The range of cathode size is illustrated in Fig. 78. The largest cathode, shown at the extreme left, is that of the 5J26 magnetron, operating at about 23 cm., the smallest, that of the 3J21 magnetron operating near 1 cm. The range of operating conditions to be met, as well as the magnitude of the problem at shorter wavelengths, is illustrated by these two extremes. The cathode of the 3J21 magnetron, although its surface area is only 0.31 sq. cm., is called upon to deliver peak currents comparable to those demanded of the cathode of the 5J26, having a surface area of 17.1 sq. cm. The ratio of current densities is 25 to 1. The peak back bombardment of the two cathodes is comparable. Other cathodes shown in Fig. 78 operate under conditions intermediate between these extremes. Needless to say, the 5J26 cathode is operated quite conservatively, the 3J21 cathode under extremely severe conditions.

Little difficulty with cathodes has been experienced in pulsed magnetrons above 10 cm. wavelength. For the most part they are plain, nickel sleeves coated with active material. The highest emission density (10.1 amps./cm.^{2}) used successfully with this type of cathode was in the 720A-E, which operated satisfactorily at 1 μs but was not satisfactory at 5 μs. The operation at 5 μs required a modification of the cathode as described. When the simple sprayed cathode was tried in developmental models of the 725A magnetron, the life at 1 μs was of order 10 hours. At the high emission density required (approximately 30 amps./cm.^{2}) the active coating was rapidly lost as a result of arcs, and frequently the nickel support itself was fused and vaporized.

The problem of arcing to the cathode surface in small magnetrons was soon recognized as the most important cathode problem. It prevented steady operation and hastened destruction of the cathode surface and the end of useful magnetron life. All of these cathodes were found to require an initial break-in period during which the arcing is particularly violent. As the input voltage and current are gradually increased, the violent arcing gradually subsides. The tendency to arc at any time subsequent to this initial period depends on the nature of the cathode surface, but beyond that, it depends also on the operating conditions to which the magnetron is subjected. Increase in power input, either as increased voltage or current, or both, rapidly increases the frequency of arcs. Similarly, increased pulse

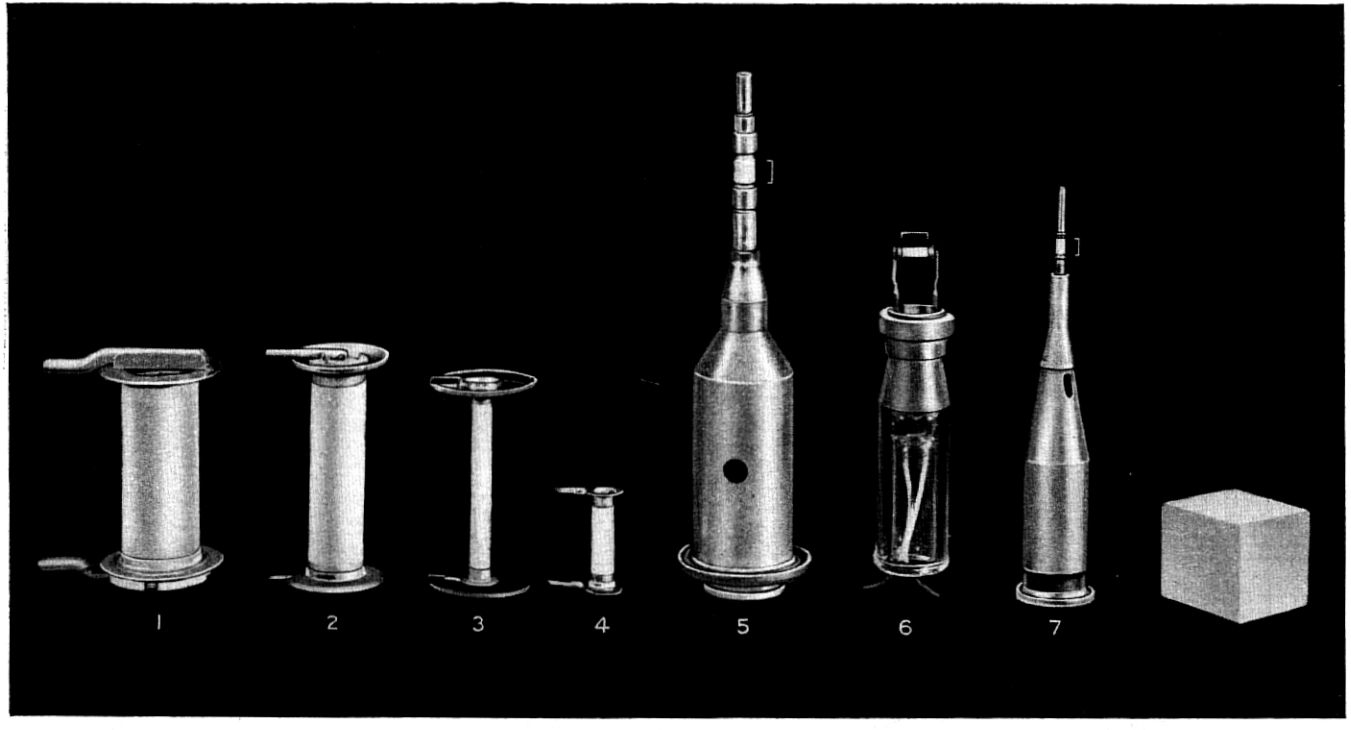

Fig. 78—A group of cathode structures for centimeter wave magnetrons. From left to right they are: (1) the 5J26 cathode—oxide coating on roughened nickel base; (2) the 4J21-30 cathode—oxide coating on roughened nickel base; (3) the 720A-E cathode—metallized, oxide coating on nickel wire mesh base; (4) the 706AY-GY cathode—oxide coating on smooth nickel base; (5) the 4J50 cathode and support structure—oxide coating on sintered, nickel powder, matrix base; (6) the 725A cathode and support leads—oxide coating on sintered, nickel powder, matrix base; and (7) the 3J21 cathode and support structure—oxide coating on sintered, nickel powder, matrix base. The active cathode portion in each of the structures (5), (6), and (7) is indicated by a bracket.

length makes the arcing much worse; in the 725A for example, changing the pulse length from 1 μs to 2 μs may increase the arcing rate by a factor of 10 to 20. A decrease in recurrence rates with some types of cathodes also causes a noticeable increase in the rate of arcing.

In the great majority of cases, magnetron cathodes have employed coatings of the ordinary strontium and barium carbonates as the source of primary and secondary electrons. All-metal, secondary emitting cathodes with primary emitting, starter cathodes have been tried in some laboratories with some success but have not yet come into general use. The efforts at the Bell Laboratories have been directed toward developing and improving the oxide coated cathode along lines making it more nearly possible to satisfy requirements (3), (4), (5), and (6) listed in Section 10.7 *Magnetron Cathodes* of PART I without impairing the ability to meet requirements (1) and (2).

Most of the cathode developments were made in connection with the 725A. This magnetron served as a convenient "laboratory" or "proving ground" for magnetron cathode studies. Its cathode is small enough and the demands made upon it stringent enough to make apparent any cathode weaknesses and any improvements which may be made. A large number of life racks were kept in constant operation for 725A magnetron life tests over a long period of time under various conditions in which the cathodes were generally run to destruction.

Attempts were made to make the data reproducible by controlling the activation, by controlling the initial break-in of the operating magnetron, and by devising means of quantitatively determining some measure of the adequacy of any given cathode. The last of these items involved the development of an automatic counter which registers the number of arcs or bursts of arcs which cause the current to exceed a predetermined value. By recording the accumulated number of arcs at intervals throughout the life of the magnetron, it is possible to get a picture of the arcing pattern with life. Such counters have done much to put the life testing and initial break-in of magnetrons on a semi-quantitative basis. The smoothed curves shown in Fig. 80 were obtained through the use of these counters.

Early attempts at building a cathode upon which sufficient active material may be held, made at both the M. I. T. Radiation Laboratory and the Bell Laboratories, involved winding coated cathodes with nickel wire to provide a reservoir of active material under the wires. In this manner, the material was protected from direct arcing effects, allowing the active material to migrate slowly to the outside surface of the wires. This general idea was greatly improved upon when the wire winding was replaced by a woven nickel mesh into the interstices of which the active material was packed. The

nickel mesh, being spot welded or sintered directly to the nickel base, formed a part of the cathode foundation, helping to reduce the coating resistance. It was found that arcs, rather than striking directly to the active material, tended to strike to the nickel wires. In spite of this fact, sudden bursts of current in arcing would erupt some of the active material from the cathode.

The mesh used in the 725A cathode is made of 6 mil nickel wire woven with 75 wires to the inch. The radial thickness of the mesh on the cathode is 10 mils. The average amount of active double carbonate mixture which the cathode holds is 23 mg. per sq. cm. The mesh cathode is shown in Fig. 79 in three stages of its fabrication. With this cathode, it was possible to

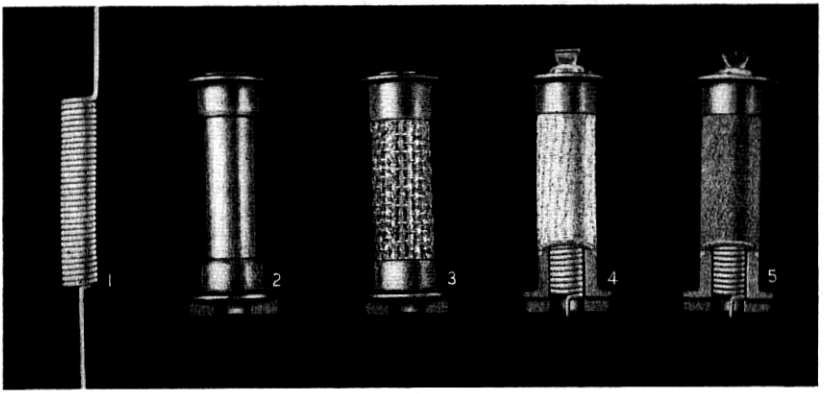

Fig. 79—725A cathode construction. Shown are: (1) the heater element; (2) the machined nickel cathode blank; (3) the cathode blank with the nickel wire mesh, welded or sintered in place; (4) the mesh type cathode with oxide coating applied, cut away to show heater element in place; (5) the more recent cathode with sintered, nickel powder, matrix base (uncoated).

produce 725A magnetrons having a guaranteed life at rated operating conditions of at least 500 hours, the average value being considerably higher. The arcing characteristic of the mesh cathode, excluding the initial break-in period, is shown in Fig. 80. The abrupt failure is typical of magnetron cathodes. At shorter pulse lengths failure occurs considerably later but in the same abrupt fashion. The life curve of the early type of cathode consisting of an oxide coated nickel cylinder, if plotted with the data on other cathodes in Fig. 80, would be crowded very close to the axis of zero hours.

Even with cathodes of mesh construction, operation of the magnetron was generally inadequate at 5 μs pulse duration. Furthermore, considerable break-in time was necessary before stable operation at 1 μs pulse duration was achieved. Some of the first mesh cathodes used in the 725A,

for example, took as long as 45 minutes of intense arcing during gradual increase of input voltage and current before satisfactory operation was attained. It seemed unlikely that the arcing during the break-in period could be completely eliminated, but it was found that improvements in cathode construction which made steady operation at higher current possible also reduced the time of initial break-in to attain these conditions.

It appeared that the resistance of the cathode coating might be lowered by distributing nickel more uniformly throughout the coating. Accord-

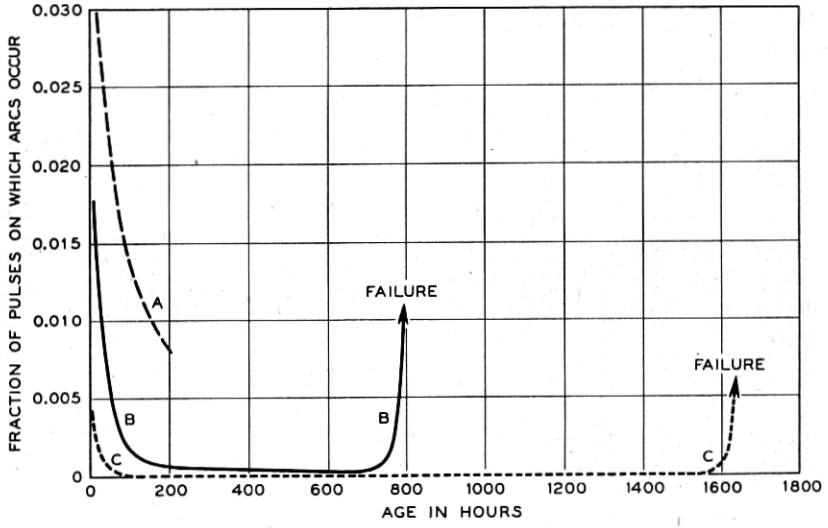

Fig. 80—Curves of arcing during life for 725A magnetrons, having various types o cathodes, operating at 5.7μs pulse duration, 165 pulses per second, and 210 kw. peak powe input. It is to be emphasized that these conditions are considerably more stringent than the normal operating conditions. Curve (a) is for a cathode having oxide coating on a nickel wire mesh base; curve (b), metallized coating on a nickel wire mesh base; curve (c), either plain oxide or metallized coating on a sintered, nickel powder, matrix base.

ingly, mesh cathodes were coated with a mixture of double carbonates in which was distributed a fine nickel powder of high purity having an average particle size of 2 microns. The carbonate particle size is between 1 and 2 microns. The amount, found not to be critical, was 55 per cent by weight of the combined dry ingredients of the coating mixture. Although this reduced the amount of active material present on the cathode surface, as seen in Fig. 80 it resulted in a cathode having considerably improved arcing characteristics with considerably longer useful life. This cathode construction was adopted finally for the 725A production and was also utilized in the 10 cm. high power magnetrons, the 4J45–47, for operation at 5 μs pulse duration.

The next step in the development was the replacement of the nickel mesh by a sintered matrix of coarse nickel powder (see Fig. 79). The average particle size was 55 microns. The active material is packed into this matrix in much the same manner as in the mesh cathode. Little difference was observed in the addition of fine nickel powder to the active coating in this type of cathode. The matrix cathode has the best life characteristic of any yet devised for the magnetron oscillator. Its life characteristic is shown in Fig. 80 with those of the earlier types.

The sintered matrix type of cathode has been used extensively in the 4J50 and 4J52 magnetrons at 3 cm. and in the 3J21 magnetron at 1 cm. In these cathodes, it was important to have high heat dissipation. This was achieved by designing a high thermal conductivity support and providing considerable radiating area immediately adjacent to the cathode surface by extending the cathode, as shown in Figs. 75 and 77, into the pole piece opposite that carrying the cathode mount.

22. Acknowledgments

During the war, the interchange of ideas and results among authorized persons concerned with magnetrons has been rapid and effective. Because of this it would be difficult to trace the origins of much of the general material presented in PART I and no attempt has been made to do so. It must be clear that the results reported have involved the efforts of many people. In the Bell Laboratories, the authors were members of a group which, as the work progressed, grew to a considerable size. In the early stages they were joined by G. E. Moore and W. B. Hebenstreit, later by N. Wax, L. M. Field, A. T. Nordsieck, and R. D. Fracassi. Other members of the Technical Staff in the magnetron group were A. J. Ahearn, H. W. Allison, B. B. Cahoon, C. J. Calbick, M. S. Glass, R. K. Hansen, J. G. Potter, R. Rudin, H. G. Wehe, A. E. Whitcomb, and C. M. Witcher, as well as several technical assistants.

The NDRC Radiation Laboratories at the Massachusetts Institute of Technology and at Columbia University generously supplied personnel for several cooperative projects and information on new results. In the 725A development, A. T. Nordsieck, then of Columbia, took part. L. R. Walker of M. I. T. contributed not only to the development of the 725A but took part in the development of the 4J50, 4J52, and 4J78. Other M. I. T. Staff Members in residence from time to time were F. Hutchinson, E. Everhart, and D. B. Bowen. The developments of the 2J51 and the 3J21 were effected jointly with the Columbia Laboratory.

Prof. J. C. Slater, first as a member of the M. I. T. Radiation Laboratory and later as a member of the Bell Laboratories, made numerous studies in our Laboratories and consulted generally on magnetron problems.

Mechanical design, as well as constructional work and preparation of the detailed specifications for manufacture, was carried out by V. L. Ronci, D. P. Barry, F. H. Best, J. E. Clark, D. A. S. Hale, J. P. Laico and their associates, including T. Aamodt, C. J. Altio, D. I. Baker, C. Blazier, R. H. Griest, F. B. Henderson, W. Knoop, W. J. Leveridge, J. B. Little, C. Maggs, J. A. Miller, H. W. Soderstrom, and F. W. Stubner.

Permanent magnets were designed by P. P. Cioffi of the magnetics group in the Physical Research Department. Numerous physico-chemical problems were solved by L. A. Wooten and his associates of the Chemical Department. The work of J. B. Johnson and J. R. Pierce in allied fields contributed to that described in this paper. In addition, many users of magnetrons for radar purposes throughout the Laboratories collaborated by conducting tests of magnetrons used in radar equipments. We wish to acknowledge the support and advice of M. J. Kelly and J. R. Wilson under whose general direction the work proceeded.

Finally, the authors wish to thank L. M. Field, W. B. Hebenstreit, G. E. Moore, A. T. Nordsieck, and N. Wax, who have read parts of the paper critically.